EDITORIAL STAFF

R. M. Burns, *Chairman*
Norman Hackerman, *Technical Editor*
Ruth G. Sterns, *Managing Editor*
Cecil V. King, *Acting Editor*
U. B. Thomas, *News Editor*
Natalie Michalski, *Assistant Editor*
Eleanor Blair, *Assistant Editor*

DIVISIONAL EDITORS

W. C. Vosburgh, *Battery*
J. V. Petrocelli, *Corrosion*
John J. Chapman, *Electric Insulation*
Abner Brenner, *Electrodeposition*
H. C. Froelich, *Electronics*
Sherlock Swann, Jr., *Electro-Organic*
Irvin R. Kramer, *Electrothermics and Metallurgy, I*
A. U. Seybolt, *Electrothermics and Metallurgy, II*
W. C. Gardiner, *Industrial Electrolytic*
Carl Wagner, *Theoretical*

REGIONAL EDITORS

Howard T. Francis, *Chicago*
Joseph Schulein, *Pacific Northwest*
J. C. Schumacher, *Los Angeles*
G. W. Heise, *Cleveland*
Paul S. Brallier, *Niagara Falls*
Oliver Osborn, *Houston*
Earl A. Gulbransen, *Pittsburgh*
A. C. Holm, *Canada*
J. W. Cuthbertson, *Great Britain*
T. L. Rama Char, *India*

ADVERTISING OFFICE

Jack Bain
Advertising Manager
545 Fifth Avenue
New York 17, N. Y.
PHONE—*Murray Hill 2-3345*

Journal of the
Electrochemical Society

JULY 1955 VOL. 102 • NO. 7

CONTENTS

Editorial

Protecting Our Air Resource 155C

Technical Papers

Dissolution of Metals in Aqueous Acid Solutions, I. Current-Potential Relations for Iron and Mild Steel. *A. C. Makrides, N. M. Komodromos, and Norman Hackerman* 363
A Method for the Isolation of Surface Films from Aluminum Alloys and the Mechanism of the Reactions Involved. *M. J. Pryor and D. S. Keir* 370
The Rate and Mechanism of Dissolution of Purest Aluminum in Hydrofluoric Acid. *M. E. Straumanis and Y. N. Wang* 382
Brightening Agents for the Tin-II Sulfate-Sulfuric Acid Electrolyte. *C. A. Discher and F. C. Mathers* 387
Antimony Oxide Phosphor with Red Emission. *Yoshihide Kotera and Tadao Sekine* 390
Bomb Reduction of Molybdenum Trioxide by Calcium Metal. *H. L. Gilbert and F. E. Block* 394
The Thermodynamic Stability of Refractory Borides. *Leo Brewer and Haakon Haraldsen* 399
High Temperature Oxidation of Two Zirconium-Tin Alloys. *M. W. Mallett and W. M. Albrecht* 407
Application of Backside Luggin Capillaries in the Measurement of Nonuniform Polarization. *M. Eisenberg, C. W. Tobias, and C. R. Wilke* 415
Mathematical Studies of Galvanic Corrosion, III. Semi-infinite Coplanar Electrodes with Equal Constant Polarization Parameters. *James T. Waber* 420
Conductances of Some Moderately Concentrated Solutions of Metallic Perchlorates in the Mixed Solvent Methanol-Acetone at Low Temperatures. *Paul G. Sears, Walter W. Wharton, and Lyle R. Dawson* 430

Technical Reviews

A Rapid Test for Sulfation. *C. C. Rose* 157C
Review of High Temperature Metal-Ceramic Seals. *Hayne Palmour, III* 160C

Current Affairs

Becco—ECS Sustaining Member 165C
Pittsburgh Meeting, October 9 to 13, 1955 ..... 166C
Annual Report of the Board of Directors for 1954 ..... 167C
Annual Report of the Secretary for 1954 ..... 167C
Treasurer's Report for 1954 ..... 167C
Auditor's Report 168C
Division News 170C
Section News 172C
Personals 175C
New Members 175C
Recent Patents 176C
Announcements from Publishers 177C
Literature from Industry 177C
New Products 178C

Published monthly by The Electrochemical Society, Inc., Mount Royal and Guilford Aves., Baltimore 2, Md., combining the JOURNAL and TRANSACTIONS OF THE ELECTROCHEMICAL SOCIETY. Editorial offices: 216 West 102nd Street, New York 25, N. Y. Statements and opinions given in articles and papers in the JOURNAL OF THE ELECTROCHEMICAL SOCIETY are those of the contributors, and The Electrochemical Society assumes no responsibility for them. Nondeductible subscription to members $5.00; subscription to nonmembers $15.00. Single copies $1.25 to members, $1.50 to nonmembers. Copyright 1955 by The Electrochemical Society, Inc. Entered as second-class matter November 15, 1947, at the Post Office at Baltimore, Md., under the act of August 24, 1912.

HOW DO YOU BENEFIT WITH KARBATE BRAND IMPERVIOUS GRAPHITE PROCESS EQUIPMENT?

ANSWER:

By using "Karbate" products, you can:

- **Eliminate corrosion, metallic contamination and the effects of thermal shock**
- **Utilize proved, rugged designs for long life, low maintenance**
- **Order standard stock items for lower cost, faster delivery**
- **Rely on service and application recommendations from National Carbon's technical staff**

Many features recommend "Karbate" chemical process equipment for a prominent place in your plant. Its low first-cost, long service life and freedom from mechanical troubles merit your *first* consideration — not only in those highly corrosive services where nothing else will do, but *wherever* corrosion is a factor.

Write for literature!

The term "Karbate" is a registered trade-mark of Union Carbide and Carbon Corporation

NATIONAL CARBON COMPANY
A Division of Union Carbide and Carbon Corporation
30 East 42nd Street, New York 17, N. Y.
Sales Offices: Atlanta, Chicago, Dallas, Kansas City, Los Angeles, New York, Pittsburgh, San Francisco
IN CANADA: Union Carbide Canada Limited, Toronto

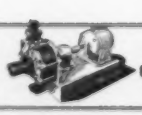
Pumps—Catalog Section S-7250

Pipe and Fittings—Catalog Section S-7000

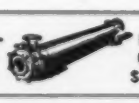
Heat Exchangers—Catalog Sections S-6740 and S-6940

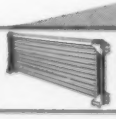
Cascade Coolers—Catalog Section S-6820

HCl Absorbers—Catalog Section S-7460

For Your File! **IMPROVED PLATING TECHNIQUES** *By Baker & Adamson®*

How You Can Make "Printed Circuits" Faster and Better Than Ever!

Use B&A Copper Fluoborate for High-Speed Electroforming—The time required for the copper plating of thick, high quality circuits is reduced sharply by high purity B&A Copper Fluoborate.

Get the Excellent Solderability Produced by B&A Lead-Tin Fluoborate—Assembly is expedited through the use of B&A Lead-Tin Fluoborate giving a 60:40 tin-lead deposit of maximum solderability.

FREE! Technical Bulletins on the Production of Printed Circuits. Mail coupon for them today!

BAKER & ADAMSON® *Fine Chemicals*

GENERAL CHEMICAL DIVISION

ALLIED CHEMICAL & DYE CORPORATION

40 Rector Street, New York 6, N. Y.

The trend throughout the electronics industries is to low-cost "printed circuits" . . . for radios, for television sets, for more and more types of products with electric circuits.

Now these economical circuits can be made better and faster than ever, your products improved, your costs lowered, with the use of B&A Fluoborates. These high purity plating solutions come in concentrated solution form, require no mixing or dissolving, give stability in bath composition and practically 100% anode and cathode efficiencies.

B&A technical bulletins describing these improved plating techniques are available on request. Send coupon for them today.

BAKER & ADAMSON PRODUCTS
General Chemical Division
Allied Chemical & Dye Corporation
40 Rector Street, New York 6, N. Y.

Please send technical bulletins on the use of B&A Fluoborates in the production of printed circuits.

Name_____

Company_____

Title_____

Address_____

City_____ Zone____ State_____

JE-7

FISHER
TITRIMETERS®

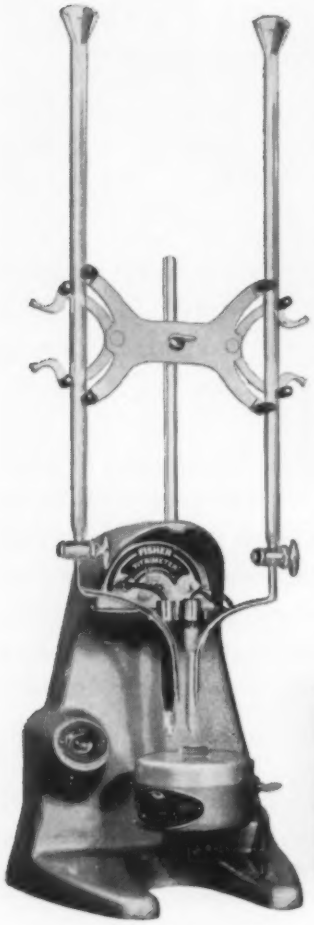

- **THE STANDARD TITRIMETER** . . . the basic analytical instrument for every kind of titration.
- **THE AUTOMATIC TITRIMETER** . . . titrations in half the time.
- **THE HIGH FREQUENCY TITRIMETER** . . . for "hands off" titrations.
- **THE AMPEROMETRIC TITRIMETER** . . . for trace concentrations.

There's a Fisher Titrimeter for every kind of titration. Acids and bases, oxidation-reduction reactions, precipitations and complexing reactions, non-aqueous or two-phase titrations, big samples or tiny ones — all are handled with speed and accuracy.

The four Fisher Titrimeters are key analytical instruments in any busy modern laboratory. Using them, technicians with a minimum of training can perform routine titrations easily, accurately, and fast.

Write today to 717 Forbes Street, Pittsburgh 19, Pa. for Booklet FS-247-20. It tells the whole story of the versatile Fisher Titrimeter family and the type of work which each Titrimeter does best.

FISHER SCIENTIFIC

Boston	Cleveland	Philadelphia	Washington
Buffalo	Detroit	Pittsburgh	Montreal
Chicago	New York	St. Louis	Toronto

America's Largest Manufacturer-Distributor of Laboratory Appliances and Reagent Chemicals

...a practical refresher in chemical arithmetic

JUST PUBLISHED
6th EDITION

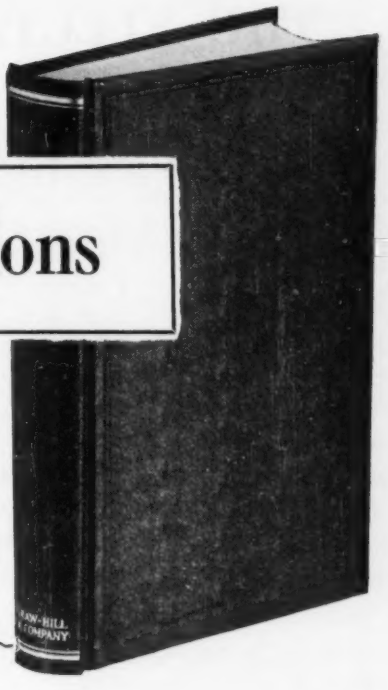

Chemical Calculations

By H. V. ANDERSON

Professor of Chemistry, Lehigh University

Sixth Edition, 299 pages, 27 tables, 11 figures, $4.75

THIS valuable book provides you with a sound review and analysis of calculations common to chemical research and practice—serves as a helpful guide spotlighting the "common-sense" method of approach in solving everyday problems. It includes scores of illustrative examples dealing with equation writing, thermometric calculations, gas-volume relations, oxidation reduction, gram-equivalent, molar and normal concentration, principle of equivalency, thermochemical reactions, electrochemistry, chemical equilibrium, solubility-product principle, and so on.

This revised Sixth Edition is packed with useful explanations and data for the practicing chemist. The step-by-step presentation in solving illustrative examples in logical sequence leads to a better, more thorough understanding of the solution. The use of dimensional units as an aid in solving various problems is stressed, and the use of significant figures is emphasized.

Revised material includes data on exponents and significant figures, gram-atom and gram-mole relations, fundamental gas laws, subject of percentage concentration, and so on. Emphasis is placed on chemical equation writing. You'll find this book a reliable guide in making a wide variety of common calculations.

Here's some of the information packed into 27 helpful tables:

—Conversion Table for Pressure
—Vapor Pressure of Water in Millimeters of Mercury
—Common Radicals with Names, Formulas and Valence
—Boiling-point and Freezing-point Constants for Various Solvents
—Calorific Power of Some Substances
—Heats of Formation of Some Oxides
—Calorific Power of Some Gases and Liquids
—Conversion Factors for Weights and Measures
—Density of Gases
—Percentage of Effective Ionization of Electrolytes at 18°C

Keep this handy reference on common calculations at your fingertips—to help you solve a wide variety of chemical problems

CONTENTS

1. Measures and Weights
2. Density
3. The Language of Chemistry
4. Gram-Atom and Gram-Mole
5. The Measurement of Temperature
6. Effects of Changes in Pressure and Temperature on the Volume of Gases
7. Mole-weight—Gas-volume Relations
8. Derivation of Chemical Formulas
9. Chemical Equations. Nonredox Type
10. Oxidation-reduction
11. Gram-equivalent
12. Molar and Normal Concentration
13. Principle of Equivalency
14. Combination of Gases
15. Thermochemical Reactions
16. Electrochemistry
17. Chemical Equilibrium; Reversible Reactions
18. Solubility-Product Principle

THE ELECTROCHEMICAL SOCIETY, INC.
216 West 102nd Street
New York 25, New York

Please send me _____ copies of the 6th edition of Anderson's "Chemical Calculations":

Name_____

Street_____

City, State_____

Price: $4.75 plus postage

THE ELECTROCHEMICAL SOCIETY, INC.

The Electrochemical Society is an international organization of individuals and companies concerned with or interested in Electrochemistry and allied subjects.

The Society is dedicated to the advancement of the theory and practice of Electrochemistry and related subjects, as shown in the following divisions:

Battery	Electro-Organic
Corrosion	Electrothermics and Metallurgy
Electric Insulation	Industrial Electrolytic
Electrodeposition	Theoretical Electrochemistry
Electronics	

Among the means to this end are the holding of meetings for the reading and discussion of professional and scientific papers on these subjects, the publication of such papers, discussions, and communications as may seem appropriate, and cooperation with chemical, electrical, and other scientific and technical societies.

It is an incorporated society without capital stock. The affairs of the Society are managed by a Board of Directors under a Constitution and Bylaws. Officers are nominated by a nominating committee appointed by the Board of Directors and elected by the members.

Direct all general correspondence and inquiries regarding membership to Society headquarters at 216 West 102nd Street, New York 25, N. Y.

Officers of the Society

President ..... HERBERT H. UHLIG
Past President ..... MARVIN J. UDY
Vice-President ..... HANS THURNAUER
Vice-President ..... NORMAN HACKERMAN
Vice-President ..... SHERLOCK SWANN, JR.
Treasurer ..... LYLE I. GILBERTSON
Secretary ..... HENRY B. LINFORD

WILEY BOOKS

First in their fields

VAPOR-PLATING

The Formation of Metallic and Refractory Coatings by Vapor Deposition

By C. F. POWELL, I. E. CAMPBELL, and B. W. GONSER,
all at the Battelle Memorial Institute

This is the first single source of reference for data and information on these processes. Provides a critical and authoritative review of the applications and techniques of vapor deposition of metals and non-metals.

The versatility of vapor-plating processes is stressed by the authors in an effort to stimulate the use of these processes as a flexible tool in many fields of technology. Sponsored by THE ELECTROCHEMICAL SOCIETY.

1955 158 pages Illus. $5.50

MODERN ELECTROPLATING

Edited by ALLEN G. GRAY
Technical Editor, STEEL Magazine

Based on the combined experience of 39 outstanding experts, this book gives you a complete, up-to-date, one-volume summary of current electroplating processes. The only book to emphasize the practical aspects of the science and theory upon which its modern applications rest, it reflects the developments which have made electroplating indispensable in both decorative and utility fields. Sponsored by THE ELECTROCHEMICAL SOCIETY.

1953 653 pages Illustrated $9.50

ELECTROCHEMISTRY in BIOLOGY and MEDICINE

Edited by THEODORE SHEDLOVSKY,
Rockefeller Institute for Medical Research

In this new work based on a symposium held by The Electrochemical Society, Inc., twenty-three experts cover important advances in the field. The nineteen papers included present discussions ranging from membranes and the application of electrochemical methods in problems of biological interest —to the behavior of living tissues as electrochemical systems. Rather than providing an exhaustive treatise, the papers indicate the trend of modern thinking. Stimulating and sometimes controversial, the book should provoke a great deal of further interest in this increasingly important area of biological knowledge.

1955 369 pages 151 Illus. $10.50

CORROSION HANDBOOK

By H. H. UHLIG,
The Massachusetts Institute of Technology; and an Editorial Board of Nine

Prepared by a staff of 100 experts, this book considers the causes of corrosion in practically every type of metal and alloy, including high-temperature corrosion. Presents detailed information on prevention of corrosion and on corrosion testing. Sponsored by THE ELECTROCHEMICAL SOCIETY.

1948 1188 pages 503 Illus. $15.00

Mail Coupon for your ON-APPROVAL copies today!

JOHN WILEY & SONS, Inc.,
440 Fourth Ave., New York 16, N. Y.

JE-75

Please send book(s) checked for me to examine ON APPROVAL. Within 10 days I will either return same and owe you nothing or will remit the price(s) indicated, plus postage.

- ☐ VAPOR-PLATING $5.50
- ☐ ELECTROCHEMISTRY IN BIOLOGY AND MEDICINE $10.50
- ☐ MODERN ELECTROPLATING $9.50
- ☐ CORROSION HANDBOOK $15.00

NAME_____
ADDRESS_____
CITY_____ ZONE____ STATE_____

☐ SAVE POSTAGE! Check here if you enclose payment, in which case we pay postage. Same return privilege.

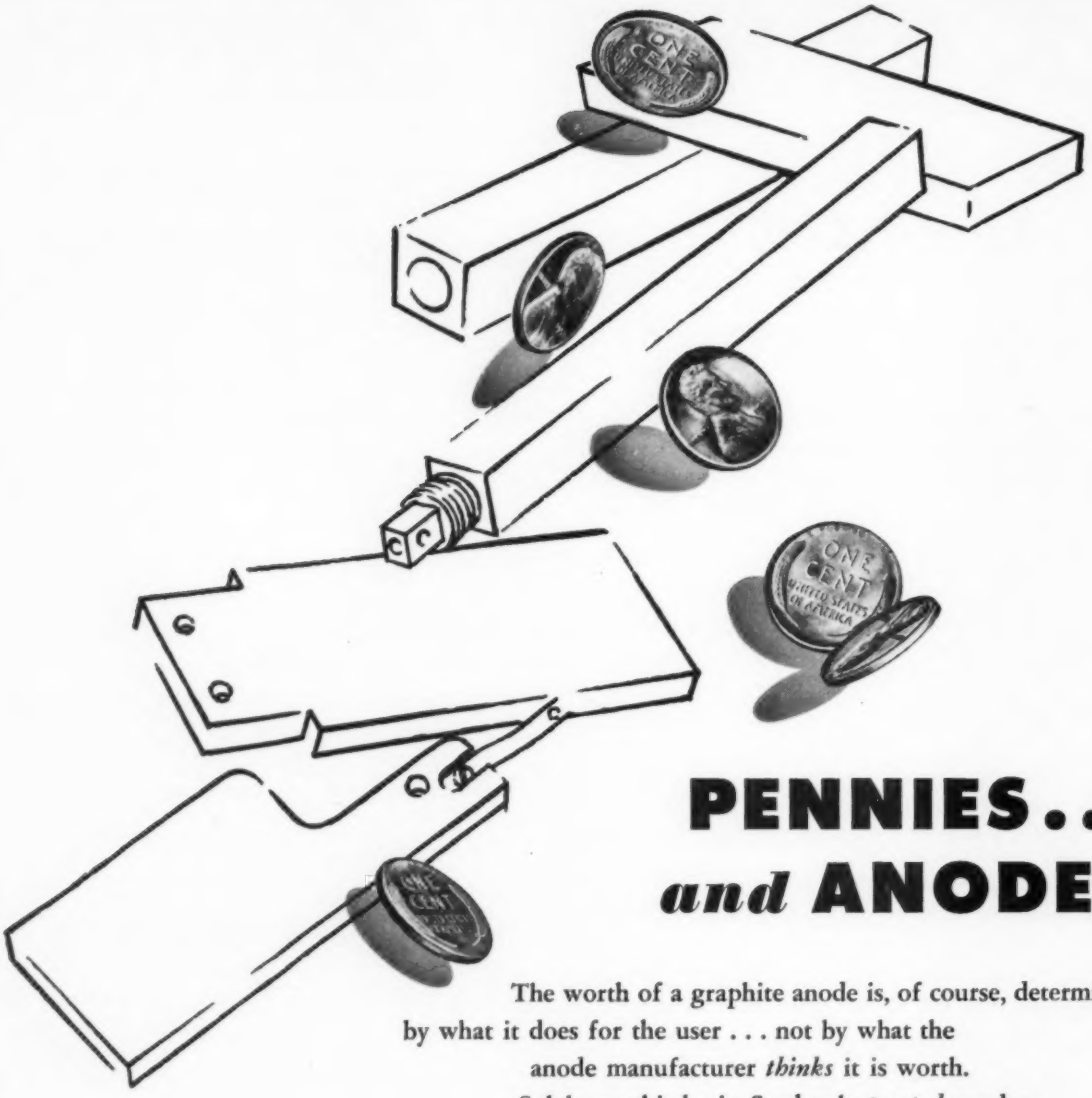

PENNIES... *and* ANODES

The worth of a graphite anode is, of course, determined by what it does for the user . . . not by what the anode manufacturer *thinks* it is worth.

Solely on this basis, Stackpole *treated* anodes, priced only pennies higher than untreated types, are more than justifying their use by leading chemical producers.

They last longer, deliver low-voltage operation in fullest measure. Write for Catalog 40A . . . or send details of your carbon-graphite requirements for recommendation by Stackpole engineers.

Address: **Stackpole Carbon Company, St. Marys, Pa.**

STACKPOLE

long-life, low-voltage

ANODES

BACKED BY THE KEEN PERSONAL INTEREST AND FULL COOPERATION OF THE SPECIALISTS WHO PRODUCE THEM.

Editorial

Protecting Our Air Resource

AIR POLLUTION has become a menace to animal and plant life and a serious discomfort to the residents of urban communities. Impairment of health, damage to vegetation, corrosion of metals, and deterioration of rubber and other organic products is the mounting cost of permitting the emission of pollutants into the atmosphere. The fatalities that occurred in Donora, Pennsylvania, and London emphasize the hazard that threatens other congested and industrialized areas. With greater frequency in recent years the larger cities in this country and abroad have experienced periods of atmospheric contamination resembling in some degree the conditions known in Los Angeles as "smog." This term, inaccurately applied to Los Angeles, was coined to describe the combination of smoke and fog prevailing at times in London. It is a more subtile phenomenon that has made Los Angeles notorious. Indeed, this city, now better known for its contaminated air than for its sunshine, has become the laboratory for air pollution study. Here and in many other communities the citizens are coming to realize the need for preserving the purity of the atmosphere and the effort and the cost that this entails.

The Los Angeles smog presents a complex chemical-meteorological problem. Masses of air from a persistent anticyclonic high pressure area over the north Pacific Ocean sweep down along the California coast and are heated by compression giving rise to a temperature inversion layer. This becomes trapped in the Los Angeles basin by the surrounding mountains and, remaining more or less stationary for days at a time, prevents the escape of atmospheric pollutants originating in the area. Thus there is formed a huge chemical reaction chamber in which, with the aid of sunshine, a multitude of obnoxious substances are brewed. These cause eye and pulmonary irritation, crop damage, and reduced visibility. While the sources of pollution have not been established with certainty, the best evidence indicates that half are of industrial origin, forty per cent from automobile exhaust, and the remaining ten per cent from the quaint practice of backyard incineration of garbage.

The chemical reactions that give rise to the Los Angeles smog are still somewhat obscure and need further study. The daily smog cycle that reaches maximum intensity in the middle of the day is characterized by abnormally high ozone concentrations. The key to the phenomenon now appears to be the production of nitrogen oxides by motor vehicles and other oil and gasoline combustion processes. Nitrogen dioxide is readily decomposed photochemically into nitric oxide and nascent oxygen, the latter giving rise to ozone. Presumably these strong oxidants, nascent oxygen and ozone, react with hydrocarbons that are present up to three parts per million in the Los Angeles atmosphere. The resulting products include aldehydes, acids, a variety of free radicals, and other objectionable contaminants.

What to do about the Los Angeles smog awaits further knowledge of its sources and its chemistry. Measures that have succeeded in improving the atmospheres of Pittsburgh and St. Louis would be neither applicable nor effective. Many fantastic schemes have been proposed and the citizens have been confused and perplexed by politicians, crackpots, and the conflicting accounts of incomplete and inadequate scientific findings. This situation has led one impatient pressure group to demand that any further expenditure of public funds be devoted to stopping smog and not studying it!

Obviously, heroic measures will be necessary to prevent progressively greater pollution of the air in all populous regions. Expensive and laborious studies will be required to establish the facts upon which sensible air pollution control measures can be based. Only an informed and enterprising public willing to support such investigations can expect to enjoy clean air.

—RMB

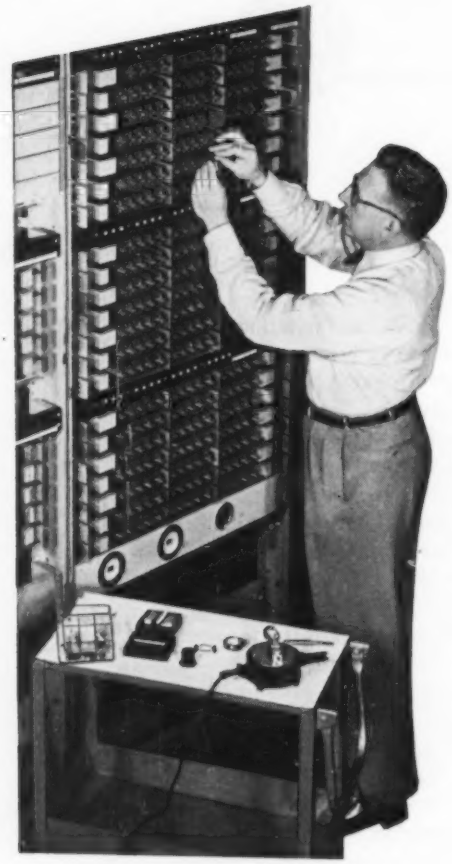

He's "fingerprinting" a relay contact

Bell Laboratories microchemists have perfected an ingenious new technique for "fingerprinting" relay contacts, the tiny switches on which a dial telephone system critically depends.

Using a portable test set, a chemist makes a plastic print of a contact. On-the-spot examination of the print with a microscope and chemical reagents quickly reveals the effects, if any, of arcing, friction, dust or corrosive vapors. While the chemist studies the print, urgently needed contacts continue in service. Findings point the way to improve relay performance.

This is another example of how Bell Telephone Laboratories research helps to keep your telephone system the world's best.

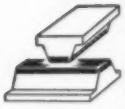

Above, Bell Laboratories microchemist applies plastic disc in heated clamp to relay contact. Imprint reveals contours of surface and picks up contaminants, if any. Part of portable test set is shown on table. Contacts, shown in small sketches, are of precious metal fused to base metal.

Preparing disc for microscopic examination. On-the-spot examination may reveal acid, alkali, sulfur, soot or other polluting agents peculiar to an area.

A microscopic look at disc often provides lead to nature of trouble. Unlike actual contact, print can be examined with transmitted light and high magnification.

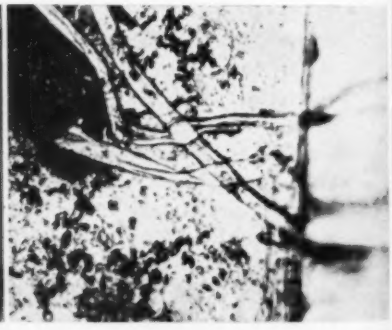

Here the plastic disc has picked up microscopic lint that insulates contact, stops current. (Picture enlarged 200 times.) Traces of contaminants are identified in microgram quantities. Inert plastic resists test chemicals that would damage contact.

Bell Telephone Laboratories

Improving telephone service for America provides careers for creative men in scientific and technical fields

A Rapid Test for Sulfation[1]

C. C. Rose[2]

Abstract

Lead-acid storage batteries are subject to early failure by operation or storage in a condition of partial discharge. This type of failure is commonly called "sulfation." It has not been defined accurately and has been difficult to produce and evaluate in the laboratory. A method is proposed which is fairly rapid, consistent, and significant, and which measures the contribution of various factors involved.

Lead-acid storage batteries in automotive service fail generally from three principal causes: overcharge, undercharge, or mechanical defects. Cycling failure of positive plates is seldom encountered in this service any longer. Normal failure in batteries which last at least their guarantee life is generally positive grid corrosion.

The modern battery of proper size, in normal service, with proper voltage regulator setting to provide full charge gravity in the battery with a minimum of overcharge, is capable of lasting from 50,000–100,000 miles of driving. One of the most serious causes of damage is undercharge, which often results in premature battery failure because of "sulfation." This is easily recognized, chiefly by the condition of the negative plate. Even after being carefully recharged, such negatives tend to be hard and dense when scratched instead of showing the soft gray metallic luster of good sponge lead. They are often sandy or gritty, particularly if they have been subjected to high acid gravity and high temperatures, and most characteristically they do not show a reverse cadmium reading even when fully charged. This is not because the plates are sulfated, but rather is a symptom of antimony contamination of negative active material and an indication that such plates will sulfate rapidly on open circuit.

This condition results in a high open circuit loss of three or more points per day in gravity and often a loss of 75% or more of cold starting capacity. There is no practical or economically feasible method of restoring such batteries to a normal healthy condition. Sodium and magnesium sulfates or other battery dopes do not help. Sulfation is distinct from the simple condition of discharge, or sulfation brought about by short circuits through battery separators, or the result of complete battery breakdown.

Sulfation does not "account for 70% of all battery failures" as has been stated, or any appreciable fraction thereof. Scrap battery surveys indicate that only about 18% had sulfated negatives even though most of them had given normal life. Of some 4000 batteries which failed prematurely for one reason or another and were returned for adjustment, approximately 13% were judged sulfation failures or neglect failures. There is no good way of translating this figure to total production, but assuming 1% returns, it represents not over 0.13% of the total. There is no reason then to say that sulfation is a major cause for battery failure, although it still is a major weakness of the lead-acid battery and it generally causes failure before normal life is attained.

The real importance of this characteristic is that it limits the stand-by time of lead-acid batteries either in stock or vehicle storage. It has been a difficult situation to understand clearly and even more difficult to explain and prevent. This is because a lead-acid battery stands a great deal of abuse and neglect without suffering permanent damage.

For this reason a simple and practical test for sulfation is in order. Strangely enough, no test has been devised or at least agreed on to date to do this, and such a test procedure is not too obvious. It is felt that neglect in keeping batteries fully charged while in stock, particularly in hot weather, is a factor contributing to sulfation failure. This is especially harmful when such batteries are installed in service without being fully charged, and it is almost certain to be fatal when such service continues to provide inadequate input, and the undercharged condition is allowed to prevail.

Admitting this, it was still not possible to explain all that was happening in the field or to duplicate it in the laboratory. Quite by accident the additional factor or a combination of factors contributing to the condition was found, and a rapid, consistent, and significant test for measuring the influence of the various battery components involved has been devised.

The Sulfation Test

The basis of the test is high temperature open circuit stand and high temperature charge. Whether the latter condition is critical or not, it ties in with field conditions, and it does seem to accelerate the test. Readings taken on batteries under the hood in cars parked in the sun have shown temperatures as high as 165°F. At these temperatures with normal regulator settings charging rates are high because battery voltage is low. Under such conditions it is hard to anticipate battery failure from sulfation except that self discharge is extremely high both day and night while the car is idle. Water loss is also very high resulting in low levels and high gravity which again is extremely harmful to negative plates. Thus, a test devised to include charge and open circuit stand at 150°F seems reasonable and practical for laboratory purposes.

The exact times, sequence, and rate of capacity measurement, etc., for such a test are not too critical. Several different schedules have been tried including recharge and capacity testing at 80°F. Such procedure slowed up the testing and showed no advantage. Also it may be found that one or more of the discharge cycles in the proposed schedule can be eliminated and yet here again it may be said that such a cycle is not unfavorable to a battery normally and that it further simulates operating conditions.

[1] Manuscript received November 12, 1954. This paper was prepared for delivery before the Boston Meeting, October 3 to 7, 1954.

[2] Automotive Division, Electric Storage Battery Company, Cleveland, Ohio.

TABLE I. *Test schedule 150°F water bath temperature*

Friday	9:00 A.M.	Batteries begin open circuit stand.
Saturday		On open circuit.
Sunday		On open circuit.
Monday		On open circuit.
Tuesday	9:00 A.M.	Catchout. Discharge at 40 amp to 1.7 volts per cell.
	11:00 A.M.	On charge at 5 amp.
Wednesday	9:00 A.M.–10:00 A.M.	Discharge at 40 amp.
	10:00 A.M.–3:00 P.M.	Charge at 10 amp.
	3:00 P.M.	On open circuit.
Thursday	9:00 A.M.–9:30 A.M.	Discharge at 40 amp.
	9:30 A.M.–3:30 P.M.	Charge at 10 amp.
	3:30 P.M.–4:00 P.M.	Discharge at 40 amp.
	4:00 P.M.	On charge at 5 amp.
Friday	9:00 A.M.	Stop charge.

The recommended schedule (Table I, S-40 Test) is workable in any battery laboratory with S.A.E. cycling circuits plus a simple water bath to maintain temperature. The comparison of residual capacity after O.C. stand is just as accurately measured by the 40 amp discharge normal to cycle testing as it is at higher rates. Results are consistent and significant and are available in 10–12 weeks. Tests were all run on 100 amp-hr S.L.I. batteries.

Fig. 1 indicates the effect of electrolyte gravity on negative sulfation. That this has been recognized by the industry is shown by the change to high level lower gravity in many batteries now offered, although it is doubtful that many of these manufacturers know the exact effect of this change. The change from 1.280 to 1.260 practically doubled the resistance of a battery to sulfation failure, all other factors being equal, with still further improvement possible at 1.240 gravity.

In Fig. 2 the combined effect of insulation and of positive grid alloy is shown. Rubber insulation is outstanding in all comparisons and the indication is that improved types of glass fiber and diatomaceous earth can approach rubber in this characteristic. These batteries ran 34 or more weeks, failed apparently from positive grid corrosion plus some loss of active material and with negatives still showing good negative cadmium readings at the end of life. The function here is apparently a filtering or sequestering action protecting the negative from the antimony dissolved from the positive. That this is so is clearly indicated in the direct comparison of the 11% and 6% positive alloys with wood insulation, the high antimony alloy failing much more rapidly than the low. Comparison of the wood and rubber insulation with the low antimony alloy is quite obviously in favor of rubber again at a favorable low 1.260 gravity.

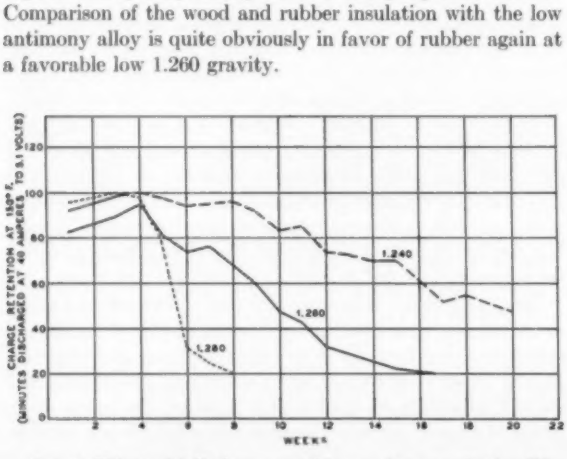

FIG. 1. Effect of full charge specific gravity on sulfation life; 6% Sb positive grid alloy; mechanical insulation.

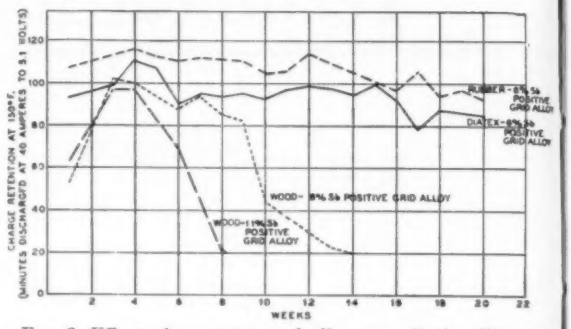
CHARGE RETENTION AT 150°F.
(MINUTES DISCHARGED AT 40 AMPERES TO 5.1 VOLTS)
WEEKS
RUBBER - 6% Sb POSITIVE GRID ALLOY
DIATEX - 6% Sb POSITIVE GRID ALLOY
WOOD - 6% Sb POSITIVE GRID ALLOY
WOOD - 11% Sb POSITIVE GRID ALLOY

FIG. 2. Effect of separator and alloy on sulfation life; specific gravity, 1.260.

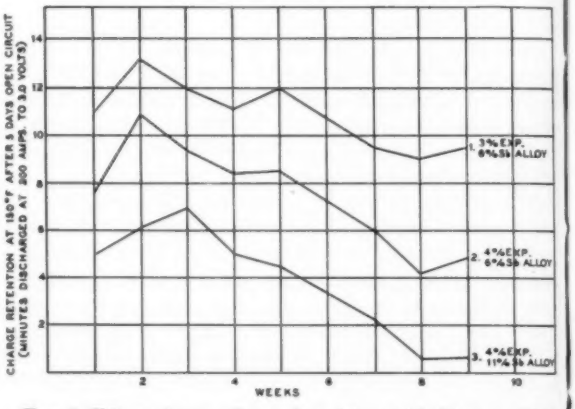
CHARGE RETENTION AT 150°F AFTER 5 DAYS OPEN CIRCUIT
(MINUTES DISCHARGED AT 200 AMPS. TO 3.0 VOLTS)
WEEKS
1. 3% EXP. 6% Sb ALLOY
2. 4% EXP. 6% Sb ALLOY
3. 4% EXP. 11% Sb ALLOY

FIG. 3. Effect of expander and positive grid alloy on sulfation; 1.285 specific gravity; rubber insulation.

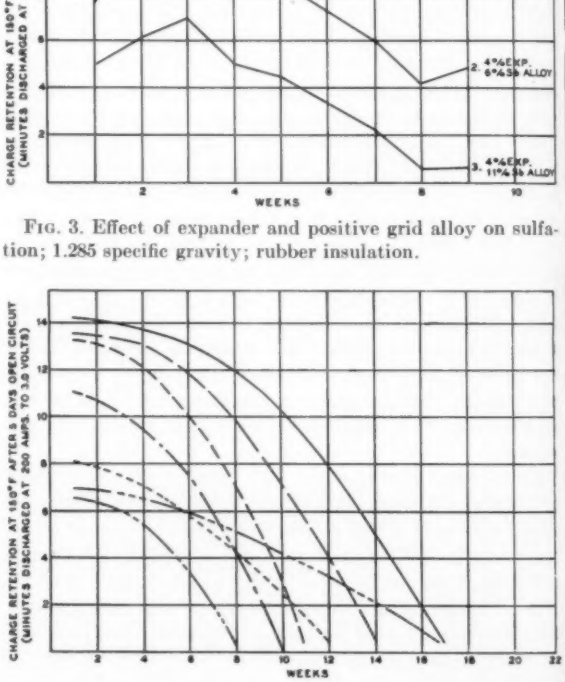

FIG. 4. Comparison of competitive batteries on sulfation test.

This test may be used to advantage in testing the new mechanical separators as well. By mechanical separators is meant those other than wood or rubber, made from cellulose, or glass fibers plus diatomaceous earth filler, and bonded with some kind of plastic acid resisting resin. A distinct difference in resistance to sulfation is shown which cannot be predicted from appearance or from other normal battery or separator tests. It was found that the particular brand of separators which showed up weakest on this sulfation test corresponded with field returns from this same cause of failure.

In Fig. 3 two variables are involved. The principal variable was expander which governs the activity of the negative plate and the difference between 3% and 4% is quite ap-

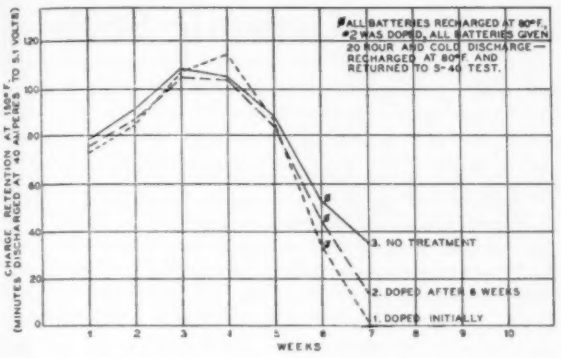
ALL BATTERIES RECHARGED AT 80°F.
#2 WAS DOPED, ALL BATTERIES GIVEN
20 HOUR AND COLD DISCHARGE—
RECHARGED AT 80°F AND
RETURNED TO S-40 TEST.
CHARGE RETENTION AT 150°F
(MINUTES DISCHARGED AT 40 AMPERES TO 5.1 VOLTS)
WEEKS
3. NO TREATMENT
2. DOPED AFTER 6 WEEKS
1. DOPED INITIALLY

FIG. 5. Effect of battery dope on high temperature sulfation life. 11% Sb positive alloy; wood insulation; 1.285 specific gravity.

preciable. This test was run with rubber insulation, which is favorable and eliminates the separator variable, but at high gravity to accelerate testing. Also the discharge was run at 200 amp instead of 40 and is recorded on a somewhat different scale, which does not affect the shape of the curves. The effect of grid alloy is again shown and it is apparent that these factors are cumulative.

Fig. 4 is a comparison of commercial batteries all of the same ampere-hour capacity, of different makes, and as purchased on the open market. It is evident that all of these batteries are subject to this type of failure and that the benefits gained by proper selection of expander, grid alloy, and acid gravity are cumulative. The top curve represents a favorable combination of these variables.

The difference in the position of the curves at the start is not a significant part of this comparison since it probably is caused largely by their difference in age and care in stock. However, it certainly does indicate what happens to batteries not properly maintained prior to installation in service.

Fig. 5 represents the results of a test carefully designed to determine the effect of a battery dope on sulfation. Three identical batteries were built and one of them was doped just before starting this test. This is battery No. 1. At the end of six weeks this battery had definitely failed with the other two not far behind. At this point the second battery was

TABLE II

Battery No.	1	2	3
Additional treatment	None	Doped	None
Twenty-hour discharge			
Specific gravity (80°F)	1.276	1.280	1.272
Capacity (hr)	<18	<18	18.7
Cold discharge			
Specific gravity (80°F)	1.289	1.293	1.282
Neg. cadmium	+.04	+.04	+.02
5 sec volts	4.20	4.40	4.50
Minutes	0.82	1.00	1.21
Recharge 80°F returned to sulfation test			

TABLE III

Battery No.	1	2	3
Sulfation cycle #7 (min)	0	13.1	36.2
Twenty-hour discharge (hr)	<12	<12	<12
Open circuit at 95°F (14 days)			
Start specific gravity (80°F)	1.237	1.258	1.247
Finish specific gravity (80°F)	1.188	1.192	1.173
Loss	.049	.066	.074
Twenty-hour capacity (hr)	0.0	0.2	2.0
Cold capacity			
Minutes	0.49	0.66	0.85
5 sec volts	4.00	4.03	4.25
Twenty-hour capacity (hr)	11.8	13.2	16.7

doped to determine whether a dope could salvage a battery otherwise sound but in a sulfated condition. This was battery No. 2.

At this point a 20 hr and a 300 amp discharge at 0°F were run not only to measure the capacity of the batteries but to favor the dope by at least three careful and complete recharges at 80°F. Results are indicated in Table II.

The batteries were returned to the sulfation test where continued deterioration was clearly indicated. They were again removed and final data obtained as indicated in Table III. Capacity after open circuit stand was practically nil although the comparison distinctly favors the undoped battery. It is interesting to note that gravity loss did not indicate the true capacity loss at this point and that it actually favored the doped batteries. Full charge cold capacity likewise had been lost almost completely in the doped batteries—certainly it was not better than in the undoped one.

Final inspection of the elements indicated a slight but significant difference in the appearance of the negatives. Those in the doped batteries were hard, lacked good metallic luster, and the outside negatives were partially washed out. The positive plates also showed a similar slight difference in favor of the undoped battery, with less sulfate and better appearing active material. The positive plates of the doped batteries had not lost active material as was expected, probably explained by the fact that this was not a cycling test.

Conclusions

The proposed test results in a definite negative plate failure which duplicates in appearance and electrochemical characteristics that encountered in service. Test results are not complicated by the failure of other components of the battery as is often the case in other storage battery tests. The effect of the contributing factors, such as acid gravity, positive grid alloy, expander, and separators, is clearly indicated both singly and collectively. The test indicates very definitely that battery dopes do not prevent negative plate failure, i.e., sulfation, nor can they restore batteries in this condition. The combination of rubber insulation, 1.260 or lower acid gravity, 6% antimony lead positive grids, and minimum expander results in a battery with the least tendency to failure from sulfation.

Review of High Temperature Metal-Ceramic Seals[1]

Hayne Palmour, III[2]

Abstract

A technical review of the development of metal-ceramic seals is presented, with emphasis on methods devised for high temperature brazing of metals to low-loss technical ceramics for electronic applications. Basic mechanisms of metal-ceramic bonding are discussed briefly, as are the problems resulting from mis-match between thermal expansivities of metals and ceramics. Illustrations of feasible design types are shown, and comparative data on electrical and mechanical properties of various technical ceramics (including glass) are listed.

Today's demand for high temperature hermetically sealed metal-ceramic assemblies is an outgrowth of the constant push by the electronics industry toward higher operating frequencies and miniaturized components with resultant high power ratings and high temperatures for components and systems alike.

If we were to reduce the complex requirements of modern electronic design to extremely simple terms, we might come up with the idea that all circuits are composed of appropriately chosen conductors, semiconductors, and nonconductors, operating in suitable environments. In these simple terms, this paper shall be particularly concerned with the matter of effecting combinations of appropriate metal conductors and ceramic nonconductors to isolate and control an environment, like the atmosphere within a vacuum tube.

One of the earliest and most useful man-made nonconductors was glass, and the development of vacuum tight glass-to-metal seals near the end of the last century made the incandescent light a practical commodity; the same glass seals, with some refinements in materials and techniques, helped to launch the infant radio industry on its way with adequate vacuum tubes in glass envelopes.

But as the radio industry grew into an electronics industry and began to add words like "radar" and "microwave" to our common vocabulary, the usefulness of glass as a nonconductor dropped in more or less direct ratio to the frequencies and temperatures involved because of its inherent high dielectric losses at elevated temperatures and its poor heat shock resistance (Table I).

Fortunately, there is available a group of dense, essentially crystalline ceramics which demonstrate superior low-loss properties at high frequencies and high temperatures (Table I). In addition, these low-loss ceramics offer higher mechanical strength and generally better thermal shock behavior than can be expected from glass. While they do not always lend themselves to fabrication in the complex shapes which are possible with plastic molten glass, they are amenable to fabrication in a broad range of useful shapes to close dimensional tolerances. Consequently, these low-loss ceramics might be expected to solve many of the problems which have heretofore bedeviled the tube designer restricted to working with glass. Low-loss ceramic materials have not been limited to vacuum tubes alone, but have found wide use in many other electronic components.

For the low-loss ceramics to become useful in the full range of electronic applications, there must first be the counterpart of the glass-to-metal seal—a metal-to-ceramic seal to bond the conductor and nonconductor together into a mechanically strong, pressure-, vacuum-, or water-tight unit.

A metal-ceramic seal, or more precisely, a hermetically sealed metal-ceramic assembly, is composed of at least one metal unit, in conjunction with one or more ceramic units, or of several ceramic units sharing metallic bonding interfaces; the ceramic, the metal, and the bond areas must be impervious to the passage of liquids or gases. Obviously, the ceramic may function as a nonconductor, as a structural member, or as both. Likewise, the metal may be only a structural or bonding member, an electrical conductor, or both.

There are two general uses of metal-ceramic seals. One is in the production of ceramic envelopes and "windows" for electron tubes, and, because sealing in this case constitutes assembly, the sealing operation is generally accomplished by the tube manufacturer.

The second use is a broader one, where there is an increasing demand for ready-sealed metal-ceramic units, such as feed-through insulators for hermetic-sealed transformers, capacitors, and the like, which the manufacturer solders or brazes into his product.

It should be pointed out that metal-to-ceramic seals represents a special case of a more general, and much older matter—that of metal-to-ceramic bonding. The ceramic field is a very broad one, including glass, porcelain enameling, ordinary dinnerware, decorative pottery, and other inorganic, nonmetallic materials which are processed at high temperatures.

The ceramics which are of interest in electronics, usually called "technical ceramics," are among the most recent developments in a ceramic technology which extends back over a history of several thousand years. During a great part of that long history ceramic-to-metal bonding has played an important part in the aesthetic appeal and usefulness of ceramic materials.

Metal-to-ceramic bonds fall into three general categories, based in large part on the mechanism by which the required intimacy of contact at the ceramic-metal interface is obtained.

The first of these utilizes a molten ceramic wetting a relatively more refractory metal. Porcelain enamel on metal is of this type, and so are the glass bonded decorative metals applied to pottery and glass. Another application of this type of bond is found in the glass-to-metal seals commonly used in electronic work. Since this bond employs a molten or glassy ceramic phase, the finished unit displays many of the brittle properties of glass. Fairly low melting ceramic compositions are required, so the bond is generally restricted to low temperature operations.

The reverse situation is found in type two, where the metal provides the fluid phase to wet a relatively more refractory ceramic. Examples of this sort may be found in certain classes

[1] Manuscript received October 21, 1954. This paper was prepared for delivery before the Chicago Meeting, May 2 to 6, 1954.

[2] Research Department, American Lava Corporation, Chattanooga, Tennessee.

of cermets, and in the "hard solder" metal-to-ceramic seals which are of particular interest in this discussion.

The third type of bonding comes about in solid-state reactions. The intimacy of contact is provided mechanically by pressure, spraying, dipping, or painting, or granular mixing techniques, and solid-state reactions occur during firing at a temperature slightly below the melting point of either metal or ceramic. This reaction is typical of refractory cermets.

In each of these categories, a mechanism for obtaining intimate contact between the metal and ceramic components has been described. The actual nature of the bond, and the resultant bond strength, are dependent on more complex factors.

There can be a simple mechanical bond, deriving its strength from interlocking particles, or from penetration of the liquid phase into surface pores and grain boundaries at the refractory interface, or from van der Waals forces.

There can be a chemical bonding which depends on solvent action, transferring constituents from the solid phase into the liquid phase. In this case there is the possibility that new solid phases may form within the matrix to produce a crystalline bridging structure across the interface.

There may be a chemical bonding when an active metal constituent, either in a melt, or by solid-stage change, undergoes a valence shift toward a metalloid or nonmetallic state, progressing continuously from metal to suboxide to oxide across the interface, becoming finally an integral part of the refractory ceramic structure.

Certain metals, because of their atomic size and chemical properties, exhibit an affinity for chemical bonding with ceramics. They share the common property of relatively easy oxidation, yielding refractory oxides which are compatible with the oxides normally used in ceramic compositions. The active metals, titanium and zirconium from Group IV of the atomic chart; the transition metals, iron, cobalt, and nickel; chromium and molybdenum in Group VI; and manganese in Group VII are useful in this respect.

It is extremely difficult to observe directly or measure quantitatively conditions at a bond interface. Pincus (1) has described a tapered sectioning technique to produce a cross section of the bond having an apparent thickness 10 times greater than the width, as an aid to microscopic examination. Kingery (2) has reported on studies of the relationship between bond strength and interfacial contact angles, using a sessile drop of molten metal on a ceramic surface, where good bonding is always accompanied by very low contact angles.

The matter of thermal expansion is an essential consideration in any metal-to-ceramic bond. The expansion characteristics of metals and ceramics are inherently dissimilar, and where the bonding material is nonductile over a considerable temperature range, careful selection of metal and ceramic and proper design of the unit, to utilize high compressive strength of the ceramic rather than the much weaker tensile strength, determine whether or not the bond will be successful.

The mechanisms of bonding constitute a major field of investigation and study beyond the scope of this review. However, the subject is well covered in the literature, particularly under the heading of porcelain enamelling on metals, and in the field of cermets (3–5).

There are four basic techniques for developing metal bonds suitable for ceramic-to-metal seals. The first technique, that of using glass as a bond between metal and ceramic, fails to meet the most stringent requirements of high temperature, high-frequency electronic service. For this reason, and because the various methods are well understood and well covered in the literature, glass bonded seals will be excluded from this discussion.

TABLE I. *Comparative electrical and mechanical properties of glasses and ceramics*

	Soft glass	Hard glass	Alumina ceramic
Safe temperature at continuous heat	Below 450°C	Below 450°C	1100°C
Thermal shock resistance	Poor	Fair	Excellent
Tensile strength	Low	Low	Good
Compressive strength	Good	Good	Excellent
Te value	300°C	300°C	800°C
Power factor at 1 mc room temperature	0.0090	0.0040	0.0007
Dielectric constant	7.0	4.7	8.3

The remaining three are similar in that each technique utilizes one or more of the metals which exhibit an affinity for ceramic bonding as the "active ingredient," and in the fact that a reducing or inert atmosphere is necessary during firing to prevent excessive oxidation of the metal before it can seal with the ceramic. They are commonly known as the moly-manganese process, the titanium hydride process, and the active metals process.

The present day moly-manganese process is the outgrowth of the first successful high temperature seals, developed in Germany, near the beginning of World War II (6). The Telefunken process utilized an initial coating of molybdenum powder with admixtures of iron and nickel painted on a steatite ceramic, which was fired on in hydrogen atmosphere to develop a strong bond at a temperature near the softening point of the ceramic. There was little knitting of the moly particles with each other, so the initial layer was augmented with nickel powder painted on and fired in hydrogen to alloy with the moly and produce a bright metal surface which could subsequently be silver brazed. The final assembly of the metallized ceramic with metal parts which had also been nickel alloyed was made in hydrogen with silver solder. Telefunken produced acceptable radar tubes, but experienced considerable variations in the quality of bonding with the moly-iron-nickel mixture (7).

Nolte and Spurck (8) have since modified the process to utilize manganese rather than nickel and iron to promote bonding with the ceramic, and substituted electrodeposited nickel and copper in the alloying operation. The moly-manganese bond is less sensitive to slight process and kiln atmosphere variables than was the case with nickel-iron-moly used in the Telefunken process.

The moly-manganese process appears to have these advantages: strong bond; good reproducibility; and excellent dimensional control of metallized areas.

Disadvantages are: multistep process (3 firings); hydrogen firing tends to discolor ceramics and glazes and may impair electrical properties.

Bondley, in 1947, introduced the use of titanium hydride in conjunction with silver solder, copper, or silver (9). The area to be metallized is painted with titanium hydride; the ceramic and metal parts are assembled with silver solder wire in contact with the hydride area to provide the fill material. One firing in vacuum or inert atmosphere completes the seal, at a temperature just above the melting temperature of the solder. The hydride dissociates during the early stage of firing to leave a thin layer of finely divided active metal. The

TABLE II. *Mechanical and electrical properties of dense, low loss ceramics*

Property	Forsterite $2MgO \cdot SiO_2$	Alumina 85% Al_2O_3	Alumina 97% Al_2O_3
Specific gravity, g/cc.	2.8	3.4	Above 3.6
Safe temperature at continuous heat, °C	1000	1100	1500
Hardness, Mohs' scale	7.5	9.0	9.0
Coefficient of thermal expansion			
25°–100°C	9.1×10^{-6}	5.8×10^{-6}	5.0×10^{-6}
25°–700°C	10.6×10^{-6}	7.5×10^{-6}	7.8×10^{-6}
Tensile strength, psi	10,000	20,000	25,000
Compressive strength, psi	85,000	140,000	170,000
Heat shock resistance	Fair	Excellent	Excellent
Impact resistance, (Charpy)	4.0	6.3	8.2
Dielectric strength, v/mil	240	250	260
Dielectric constant, 1 mc	6.20	8.30	9.85
Power factor, 1 mc	0.0004	0.0007	0.0003
Loss factor, 1 mc	0.0020	0.0060	0.0029

hydrogen given off is credited with a beneficial cleaning action to further condition the metal and ceramic sealing surfaces.

Later work by Pearsall and Zingeser demonstrated the suitability of other hydrides, notably zirconium, and also showed that the active metals themselves produced comparable results (10)

We may list these advantages for the hydride technique: strong bond, excellent reproducibility; only one firing operation; vacuum or inert atmosphere rather than hydrogen; firing temperatures well below the softening point of the body; use with silver, copper, silver solder, lead and soft solders.

Disadvantages include: high fluidity of the solder at the alloying temperature, which may make dimensional control of the metallized area difficult; and application of the hydride involves hand work of considerable skill to achieve product uniformity.

Pearsall and Zingeser's work (10) opened up several new avenues of approach, which might be grouped together and called the active metal techniques.

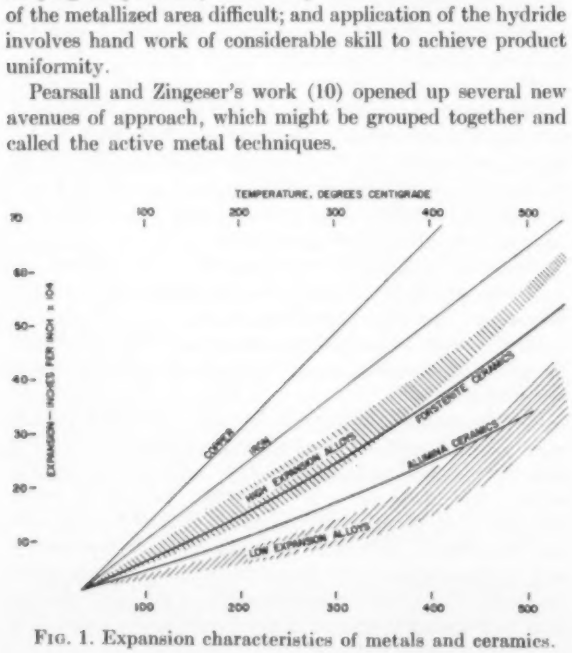

FIG. 1. Expansion characteristics of metals and ceramics.

Briefly, they found that active metals, particularly titanium and zirconium, could be used to produce excellent seals in the form of an alloy with silver, copper, or silver solder, or in powder form used much like the hydrides, or as a sandwiched thin layer between sheets of solder (7).

A titanium cored silver solder is now commercially produced in wire form, available with 3%, 5%, or 8% titanium (11). The cored wire, in preformed rings or other shapes, is assembled with the metal and ceramic, or with ceramics alone, and fired in vacuum or inert gases, such as helium and argon. The silver-copper eutectic solder melts at 760°C, and with further heating to 950°C, alloys with the titanium core and wets the ceramic and metal parts to effect the seal.

It is the simplest technique yet devised for metal-ceramic brazing, but there are several design limitations which are necessary to control the flow of the superheated solder.

It seems to be most applicable where the sealing zone is almost totally enclosed between matching parts of the assembly, where the length of the flow is relatively short, and where the final brazed zone is quite thin.

Advantages are: strong bond, excellent reproducibility with proper design configurations; simple mechanical assembly; and only one firing in vacuum, helium, or argon.

Disadvantages are: design limitations; and flow difficult to control.

There is some evidence that the titanium-cored wire technique may be improved by using high silver content solders, rather than the rapidly melting eutectic composition. With sterling silver, for example, the solder is plastic rather than fluid from 760° almost to the alloying temperature at 950°C, and does not tend to flow away from the titanium core. Consequently, alloying is more uniform, and the flow is more easily controlled.

The processes already described are most appropriate for direct assembly with formed metal parts. There are many applications where a bare metallized pattern on ceramics is desirable. Paintable powder mixes of silver solder with active metals may be used where a metallized band or other configurations to close dimensional tolerances are required on ceramics (12). Controlled flow, excellent wetting, and strong bonds have been obtained using eutectic silver solder with 8% titanium metal, suitably suspended and applied by brushing, and fired to about 850°C in vacuum. These metallized ceramics can be silver brazed in protective atmospheres. If precautions are taken to avoid heat shock, they may be brazed with a torch using a reducing flame.

There are certain other techniques which have promise, although there are certain inherent difficulties in processing which make them less attractive, at the present time, than the methods mentioned.

Knecht (12) has described a solid-state bonding of metal and ceramic powders formed under high pressures in layered zones, somewhat like powder metallurgy practice, and matured at elevated temperatures in protective atmospheres.

Strong bonds can be developed on alumina ceramics with vapor-deposited Inconel-copper films, which can then be silver brazed with fair success.[3] Processing offers real technical problems, including suitable means of masking, rotating the work, and controlling deposition rates, to achieve uniformly metallized areas, to close dimensions, on a great variety of sizes and shapes.

Selection of metals and ceramics for these high temperature seal applications is of great importance. As mentioned earlier,

[3] Author's experimental work.

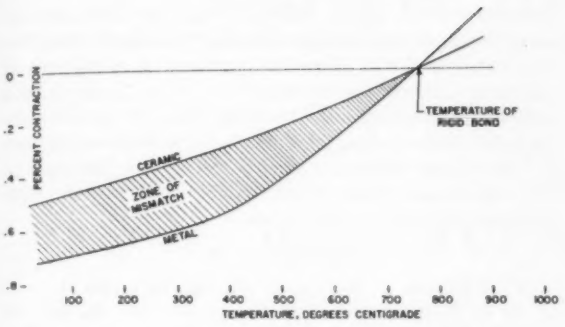

FIG. 2. Stresses on cooling below melting point of silver solder.

thermal expansion differences between metal and ceramic create the most difficult technical problems in sealing practice.

Three ceramic body types are most desirable from the standpoint of electrical and mechanical properties for use in high temperature seals. They are Forsterite, $2MgO \cdot SiO_2$; 85% alumina; and the 95–97% alumina bodies (Table II).

Forsterite has relatively high thermal expansion characteristics, making the choice of matching metals somewhat easier, but it is inferior to the alumina ceramics in mechanical strength and particularly in heat shock resistance. Low expansion metals of the Kovar type, nickel-cobalt-iron alloys, provide a fairly satisfactory match with the aluminas.

Metals for sealing purposes must first of all be adequately workable, and must possess reasonable electrical characteristics, but the thermal expansion characteristics are generally determining factors in selecting a suitable metal. Copper would be highly desirable, were its thermal expansion not so very much higher than any of the usable ceramics (Fig. 1).

The chrome-iron and nickel-iron alloys, and the nickel-cobalt-iron alloy developed for glass sealing cover a fairly wide expansion range between room temperature and the annealing point of glass at about 400°C, but above that temperature there is a sharp inflection toward much higher expansion rates. The conductivity of these sealing alloys is considerably lower than copper, which, in some cases, makes them unsatisfactory for the intended electrical use, or requires an excessively large wire size.

Fig. 2 illustrates the contraction experienced on cooling a seal between an alumina ceramic and the best available metal alloy.

The silver solder, which makes the seal, becomes rigid and nonductile at about 700°C above room temperature, and the

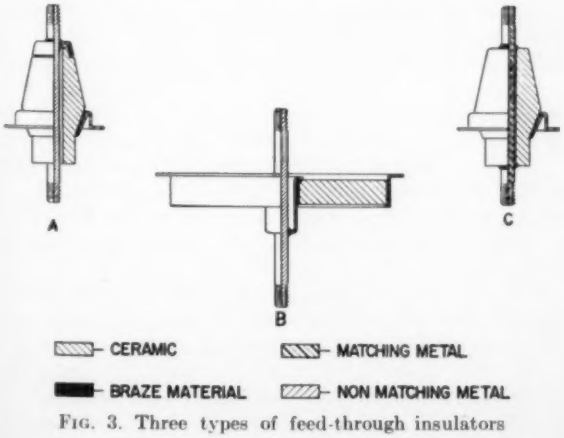

FIG. 3. Three types of feed-through insulators

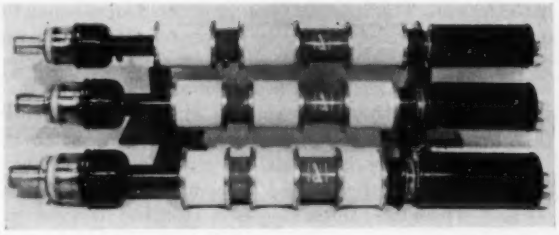

FIG. 4. Large metal-ceramic sealed klystrons

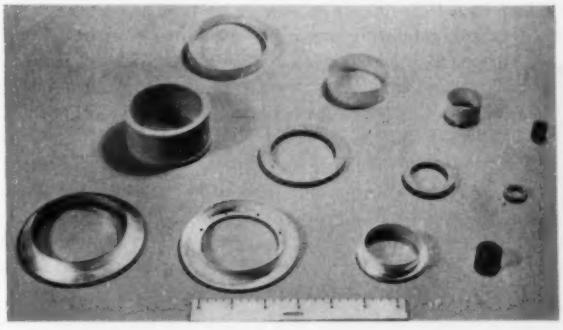

FIG. 5. Component metal and ceramic parts of experimental tetrode prior to assembly.

FIG. 6. (*left*) Assembled tetrode

FIG. 7. (*right*) High-frequency triode with metal-ceramic envelope.

mismatch in contraction rates, must result in stresses which under certain conditions may be disruptive. There are no metals available which really match ceramics in expansivity and careful design to achieve a safe distribution of stresses is required. Thus, the resolution of expansion mismatches is the chief aspect, the basic function, of the specialized design configurations which are employed in making high temperature seals.

From the mechanical standpoint, there are two distinctly different types of seals. The outside seal has a band of metal surrounding the ceramic, generally giving compressive stresses

in the ceramic. The inside seal has the ceramic surrounding the metal and gives rise to tensile stresses, usually considered dangerous.

Three types of feed-through insulators will serve to indicate the basic principles of design (Fig. 3). In the first example, (Fig. 3*a*), outside seals of matching or compatible metals are employed in both positions, and the center conductor, which may be nonmatching, is brazed to the upper cup to complete the seal. Where mechanical stresses or electrical requirements demand that the center conductor be completely sealed within the ceramic, a matching metal is mandatory, and the dimensional tolerances should insure a close fit to limit the solder to a thin film (Fig. 3*b*).

A tapered mounting ring is preferred over straight cylindrical shapes to avoid sudden discontinuities in the ceramic. The shape and thinness of the metal stock prevent excessive loading which might rupture the ceramic, particularly under thermal shock conditions.

The ceramic wafer (Fig. 3*c*) illustrates another condition where a nonmatching center conductor must be used, and the shape will not allow an outside seal. A thin walled cup of a matching metal is used, with the hope that the tensile stresses it transmits do not exceed the tensile strength of the ceramic.

By careful design, very intricate assemblies are now being commercially produced by several manufacturers.

High-frequency klystrons with low-loss ceramic envelopes and high temperature seals of the moly-manganese type are commercially produced as are various types of triodes and tetrodes for radar and other high frequency uses (Fig. 4, 5, 6, and 7).

Conclusion

The future for these seals is bright, and the demand for them is increasingly urgent. Those who are working with them wish hopefully that the expansion characteristics of available ceramics could be ideally matched over a broad temperature range with new metal alloys. Electronics designers should be acquainted with the particular problems of metal-ceramic sealing so that cooperative designing could aid in eliminating some of these problems. But the fact remains that, with existing metals and ceramics, there are enough techniques, methods and design strategems now available to produce high quality high temperature seals which should amply satisfy high-frequency electronic requirements.

REFERENCES

1. A. G. Pincus, *J. Am. Ceram. Soc.*, **36**, 152 (1953).
2. W. D. Kingery, *et al.*, *J. Am. Ceram. Soc.*, **36**, 363, 403 (1953); *ibid.*, **37**, 18, 42 (1954).
3. A. I. Andrews, "Enamels," Twin City Printing Co., Champaign, Ill. (1935).
4. J. A. Stavrolakis, *et al.*, WADC Technical Report 53-356, October (1953) (Armour Research Foundation, Illinois Institute of Technology).
5. "Proceedings of the WADC Ceramic Conference on Cermets, 6-8 October, 1952," WADC Technical Report 52-327. Restricted.
6. "German Centimeter & Decimeter Tubes," Intelligence Report (TUB-1) Office of the Theater, Chief Signal Officer, APO 887 (1945).
7. L. Navias, General Electric Research Laboratory Report RL-833, April (1953).
8. H. J. Nolte and R. F. Spurck, *Television Eng.*, **1**, 14 (1950).
9. R. J. Bondley, *Electronics*, **20** (7), 97 (1947); *Ceramic Age*, **58** (1), 15 (1951).
10. C. S. Pearsall and P. K. Zingeser, Technical Report #104, Research Laboratory of Electronics, Massachusetts Institute of Technology (1949).
11. H. Bender, *Ceramic Age*, **63** (4), 15, 46 (1954).
12. W. Knecht, Air Force Technical Report No. 6101, February (1950).
13. W. H. Kohl, "Materials Technology in Vacuum Tubes," Reinhold Publishing Co., New York (1951).

Current Affairs

Becco—ECS Sustaining Member

Fifty years ago the only way to produce hydrogen peroxide was to react barium peroxide with an acid. Rather dilute and somewhat unstable solutions of hydrogen peroxide were obtained in this way and used on a relatively small scale for the bleaching of wool, silk, hair, feathers, etc.

Forty-five years ago the first plant using an electrolytic process for hydrogen peroxide manufacture went into operation at Weissenstein in Austria, and during the next forty years or so this and related processes produced the bulk of hydrogen peroxide manufactured in the world.

Thirty years ago the Buffalo Electro-Chemical Company was founded in Buffalo by Mr. Charles A. Buerk, and in 1952 the company became part of the Food Machinery and Chemical Corporation and is now operated as Becco Chemical Division of that company.

From the beginning Becco has been one of the major producers of hydrogen peroxide in the U. S. A. The process depends upon electrolytic oxidation of a bisulfate solution, on platinum anodes, to yield a persulfate solution. This solution is subsequently hydrolyzed by heating in a vacuum still, so that hydrogen peroxide is formed and almost immediately distilled off. The basic reactions may be summarized as follows:

$$\left.\begin{array}{l} \longrightarrow \quad 2HSO_4 \quad \longrightarrow \quad S_2O_8 \quad + \quad H_2 \uparrow \\ S_2O_8 \quad + \quad 2H_2O \quad \longrightarrow \quad H_2O_2 \uparrow \quad + \quad 2HSO_4 \quad \longrightarrow \end{array}\right\}$$

The resulting hydrogen peroxide is then fed into Becco designed distillation equipment to concentrate the product to nearly any desired degree. Becco hydrogen peroxide is regularly marketed at concentrations up to 90%.

Although manufacturing methods have changed but little in principle over all these years, production capacity has risen to very high levels, as new uses for hydrogen peroxide were discovered and the markets for established uses expanded.

World production capacity in 1950 was an estimated 20,000 tons 100% hydrogen peroxide, half of which was produced in the United States.

By 1955 U. S. yearly production will have reached the impressive total of about 20,000 tons hydrogen peroxide 100%, equalling estimated world production in 1950.

About 60% of the total hydrogen peroxide produced in 1951 was used by the textile industry, essentially for bleaching purposes. Assuming an average consumption of about ½ lb of 100% hydrogen peroxide for every 100 lb of textile goods bleached, we see that well over 20,000,000 lb of assorted textile goods were treated in one way or another with hydrogen peroxide, and that's an awful lot of shirts, sheets, towels, and hankies.

Of course, the textile industry is by no means the only important consumer of hydrogen peroxide. The bleaching of wood pulp and particularly of groundwood pulp is beginning to absorb substantial quantities of hydrogen peroxide. In recent years its use has also substantially increased in the manufacture of synthetic organic chemicals, largely due to the development of commercially useful epoxidation and hydroxylation reactions.

An electrolytic cell room in one of Becco's hydrogen peroxide plants.

Although hydrogen peroxide is Becco's main product, there are other important peroxygen compounds on the manufacturing program. Persulfates, for instance, are well established in polymerization techniques for the production of synthetic rubber and find many other uses. Peracetic acid produced from highly concentrated hydrogen peroxide and acetic acid is an extremely useful oxidizing agent widely applied to epoxidation and hydroxylation reactions in the manufacture of a number of important insecticides and other organic synthetic chemicals. Sodium perborate, another Becco product, is consumed in large quantities by the textile industry in the development of dyes and is an important ingredient in powder bleaches for home laundry use. Zinc peroxide finds use in the pharmaceutical industry and a related product, calcium peroxide, is well established as a dough conditioning agent.

The steady growth in production and sales of Becco's peroxygen compounds is a reflection of the forward looking spirit of management, engineering, and research groups of the company. Production procedures have been constantly improved over the years to their present high level of efficiency and applications, unknown not too many years ago, investigated and developed by the staff of the Research Department. Today well over 60 qualified men in the Research and Engineering Departments continue to work on improving existing, and developing further, uses for the company's products and manufacturing processes.

Pittsburgh Meeting, October 9 to 13, 1955

© PITTSBURGH CHAMBER OF COMMERCE

Artist's conception of the completed Point Park, Pittsburgh

The Fall Meeting of the Society will be held October 9 to 13 in Pittsburgh, Pa., at the William Penn Hotel, near the point.

More than one electrochemist will be coming to Pittsburgh this fall for the first time since the 1943 meeting of The Electrochemical Society. He will hardly recognize the place. Basically, it is still a steel city—its output is greater than the entire production of England or Germany. But, instead of the old corroded topography, he will see a brightened exterior in a highly purified atmosphere. Over 98% of the heavy-smog days have succumbed to smoke control. If he arrives by plane, he will find that the new Pittsburgh airport is like a little city, complete with hotel and movie. Multilane parkways replace the old hilly roads and speed traffic to the "point." There he will find that many of the old buildings have disappeared, being replaced by a large park fringed with stainless steel skyscrapers.

Employment Posters for Pittsburgh Meeting

Companies which desire to recruit employees at the Pittsburgh Meeting, October 9 to 13, 1955, are invited to prepare posters (not to exceed 8½ in. × 11 in.) to be placed on a bulletin board near the registration desk.

Company representatives can contact Mr. Robert A. Woofter, Registration Chairman, during the meeting to make arrangements for posters to be displayed.

Technical Program

The following Divisions have planned technical sessions: Battery, Corrosion, Electrodeposition, Electro-Organic, and Electrothermics and Metallurgy.

Palladium Medal

On Tuesday, October 11, the Palladium Medal address will be given by Dr. Ulick R. Evans, Cambridge University, England. Dr. Evans is well known in this country through his important contributions to electrochemical corrosion.

Other Activities

Pittsburgh, a focus of industrial production and development, offers too much to see during one short visit. Realizing this, the convention planners have made a careful selection of plant trips, both for the men and ladies.

According to Paul Fugassi, General Chairman of the Convention, considerable effort is being expended to make the Pittsburgh Meeting one that will be long remembered. Co-workers in this task are the following members of the Pittsburgh Section: E. K. Camp, arrangements; F. L. Jones and J. S. McKay, entertainment; E. A. Gulbransen, finance; M. T. Simnad, membership; D. S. McKinney, plant trips; S. Barnartt, publicity; and R. A. Woofter, registration. John C. Warner, President of Carnegie Institute of Technology and Past President of the Society, is Honorary Chairman.

A Ladies' Program that promises to be a real social success is being organized by Mrs. R. A. Woofter.

Further details will appear in the August issue of the JOURNAL.

Mr. Holian Resigns

William J. Holian resigned as Assistant Secretary of the Society, effective July 1, because of ill health and the rigors of commuting from his home in Springdale, Conn., to New York. Mr. Holian joined the staff of the Society in September 1948 and is known to many members who met him at semiannual meetings of the Society.

Pittsburgh Program Booklet Not to be Mailed Separately

For the Pittsburgh Meeting, separate Program Booklets *will not* be mailed to members of the Society. For this meeting complete information, which in the past has appeared only in the Program Booklet, will be included in the September issue of the JOURNAL. In other words, the September JOURNAL will carry General Information, Technical Program, and Abstracts. Reprints from the JOURNAL will be available at the Pittsburgh Meeting in the former Program Booklet size.

Annual Report of the Board of Directors for 1954

During the year 1954, the following awards were made:

Acheson Award—George W. Heise.

Young Author's Prize—J. Halpern, Dept. of Mining and Metallurgy, University of British Columbia, Vancouver, B. C., Canada, for his paper: "Kinetics of the Dissolution of Copper in Aqueous Ammonia."

Honorable mention—R. A. Powers and J. C. Griess, Jr.

Francis Mills Turner Memorial Award, Sponsored by the Reinhold Publishing Corporation—Robert B. Holden, Chemistry Section, Sylvania Electric Products Inc., Atomic Energy Division, Bayside, N. Y., for his paper: "The Hot-Wire Process for Zirconium."

Prize Essay Contest—First prize—Ralph J. Brodd, 2709 Hemphill Park, Austin, Texas. Second prize—A. C. Makrides, Dept. of Chemistry, University of Texas, Austin, Texas. Honorable mention—Francis van Hecke, 183 Avenue de Tervueren, Brussels, Belgium; and William E. Tragert, Research Laboratory, General Electric Company, Schenectady, N. Y.

As a result of the success of the Ten-Year Index, for the period 1942–1952, the Board of Directors authorized the publication of the Index for the years 1952–1962. This publication will be underwritten by the Publication Reserve, a fund to which the profits of the 1942–1952 Index were directed.

During 1954, an ABC rating was obtained for our JOURNAL.

During this past year, there was a change in the allocation of interests of Divisions. The Rare Metals group of the Electronics Division was incorporated with the old Electrothermics Division, along with the change in name of that Division to "The Electrothermics and Metallurgy Division."

Also, during this past year, a new Constitution was approved and put into operation, and a very active committee was working on the revision of the Bylaws. These were to be approved, however, early in 1955. The revision of the Bylaws was necessary as a result of changes in the Constitution.

Two promotions of note should be recorded: Miss Natalie Michalski, an employee of seven years' standing, was advanced to the title of Assistant Editor, and Miss Anne Zino was promoted to Assistant Business Manager. This latter promotion was also recorded in the Report of the Secretary.

The Board approved Social Security for the office staff.

Also, a very notable event, namely, the formation of a new Section, was consummated. This is the Ontario-Quebec Section, which now contains a total of 53 members. This Section is a very active group, and is holding some very interesting and informative meetings. The latest one was announced in a flyer just received describing a session on titanium.

Annual Report of the Secretary for 1954

During the year of 1954, the Secretary's Office suffered the partial loss of services of our highly esteemed Assistant Secretary, Mr. William J. Holian. He did, however, recover sufficiently by the end of the year to make it possible for him to return to the office part time. The affairs of the Society, however, did not suffer materially due to the wonderful cooperation of the staff, and, in particular, Miss Anne Zino who should be complimented on the wonderful job that she has done in stepping into and carrying on the work for which Mr. Holian had previously been responsible.

During this last year, all arrangements were completed so that as of January 1 the wrappers were addressed from the plates in the Secretary's Office. This was a major undertaking since the Addressograph plates now must be maintained in a geographic rather than alphabetic listing. However, the system is working in a very satisfactory manner, resulting in considerable saving to the Society. At the same time, the Secretary's Office now, for the first time, can maintain an accurate count on JOURNALS mailed. For those not so close to the business affairs of the Society it should be pointed out that, ever since Waverly Press has been doing our printing, all publications have been addressed from Addressograph listings maintained in Baltimore. The Society, therefore, has had duplicate Addressograph listings. This has amounted to increasing our costs by approximately $40.00 a month.

The Annual Report of the Secretary, in the past, has always contained a membership count. This has been necessary due to the fact that these figures have been published only in the Secretary's Report. That practice will be discontinued as of this report, since every three months a complete listing of membership by class, Section, and Division is now published in the JOURNAL.

Report of Tellers of Election

For President: H. H. Uhlig, 793; 8 write-ins; 34 abstentions

For Vice-President: Sherlock Swann, Jr., 309; W. C. Gardiner, 298; F. A. Lowenheim, 220; 4 write-ins; 4 abstentions

For Treasurer: L. I. Gilbertson, 802; 1 write-in; 31 abstentions

Sixteen ballots were declared invalid for the following reasons: 12 ballots had more than one candidate marked for the same office; 4 ballots were completely blank.

The ballot tabulations have been placed in a sealed envelope in the charge of the Office Manager at The Electrochemical Society office.

(Signed) ATTILIO BISIO, *Chairman*
PAUL E. GRUBB
HENRY T. WOLLMAN

The Tellers' Report was unanimously accepted and a motion was made declaring the candidates, H. H. Uhlig (President), Sherlock Swann, Jr. (Vice-President), and L. I. Gilbertson (Treasurer), duly elected.

HENRY B. LINFORD, *Secretary*

Treasurer's Report for 1954

Edward Goodrich Acheson Fund

Capital Funds Securities—1/1/55

$5,000	USA 3¼% Treasury Bonds of 1978/83, due 6/15/83
$2,000	Pennsylvania Railroad Co. 3⅛% General Mortgage Series F, due 1/1/85
$2,000	American Telephone and Telegraph Co. 2¾% Debenture Bond, due 10/1/75
52 shares	American Can Co. 7% Cum. Pfd.
14 shares	Corn Products Refining Co. 7% Cum. Pfd.
10 shares	Eastman Kodak Co. 6% Cum. Pfd.
10 shares	Ingersoll-Rand Co. 6% Cum. Pfd.
25 shares	International Harvester Co. 7% Cum. Pfd.
20 shares	National Lead Co. Class A 7% Cum. Pfd.
28 shares	Pacific Gas and Electric Co. 6% Cum. 1st Pfd.

$10,000 Cash in Guaranty Trust; in Process of Investment

GUARANTY TRUST COMPANY OF NEW YORK, Custodian
Fifth Ave. at 44th St., New York 18, N. Y.

Guaranty Trust Co., Custodian

Acheson Fund Total Income Balance 1/1/55		
Income Balance 1/1/55 (incl. Prin. Fds. of $97.43).		$1,713.08
Credit: Dividends and interest on stocks and bonds		1,310.66
USA 2½% Savings Bonds matured 11/1/54		10,000.00
Transfer from East River Savings Bank		755.01
		$13,778.75
Debit: Custodian charges	$66.00	
Honorarium to G. W. Heise	1,000.00	
Medallic Art Co.	401.95	
Medallist expenses	177.39	
Purchase 28 shares Pac. Gas & Elec.	1,050.09	2,695.43
Income Balance 1/1/55 (incl. Prin. Fds. $10,000)		$11,083.32

East River Savings Bank, Amsterdam Ave. at 96th St., New York, N. Y.

Principal Funds Balance, 1/1/54	$755.01
Transferred to Guaranty Trust Co. Feb. 1954	755.01
	$000.00

Edward Weston Fellowship Fund for 1955

The Hanover Bank, Trustees

Capital Funds Securities, 1/1/55
1160 Units—Hanover Bank Co., Common Trust Fund A, value Jan. 1, 1955—$13,548.33
$1,817.66—AC 1330 Brook Ave., Bronx, N. Y., N.Y.T. & M. Co., allowed claims
1—Prudence 422, 34 East 86th St., New York, N. Y., Mortgage Certificate

Principal Account Balance 1/1/55	$72.51	
Checking Account Balance 1/1/54		$401.36
Credit: Deposit from Income Account 9/15/54		395.55
Checking Account Balance 1/1/55		$796.91
Income Account Balance 1/1/54		103.41
Credit: Dividends from H.B., C.T. Fd. A for 1954		418.76
		$522.17
Debit: Trustees charges for 1954	$20.82	
Transfer to checking account 9/10/54	395.55	416.37
Income Account Balance 1/1/55		$105.80
The Hanover Bank Balance for Fellowship 1/1/55		$902.71

THE HANOVER BANK, Trustees
70 Broadway, New York 15, N. Y.

Consolidated Fellowship Fund for 1954

Capital Funds Securities

Wellington Fund, Inc.
The Corporation Trust Co., Agent
120 Broadway, New York 5, N. Y.

Total number of shares 1/1/54	331.156	
Credit: Dividend shares	21.204	
Total number of shares 1/1/55	352.360	
Net asset values 1/1/55 at $24.60 per share		$8,668.06

Fundamental Investors, Inc.

City Bank Farmers Trust Company, Agent
22 William St., New York 15, N. Y.

Total number of shares 1/1/54	326.429	
Stock split 2 for 1, 9/30/54	652.858	
Credit: Dividend shares	24.449	
Capital gain shares	24.354	48.803
Total number of shares	701.661	
Net Asset Value 1/1/55 at $13.49 per share		$9,465.07
Total Value of Fund Securities 1/1/55		$18,155.08

Corrosion Handbook Fund for 1954

Total Corrosion Handbook Fund 1/1/54		$14,920.60
1/1/55		$16,501.19

Corn Exchange Bank
102nd St. and Broadway
New York, N. Y.

USA Savings Bonds Series F (earmarked in safe deposit box)	$10,471.37

New York Savings Bank
8th Ave. and 14th St.
New York, N. Y.

Bank Balance 1/1/54		$4,449.23
Credit: Interest for 1954	$138.20	
Royalties for 1954	1767.39	1,905.59
		$6,354.82
Debit: Prizes, Travel Expenses, Journal subscriptions, etc.		325.00
Bank Balance 1/1/55		$6,029.82
Total Handbook Fund 1/1/55		$16,501.19

Joseph W. Richards Memorial Fund

Central Savings Bank
Broadway at 73rd St.
New York, N. Y.

Bank Balance 1/1/54	$749.41
Credit: Interest for 1954	20.31
Bank Balance 1/1/55	$769.72

Columbus Convention Fund

Corn Exchange Bank
102nd St. and Broadway
New York, N. Y.

USA Gov't Bonds Series F (earmarked in safe deposit box)	$400.00

(Signed) E. G. WIDELL, *Treasurer*

Auditor's Report

BALANCE SHEET
December 31, 1954

Assets

Furniture and Office Equipment	$4,685.31	
Cash	27,558.19	(A)
U. S. Savings Bonds (Cost)	28,860.00	(B)
Inventory—Bound Volumes	2,682.96	
Accrued Income on Investments	7,315.00	
Guarantee Deposits	420.00	
	$71,521.46	

Liabilities, Reserves, and Surplus

Accounts Payable—Suppliers	$3,182.56
Taxes Withheld from Salaries	653.90
Life Memberships	1,299.16
Prepaid Sustaining Memberships	1,100.00

Prepaid Subscriptions	9,374.70
Reserve for Depreciation	1,072.38
Deferred Income (India Section)	18.46
Surplus	54,820.30
	$71,521.46

(A) Includes:

General Funds	
National City Bank	$14,077.85
Chemical Corn Exchange Bank	2,656.23
Petty Cash	44.78
	16,778.86
Corrosion Handbook Fund	
New York Savings Bank	5,922.20
Publication Reserve Fund	
National City Bank	3,743.67
Electrodeposition Division	
National City Bank	1,113.46
	$27,558.19

(B) Includes:

General Funds	$17,988.63
Corrosion Division Fund	10,471.37
Columbus Convention Fund	400.00
	$28,860.00

Cash Statement

January 1 to December 31, 1954

National City Bank		
Book balance December 31, 1953		$12,886.00
Receipts—1954 (Gross)	$98,059.34	
Disbursements—1954 (Gross)	92,010.36	
Excess receipts over disbursements		6,048.98
Book balance December 31, 1954		18,934.98
New York Savings Bank		
Book balance December 31, 1953		4,970.67
Interest 1954		64.86
Transferred from National City Bank		886.67
Book balance December 31, 1954		5,922.20
Chemical Corn Exchange Bank		
Book balance December 31, 1953		1,718.55
Receipts—1954 (Gross)	49,493.26	
Disbursements—1954 (Gross)	49,005.58	
Excess receipts over disbursements		937.68
Book balance December 31, 1954		2,656.23
Cash on hand—Agent—December 31, 1954		44.78
Total		$27,558.19
Total accounted for as follows:		
National City Bank per bank statement	23,233.23	
Less outstanding checks	4,298.25	18,934.98
New York Savings Bank per bank statement		5,922.20
Chemical Corn Exchange Bank per bank statement	1,475.27	
Less outstanding checks	819.04	656.23
Deposit in transit		2,000.00
Cash on hand—Agent		44.78
Total, as above		$27,558.19

Analysis of Expenditures

January 1 to December 31, 1954

Furniture and Office Equipment		$234.78
Publication Expenses		
Journal	$27,730.98	
Reprints	2,491.28	30,222.26
General Expenses		
Salaries, full-time employees	33,813.94	
Wages, part-time employees	869.00	
Rent	2,400.00	
Stationery and supplies	1,559.42	
Postage and express	1,541.46	
Miscellaneous office expenses	2,815.45	
Audit	175.00	
Prizes	100.00	
Local Sections:		
Philadelphia	135.50	
Cleveland	136.00	
Midland	52.00	
India	75.00	
Wash.-Baltimore	50.00	
Pacific No. West	50.00	
N. Y. Metropolitan	200.00	
Publication Committee	230.66	
Corrosion Division	289.00	
Conventions	3,518.57	
Emblems	46.70	
Advertising	386.18	
Sale of Publications	36.00	
Federal Insurance Contr. Tax	91.54	
Advertising Agent	5,199.96	
10-Year Index	1,559.81	
Audit Bureau of Circulation	798.08	
Volume 100 (binding and mailing)	915.71	
Monograph on Electro-Organic Chemistry Bibliography	500.00	
National Academy of Sciences	3.00	57,547.98
		$88,005.02

Analysis of Income

January 1 to December 31, 1954

Dues:	
1953	$60.00
1954	10,585.90
1955	18,885.60
Volumes:	
1952	479.73
1954	535.50
1955	1,404.00
Publications	277.79
Nonmember subscriptions—Journal	22,488.20
Advertising	16,903.01
Conventions	4,170.20
Preprints	15.45
Reprints	2,773.35
Emblems	148.00
Thompson Monograph	19.50
Membership Directory	26.00
Sustaining Memberships	10,300.00
Bank interest	64.86
Cathodic Protection	374.65
10-Year Index	1,342.60
Modern Electroplating	2,858.64
Journal	458.65
Corrosion Division	1,767.39
Consolidated Fellowship Fund	12.00
	$95,951.11
Excess income over expenditures	7,946.09

Accounted for as follows:	
Surplus (increase)	$8,180.87
Less: Furniture and office equipment	234.78
	$7,946.09

ANALYSIS OF INVESTMENT IN U. S. SAVINGS BONDS
December 31, 1954

Date of Issue	*Serial No.*	*Face Value*	*Cost*	*Value 12/31/54*
Oct. 1943	M-673354-F	$1,000	$740	$945
Oct. 1943	M-673355-F	1,000	740	945
Oct. 1943	M-673356-F	1,000	740	945
Oct. 1943	M-673532-F	1,000	740	945
Oct. 1943	M-673533-F	1,000	740	945
Oct. 1943	M-673534-F	1,000	740	945
March 1944	M-749592-F	1,000	740	945
March 1944	M-749593-F	1,000	740	945
March 1944	M-749594-F	1,000	740	945
March 1944	M-749595-F	1,000	740	945
March 1944	M-749605-F	1,000	740	945
March 1944	M-749606-F	1,000	740	945
March 1944	M-749607-F	1,000	740	945
March 1944	M-749608-F	1,000	740	945
June 1944	V-54568-F	5,000	3,700	4,725
Dec. 1944	V-58025-F	5,000	3,700	4,645
May 1945	X-62428-F	10,000	7,400	9,140
Jan. 1946	M-1059303-F	1,000	740	887
Jan. 1946	M-1059304-F	1,000	740	887
Jan. 1946	M-1059305-F	1,000	740	887
Jan. 1946	M-1059306-F	1,000	740	887
Jan. 1946	M-1059307-F	1,000	740	887
Total		$39,000	$28,860	$36,175

(Signed) H. K. LEICHT, *Auditor*

Candidates Nominated for Society Offices, 1956

The Nominating Committee, appointed by President H. H. Uhlig, having met at Cincinnati, Ohio, during the 107th Meeting of The Electrochemical Society, presents the following list of candidates for office for the term 1956–1957:

For President—
Hans Thurnauer

For Third Vice-President—
W. C. Gardiner
John Musgrave
Eugene Willihnganz

These candidates have been notified, and each has expressed his willingness to run for office and to serve if elected.

The two other Vice-Presidents, Norman Hackerman and Sherlock Swann, Jr., since they were elected for a three-year term, will automatically become first and second Vice-President, respectively.

The above slate will be voted on in the fall ballot-by-mail election—the successful candidates to assume office in the spring of 1956. This report was submitted by Charles Faust, Ernest Yeager, Ivor Campbell, and R. M. Hunter, Chairman.

DIVISION NEWS

Electric Insulation Division

Dr. C. Frank Miller, Chairman of the Electric Insulation Division, presided over an informal meeting on Sunday, May 1. The past, present, and future of the Division were critically reviewed, resulting in the appointment of committees covering the important areas of interest in electric insulation and dielectrics in an effort to make the program of the Division more effective.

At the annual Division luncheon and business meeting, the following officers were elected:

Chairman—L. L. Deer
Vice-Chairman—D. A. Lupfer
Secretary-Treasurer—L. J. Frisco

Dr. Andrew Gemant, the guest of honor,, presented a brief address of philosophical and historical interest.

The Division program consisted of 28 papers and one round-table discussion. All six sessions were well attended and particular interest was shown in the subjects of radiation, electrophysics, new materials, and capacitors.

Plans have been made to present a program of at least four sessions at the 109th Meeting of the Society in San Francisco in 1956.

L. J. FRISCO,
Secretary-Treasurer

Electronics Division

The annual business meeting of the Electronics Division was held in Cincinnati on May 4. The Chairman reported on the activities of the Division as follows:

"The Electronics Division is presenting four symposia at the Cincinnati Meeting. A total of 73 papers cover the fields of (*a*) Luminescence, (*b*) Oxide Cathodes, (*c*) Phosphor Application, (*d*) Semiconductors.

"The Semiconductor symposium continues to show healthy growth. The symposium on Phosphors and Screen Application is also maintaining a healthy position. The new effort in the field of Oxide Cathodes has shown remarkable response.

"This past year has seen the final steps taken to make the Semiconductor Group a separate activity with its own chairman. This will again give the Electronics Division three separate sections, the Semiconductor Group having taken the place of the Rare Metals Group.

"Once again a booklet of enlarged abstracts has been published. The price has been maintained at $2.00 per copy and for the first time the Division will stand a loss. We have experimented with having the typing and setup done entirely by Edwards Brothers, relieving the various chairmen of this burden. It is believed that to offset this added cost a slight increase in the charge of the booklet should be made during the next year. However, the monies made from the abstract booklets in the past have again permitted us an assessment-free year. This booklet continues to grow in popularity and the 500 copies ordered this year were completely sold out before the end of the meeting in Cincinnati. A re-run of 100 copies has been ordered to fill the unsatisfied demand.

"Our Division membership, as of 3/1/55, stands at 357, an increase of only 15 from the previous year. With our increased activities, a further growth is to be expected.

"At the conclusion of the Chicago meeting in 1954, it was decided that the Electronics Division would investigate the possibility of assuming the publication of a Digest of Semiconductors and Luminescent Materials literature. This would be taken over from the National Conference on Electronics, which had previously published such a work.

"Battelle Memorial Institute also had published such a Digest, and it was felt that if some suitable arrangements could be made between these groups a single expanded work could be pub-

lished which would be of benefit to all workers in these fields.

"The Board of Directors of The Electrochemical Society agreed to sponsor such a publication in the name of the Society under the auspices of the Management and Editorial Committee designated by the Electronics Division.

"Battelle Memorial Institute agreed to continue to compile such a Digest and graciously consented to donate their efforts for a limited number of complimentary copies. A working arrangement between the Management Committee and Battelle Memorial Institute has been effected. John Wiley and Sons undertook the actual publication of the booklet."

Symposia planned for next year include: Luminescence, Semiconductors, Oxide Cathodes, and Instrumentation.

The new officers of the Division elected at the business meeting are:

Chairman—C. W. Jerome

Vice-Chairman (Luminescence)—J. H. Schulman

Vice-Chairman (General Electronics)—Channing Dichter

Vice-Chairman (Semiconductors)—F. J. Biondi

Secretary-Treasurer (3-year term)—M. F. Quaely

The fiscal year of the Division continues until May 31. Since the results of this year's sale of abstract booklets are not yet complete, the financial report given below does not include data of those transactions:

Balance on hand 5/11/54...	$444.66
Net profit from 1954 booklet	419.73
Interest on bank balance...	21.60
Total Assets.....	$885.99
Total paid out.....	52.00
Balance carried forward	$833.99

CHARLES W. JEROME, *Secretary-Treasurer*

Semiconductor Group Electronics Division

The newly organized Semiconductor Group of the Electronics Division of the Society held a group luncheon meeting on May 5 at the Sheraton-Gibson Hotel in Cincinnati with approximately 63 persons in attendance. Mr. F. J. Biondi, newly elected Vice-Chairman (Semiconductors), presided.

Announcement was made that Mr. J. W. Faust, Jr., of the Westinghouse Electric Corporation, has taken on the responsibility for organizing the Semiconductor Symposium for the May 1956 meeting.

It was further the consensus of the group that this rapidly moving field would best be served by having two symposia a year, rather than one, and that the time interval involved with abstracts, etc., be shortened. The Chairman of the group and Mr. Faust will survey interest in having a symposium at the October Pittsburgh Meeting. If an October Semiconductor session is organized the timing is such that extended abstracts will not be made up and the bulk of the papers may well be of the "recent news" type. Those who wish to participate should contact Mr. F. J. Biondi, Bell Telephone Laboratories, Inc., Murray Hill, N.J., or Mr. J. W. Faust, Westinghouse Electric Corporation, East Pittsburgh, Pa., as soon as possible.

F. J. BIONDI, *Vice-Chairman*
Semiconductor Group

Electrothermics and Metallurgy Division

The Electrothermics and Metallurgy Division's luncheon and annual business meeting were held on Wednesday, May 4, at the Sheraton-Gibson Hotel, headquarters for the Society's Spring Meeting in Cincinnati.

After the luncheon, Dr. I. E. Campbell, retiring Division Chairman, reviewed the activities and accomplishments of the Division during the past two years. Symposia were held at every meeting of the Society. The session on "Vacuum Metallurgy," held at the Boston Meeting, was perhaps the most successful, contributing substantially to the large attendance at that meeting. A printed record of the papers presented at that session was made available to members of the Society at a price of $4.00. Dr. John M. Blocher, Jr., organized the session and, with the cooperation of the authors, was primarily responsible for the early appearance of this publication. Copies of this volume are available from the Society.

A more active program in "classical" electrothermics was developed during the past two years, largely through the efforts of A. C. Haskell, Jr., with the excellent help of Mr. Marvin Udy, President of the Society.

Continuing his remarks, Dr. Campbell pointed out that consolidation of the former Electrothermics Division and the Rare Metals group of the Electronics Division had been effected, the new name for the Division becoming "Electrothermics and Metallurgy." The Bylaws of the Division were amended to conform with this consolidation as well as with the recently revised Constitution of the Society. The Beckett Memorial Award was established to stimulate student interest in electrothermics.

Two additions were made to the list of Society Monographs. One of these, a book titled "Vapor-Plating," is now available from John Wiley and Sons. The other, "High Temperature Technology (Materials, Methods, and Measurements)," should be available from the same publisher, either in December 1955, or January 1956.

The resignation of Jack Dewar, from both the Division and the Society, was reported with regret. The Secretary was instructed, by Division vote, to draft a letter of appreciation to Jack for his outstanding service to the Society and the Division, in particular, for his management of the Montreal Meeting of the Society.

Dr. Campbell extended his appreciation to the chairmen of the various symposia for their active efforts in securing papers and organizing meetings.

This portion of the meeting was concluded with a standing ovation for Mr. Udy and his fine work for the Society during the past year.

There being no old or new business, election of Division Officers was held. Dr. B. W. Gonser, Chairman of the Nominating Committee, which consisted of A. T. Hinckley, C. P. Zergiebel, and himself, presented the following slate of candicates, for which a unanimous vote was cast:

Chairman—A. C. Haskell, Jr., Titanium Alloy Manufacturing Div., National Lead Co.

Vice-Chairman—A. U. Seybolt, General Electric Co.

Vice-Chairman—G. M. Butler, Carborundum Co.

Secretary-Treasurer—E. M. Sherwood, Battelle Memorial Institute

Members-at-Large—G. Steven, Armour Institute of Technology; M. J. Udy, Consultant; J. H. Westbrook, General Electric Co.; J. C. McMullen, Carborundum Co.

The newly elected Chairman, Mr. Haskell, conducted the remainder of the meeting. He paid tribute to Dr. Campbell for his excellent conduct of the business of the Division during his term of office, stressing the teamwork of all concerned.

Plans for future meetings then were discussed. A symposium on "Fluidized-Bed Roasting" is being organized by Dr. Toemé of the National Lead Company for the 1955 Fall Meeting at

Pittsburgh. Also for the Pittsburgh Meeting, in cooperation with the Electrodeposition Division, a symposium on "High Temperature Protective Coatings" is being organized by Dr. Cloyd Snavely, immediate Past-Chairman of the Electrodeposition Division, and Dr. E. M. Sherwood, both of the Battelle Memorial Institute. "The Electric Arc in Vacuum or Inert Atmospheres" will be discussed at the San Francisco 1956 Spring Meeting and, for the 1956 Fall Meeting in Cleveland, "Physical, Chemical, and Thermal Properties of Slags of the Electric Arc Furnace" has been selected as the symposium subject. Those who wish to present papers at these symposia are urged to so inform the Secretary of the Electrothermics and Metallurgy Division.

The meeting was then closed.

E. M. SHERWOOD,
Secretary-Treasurer

Vacuum Metallurgy Book Available

Papers presented at the Vacuum Metallurgy Symposium, October 6 and 7, 1954, in Boston are now available in book form.

Sponsored by the Electrothermics and Metallurgy Division of the Society this symposium brought together, for the first time, those interested in the relation of vacuum to metallurgy.

In the keynote address, J. D. Nisbet, Director of Research of the Universal-Cyclops Steel Corporation, outlines the rapid progress in this field, together with a consideration of what the future may hold. Eighteen papers follow on vacuum melting, vacuum heat treating, vacuum distillation of metals, and on new apparatus. A valuable review of the present status of theory and techniques for the determination of the vapor pressures of metals and alloys is included.

Copies of this 216-page book in hard paper binding may be obtained from Society Headquarters, 216 West 102nd St., New York 25, N. Y., The cost is $5.00, less a 20% discount to Society members.

Theoretical Electrochemistry Division

At the business meeting of the Theoretical Division held during the Cincinnati Meeting of the Society in May, the following officers were elected:

Chairman—E. B. Yeager, Western Reserve University, Cleveland, Ohio

Vice-Chairman—Paul Delahay, Louisiana State University, Baton Rouge, La.

Secretary-Treasurer—Ralph Roberts, Office of Naval Research, Washington, D. C.

Executive Committee Members-at-Large—E. L. Eckfeldt, Leeds and Northrup Co., Philadelphia, Pa.

C. W. Tobias, University of California, Berkeley, Calif.

RALPH ROBERTS,
Secretary-Treasurer

1955 Extended Abstracts

The Electronics Division has arranged for an additional 100 copies of the "Enlarged Abstracts of Papers Presented by the Electronics Division" at the Cincinnati Meeting.

Please send check for $2.00 to Charles W. Jerome, Sylvania Electric Products Inc., 60 Boston St., Salem, Mass.

* * *

The Theoretical Electrochemistry Division has available 40 copies of the "Enlarged Abstracts" of papers presented at its symposia at the Cincinnati Meeting. The booklet also includes abstracts of the Fused Electrolytes Symposia sponsored jointly by the Theoretical Electrochemistry and Industrial Electrolytic Divisions.

Please send check for $2.00 to Ernest Yeager, Department of Chemistry, Western Reserve University, Cleveland 6, Ohio.

SECTION NEWS

Chicago Section

At the regular monthly meeting on April 1, Dr. L. F. Yntema of the Fansteel Metallurgical Corporation discussed "Protection of Molybdenum at High Temperatures."

The greatest needs for materials for use at high temperatures are for heating elements and jet motor components. Requirements for such materials are good mechanical properties at elevated temperatures, chemical inertness to the environment, and that they are able to be fabricated and are available in sufficient quantity.

Three classes of materials have been and are being developed to meet these requirements: (*a*) Borides of groups 4, 5, and 6, transition elements. These boron compounds have reasonable high temperature strength. They are in some instances sufficiently stable chemically but are generally quite brittle. (*b*) Cermets: metal-ceramic mixtures. These are in the process of development with the ceramics largely being oxides. (*c*) Metals.

The most interesting metals can be determined by considering those with the highest melting point first and working down. Tungsten is difficult to fabricate, has been scarce, and oxidizes badly. Rhenium is rare and expensive. Tantalum is difficult to fabricate and rather scarce. Molybdenum is able to be fabricated, is available, and is in reasonable supply, especially on this continent, although it also poses the oxidation problem. Alloying has been tried in an effort to control the problem of oxidation. It is not successful except by high alloy content; brittleness results. Alloying elements with high vapor pressures cannot be used. This approach consequently has not been particularly successful.

Ceramic protective coatings on a metal such as molybdenum must have a high melting point, good adherence, lack of permeability to oxygen, and a coefficient of expansion close to that of molybdenum. One such coating has been made in which a base of borosilicate glass containing 25% ZrO_2 is applied to the molybdenum, then covered with ZrO_2 and kaolin; this is in turn covered with a coating of the glass. In another coating system, a molybdenum-chromium alloy layer is made on the surface, then in turn covered with a cermet containing spongy chromium impregnated with the borosilicate glass. Such coated pieces of molybdenum last about 7 hr at a temperature of 1540°C. Considerably longer lifetimes are obtained at lower temperatures.

The metal has also been successfully clad mechanically using nickel metal. Such bimetal structures can be hot rolled and the nickel molybdenum alloy kept thin. Reasonable lifetimes of such clad molybdenum can be obtained up to perhaps 1200°C. They fail by the oxidation of the nickel cladding.

In another coating technique, a silicide layer is formed on the molybdenum base metal. The external surface of this layer is $MoSi_2$ and is resistant to oxidation. Apparently some SiO_2 forms as a result of oxidation and retards subsequent reaction. Beneath the

surface layer there is characteristically formed Mo_2Si_2 which is also oxidation resistant. At the region of attachment to the base metal, Mo_5Si forms, and this is not resistant to oxidation. During use of such a coated material, the Mo_5Si layer grows thicker. When it reaches the external surface, the piece fails. There are several methods of production of such coatings. One successful method requires heating the molybdenum in a silicon tetrachloride plus hydrogen atmosphere. If the temperature of formation is above 1440°C, the silicide layers described are formed. If a lower formation temperature is used, there is usually a metallic silicon layer over the molybdenum silicide. Life expectancy of molybdenum coated with silicide layers diminishes from above 3000 hr at 800°C to about 30 hr at 1800°C.

Other methods of protection are being developed. A short dip of molybdenum in molten aluminum plus silicon forms a layer of aluminum silicide upon the base metal. When such a coated piece is exposed to air, $AlSiO_5$ is formed on the surface, as well as a molybdenum silicide layer next to the base metal.

J. E. Draley, *Secretary*

Detroit Section

A symposium on Leveling in Electrodeposition was held on April 22 at Wayne University. Participating in this symposium were F. I. Nobel of Lea-Ronal Inc., A. H. DuRose of Harshaw Chemical Company, and J. D. Thomas of General Motors Research.

Mr. Nobel, discussing leveling in copper deposits, stated that zero or negative leveling existed in the cyanide copper bath, and only by the use of additives could positive leveling be obtained. No leveling was possible at all if the rms value of the original surface was greater than 10 μin. In the case of the acid copper bath, good leveling could be expected with additives, regardless of the smoothness of the original surface. The obvious advantage of a bath having satisfactory leveling properties is the elimination of buffing. Leveling ability, however, is not sufficient in cases where a mirror finish is required. Mr. Nobel indicated that a satisfactory theory on leveling is still lacking, and more extensive research is required in this field of electrodeposition.

Mr. DuRose reported on some polarization studies made in conjunction with leveling in nickel baths. He described the use of fine wire cathodes where deposition was made on the wire tip, or on projections along the wire, or over scratches in the wire. Leveling efficiency was evaluated by the ability of the tips or projections to be smoothed over, or by the filling in of the scratches. An equation based on throwing power as calculated in a Haring cell was derived which showed that throwing power within a scratch increased with increasing size of that scratch. Polarization measurements were made which indicated that such additives as Perflow increased the cathode potential, and at the same time improved leveling. A discrepancy was found in comparison of the commutator and Luggin capillary methods of potential measurement in that, whereas the polarization curves with and without additive were parallel in the case of the capillary method, this did not hold true for the commutator measurements. In summarizing, Mr. DuRose stated that leveling increased with increase of cathode potential, temperature, and *p*H, but decreased with increasing current density. It was further pointed out that, although the depth of a scratch was decreased by leveling, the width was increased.

Mr. Thomas described the interference microscope method of studying leveling in electrodeposition. By the use of colorful and masterfully prepared slides, the principle and application of the two-beam interference microscope was illustrated. In principle, a beam of light reflected from the specimen surface forms an interference pattern with the reflected beam from a reference reflector (both beams having the same source). This interference pattern is viewed through the eyepiece of a microscope, and by measurement of fringe shift, quantitative data can be obtained as to the peak-to-valley distances. Although qualitative information is possible using ordinary polished surfaces, for exacting work, reference standards of surface roughness must be used as the basis metal. With the use of such standards reproducible surfaces can be made, and a specific number assigned, denoting leveling ability. Thus, for a surface having an original peak-to-valley roughness of 80 μin., and a final roughness following plating of 30 μin., the leveling ability of the electrodeposit is calculated as $\frac{80 - 30}{80} \times 100 = 62.5\%$. Slides of microinterferograms were shown of copper deposits on a standard surface using different proprietary solutions, which clearly illustrated the relationship between leveling and fringe shift. After listening to Mr. Thomas' talk and viewing the slides, one was left with the feeling that use of the two-beam interference microscope will lead to marked advances in electrodeposition research.

M. Shaw, *Secretary-Treasurer*

The following have been elected to office in the Detroit Section for the year 1955–1956:

Chairman—A. W. Liger
1st Vice-Chairman—G. V. Kingsley
2nd Vice-Chairman—Manuel Ben
Secretary-Treasurer—Manuel Shaw
Representative on Council of Local Sections—L. O. Case

M. Shaw, *Secretary-Treasurer*

Pacific Northwest Section

The January meeting of the Pacific Northwest Section was held Thursday, January 27, in Chief Joseph Junior High School, Richland, Wash. The meeting was held jointly with the Richland Section of the American Chemical Society.

The speaker was Dr. Pierre Van Rysselberghe, Professor of Chemistry at the University of Oregon. The title of Dr. Van Rysselberghe's talk was "The International Picture in Electrochemistry." Approximately 45 members and guests were in attendance.

Dr. Van Rysselberghe traced the growth of the International Committee of Electrochemical Thermodynamics and Kinetics (CITCE). The CITCE, after a modest beginning, gained stature rapidly, and was later requested to ally itself with The International Union for Pure and Applied Chemistry in an effort to strengthen the attack on problems existing within the field of electrochemistry.

The CITCE, with which Dr. Van Rysselberghe had worked by correspondence prior to 1950, and with which he was able to work more closely during the years 1950–1951 while a Fulbright Visiting Lecturer in Italian Universities, had made very commendable progress in spite of many difficulties. When approached by the International Union, much work had been accomplished in completing potential-*p*H diagrams for various metal-oxide-hydroxide systems. The International Union requested that this work be continued and that additional problems such as sign conventions be added to their agenda.

Dr. Van Rysselberghe showed examples of the potential-*p*H diagrams, some of which had been mapped by his European colleagues. Their use in predicting the stable form of metal salts or

hydroxides in various *p*H ranges and in helping to explain the sources of electrochemical energy was explained.

Prior to the meeting, members and guests, many of them former students of Dr. Van Rysselberghe, were privileged to meet and talk with him at a dinner held at the Desert Inn Hotel in Richland.

KENNETH L. SANBORN,
Secretary-Treasurer

San Francisco Section

The regular January meeting of the San Francisco Section was held on January 26 at the Faculty Club, University of California, Berkeley, Calif.

Following dinner, a short business meeting was held. The technical program consisted of a discussion of "Chlorine-Caustic Electrolysis and Related Operations" by Mr. Richard F. Bechtold, Superintendent, Electrochemical Department, The Dow Chemical Company, Pittsburg, Calif. Mr. Bechtold's talk covered a general explanation of both diaphragm and mercury chlorine cells, brine preparation, and chlorine purification and liquefaction. Several typical operating problems encountered were explained which indicated some of the practical aspects of this type of process and their relationships to the theoretical considerations.

The talk was frequently punctuated by questions from the floor and a very interesting informal question and answer period followed.

On March 14, Mr. Marvin Udy, Society President, paid an informal visit to the San Francisco Section. Society affairs were discussed, and a review of the membership and financial status of the Society was presented by Mr. Udy. It was pointed out that there are a great number of nonmember subscribers to the JOURNAL, which attests to its high caliber. It was noted that the San Francisco Section has shown the largest percentage increase in membership of any local section in recent years, and that an unusually large fraction of the membership attends meetings.

Preliminary plans for the Spring 1956 National Convention were discussed. Mr. Udy was confident that there would be a large attendance at the San Francisco meeting.

The regular March meeting of the San Francisco Section was held on March 30 at the University of California Faculty Club. The speaker on this occasion was Dr. Robert M. Burns, Editor of the JOURNAL, who is at present on the West Coast as a consultant.

The topic for the evening was "Electrochemical Problems in the Telephone Industry." Dr. Burns first pointed out the great variety of corrosion problems encountered in communications, both from the use of new materials and from unusual conditions (stray currents, unusual soil conditions, etc.).

The speaker mentioned that research in solid-state physics is just coming of age; it has already led to the development of the transistor and the silicon solar energy converter. The transistor is displacing the vacuum tube in an increasing number of applications, having the advantage of small size and small power requirement. Impurities are extremely critical in that even parts per billion of certain contaminants will render germanium practically useless for transistor manufacture. As a result, new techniques had to be devised both for preparation (zone melting) and analysis of the raw materials.

The silicon solar energy converter is commonly called a "solar battery," although it is not a battery, strictly speaking. It will convert solar energy falling upon it directly to electricity, but will not store it. The conversion efficiency is steadily being increased: 10% has been achieved and 15% is in sight. A model silicon converter was demonstrated to the audience.

The great number of questions following the talk attested to lively interest on the part of the audience.

BERNARD PORTER

Washington-Baltimore Section

The 32nd technical meeting of the Section was held on April 21 at the National Bureau of Standards. The speaker was Dr. Theodore Shedlovsky, of the Rockefeller Institute for Medical Research, who spoke on Electrochemistry in Medicine. Dr. Shedlovsky is editor-in-chief of the treatise on this subject published under the sponsorship of the Theoretical Division of The Electrochemical Society.

Dr. Shedlovsky pointed out that electrochemistry is related to medicine in two ways: first, it provides laboratory tools for the study of biologically important substances and for the determination and control of many biological environmental factors; second, living organisms are complicated electrochemical systems capable of transforming chemical energy into electrical signals. Historically, the relation of biology and electricity was recognized before that of chemistry and electricity. Dr. Shedlovsky read from the scientific papers of the late 18th century reporting the early observations of physiological reaction to electrical stimulation. Electrical signals originating in living tissue have resulted in the use of the electrocardiograph and encephalograph as monitors of the normalcy of the heart and brain functions.

Electrophoresis is an example of an electrochemical tool that has been used successfully for the study of blood plasma and serum in health and disease. In this technique, protein components of these fluids produce strata of varying index of refraction in the vicinity of the electrodes. These strata are observed by Schlieren techniques, and the number and relative amounts of the protein species may be recorded photographically. In addition to normal serum and plasma photographs, Dr. Shedlovsky showed some obtained from specimens taken in various disorders.

The study of the living cell itself has shown that, commonly, a potential of 0.1 v is associated with it at rest. The cell membrane is described as a potassium electrode of high ohmic resistance at rest, and as a sodium electrode of low resistance under stimulation. In the physiological environment, conductivity and the source of emf are considered to result from the Bronsted proton exchange in acid-base reactions rather than electron transfer and oxidation-reduction reactions. Prototype cell membranes include such structures as the glass electrode, and circuit analogues have resulted in series-parallel pictures of capacitances and resistances common to surface phenomena.

In conclusion, Dr. Shedlovsky read, from the scientific papers of Galvani and Volta, illustrations of the remarkable intuition and foresight of these early observers of the relation of electrochemistry and medicine.

The interesting discussion period encompassed remarks by Dr. Karl Sollner on the mechanism of proton exchange at cell walls, and extended to Dr. Shedlovsky's description of the electrical apparatus of the electric eel.

JEANNE BURBANK,
Secretary-Treasurer

Cleveland Section

At the May 13 meeting of the Cleveland Section, the following slate of officers was installed:

Chairman—W. H. Stoll

Vice-Chairman—K. S. Willson
Secretary—P. S. Brooks
Treasurer—D. E. Kinney
K. S. Willson, *Secretary*

PERSONALS

William Giesker

William Giesker has been appointed Superintendent of The Autoyre Co., Oakville, Conn., the world's largest manufacturer of bathroom, kitchen, and closet accessories. Previously he was the company's chief chemist.

J. E. Stareck

J. E. Stareck recently became Director of Research of the Metal & Thermit Corp., producers of metals, industrial chemicals, welding equipment, and supplies. In his new post he will also continue to direct the research activities of United Chromium, Inc., a subsidiary of Metal & Thermit.

Nonmember Journal Subscribers

Nonmember subscription rates to the Journal in 1956 will be $18.00 instead of the $15.00 previously charged. Current subscribers will be mailed invoices for $18.00 late in September.

Earle D. Moiles, Jr., has been promoted from sales field engineer to District Manager of the Boston Office of the Leeds & Northrup Co. He was attached to the Philadelphia sales office before going to Boston.

NEW MEMBERS

In May 1955 the following were approved for membership in The Electrochemical Society by the Admissions Committee:

Active Members

John V. H. Berdan, National Carbon Div., Union Carbide & Carbon Corp.; Mail add: Apt. A, 6627 Buffalo Ave., Niagara Falls, N. Y. (Electrothermics & Metallurgy)

Oliver J. Blaber, Sylvania Electric Products Inc.; Mail add: 163-54 23 Ave., Flushing 57, N. Y. (Electrothermics & Metallurgy)

Thelma C. Buescher, P. R. Mallory & Co.; Mail add: 3835 Carson Ave., Indianapolis 27, Ind. (Electronics, Electrodeposition)

Paul Carus, Carus Chemical Co.; Mail add: Box 364, La Salle, Ill. (Industrial Electrolytic)

Bruce E. Deal, Dept. of Metallurgical Research, Kaiser Aluminum & Chemical Corp., Spokane 69, Wash. (Corrosion, Theoretical Electrochemistry)

John W. Faust, Jr., Westinghouse Research Labs.; Mail add: 715 Beulah Rd., Pittsburgh 35, Pa. (Electronics)

Attilio Grandinetti, Lakeshore Electrotype Div.; Mail add: 5938 W. 16 St., Cicero 50, Ill. (Electrodeposition)

David W. Hardesty, General Motors Corp.; Mail add: 27768 Lathrup St., Birmingham, Mich. (Corrosion, Electrodeposition)

William M. Hetherington, Jr., Philco Corp. Development Lab.; Mail add: 2161 Princeton Ave., Philadelphia 49, Pa. (Electronics)

William L. C. Huis, RCA Victor Div.; Mail add: 523 W. Highland Ave., Marion, Ind. (Electronics, Electro-Organic, Theoretical Electrochemistry)

Vernet C. Kauffman, General Electric Co., Lamp Division, Large Lamp Dept., Nela Park, Cleveland 12, Ohio (Electrodeposition, Electronics, Electro-Organic, Electrothermics & Metallurgy, Theoretical Electrochemistry)

Paul H. Keck, Signal Corps Engineering Labs.; Mail add: 39 Queens Dr., Little Silver, N. J. (Electronics)

Karl Kordesch, National Carbon Research Labs.; Mail add: 1415 W. 81 St., Cleveland, Ohio (Battery)

Russell G. McGhee, Speer Carbon Co.; Mail add: 463-81st St., Niagara Falls, N. Y. (Industrial Electrolytic)

Paul McVicker, Electro Metallurgical Co.; Mail add: 938 Rankine Rd., Niagara Falls, N. Y. (Electrothermics & Metallurgy)

Leslie E. Othmer, Sr., Keokuk Electro-Metals Co.; Mail add: 1800 Grand Ave., Keokuk, Iowa (Electrothermics & Metallurgy)

Hayne Palmour, III, Research Dept., American Lava Corp., Chattanooga 5, Tenn. (Electric Insulation)

Jacob G. Rabatin, General Electric Co.; Mail add: R. F. D. #4, Chardon, Ohio (Electronics)

Joseph C. Schumacher, American Potash & Chemical Corp.; Mail add: 1559 Ensley Ave., Los Angeles 24, Calif. (Battery, Industrial Electrolytic)

Peter Seats, Thomas Electronics Inc., 118-9th St., Passaic, N. J. (Electronics)

Selby M. Skinner, Dept. of Chemistry, Case Institute of Technology, University Circle, Cleveland 6, Ohio (Theoretical Electrochemistry)

James S. Smith, Sylvania Electric Products Inc., Towanda, Pa. (Electronics)

Dmitri N. Vedensky, The M. A. Hanna Co., 1300 Leader Bldg., Cleveland 14, Ohio (Electrothermics & Metallurgy)

Piotr Zenczak, Evans Products Co., Coos Bay, Oreg. (Battery)

Associate Member

Jack E. Norbeck, General Electric Co.; Mail add: 12204 Craven Ave., Cleveland 5, Ohio (Electronics)

Student Associate Member

Aleksandrs Martinsons, University of Michigan; Mail add: 513½ E. William, Ann Arbor, Mich. (Theoretical Electrochemistry)

Transfers to Active Membership

David O. Feder, Bell Telephone Labs., Inc.; Mail add: 205 E. 72 St., New York 21, N. Y. (Corrosion, Electrodeposition, Electronics, Electrothermics & Metallurgy, Theoretical Electrochemistry)

Norman H. Kirk, Park Bros. Ltd., Bankfield Works, Ordnance St., Blackburn, Lancs., England (Battery)

Reinstatement and Transfer to Active Membership

DAVID B. JOY, National Carbon Co., 30 E. 42 St., New York, N. Y. (Industrial Electrolytic)

Reinstatements to Active Membership

HEBERT J. FLEISCHMANN, Saturnium Corp., Inc.; Mail add: California, Ky. (Industrial Electrolytic, Theoretical Electrochemistry)

JAMES A. B. MILNE, North American Cyanamid, Ltd., Niagara Falls, Ont., Canada (Electrothermics & Metallurgy)

ARTHUR J. SHERBURNE, General Electric Co.; Mail add: 907 Walnut St., Coshocton, Ohio (Electric Insulation)

BERT W. WHITEHURST, Hawkridge Metals Corp.; Mail add: 27 School St., Boston, Mass. (Electrodeposition)

Adjustment from Associate to Active Membership

BEN MATCHEN, Norton Co.; Mail add: 1567 Ontario Ave., Niagara Falls, Ont., Canada (Industrial Electrolytic) (Elected Dec. 6, 1954)

NEWS ITEM

First U. S. Reagent Chemical Plant

On May 17, production lines started rolling in the manufacturing laboratories of Fisher Scientific Company's giant reagent-chemical plant in Fair Lawn Industrial Park, N. J. Fisher/Fair Lawn is the first plant in America designed exclusively for reagent chemicals: the ultrapure, laboratory-analyzed chemicals used by researchers and scientists engaged in every sort of activity.

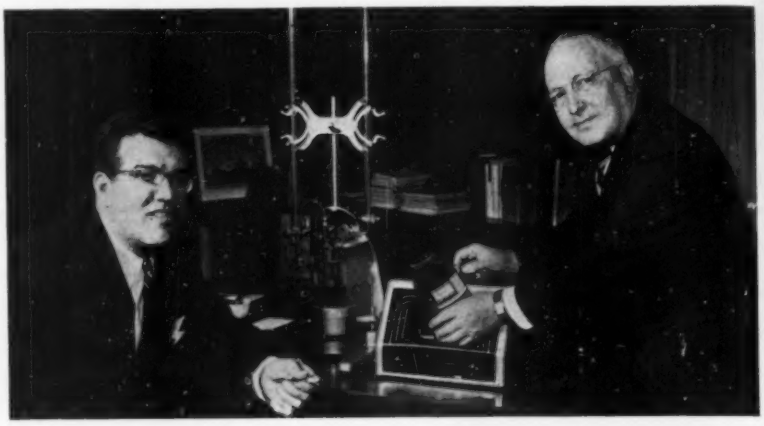

In the Presidential office of J. C. Warner, Aiken Fisher, President of Fisher Scientific Company (*left*), waits to give signal to Dr. Warner (*right*) to open Fisher plant in New Jersey.

To emphasize the unique laboratory nature of the new plant, where chemicals are made in small lots of a few hundred pounds and receive up to 14 laboratory tests each, the cornerstone of the plant was laid last year by plant manager—Fisher vice president A. L. Abbitt with a *gold laboratory spatula*.

On May 17, to carry out the reagent theme further, Dr. J. C. Warner, President of Carnegie Institute of Technology, and President-Elect of the American Chemical Society and Past President of The Electrochemical Society, poured some Fisher sodium hydroxide reagent into a beaker of acid on a Titrimeter. The action of base and acid closed the instrument's "magic eye," which set off a signal that was carried by telephone to Fair Lawn, where the signal started a conveyor belt. This instantly started the automatic bottling, capping, and labeling of Fisher sodium hydroxide at Fair Lawn, conveying the finished products into the plant's warehouse—all untouched by human hands.

RECENT PATENTS

Selected from the Official Gazette by M. S. Wright, Librarian, National Carbon Research Laboratories, Cleveland, Ohio.

April 19, 1955

Bircher, J. A., 2,706,411, Thermoelectric device for measuring high temperatures

King, A. J., 2,706,554, Getter assembly

Burling, E. R., and Rich, J. P., 2,706,673, Method of bleaching with chlorine dioxide

Ladisch, R. K., 2,706,710, Portable polarographic half cell

Ladisch, R. K., 2,706,711, Portable polarographic half cell

Ladisch, R. K., 2,706,712, Portable polarographic half cell

MANUSCRIPTS AND ABSTRACTS FOR SPRING MEETING

Papers are now being solicited for the Spring Meeting of the Society, to be held at the Mark-Hopkins Hotel in San Francisco, April 29 and 30, and May 1, 2, and 3, 1956. Subjects to be covered at the technical sessions will be Electric Insulation, Electronics (including Luminescence, Oxide-Cathodes, Phosphor Application, Semiconductors, and Instrumentation), and Industrial Electrolytics, and probably Electrothermics and Metallurgy and Theoretical Electrochemistry.

To be considered for this meeting, triplicate copies of abstracts (not to exceed 75 words in length) must be received at Society headquarters, 216 West 102nd St., New York 25, N. Y., *not later than January 2, 1956*. Complete manuscripts should be sent in triplicate to the Managing Editor of the JOURNAL at the same address.

***

The Fall 1956 Meeting will be held in Cleveland, Ohio, October 28, 29, 30, and 31, and November 1, at the Statler Hotel. Sessions will be announced in a later issue.

DECEMBER 1955 DISCUSSION SECTION

A Discussion Section, covering papers published in the January–June 1955 JOURNALS, is scheduled for publication in the December 1955 issue. Any discussion which did not reach the Editor in time for inclusion in the June 1955 Discussion Section will be included in the December 1955 issue. Those who plan to contribute remarks for this Discussion Section should submit their comments or questions in triplicate to the Managing Editor of the JOURNAL, 216 West 102nd Street, New York 25, N. Y., not later than August 15, 1955. All discussions will be forwarded to the author, or authors, for reply before being printed in the JOURNAL.

Hughes, W. B., and Lembcke, R. E., 2,706,714, Method of inhibiting corrosion of metals

April 26, 1955

Ransburg, E. M., and Miller, E. P., 2,706,964, Apparatus for electrostatic atomization

McKinley, T. D., 2,707,149, Recovery of titanium metals

Brown, H., and Fellows, R. A., 2,707,166, Electrodeposition of copper from an acid bath

Hoover, E. W., 2,707,167, Electrodeposition of copper from an acid bath

Wainer, E., and Sibert, M. E., 2,707,168, Preparation of titanium monoxide by electrolysis

Steinberg, M. A., Sibert, M. E., and Topinka, A. A., 2,707,169, Preparation of titanium metal by electrolysis

Wainer, E., 2,707,170, Electrodeposition of titanium

Ruben, S., 2,707,199, Potential producing cell and high voltage pile

Urry, L. F., Kennedy, W. L., and Brown, H. M., 2,707,200, Leak-resistant dry cell

Fernald, G. H., and Enloe, K. M., 2,707,201, Porous storage battery separator and method of making

Chubb, M. F., 2,707,202, Lead acid storage battery construction

Hollmann, H. E., 2,707,223, Electric resistor

Electrochemistry in Biology and Medicine

"Electrochemistry in Biology and Medicine," edited by Theodore Shedlovsky, sponsored by The Electrochemichemical Society, and published by John Wiley & Sons, Inc., is now available.

The book is based on a symposium on electrochemistry in biology and medicine which was held at the New York Meeting of the Society in 1953.

The book is being sold for $10.50 by John Wiley & Sons, Inc., 440 Fourth Ave., New York 16, N. Y. Members of the Society who order the book through ECS Headquarters Office, 216 West 102nd St., New York 25, N. Y., can receive a 33⅓% discount given to members. The publisher will mail the volume and invoice.

ANNOUNCEMENTS FROM PUBLISHERS

BIENNIAL REPORT 1953 AND 1954; NATIONAL BUREAU OF STANDARDS. National Bureau of Standards Miscellaneous Publication 213. Order from Superintendent of Documents, U. S. Government Printing Office, Washington 25, D. C. 162 pages, 60 cents.*

This report summarizes the research and development activities of the NBS in the physical sciences during the fiscal years 1953 and 1954. Brief descriptions are given of representative accomplishments in each area of the Bureau's responsibilities, which include maintenance of basic standards, determination of physical constants and properties of matter, development of methods and instruments of measurement, and the provision of calibration, testing, and scientific advisory services.

ASTM PROCEEDINGS, 1954 edition. Published by the American Society for Testing Materials, 1916 Race St., Philadelphia 3, Pa. 1400 pages, $12.00.

The volume records the technical accomplishments of the ASTM for 1954. It includes many technical reports and papers, together with discussion which has been offered to the society during the year and accepted for publication in the *Proceedings*.

* Foreign remittances must be in U. S. exchange and should include an additional one-third the publication price to cover mailing costs.

ORGANIC SYNTHESES, Collective Volume III, edited by E. C. Horning. Published by John Wiley & Sons, Inc., 440 Fourth Ave., New York 16, N. Y., March 1955. 890 pages, $15.00.

The new book encompasses all the material in Annual Volumes 20–29, revised and brought up to date with new and improved methods of preparation.

LITERATURE FROM INDUSTRY

CHLORINE ANALYZER. Data sheet available on a new residual chlorine analyzer which provides an automatic check on Cl_2 content in chlorinated water. Functioning on the coulometric principle, the instrument makes a continuous electrical titration for Cl_2 content, and incorporates an L&N Speedomax recorder to chart the variable. A high degree of inherent measuring accuracy and unusually low maintenance are the direct results of the method employed. Leeds & Northrup Co. P-308

"WHAT'S NEW FOR THE LABORATORY." 63rd edition of publication features 4 Beckman instruments; silicone rubber-coated Flexible Heating Tape; "Precision" Metabolic Shaking Incubator; Duplex Filamatic; several new glassware items; Wide-Range Zimmerli Gauge; Distilled Water Heater, Bottle Pump; Test Tube Washer; Corning Flared-Top Pipettes; Laboratory Scale; new, improved "Bronwill" Constant Temperature Circulator; plus others. Scientific Glass Apparatus Co. Inc. P-309

PULP BLEACHING. New Bulletin offers a number of test procedures for preliminary evaluation of various peroxide pulp bleaching treatments. Low, moderate, and high density bleaching procedures are outlined, as are pre-

treatments, sheet making, and chemical tests relating to hydrogen peroxide and other bleaching chemicals on the pulp. Apparatus, chemicals, procedures, and examples with typical calculations are described. Becco Chemical Div., Food Machinery and Chemical Corp. P-310

"EQUIPPING THE PICKLE HOUSE." 32-page, 2-color booklet is offered as a practical guide to greater production at lower cost in a wide variety of pickling operations. It describes the use of specially designed Monel equipment in the processing of large and small fabricated parts, hollow ware, and forgings and castings, as well as the common mill forms of steel and tin plate. The text explains how Monel's corrosion resistance, strength, and ductility cut dead weight, permit greater payloads, and assure longer service life. The International Nickel Co., Inc. P-311

"ALLIGATOR" CLIP. Catalogue sheet describes the smallest alligator clip ever made—a new steel or solid copper clip, completely insulated by vinyl plastisol sheath-type insulator. Designed for quick, temporary connections in miniaturized and subminiaturized equipment. Mueller Electric Co. P-312

NEW PRODUCTS

CONTROL VALVES. Production has been announced of a new line of control valves for NAK and similar molten metal services, designated model series 1401. Body rating of the line is 150 psi at 1600°F. Valves can be furnished in body sizes ½ in. through 6 in. with the manufacturer's Domotor, cylinder, or manual operators. A variety of end connections is also available. The Annin Co. N-176

PORTABLE OSCILLOGRAPHS. Lightweight, 4 and 6 channel portable oscillographs have been developed. Despite light weight and compactness, either model provides full range instrumentation. Each offers a range of 16 chart speeds with travel variation of from 10 in./day to 10 in./sec to simplify testing problems of electrical variables, vibration, torque, stress, strain, and other desired measurements. Both models equipped for either ink or electric writing. A control selector permits either a local or remote control setup. Brush Electronics Co. N-177

PLASTIC DRUM FAUCET. A polyethylene plastic drum faucet, reportedly a new idea in its field, has been introduced. Designed to fit all ¾ in. standard drum openings, this full-sized faucet is priced considerably lower than regular metal style faucets and is more durable and lighter weight. An important factor to many industries is the polyethylene construction which will not react with strong acids, alkalies, oils, etc. It operates smoothly and will not leak, regardless of temperature or type of material with which used. Multi-Meter Corp. N-178

MILLIVOLT INDICATOR. Seven ranges, covering values from 0.25 to 25 mv, are provided in a new portable indicating instrument. Combination of laboratory precision with ruggedness permits field use under the most adverse circumstances. Balance is indicated by a light-beam spot-type galvanometer protected by automatic short-circuiting when instrument is off, and a shunt resistor when ranges are changed. Preaged, stabilized wire-wound resistors are used, and a large meter scale indicates millivolt values directly with good precision. Accuracy is 0.5% of each range. Beckman & Whitley, Inc. N-179

GERMANIUM POWER RECTIFIER. A 35-kw liquid-cooled germanium power rectifier is available. It is a 3-phase bridge unit, rated for a maximum of 450 amp d-c continuous output, and can be supplied for input voltages of 26, 36, 52, and 66 v rms maximum. Efficiencies up to 97% are attainable and the power factor is essentially 100%. Aging is negligible or zero. Rectifier regulation as low as 2% is possible from no load to full load. International Rectifier Corp. N-180

HIGH DIELECTRIC FILM. A product known as AMF "Fiberfilm"® sheet material was introduced at the IRE Show in March. First of a new family of engineering materials, the product is made from glass microfibers and polytetrafluoroethylene. Available in both porous and nonporous forms, the films represent the refinement of the first practical method for preparing long continuous lengths or rolls up to 40 in. in width of very thin, high-quality film having all the excellent electrical properties of Teflon (duPont Trademark), and at the same time highly desirable mechanical properties. American Machine & Foundry Co. N-181

ARMORED ROTAMETERS. A nonmagnetic metal extension tube replaces the customary glass tube in the new "MAG/NA/VUE" which has been developed mainly for use with the Brooks® AR/MET Armored Rotameters. The unit is designed for use at pressures to 1200 psi at 200°F, or for metering opaque fluids. Riding inside the extension is a float with a permanent magnet imbedded in the float head. Outside the extension a lightweight indicating sleeve moves in response to any change in float position. The magnet in the float head holds the sleeve in permanent bond to the float position. Brooks Rotameter Co. N-182

OXYPHEN *p*H PAPERS. True Brite Oxyphen *p*H Papers provide a new and simpler method of testing *p*H rating of electroplating solutions. No separate color charts or comparison charts are needed with the new type papers which provide an instantaneous reading of the *p*H rating when the color of the indicator bar is compared with the nearest constant color bar. 30 separate ranges available to cover all of the practical conditions of *p*H ratings from acid copper solutions (0.3–1.8) to cyanide copper solutions (11.5–14.0). True Brite Chemical Products Co. N-183

To receive further information on any New Product or Literature from Industry listed above, send inquiry, with key number, to JOURNAL of The Electrochemical Society, 216 West 102nd Street, New York 25, N. Y.

Please print your name and address plainly.

ADVERTISERS' INDEX

Baker & Adamson, General Chemical Division, Allied Chemical & Dye Corporation 149C
Bell Telephone Laboratories, Inc. 156C
Enthone, Incorporated ..... Cover 4
Fisher Scientific Company 150C
Great Lakes Carbon Corporation ..... Cover 2
McGraw-Hill Book Company, Inc. 151C
National Carbon Company 148C
Stackpole Carbon Company 154C
John Wiley & Sons, Inc. 153C

Dissolution of Metals in Aqueous Acid Solutions

I. Current-potential Relations for Iron and Mild Steel[1]

A. C. Makrides,[2] N. M. Komodromos,[3] and Norman Hackerman

Department of Chemistry, University of Texas, Austin, Texas

ABSTRACT

The solution rate of iron in air-free hydrochloric acid solutions is a linear function of hydrochloric acid activity for activities between 1 and 10. The potential of dissolving iron is a logarithmic function of hydrochloric acid activity.

The potential of mild steel in acid solutions containing depolarizers is a linear function of the logarithm of the solution rate. It is suggested that the resulting potential-current curve (calculated from weight loss) constitutes an approximate polarization curve for the anodic reaction.

Introduction

An important step in elucidating the mechanism of wet corrosion of metals was the local-cell theory of corrosion (1). A more recent approach deals with corrosion and dissolution of metals in terms of two electrochemical reactions, an anodic and a cathodic one, rather than in terms of spatially separated local cells (2). The potential of an electrode placed in a solution containing an oxidation-reduction couple such that the electrode material takes part in the reaction is called the "mixed-potential." Measurements of potential of iron and mild steel electrodes in hydrochloric acid alone and in hydrochloric acid solutions containing depolarizers are reported in this paper and are discussed on the basis of the theory of mixed-potential.

Experimental

Iron coupons were mounted on a shaft driven by a ¼ hp motor through an arrangement of pulleys. Speeds up to 11,000 rpm could be obtained. The lower part of the shaft was covered with tygon tubing, and a rubber washer was used at the junction of the shaft with the coupon to prevent contact of the shaft with the solution. The coupons were tapped (⅜ in. thread hole along the axis) and attached to the shaft by screwing tightly on the lower part. Electrical contact was made through a mercury-filled recess drilled into the top of the shaft. The resistance of the junction was negligible.

Preparation of coupons.—Cylindrical coupons (2.5 cm x 1.9 cm) polished with 2 and 2/0 emery polishing paper to a mirror-like finish were used. Emery and iron particles were removed, and the coupons were degreased with hot benzene. After weighing to the nearest 0.1 mg, the bottom and top parts as well as the edges were coated with paraffin. Coupons were stored in a desiccator until used. The projected exposed area was 10 cm².

Procedure.—A 600 cc beaker containing 400 cc of solution was fitted with a Lucite cover with holes for calomel cell, coupon, nitrogen inlet, and thermometer. For runs in air-free solutions, nitrogen was continuously bubbled through the solution via three fritted glass bubblers placed at the bottom of the beaker. The gas was purified by passing through a vanadyl sulfate train. After passing nitrogen for 30–45 min the beaker was placed under the coupon, which had been mounted on the shaft immediately before, and raised so as to immerse it. The motor was then started. A total of 5–7 sec elapsed between immersion and starting of the motor. The motor attained its full speed in 1 sec. The temperature was 30 ± 1°C.

At the end of a run the coupon was rinsed with distilled water, then swabbed with a towel wetted with acetone. After washing in acetone, removing the paraffin with benzene, and drying, it was weighed at once or placed in a desiccator until weighed.

A student type Leeds and Northrup potentiometer and galvanometer were used. The open circuit potential, negative with respect to the saturated calomel cell, was recorded at one minute intervals. Contact with the solution was made through a 3% agar-saturated potassium chloride bridge.

Material.—Iron coupons were cut from an iron rod of 99.92–99.96% iron content supplied by the Swedish Iron and Steel Company, New York.

Steel coupons were cut from a cylindrical SAE 1020 steel rod. Spectrographic analysis showed negligible traces of copper.

[1] Manuscript received November 22, 1954. This paper was prepared for delivery before the Boston Meeting, October 3 to 7, 1954.

[2] Present address: Institute for the Study of Metals, University of Chicago, Chicago, Illinois.

[3] Present address: E. I. du Pont de Nemours & Company, Flint, Michigan.

Hydrochloric acid solutions were prepared from C.P. concentrated acid.

Ferric chloride, potassium dichromate, and ceric sulfate were of C.P. grade. Concentrations of ferric chloride and ceric sulfate solutions were determined by titration.

Benzoquinone, tolu-*p*-quinone, sodium anthraquinone sulfonate, and hydroquinone were provided by Eastman Organic Chemicals and were of highest commercial purity available. They were recrystallized from ethyl alcohol.

Results and Discussion

Solution Rates of Iron and Mild Steel in Hydrochloric Acid

Weight losses of iron and steel coupons in hydrochloric acid solutions were found to be linear functions of time. Accordingly, the weight loss in 15 min was generally obtained, and solution rates calculated on assumption of uniform dissolution during this interval.

Solution rates of stationary and rotating iron coupons in air-free and air-saturated solutions of hydrochloric acid are plotted in Fig. 1 and 2. The values given are averages of at least two runs, usually three or more. Mean deviations did not exceed 10% except at the lowest acid activity.

True surface area was calculated on assumption of a roughness factor of 4.0. The value obtained by gas adsorption using the BET method for iron coupons pickled in acid (other than the ones used in this work) was 3.6.

The weight loss is, within experimental error, a linear function of hydrochloric acid activity in air-free solutions. Hydrochloric acid activities were calculated from the data of Harned and Ehlers (3). Rotation decreases the rate of solution somewhat.

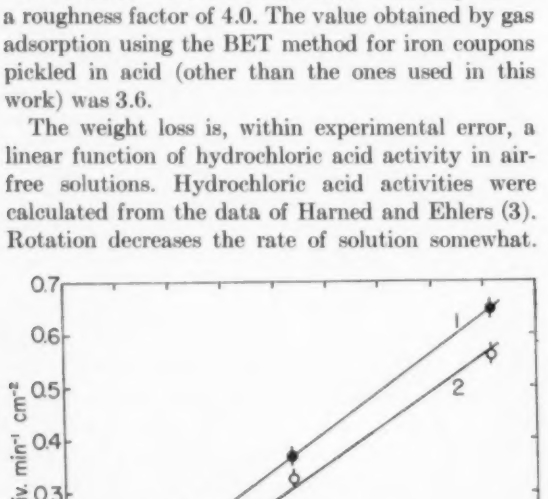

Fig. 1. Rate of solution of iron in air-free solutions as a function of HCl activity. Curve 1—Coupons stationary; curve 2—coupons rotated at 2180 rpm (12,700 cm/min).

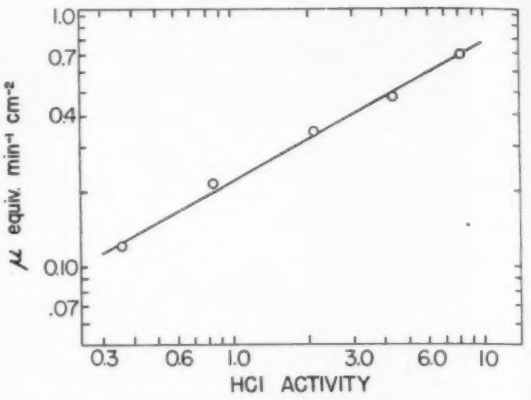

Fig. 2. Rate of solution of iron in air-saturated solutions as a function of the logarithm of HCl activity.

The slopes are 7.3×10^{-2} for stationary coupons and 6.9×10^{-2} μ equiv/min/cm^2 for rotating coupons. Fig. 2 shows that the solution rate in air-saturated solutions is a function of the 0.56 power of hydrochloric acid activity.

While the intercept of the solution rate vs. activity is zero in air-free solutions when the coupons are rotated at 2180 rpm, it is positive in solutions that either contain oxygen or are not agitated. The positive intercept in the presence of oxygen is understandable, since part of the reaction is to be accounted for by oxygen reduction. The reason for a positive intercept in air-free solutions that are not agitated is less clear; it may be connected with nonuniform conditions existing in the neighborhood of the surface and created probably by the solution process. This possibility is suggested by the fact that the intercept becomes zero on rotation of the coupons.

The solution rate in air-free 2*N* hydrochloric acid was independent of stirring speed. Rotation of coupons at 2180 rpm (12,700 cm/min) *in air-saturated solutions* increased the solution rate by a factor of about 1.6.

Similar results were obtained with mild steel coupons except that the weight loss was approximately 35% greater than with iron.

It is known that rate of solution in nonoxidizing acids is controlled by both the anodic and cathodic reaction rates (4) and is independent of ferrous ion concentration (5). When oxygen is present it is cathodically reduced and increases the solution rate; in its presence the solution rate is dependent on stirring speed (6), while in its absence it is independent of stirring speed (7, 8). Results reported above are in agreement with these observations.

In Fig. 3 the potential of dissolving iron vs. SCE is given as a function of time at various hydrochloric acid concentrations. The potential was reproducible

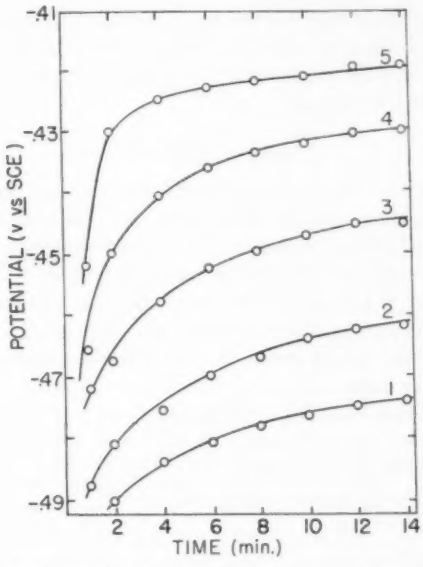

FIG. 3. Time-potential curves of iron in air-free solutions; coupons rotated at 2180 rpm. Curve 1—0.5*N* HCl; curve 2—1.0*N* HCl; curve 3—2.0*N* HCl; curve 4—3.0*N* HCl; curve 5—4.0*N* HCl.

to within ±2 mv. The potential changes rapidly in the cathodic direction in the initial 3–4 min and more gradually from there on. It is obvious from Fig. 3 that the potential has not reached a steady-state value in 15 min, and it is known from other experiments that the drift continues for at least several hours. This drift may be caused by changes with time of the overpotential of either the anodic, the cathodic, or both reactions (9), or by changes of the electrode caused by solution of hydrogen in iron. It cannot be accounted for by changes in the solution, since ferrous ion had no effect on the potential, and since the decrease in acid activity was negligible.

Although a steady-state potential has not been achieved at the end of 15 min, the shape of the time-potential curves is the same at all hydrochloric acid concentrations; consequently the potential at the 14th minute can be used for purposes of comparison. A plot of this potential against the logarithm of acid activity is given in Fig. 4. The potential moves in the cathodic direction with increasing acid activity. The equation for air-free solutions is

$$E = \text{constant} + 0.047 \log \alpha_{H^+} \qquad \text{(I)}$$

For coupons rotated at 2180 rpm in air-free solutions the constant was -0.45_7 v.[4]

Current densities were calculated from the weight loss assuming a roughness factor of 4.0. Fig. 5 gives the potential at the 14th min vs. current density for

[4] For a discussion of potentials of corroding or dissolving electrodes see reference (10).

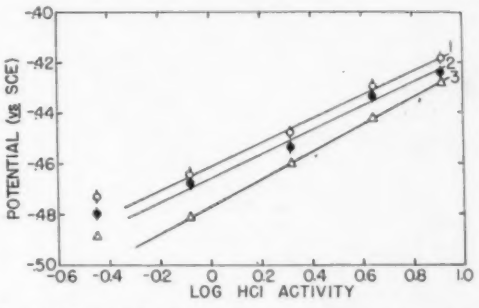

FIG. 4. Potential of iron (at 14th min) as a function of HCl activity. Curve 1—Air-free solutions; coupon revolving at 2180 rpm; curve 2—air-free solutions; coupon stationary; curve 3—air-saturated solutions; coupon stationary.

air-free solutions. It is sometimes maintained that such a plot involves the assumption that the so-called "total anodic area" does not change. Since in this case attack is uniform, and the whole of the surface undergoes dissolution at one time or another, the *total* surface area is the appropriate parameter. Thus, there is no ambiguity in the calculation of current densities.

On the assumption that a change in acid activity does not change the cathodic polarization curve but merely shifts it by an amount given by Nernst's equation, Fig. 5 can be considered to constitute an approximate polarization curve for the anodic process. This neglects any effects caused by changing the chloride ion concentration from 0.5 to 4.0*N*.

The equation obeyed for coupons rotated at 2180 rpm and at 30°C is

$$\text{Potential} = -0.415 + 0.054 \log i \qquad \text{(II)}$$

Here the potential is measured against a saturated calomel cell, and i is the current density in ma/cm².

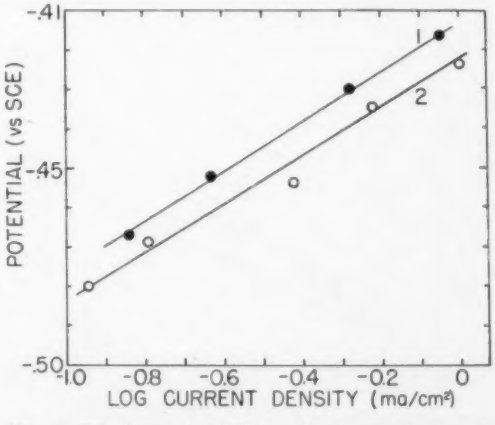

FIG. 5. Solution potential as a function of log current density (calculated from weight loss); air-free HCl solutions. Curve 1—Coupons rotated at 2180 rpm; curve 2—coupons stationary.

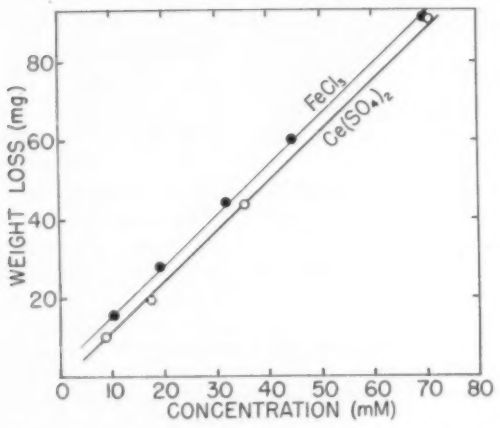

FIG. 6. Weight loss in 10 min as a function of depolarizer concentration at 2180 rpm.

Returning to solutions containing oxygen, the solution rate was partly controlled by diffusion and was dependent on stirring speed. The dissolution current density in air-saturated solutions is the sum of the limiting diffusion current for oxygen reduction and of the current for the hydrogen reaction. The relative contribution of the former (calculated from the difference between solution rates in air-saturated and air-free solutions) was about 50% at the lowest acid activity and decreased to about 10% at the highest acid activity. Its absolute contribution was approximately constant.

Since reduction of oxygen is believed to occur at a rate equal to its diffusion rate, and since its contribution to the over-all solution rate was constant, the cathode potential in solutions containing oxygen is determined by the hydrogen reaction; the polarization curve for hydrogen evolution is shifted on the current axis by a constant amount. This is only an approximation, since it neglects any changes of the polarization characteristics of the hydrogen reaction caused by oxygen.

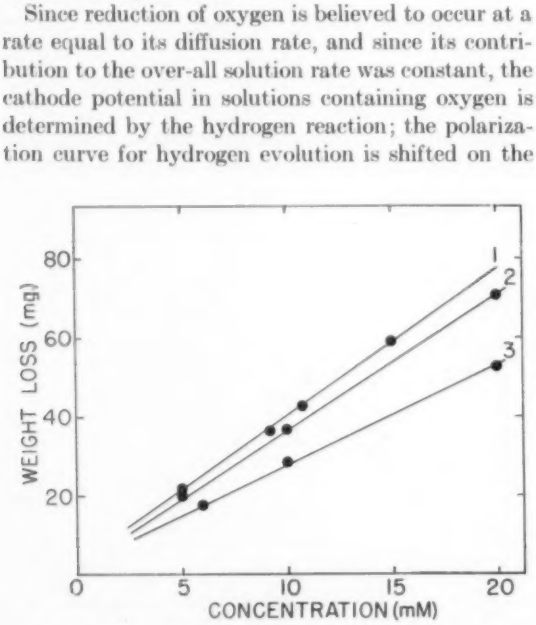

FIG. 7. Weight loss in 10 min as a function of depolarizer concentration at 2180 rpm. Curve 1—Benzoquinone; curve 2—tolu-*p*-quinone; curve 3—sodium anthraquinone sulfonate.

Depolarized Dissolution

In this series of experiments the volume, temperature, and exposed area were the same as before. Runs lasted 10 min and the solutions were $2N$ in hydrochloric acid and air-free throughout.

Fig. 6 to 8 show the weight loss as a function of depolarizer concentration at constant, 12,700 cm/min, linear speed. Points given are averages of two or more runs.

In the case of potassium dichromate the species in solution are $Cr_2O_7^{=}$ and $HCrO_4^{-}$ with an equilibrium constant $K = [HCrO_4^{-}]^2/[Cr_2O_7^{=}] = 2.3 \times 10^{-2}$ (11). Writing the weight loss as

$$W = k_1[Cr_2O_7^{=}] + k_2[HCrO_4^{-}] \qquad \text{(III)}$$

and solving the equations resulting upon substitution of experimental values, $k_1 = 6.1$ and $k_2 = 13.6$ mg/mM. In this calculation the change in the $[HCrO_4^{-}]$ to $[Cr_2O_7^{=}]$ ratio with decrease in the total chromium concentration during the run is neglected.[5] Agreement of observed and calculated values was within 5%.

Reduction products in the case of ceric sulfate and ferric chloride should have no effect on solution rate. Addition of hydroquinone, the reduction product of benzoquinone, changed neither solution rate nor potential. It is considered that this is also true for the other quinones. Any effect of the reduction product of $Cr_2O_7^{=}$ and $HCrO_4^{-}$, viz., Cr^{+3}, is negligible.

Distribution of attack at small solution rates (up to 120 mg in 10 min) was uniform, or nearly so, in the absence as well as in the presence of depolarizers.

[5] The problem can be solved exactly with

$$\frac{-d[Cr]}{dt} = k_1[Cr_2O_7^{=}] + k_2[HCrO_4^{-}]$$

where [Cr] is the total chromium concentration. Now $[HCrO_4^{-}]^2/[Cr_2O_7^{=}] = K$ and

$$[Cr_2O_7^{=}] = \frac{[Cr] - [HCrO_4^{-}]}{2}$$

substituting

$$\frac{-d[Cr]}{dt} = \frac{k_1[Cr]\,\dfrac{-K + K^2 + 8K[Cr]}{4}}{2} + \frac{k_2(-K + K^2 + 8K[Cr])}{4}$$

The differential equation is separable and can be integrated; the final expression is, however, too involved, the desired constants k_1 and k_2 being parts of logarithmic expression. Accordingly, values obtained from the simpler form were used.

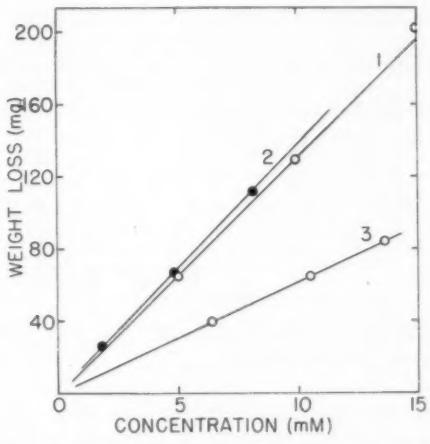

FIG. 8. Weight loss in 10 min as a function of depolarizer concentration at 2180 rpm. Curve 1—$K_2Cr_2O_7$; curve 2—$Cr_2O_7^=$ (calculated); curve 3—$HCrO_4^-$ (calculated).

With depolarizers a uniform, thin, black film appeared on the coupon surface soon after immersion. The film was easily removed at the end of the run by scrubbing with a towel wetted in acetone. No attempt was made to determine the composition or structure of this film.

From results of other investigators (12–15), and from data to be given in a subsequent paper, it was concluded that the solution rate of mild steel in 2*N* hydrochloric acid containing the depolarizers used is controlled by the rate of diffusion of depolarizer to the metal surface. Evans (4) points out that the fact that dissolution in a particular medium, say ferric chloride solution, is diffusion-controlled, does not in itself afford evidence that the reaction is chemical rather than electrochemical; it is still legitimate to divide it into anodic and cathodic reactions. In the theory of "mixed-potential" the condition for diffusion control is clearly and unambiguously defined (2).

At 12,700 cm/min and in the presence of depolarizers, the acid reaction (displacement of hydrogen) was less than 5% of the total, except at very small depolarizer concentrations where it amounted to about 10–15%. At 20,000 cm/min these percentages were smaller.

Current-Potential Relations

The variation of potential with time in the presence of potassium dichromate and at 12,700 cm/min is shown in Fig. 9. This plot is typical of the depolarizers used.

A plot of the potential at the 9th min against the logarithm of solution current density is given in Fig. 10. Current density was calculated from weight loss, assuming a roughness factor of 4.0 and uniform solution rate over the 10 min interval. This is not strictly correct since the depolarizer concentration decreases with time, but at small solution rates the decrease in depolarizer concentration is small, and the approximation is justified.

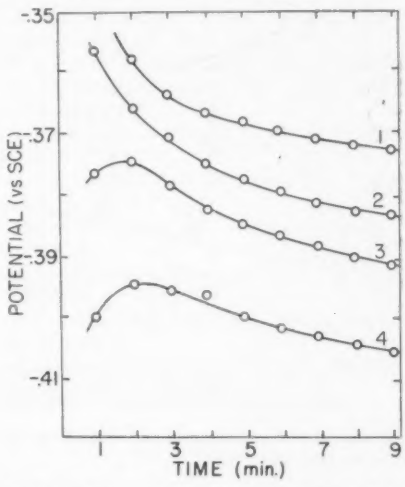

FIG. 9. Time-potential curves at 2180 rpm and at $K_2Cr_2O_7$ concentrations. Curve 1—5.0mM; curve 2—10.0mM; curve 3—15.0mM; curve 4—20.0mM.

It should be noted that in Fig. 10 points from all depolarizers at a given speed fall on the same straight line. Points with ceric sulfate did not fall on the curves and are not shown. In this case hydrochloric acid-sulfuric acid mixtures, 2*N* in total acidity, were used, and these results are therefore not directly comparable with the others.

A schematic representation of current-potential relations for dissolution in the presence of de-

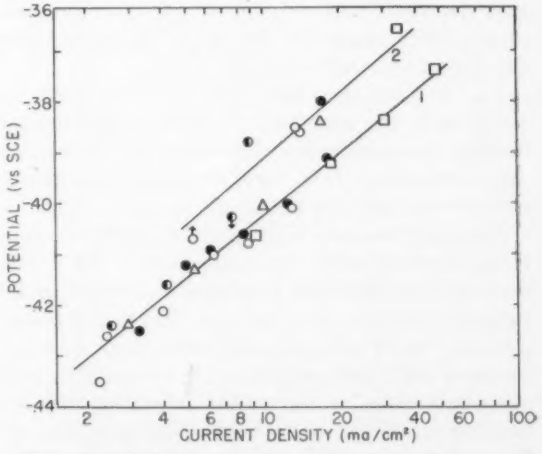

FIG. 10. Solution potential as a function of log current density (calculated from weight loss). ○—$FeCl_3$; ●—benzoquinone; △—tolu-*p*-quinone; ◐—sodium anthraquinone sulfonate; □—$K_2Cr_2O_7$. 1—12,700 cm/min; 2—20,000 cm/min.

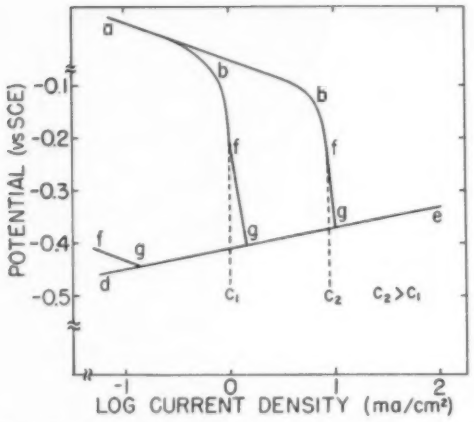

FIG. 11. Schematic representation of current-potential relations in air-free solutions.

polarizers is given in Fig. 11. Curve abc_1 is the cathodic polarization curve for reduction of depolarizer and de is the anodic polarization curve. The reaction is under diffusion control only if curve de intersects abc_1 at potentials more negative than that at point b. Curve fg is the polarization curve for hydrogen evolution. It is drawn with a slope of about 0.12.[6] Since the current accounted for by hydrogen deposition is small compared to the total, the exact shape of the hydrogen evolution curve is of secondary importance.

An increase in depolarizer concentration shifts the curve as shown in Fig. 11. It can be seen that a plot of potentials determined at various depolarizer concentrations against current density would give approximately a polarization curve for the anodic reaction. Occurrence of the hydrogen reaction makes this interpretation somewhat uncertain at small current densities; however, its contribution becomes progressively smaller (in relation to the total) as the depolarizer concentration is increased.

Fig. 10 gives the relation between measured potential and the logarithm of the solution current density. The straight line obtained at 12,700 cm/min can be considered, from the above arguments, to be a polarization curve for the anodic reaction.

A straight line was also obtained at 20,000 cm/min. It has approximately the same slope as at 12,700 cm/min but is displaced by a constant amount in the cathodic direction. It is believed that this displacement is caused by a zeta potential drop. The potential of mild steel coupons in 2*N* hydrochloric acid alone is displaced in the cathodic direction with increasing rotational speed. This is shown in Fig. 12. Since the composition of the diffuse part of the electrical double layer is approximately the same in the absence and in the presence of depolarizers (in

[6] The polarization curve for hydrogen deposition on iron was calcuated from the data of Hickling and Salt (16).

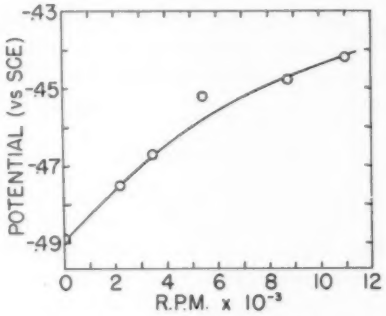

FIG. 12. Solution potential of mild steel in 2*N* HCl as a function of speed of rotation.

view of the large excess of hydrochloric acid) a similar potential shift on rotation in solutions containing depolarizers is to be expected.

The potential shift on rotation is of the right order of magnitude to be considered a zeta potential effect. It is unlikely that it is related to diffusion of ferrous or hydrogen ion since ferrous ion did not influence the potential and since the solution rate in hydrochloric acid alone was independent of stirring speed.

Returning to Fig. 10, the equation followed at 12,700 cm/min is

$$\text{Potential} = -0.44_2 + 0.04_0 \log i \qquad \text{(IV)}$$

where i is the current density in ma/cm². This equation is in reasonable agreement with the one obtained for iron in acid alone [see equation (II)].

Kuznesov and Iofa (17) and Kabanov, Burstein, and Frumkin (18) report a linear increase of potential with the logarithm of current density on anodic polarization of iron. The slope of the curve obtained by the former authors (17) was 0.07 in *N* hydrochloric acid. The slope obtained by Kabanov, Burstein, and Frumkin (18) in neutral or alkaline solutions containing chloride ions was approximately the same. The latter authors state that overvoltage values decreased with increasing chloride ion concentration. Our interpretation of the potential-solution rate curves appears therefore to lead to numerical values of the coefficient of the logarithmic term that are in reasonable agreement with direct measurement.

ACKNOWLEDGMENT

The authors gratefully acknowledge financial assistance from the Office of Ordnance Research under contract DA 23-072-ORD-216.

Any discussion of this paper will appear in a Discussion Section, to be published in the June 1956 JOURNAL.

REFERENCES

1. W. R. WHITNEY, *J. Am. Chem. Soc.*, **25**, 394 (1903).
2. C. WAGNER AND W. TRAUD, *Z. Elektrochem.*, **44**, 391 (1938); I. M. KOLTHOFF AND C. S. MILLER, *J. Am.*

Chem. Soc., **62**, 2171 (1940); J. V. Petrocelli, *This Journal*, **97**, 10 (1950).
3. H. S. Harned and R. W. Ehlers, *J. Am. Chem. Soc.*, **54**, 1350 (1932); **55**, 652, 2179 (1933).
4. U. R. Evans, "Metallic Corrosion, Passivity, and Protection," pp. 196–226, Edward Arnold Co., London (1937).
5. S. Ram, *J. Soc. Chem. Ind.*, **54**, 107 (1935).
6. C. H. Welling, R. P. Russel, and W. C. Whitman, *Ind. Eng. Chem.*, **15**, 672 (1923).
7. Ya. V. Durdin and M. A. Oranskaya, *Zhur. Obschei Khim.*, **21**, 604 (1951).
8. A. K. Krasil'shchikov, *ibid.*, **14**, 261 (1944).
9. J. O'M. Bockris, *Chem. Rev.*, **3**, 525 (1948); *see* also reference (16).
10. H. H. Uhlig, *Proc. Nat. Acad. Sci.*, **40**, 276 (1954).
11. W. M. Lattimer, "Oxidation States of the Elements and Their Potentials in Aqueous Solutions," p. 231, Prentice Hall, Inc., New York (1938).
12. C. V. King, "Pittsburgh International Conference on Surface Reactions," p. 5, Corrosion Publishing Co., Pittsburgh (1948).
13. M. B. Abramson and C. V. King, *J. Am. Chem. Soc.*, **61**, 2290 (1939).
14. R. G. van Name and D. U. Hill, *Am. J. Sci.*, **42**, 301 (1916).
15. M. Hochberg and C. V. King, *This Journal*, **97**, 191 (1950).
16. A. Hickling and F. W. Salt, *Trans. Faraday Soc.*, **36**, 1226 (1940).
17. V. A. Kuznesov and Z. A. Iofa, *J. Phys. Chem.* (*USSR*), **21**, 201 (1947).
18. B. Kabanov, R. Burstein, and A. Frumkin, *Disc. Faraday Soc.*, **1**, 259 (1947).

A Method for the Isolation of Surface Films from Aluminum Alloys and the Mechanism of the Reactions Involved[1]

M. J. Pryor and D. S. Keir

Kaiser Aluminum and Chemical Corporation, Spokane, Washington

ABSTRACT

Warm solutions of iodine in methanol were found satisfactory for isolating surface films from aluminum alloys not containing copper. Addition of sulfosalicylic acid to these solutions renders them satisfactory for isolation of films from aluminum-copper alloys. Attack is not selective at the film-metal interface, so all aluminum must be dissolved before uncontaminated films can be obtained. Hydrogen evolved during dissolution of the aluminum is believed due to the formation of aluminum methoxide. Iodide ions are also formed in these solutions. Aluminum methoxide is insoluble in dehydrated solutions but is decomposed by traces of water to soluble reaction products. A mechanism for the dissolution of aluminum in iodine-methanol solutions is suggested.

Introduction

Isolation of surface films from metals is a valuable tool for studying certain corrosion reactions. Although several techniques are available for isolating surface films from aluminum alloys, some are unsatisfactory because they yield contaminated films, and others because they involve highly toxic chemicals.

In the electrochemical method (1), specimens are subjected to anodic attack which dissolves the metal electrochemically from the surface film. This method is time-consuming and often leaves residual spots of metal. The saturated mercuric chloride (2, 3) and metallic mercury (4) methods depend on preferential corrosion of the film/metal interface by metallic mercury. Contamination limits the use of these methods since insoluble hydrated alumina is formed as a corrosion product. Dry hydrogen chloride at 300°–400°C (5) is effective for the rapid removal of aluminum from surface films. However, it is inconvenient to use, and the high temperature can result in transformation of films that are stable at low temperatures only. A solution of iodine in methanol was developed by Rooney and Stapleton (6), and has been successfully used for rapid and quantitative isolation of surface films from steel and stainless steel (7–9). The solution selectively attacks the film/steel interface, so that the film can be removed before the steel is completely dissolved. Under deaerated conditions this anhydrous solution prevents contamination of surface films with hydrated corrosion products. Use of iodine-methanol solutions on aluminum alloys demonstrated that all the aluminum must be dissolved before clean films could be obtained (10). It was suggested that air need not be excluded during film isolation from aluminum, but it was not found possible to obtain uncontaminated films from aluminum alloys containing large additions of copper or silicon. The same authors (10) indicated that a solution of bromine in methanol containing 1% water resulted in a faster isolation of surface films from aluminum alloys.

Since excellent results were obtained previously on other metals using nonaqueous solutions containing either iodine or bromine, a suitable method of isolating surface films from aluminum alloys with similar solutions was investigated. Furthermore, since bromine is not as convenient for general use as iodine, this work was confined to iodine-methanol solutions, although satisfactory film isolation with methanol-bromine solutions has been reported (11). In addition, the mechanism by which aluminum dissolved in these solutions was investigated since there have been little published data on this subject.

Method of Isolating Surface Films from Aluminum Alloys

All chemicals were of C.P. quality. The absolute methanol used had the following composition: acetone and aldehydes, 0.001% maximum; acidity (as formic acid), 0.002%; alkalinity (ammonia), 0.0003%; residue after evaporation, 0.001% maximum; water, 0.1% maximum.

The water content was typical of so-called "absolute" methanol and represents about the minimum concentration obtainable without additional drying.

High purity aluminum as cold-rolled, ¾ hard sheet, 0.16 cm thick had the following analysis: silicon, 0.0015%; iron, 0.001%; copper, 0.001%; balance, aluminum.

[1] Manuscript received November 10, 1954. This paper was prepared for delivery before the Boston Meeting, October 3 to 7, 1954.

TABLE I. *Composition of the aluminum alloys whose rates of solution in iodine/methanol are shown in Fig. 2 and 3*

Alloy	Temper	Wt %						
		Si	Fe	Cu	Mn	Mg	Cr	Zn
1100	H14	0.11	0.54	0.14	0.01	Tr	0.00	0.00
3003	H14	0.19	0.54	0.13	1.08	0.01	0.00	0.00
2024	T3	0.13	0.27	4.36	0.56	1.60	0.01	0.03
4043	H14	4.98	0.24	—	—	—	—	—
5050	H34	0.22	0.47	0.12	0.02	1.38	—	—
5052	H34	0.07	0.20	0.05	0.00	2.36	0.21	0.04
5056	H16	0.10	0.19	0.02	0.11	4.86	0.10	0.00
6061	T6	0.63	0.43	0.31	0.05	0.88	0.26	0.02
7075	0	0.11	0.26	1.63	0.01	2.60	0.25	5.69

Compositions of aluminum alloys used are shown in Table I.

Preliminary experiments were carried out at room temperature in Petri dishes using 1 cm² specimens of high purity aluminum. To observe better the progress of film isolation, specimens were anodized in sulfuric acid, dyed, and sealed. Scratch lines were ruled through the anodic coating in order to expose aluminum to the iodine-methanol solution (10 g iodine/100 ml absolute methanol). Although dissolution of the aluminum occurred slowly at room temperature, there was no preferential corrosion along the aluminum/film interface. After exposure periods of about 24 hr the aluminum was completely dissolved and the anodic film could be removed. The reaction products were completely soluble in the solution. The observation by previous workers that all the aluminum must be dissolved before the films could be obtained in the uncontaminated condition (10) was confirmed. Despite the fact that a wide variety of iodine contents and temperatures were investigated, no evidence of selective attack at the film/aluminum interface was observed. However, continuous evolution of gas always accompanied dissolution of the aluminum. Solutions from separate experiments together with any residue were carefully examined at a magnification of 500 diameters to determine whether any "spurious"[2] or secondary films were formed as a contaminant during the dissolution of the aluminum. In no case were these spurious films detected.

The experiments described above were next repeated at 50°C and in boiling iodine-methanol solutions. The dissolution rate of aluminum was greatly increased, and a brisk evolution of gas occurred at 50°C. In boiling solutions the aluminum was destroyed even more rapidly, but violent gas evolution shattered the films. Consequently, boiling iodine-methanol solutions are unsatisfactory unless the films are supported by some means. However, even where relatively thick anodic films were supported with plastic films appreciable disintegration occurred in boiling solutions. Therefore, further work was confined to solutions at lower temperatures.

The action of iodine-methanol solutions was investigated at 50°C on aluminum alloys 1100, 3003, 2024, 4043, 5050, 5052, 5056, 6061, and 7075 (see Table I for chemical compositions), carrying surface films ranging from air-formed oxide films through films of increasing thickness formed in various passivating solutions to very thick anodic films. Excellent film isolation could be obtained from the alloys 1100, 3003, 5050, 5052, 5056, and 6061 of 0.16 cm thickness within a 4–8 hr period; Fig. 1 (*a*) shows a colored anodic film isolated from high purity aluminum. The copper-containing alloy, 2024, yielded films contaminated by metallic copper at 50°C and by cuprous iodide at 25°C, whereas the silicon-containing alloy 4043 yielded films contaminated by silicon. Silicon contamination was overcome by supporting the surface films with vinyl or formvar films and removing loosely adhering silicon by washing with methanol or by brushing gently with a soft bristle brush.

In order to eliminate contamination of surface

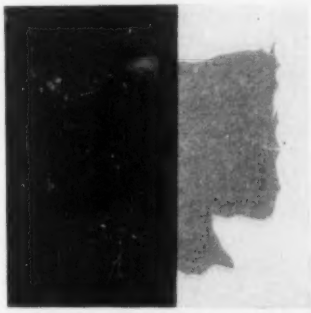

FIG. 1*a*. Surface films isolated from different aluminum alloys. Color anodized film from high purity aluminum.

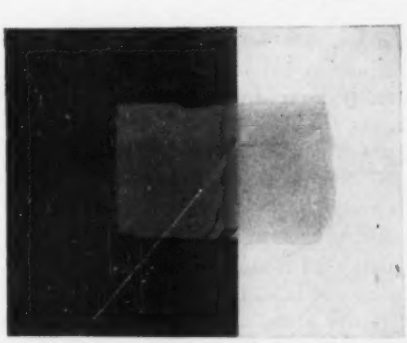

FIG. 1*b*. Anodic film from 2024 showing absence of copper and cuprous iodide.

[2] If the specimens are first abraded with emery paper, thin surface films carry abrasion marks inherited from the underlying metal. Secondary or spurious films are invariably free from these abrasion marks and thus can easily be distinguished from the original film.

films from aluminum-copper alloys, various additions were made to the original solution which would be expected to dissolve copper or cuprous compounds as soluble complexes. Additions of ethanolamine, triethanolamine, triethylamine, and ethylene diamine proved to be ineffective at keeping the copper completely in solution. Furthermore, they very greatly reduced the dissolution rate of aluminum-copper alloys. Dithizon (diphenyl thiocarbazone) was reasonably effective when added in concentrations of 0.05 g/100 ml solution in that it prevented precipitation of cuprous iodide for a period of about 30 min. However, sulfosalicyclic acid ($C_7H_6O_6S \cdot 2H_2O$) proved to be by far the most effective of these additions in forming soluble complexes with the copper in aluminum-copper alloys. Sulfosalicyclic acid is believed to form a 1:1 complex with copper in acidic solutions and a chelate containing double this proportion of sulfosalicyclic acid in alkaline solutions (12) (pH = 9.0). It is also capable of forming a complex with zinc (13) and is thus very useful for film isolation from such alloys as 7075. It was determined that additions of sulfosalicyclic acid should be used on aluminum alloys containing more than 1% copper. Fig. 1 (*b*) shows an anodic film that was isolated from 2024 by this method and emphasizes the lack of contamination. The presence of sulfosalicyclic acid in a solution of 10 g iodine in 100 ml absolute methanol does not entirely prevent formation of cuprous iodide at 25°C or that of metallic copper at 50°C because the aluminum dissolves much faster than the copper. However, once all the aluminum is dissolved, the contaminant, either cuprous iodide or copper, will then dissolve, yielding uncontaminated films. Addition of 3 g sulfosalicyclic acid/100 ml of the original iodine-methanol solution is recommended for this procedure.

However, to prevent contamination entirely, the action of the iodine-methanol solution on the aluminum must be reduced in rate. This can be achieved by using a solution containing 2.5 g iodine and 3.0 g sulfosalicyclic acid/100 ml absolute methanol at 25°C. Although this solution attacked aluminum-copper alloys much more slowly, the dissolution rate of the aluminum did not exceed that of the copper. Consequently, no contamination was obtained at any stage during the dissolution of the alloy. This procedure, which is suitable for alloys of the 2024 and 7075 types, is best used when freedom from contamination is mandatory.

Subsequent experiments, described in the next section, indicated that:

1. The rate of attack of iodine-methanol solutions on high purity aluminum increases with increasing iodine concentration and with increasing temperature. A solution containing 10 g iodine/100 ml absolute methanol is the optimum concentration for most film isolation.

2. If the solution is dried, or if access of moisture from the atmosphere is prevented, precipitation of bulky aluminum methoxide occurs and films are contaminated.

3. Addition of water to the iodine-methanol solution progressively reduces the rate of attack of the solution on the aluminum.

4. The dissolution rate of the aluminum is unaffected by the presence of dissolved oxygen.

Consequently, the best film isolation technique involves a solution containing 10 g iodine in 100 ml absolute methanol. 200 ml of solution should be used per gram of aluminum to be dissolved. The reaction should be carried out in contact with the atmosphere at about 50°C.

Film isolation can be performed most conveniently on foil specimens since the weight of metal to be dissolved is small. Thicker sections are best handled by grinding down one surface of the specimen. For very rapid film isolation the final thickness of the specimen should not exceed about 0.05 cm. The side of the specimen carrying the film can be cemented face downward with a vinyl chloride-vinyl acetate adhesive or with Formvar to a polyethylene holder. The holder was rigid in the case of foil, but polyethylene tissue was used for thicker specimens. The vinyl adhesives will withstand attack by the iodine-methanol solutions, but can be dissolved slowly by acetone or methyl-ethyl ketone. Specimens, cemented to polyethylene, can be exposed to the solution until all the aluminum is dissolved. This requires 1–2 hr for foil specimens and 4–8 hr for specimens prepared from the thicker sections. The polyethylene holders

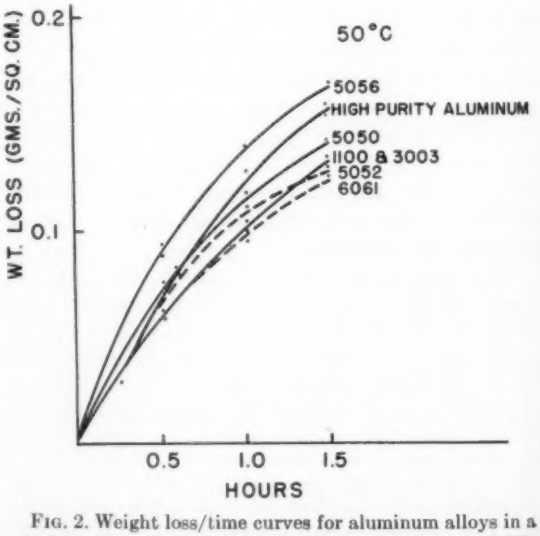

FIG. 2. Weight loss/time curves for aluminum alloys in a solution of 10 g iodine in 100 ml absolute methanol at 50°C.

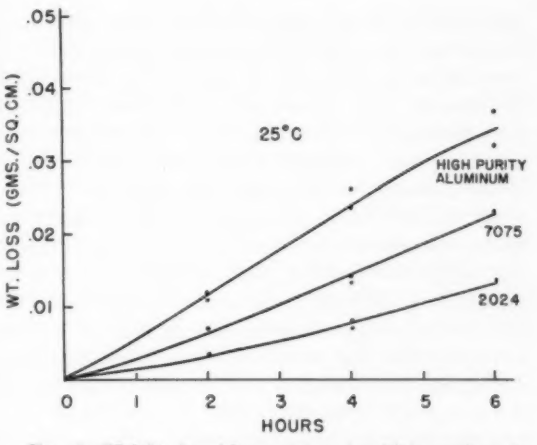

FIG. 3. Weight loss/time curves for high purity aluminum, 2024 and 7075 in a solution containing 2.5 g iodine and 3.0 g sulfosalicylic acid in 100 ml absolute methanol at 25°C.

and the films can be washed in methanol and the films subsequently removed by treatment with acetone or methyl-ethyl ketone.

The time taken for complete aluminum dissolution varies not only with the weight of metal but also with the alloy. Dissolution rates of aluminum alloys were determined at 50° ± 0.2°C in a solution of 10 g iodine in 100 ml absolute methanol. 100 ml of solution per specimen (1.5 x 1.5 x 0.16 cm) was employed. Triplicate experiments were performed under reflux to prevent loss of solution. Results are shown in Fig. 2, which indicates that 5056 is most readily attacked (probably because of the ease of formation of magnesium methoxide) and 6061 least readily attacked by this solution. The rate of attack on other aluminum alloys is very similar to that on high purity aluminum. Fig. 3 shows weight loss/time curves for the dissolution of 2024, 7075, and high purity aluminum in a dilute iodine-methanol solution containing sulfosalicylic acid. Here it is evident that both 2024 and 7075 are somewhat less readily attacked than high purity aluminum. However, the dissolution rate is high enough to permit film isolation in a reasonable length of time from thin specimens. This method will easily isolate, from any aluminum alloy, all surface films that are not affected by this reagent.

MECHANISM OF DISSOLUTION OF ALUMINUM IN IODINE-METHANOL SOLUTIONS

Experimental

Examination of gas evolved during dissolution of high purity aluminum.—It was noticed previously that dissolution of aluminum and aluminum alloys in iodine-methanol solutions was invariably accompanied by gas evolution. Furthermore, as the dissolution rate of aluminum increased the rate of gas evolution also appeared to increase. Gas evolution is not observed when similar solutions act upon steel, so it was felt that identification of this gas might throw considerable light on the mechanism of aluminum dissolution. Large volumes of the gas were collected by displacement over water from a refluxed reaction mixture containing 20 g iodine, 200 ml absolute methanol, and 1.8 g aluminum; air was expelled from the apparatus before any gas was collected. The gas could be ignited in air, and it did not contain detectable quantities of hydrogen iodide, saturated or unsaturated hydrocarbons, or carbon dioxide.

Gas analyses by ignition demonstrated that the gas was hydrogen. Tests on gas evolved from a similar reaction mixture that was not refluxed gave the same results. Consequently, it was believed that this hydrogen resulted largely from the interaction of aluminum and methanol catalyzed by the presence of iodine, possibly according to an equation such as:

$$6CH_3OH + 2Al = 2Al(OCH_3)_3 + 3H_2 \quad (I)$$

Investigations of the formation of aluminum methoxide.—Since it appears possible that aluminum methoxide might be formed as a reaction product, an attempt was made to prepare this compound in an independent manner in order to study its properties. In general such alkoxides can be prepared by the interaction of the metal and boiling alcohol in the presence of a trace of iodine and mercuric chloride (14). Since alkoxides are believed to be sensitive to water, which may cause them to decompose into the alcohol and hydrated metal oxide, absolute methanol was first dried by refluxing for 1 hr with magnesium turnings and a trace of iodine. The dried methanol was then distilled into the reaction vessel without atmospheric contact.

The reaction vessel consisted of a three-necked flask fitted with a condenser and side arm (Fig. 4). The flask contained 2 mg dried iodine and 5 mg dried mercuric chloride. A weighed aluminum specimen (1.5 x 1.5 x 0.16 cm) was suspended in a glass cradle which could be lowered into the solution by rotating the glass windlass to which it was attached by a nylon thread (Fig. 5).

100 ml dried methanol was distilled into the reaction vessel. Two drying tubes containing calcium chloride were situated between the reaction vessel and the gas collection cylinder to prevent access of water vapor. The flask was disconnected from the distillation train, and partly immersed in a water bath maintained at 50° ± 0.2°C; after the solution had come to temperature, the specimen was lowered into it; gas evolution began almost immediately. The experiment lasted 2 hr and the total volume of gas

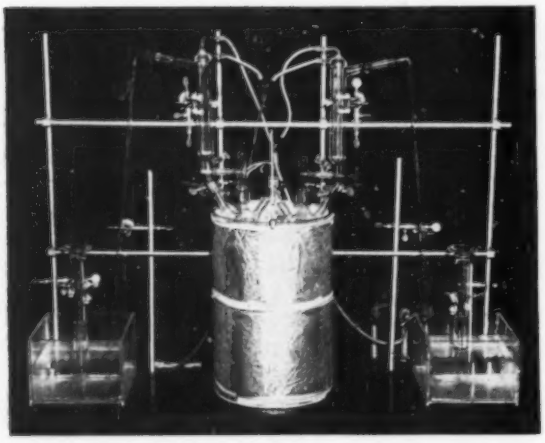

FIG. 4. Apparatus for determination of weight loss and volume of hydrogen.

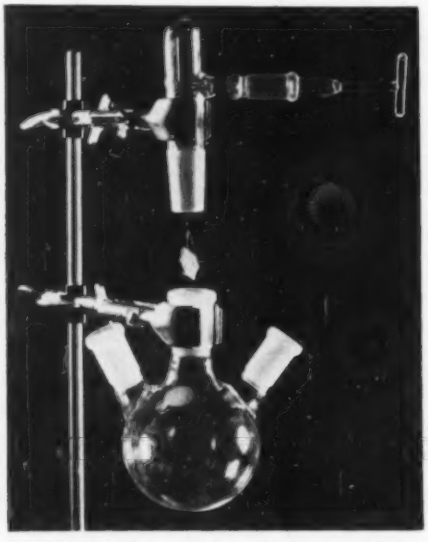

FIG. 5. Method of mounting and adjusting the specimen in the apparatus shown in Fig. 4.

evolved was determined at S.T.P. The specimen was cleaned in cold concentrated nitric acid and reweighed. Corrosion of the aluminum resulted in the formation of a voluminous white product which appeared to be insoluble in methanol. The gas was again found to be hydrogen, and calculation from the volume evolved indicated that, within the limits of experimental error, the aluminum had been corroded as aluminum methoxide.

The white product was filtered from solution and dried over calcium chloride in a desiccator. The methanol solution was then tested for soluble aluminum compounds; none was detected. The white product was insoluble in methanol and was not dissolved by a fresh solution of iodine in methanol. However, the white product could be dissolved in benzene as suggested by Hickinbottom (14). Since hydrated alumina is insoluble in benzene, it appears that the white product formed by the interaction of aluminum and methanol in the presence of traces of iodine and mercuric chloride is aluminum methoxide.

Samples of the reaction product which had been dried over calcium chloride for 6 hr were ignited and the weights of alumina, carbon dioxide, and water determined. The compound exploded when heated rapidly but, when heated more gradually, results were obtained that were consistent with aluminum methoxide contaminated with methanol. Samples of the compound that were dried for one week over calcium chloride contained about 40% aluminum methoxide and 60% alumina which presumably came from decomposition of the aluminum methoxide. These experiments confirm the suggestion that this corrosion product is aluminum methoxide and indicate that it is extremely easily decomposed by moist air and by heating. Attempts to determine a melting point on this compound were not successful as it decomposed when heated gently.

Action of absolute methanol on high purity aluminum.—To determine whether dried or absolute methanol alone had any action on aluminum, experiments similar to those described above were carried out except that iodine and mercuric chloride were not added. In no case was any detectable weight loss observed or any hydrogen evolved within a tempera-

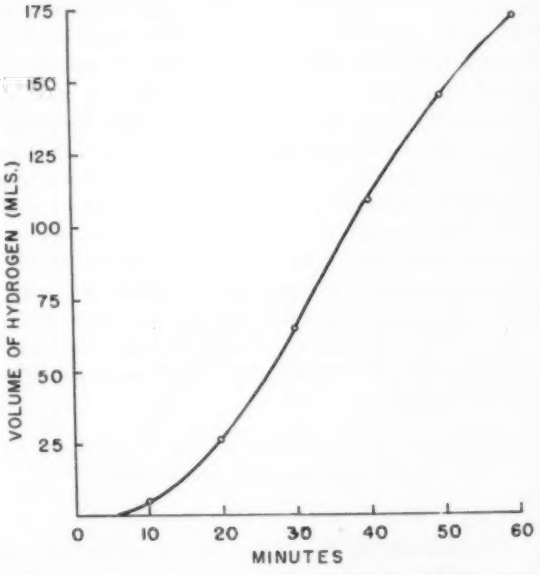

FIG. 6. Curve showing variation of volume of hydrogen with time on exposing high purity aluminum to an anhydrous solution of 5 g iodine in 100 ml dry methanol.

ture range of 25°–50°C. It was concluded that, within the temperature range studied, methanol in the absence of iodine had no action on aluminum.

Action of dried iodine-methanol solutions on high purity aluminum.—Since aluminum methoxide is insoluble in methanol, although soluble in benzene, the question arises as to whether this compound is formed in iodine-methanol solutions, since no insoluble reaction products were detected in solutions of iodine in absolute methanol which had reacted with aluminum in contact with the atmosphere. Since this absolute methanol contained around 0.1% water and undoubtedly picks up additional water from contact with the atmosphere, experiments under dehydrated conditions were next carried out.

The apparatus shown in Fig. 4 was used again. A weighed aluminum specimen was introduced into the reaction vessel together with 5 g dried iodine. Methanol was dried and introduced as described previously. The experiments were carried out at 50° ± 0.2°C. Fig. 6 shows the volume of hydrogen evolved as a function of time. A whitish coating quickly covered the specimen and flaked off intermittently. After 1 hr, 172 ml of hydrogen (S.T.P.) was evolved, which is equivalent to the calculated dissolution[3] of 0.139 g aluminum via the formation of aluminum methoxide (or by any reaction in which the equivalent weight of aluminum is 9). The measured weight loss of the aluminum was 0.234 g, which indicates that aluminum was being destroyed by more than one reaction. This experiment was repeated several times, and the presence of an insoluble white compound formed under dehydrated conditions was confirmed.

Additional experiments were carried out in a solution of 5 g iodine in 100 ml absolute (undried) methanol with the access of moisture prevented, as before. Large quantities of an insoluble whitish compound, similar to that observed under more truly anhydrous conditions, were formed. It was found that the solution after reaction with an aluminum specimen for 1 hr gave a *p*H reading of 2.1 with a glass electrode and calomel half-cell. On the addition of several drops of water to a portion of the solution, the compound dissolved very rapidly and the *p*H of the solution increased to 3.5. Further small additions of water caused no precipitation of hydrated alumina or of iodine, but large additions of water resulted in the separation of hydrated alumina. Addition of even small volumes of water to a solution of iodine in methanol that had not reacted with aluminum resulted in almost immediate precipitation of iodine. This indicates that reaction of the solution with aluminum results in the formation of appreciable quantities of iodide ion, which stabilizes the iodine and prevents its immediate precipitation on the addition of water.

A further portion of the solution was filtered, and the white residue was washed with dried methanol and dissolved in benzene. Large quantities of aluminum ion were subsequently extracted from the benzene by dilute hydrochloric acid.

These tests indicate that the insoluble corrosion product formed in dried iodine-methanol solutions was aluminum methoxide. This was confirmed by chemical analysis which showed that, after drying over calcium chloride for one week, the sample contained about 40% aluminum methoxide and some hydrated aluminum, probably due to a partial decomposition of the methoxide. Storage of the dried product in a closed weighing bottle in contact with undried air again resulted in the formation of methanol droplets.

Action of iodine-absolute methanol solutions on high purity aluminum in contact with the atmosphere.—The experiments described above indicate that the reaction between aluminum and iodine-methanol solutions under dehydrated conditions leads to the formation of insoluble aluminum methoxide as one of the products of reaction. From the standpoint of film isolation, this is clearly undesirable since surface films isolated under these conditions will be contaminated unless a further operation such as treatment with water or with a dilute acid is carried out. However, it was observed previously that when no special precautions were taken to avoid traces of water or contact with the atmosphere, other than keeping the methanol in tightly stoppered bottles and using dry apparatus, the reaction products were completely soluble and excellent film isolation was obtained. Consequently, the rate of solution of high purity aluminum was determined in iodine-methanol solutions that were not specially dried or kept out of contact with the atmosphere. The following variables were investigated: surface pretreatment; volume of solution; temperature; iodine concentration; water additions; and dissolved oxygen.

In addition, experiments were performed to determine the nature of the reaction products with a view to advancing a tentative mechanism of reaction.

The effect of surface pretreatment on the form of the weight loss-time curves was first investigated. Weight losses on triplicate specimens were determined as a function of time in Erlenmeyer flasks fitted with reflux condensers. The flasks were placed in a water bath thermostatted at 25° ± 0.2°C; 50 ml of the solution of 10 g iodine in 100 ml absolute methanol was used for each specimen. The surface pretreatments investigated were: degreasing alone; etching in 20% sodium hydroxide; etching in ½%

[3] Specimens were cleaned in cold concentrated nitric acid before weighing.

TABLE II. *Effect of surface pretreatment on weight losses at 25°C in a solution containing 10 g iodine/100 ml absolute methanol; 50 ml solution/specimen*

Surface pretreatment	Wt loss (g/cm²)											
	1 hr			2 hr			4 hr			6 hr		
Degreased in benzene	0.023,	0.025,	0.028	0.063,	0.065,	0.060	0.103,	0.099,	0.101	0.121,	0.120,	0.123
Etched in sodium hydroxide	0.005,	0.004,	0.004	0.017,	0.016,	0.024	0.069,	0.058,	0.081	0.088,	0.103,	0.130
Etched in hydrofluoric acid	0.018,	0.012,	0.012	0.035,	0.043,	0.048	0.093,	0.103,	0.092	0.129,	0.123,	0.117
Electropolished	0.001,	0.0005,	0.0005	0.004,	0.005,	0.011	0.040,	0.026,	0.042	0.042,	0.124,	0.087
Abraded under alcohol	0.030,	0.032,	0.032	0.062,	0.062,	0.062	0.104,	0.106,	0.100	0.132,	0.121,	0.120

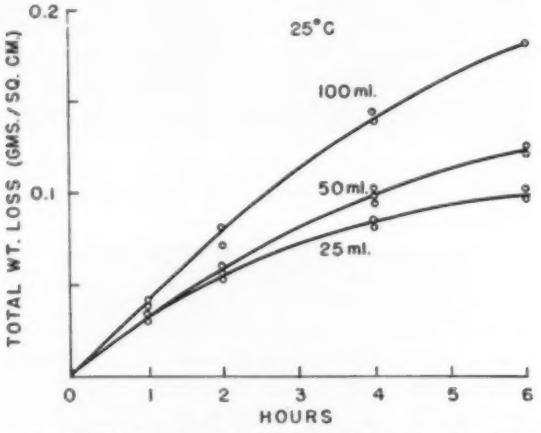

FIG. 7. Weight loss/time curves for high purity aluminum in different volumes of iodine methanol solution) 10 g/100 ml) at 25°C.

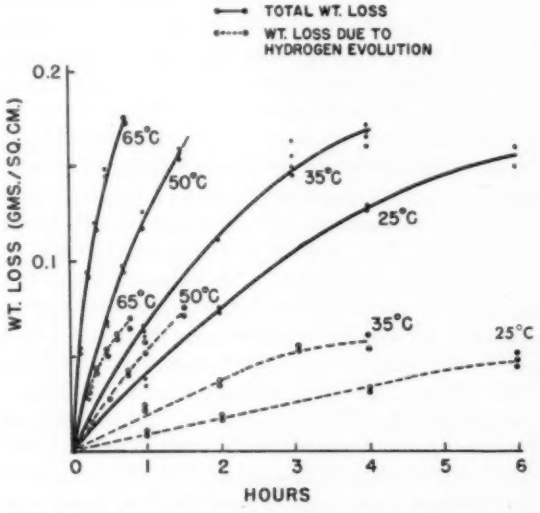

FIG. 8. Relationship between time, total weight loss, and weight loss due to hydrogen evolution at different temperatures in a solution containing 10 g I_2/100 ml absolute methanol.

hydrofluoric acid; electropolishing in 60% phosphoric acid with 40% sulfuric acid; and abrading with 320 grit emery paper under methanol.

In these experiments weight losses[4] alone were determined. The results (Table II) show that the most reproducible weight losses and the smallest induction periods were obtained after abrasion under methanol. Consequently, this surface pretreatment was used in subsequent experiments described in this section.

Experiments were next performed to determine the effect of different volumes of solution on the dissolution rate of aluminum. These experiments were performed in triplicate at 25° ± 0.2°C using solutions containing 10 g iodine/100 ml absolute methanol. The volume of solution varied between 25 ml/specimen and 100 ml/specimen. The results (Fig. 7) show that the dissolution rate has less tendency to decrease with time in larger volumes of solution. This suggests that the dissolution rate of aluminum is largely controlled by the volume of the solution. Consequently, 100 ml solution/specimen was used in subsequent experiments.

The effect of temperature within the range 25°–65°C was next investigated. In this case, weight losses and volumes of hydrogen evolved were determined using the apparatus shown in Fig. 4; drying tubes were not inserted between the reaction vessel and the gas collection cylinder. Temperatures were controlled at 25°, 35°, 50°, and 65°C ± 0.2°C by means of a thermostatted water bath. Solutions containing 10 g iodine in 100 ml absolute methanol were used. Each experiment required 100 ml of solution/specimen. The results (Fig. 8) show that the dissolution rate of aluminum and the rate of hydrogen evolution increased with increasing temperature.

Similar experiments were carried out to determine the effect of iodine concentration at temperatures of 25° and 50°C (±0.2°C) using 100 ml solution/specimen and iodine concentrations of 0, 2.5 g, 5.0 g, 7.5 g, and 10.0 g/100 ml methanol. The results (Fig. 9 and 10) confirm the previous observation that methanol alone has no detectable action on alu-

[4] Initially, specimens were cleaned in either cold concentrated nitric acid or warm chromic/phosphoric acid before weighing. Experiments indicated that, in the absence of insoluble reaction products, these cleaning operations were unnecessary.

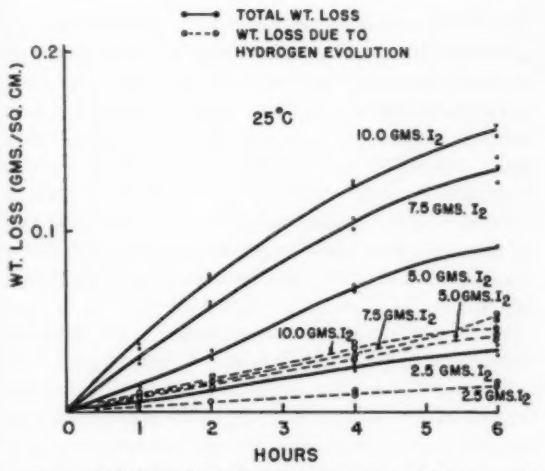

FIG. 9. Relationship between time, total weight loss, and weight loss due to hydrogen evolution at different iodine concentrations at 25°C.

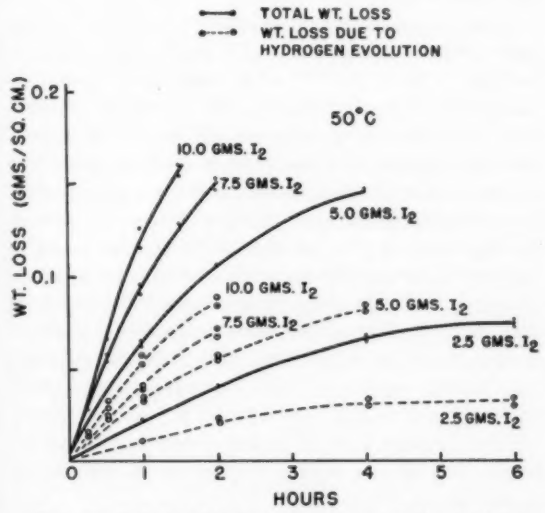

FIG. 10. Relationship between time, total weight loss, and weight loss due to hydrogen evolution at different iodine concentrations at 50°C.

minum. They also demonstrate that the dissolution rate of aluminum increases markedly with increasing iodine concentration. Calculations based on the initial slopes of these curves indicate that aluminum dissolution is first order with respect to iodine. Furthermore, the rate of hydrogen evolution increases with increasing iodine concentration, especially at 50°C.

Experiments were next carried out to determine the effect of water on the dissolution rate of aluminum. Variation of both weight loss and hydrogen evolution with time was first determined at 50°C in a solution containing 10 g iodine in 100 ml methanol containing 1% by volume of water. The results

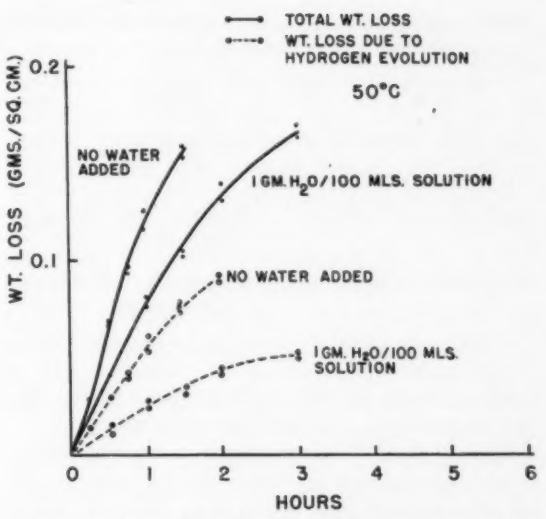

FIG. 11. The effect of 1% by volume of water on the weight loss/time curve and on the weight loss due to hydrogen evolution/time curve for high purity aluminum in a solution containing 10 g iodine in 100 ml absolute methanol at 50°C.

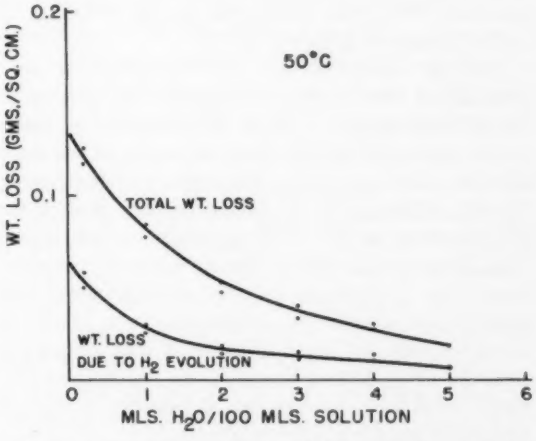

FIG. 12. The effect of water additions on the total dissolution and the weight loss due to hydrogen evolution of aluminum in a solution of 10 g I_2 in 100 ml absolute methanol at 50°C.

(Fig. 11) indicate that water additions reduced the weight losses of the specimens and the volumes of hydrogen evolved.

Additional experiments were carried out with water contents varying between 0 and 5 % by volume. The temperature of these experiments was 50°C, the duration 1 hr, and the iodine concentration of the solution was 10 g/100 ml. At the end of each experiment, weight losses and volumes of hydrogen were measured and the free iodine contents of the solutions were determined. The results (Fig. 12) showed that increasing the water content of the

TABLE III. *Effect of oxygen on the attack of iodine/methanol solutions on high purity aluminum in 1 hr*

Concentration of solution	Temp, °C	Conditions of experiment	Wt loss g/cm²
10 g I_2/100 ml CH_3OH	50°C	No bubbling	0.126
			0.117
			0.117
10 g I_2/100 ml CH_3OH	50°C	Nitrogen bubbled continuously	0.121
			0.116
			0.112
10 g I_2/100 ml CH_3OH	50°C	Oxygen bubbled continuously	0.117
			0.124
			0.122

solution decreased the dissolution rate of the aluminum and the rate of hydrogen evolution.

The effect of dissolved oxygen on the dissolution rate of aluminum in a solution of 10 g iodine in 100 ml absolute methanol (containing 0.1% of water) was next determined at 50°C. Experiments were carried out in which either tank oxygen or tank nitrogen was bubbled continuously through the solutions; weight loss determinations alone were made. The results (Table III) indicate that the rate of reaction at 50°C was unaffected by the bubbling of either oxygen or nitrogen.

The *p*H values of many of the solutions were determined after they had reacted with aluminum for different lengths of time. The reaction mixtures in all cases exhibited an acidic reaction to the glass electrode and were within the apparent *p*H range of 1.5–2.5. Although it is quite doubtful that these measurements of *p*H in organic solutions truly represent the actual hydrogen ion activities of the solutions, they do indicate that the solutions are acidic rather than alkaline in character. As a result of titration with sodium hydroxide it was calculated that the *p*H values of the solutions were within the range 3.0–3.5. In no case was it possible to boil off any acidic gas from these solutions.

Volumetric determinations of free iodine (using sodium thiosulfate) and of iodide (using cupric sulfate and sodium thiosulfate) in these reaction mixtures gave checks to within 1% with the total weights of iodine present initially in the solutions. However, when the weight of aluminum associated with the iodide was calculated and added to the weight of aluminum associated with the hydrogen evolved, the total weight appreciably exceeded the weight loss of the specimen sometimes by as much as 15%. This indicates that, in the presence of small amounts of water, either hydrogen may evolve from reactions other than the formation of aluminum methoxide or initially one aluminum ion is associated with less than three iodide ions. However, in dried solutions the order of agreement between these calculated and measured quantities is much closer. For example, an aluminum specimen exposed to a solution of 5 g iodine in 100 ml dried methanol at 50°C for 1 hr showed a weight loss of 0.234 g. The aluminum associated with the iodide in solution (assuming that one aluminum ion is associated with three iodide ions) was 0.092 g, and that associated with the hydrogen evolved was 0.139 g, making a total of 0.231 g which is approximately 1.5% less than the total weight loss. This agreement is within the limits of experimental error of the weight loss determinations.

It has previously been suggested (15, 16) that the interaction of boiling methanol, aluminum, and iodine results in the formation of methyl iodide. Consequently, methyl iodide must be considered as a possible component of the reaction mixture. Its presence had not been detected in previous experiments since the water-cooled condensers which were used would prevent the escape of any methyl iodide from the reaction vessel.

Methyl iodide gives a precipitate of silver iodide with alcoholic silver nitrate (17) and forms a constant boiling mixture (39°C) with methanol containing 74.4 mole % methyl iodide (18). Therefore, a solution containing 10 g iodine in 100 ml absolute (undried) methanol that had been in contact with 0.9 g aluminum for 1 hr was distilled and the vapors passed into fresh alcoholic silver nitrate. It was found that a component of the solution distilled over at 39°C and gave a heavy precipitation of silver iodide when passed into the alcoholic silver nitrate. This indicates that methyl iodide is formed in this reaction mixture during its action on the aluminum. A similar solution was boiled vigorously and the gases passed into water. There was no decrease in *p*H of the water, which indicates that hydrogen iodide could not be boiled out of the reaction mixture in detectable quantities.

Similar experiments were carried out on solutions resulting from the interaction of aluminum, iodine, and dried methanol. Under these conditions it was not found possible to detect the presence of methyl iodide in the reaction mixtures. This indicated that methyl iodide was formed in detectable amounts only in solutions containing traces of water.

The presence of methyl iodide in reaction mixtures containing traces of water implies that formation of aluminum Grignard compounds such as CH_3AlI_2 is possible. However, such compounds would be expected to hydrolyze in the presence of water giving methanol (19), to combine with methanol to give methane (20), and to react with methyl iodide giving ethane (21). The fact that these saturated hydrocarbons were not detected in the gas evolved indicated that the formation of aluminum Grignard compounds is unlikely under these conditions.

Discussion

Isolation of surface films from steel by means of the iodine-methanol solution occurs by a selective attack on the film-metal interface. Although a mechanism for this reaction has not been advanced, the steel is probably dissolved as a soluble iodide. There is no detectable gas evolution during film isolation from steel. The attack of similar solutions on film-covered aluminum results in the brisk evolution of hydrogen which, in dehydrated solutions, is accompanied by the formation of aluminum methoxide. Because the volume of hydrogen evolved is insufficient to account for the entire weight loss of the specimen, this suggests that a portion of the aluminum is being dissolved as a soluble iodide. Subsequent analyses of the solutions for iodide confirmed this suggestion. Since the major difference between the action of the same solution on the two different metals is the formation of the aluminum methoxide and hydrogen, it is considered that this reaction is mainly the cause of the general dissolution of aluminum rather than a selective dissolution at the aluminum/film interface.

In dried iodine-methanol solutions, the calculated weight of aluminum equivalent to the hydrogen evolved plus the weight of aluminum equivalent to the measured iodide in solution (assuming one aluminum ion is associated with three iodide ions) checks to within 1.5% with the actual weight loss of the specimen. In no case, in dried solutions, was the presence of hydrogen iodide, methyl iodide, methane, or ethane detected. Consequently, the two reactions taking place under dehydrated conditions may be represented as follows:

$$2Al + 6CH_3OH = 2Al(OCH_3)_3 + 3H_2 \quad (II)$$

$$2Al + 3I_2 = 2AlI_3[\text{ or } 2Al^{+++} + 6I^-] \quad (III)$$

The reaction mixture is distinctly acidic to a glass electrode. This might conceivably be due to reaction of the methoxide with the alcohol (Meerwein reaction) to form an alkoxyacid which is believed to resemble sulfuric, phosphoric, and perchloric acids in its electronic configuration (22).

$$Al(OR)_3 + ROH = H^+[Al(OR)_4]^- \quad (IV)$$

This is considered to be unlikely in view of the insolubility of aluminum methoxide in methanol. Instead, any acidity in these solutions is more likely to be the result of a very slow reaction between hydrogen and iodine to form minute traces of hydrogen iodide which could not be detected chemically in the vapor from the solutions.

In the presence of water the reaction mechanism suggested above becomes greatly complicated; although the presence of several different reaction products has been established, the mechanism advanced must be regarded as speculative. When solutions of absolute methanol (containing 0.1% water) were used in contact with the atmosphere no insoluble corrosion products were obtained. However, hydrogen was still evolved briskly, although in smaller quantities than in dried solutions. Furthermore, the rate of hydrogen evolution increased with increasing iodine concentration at 50°C (Fig. 10) but was almost independent of the iodine concentration at 25°C (Fig. 9). This may indicate that, at the higher temperature, hydrogen is formed by other reactions in addition to the interaction of aluminum and methyl alcohol which might be expected to be independent of the iodine concentration.[5] Additional hydrogen could be generated by the interaction of aluminum with hydrogen iodide which might form as a product of hydrolysis of aluminum iodide. This belief was supported by the detection of methyl iodide in the solutions which must result from the interaction of hydrogen iodide and methanol.

Addition of a trace of water significantly reduces the rate of attack of the iodine-methanol solution on aluminum. The reason for this is not altogether clear, although cases have been recorded in which the corrosion of aluminum by an organic compound was greatly reduced by the presence of traces of water (23). This type of behavior has been believed to be associated with the formation of protective films of oxide or hydrated oxide by the traces of water (23, 24). However, this behavior in solutions of iodine in absolute methanol would be expected to be accompanied by the formation of spurious or secondary films which were never observed. Evidently further work will be necessary to clarify this point.[6]

It is believed that the reactions occurring in iodine-methanol solutions containing traces of water may reasonably be represented by the series of reactions shown below:

Primary

$$2Al + 6CH_3OH = 2Al(OCH_3)_3 + 3H_2 \quad (V)$$

$$2Al + 3I_2 = 2AlI_3 \text{ or } [2Al^{+++} + 6I^-] \quad (VI)$$

[5] This effect may be due also to one aluminum ion in solution being initially associated with fewer than three iodide ions. However, the alternative suggested above is considered to be slightly more probable.

[6] It has been suggested that the interaction of aluminum and iodine/methanol solutions could proceed by a free radical mechanism (28) as has been proposed for the interaction of aluminum and carbon tetrachloride (29). Since the presence of water will reduce the occurrence of free radicals, this type of mechanism would explain the effect of water on the dissolution rate of the aluminum.

Secondary Reactions

$$Al(OCH_3)_3 + 3H_2O = 3CH_3OH + Al(OH)_2^+ + OH^- \quad (VII)$$

$$Al^{+++} + 2H_2O = Al(OH)_2^+ + 2H^+ \quad (VIII)$$

$$2Al + 6H^+ = 2Al^{+++} + 3H_2 \quad (IX)$$

$$CH_3OH + H^+ + I^- = CH_3I + H_2O \quad (X)$$

Dissolved oxygen has been shown to have no effect on the reactions taking place in solution (Table III). Reactions (V) and (VI) are identical to those reactions taking place in the dried solutions. However, the different course subsequently taken by the reaction is believed to be due to the action of traces of water on the primary products of reaction.

Aluminum methoxide is believed to be hydrolyzed to soluble aluminum ions of the type shown in reaction (VII). Equally well, the hydrolysis of the aluminum methoxide might give ions of the type $Al(OH)^{++}$ (25). Under the experimental conditions, hydrolysis to hydrated alumina did not occur presumably owing to the acidity developed by other hydrolysis and side reactions. However, hydrolysis of the aluminum methoxide to a soluble ion will result in the formation of hydroxyl ions.

Hydrolysis of aluminum ions (or aluminum iodide) is believed to result in the formation of such ions as $Al(OH)^{++}$, $Al(OH)_2^+$, and hydrogen ions (25). Such ions are stable in slightly acidic solutions, although they may be present in small quantities. They are considered as the first steps in the hydrolysis of aluminum ions to hydrated alumina. The dissociation constant of the reaction

$$Al^{+++} + H_2O \rightleftharpoons Al(OH)^{++} + H^+ \quad (XI)$$

has been given as 1.4×10^{-5} (25). The problem of determining hydrogen ion activity in equilibrium with aluminum ions and water is complicated by the formation of appreciable concentrations of $Al(OH)_2^+$ from the second step of the hydrolysis (27). Nevertheless, it is undoubtedly true that a rather small concentration of hydrogen ions will be formed under equilibrium conditions in a slightly acid solution. However, hydroxyl ions formed by hydrolysis of aluminum methoxide [reaction (VII)], together with reactions (IX) and (X), will consume hydrogen ions and will throw reactions (VIII) or (XI) over to the right. Consequently, hydrolysis of aluminum ions by water can provide a reservoir of hydrogen ions that can combine with hydroxyl ions formed in reaction (VII) and that can take part in reactions (IX) and (X). Examination of the weight loss and hydrogen evolution data contained in Fig. 8–10 shows that this reservoir of hydrogen ions is sufficiently large to result in the over-all formation of slight acidity in solutions containing traces of water. In addition, it is possible that some small quantities of hydrogen ions are formed by the interaction of the hydrogen evolved in reaction (V) and the iodine in solution, such as was suspected under dehydrated conditions.

It was observed that, in solutions containing traces of water, the sum of the aluminum equivalent to the combined iodine and that equivalent to the evolved hydrogen exceeded the total weight loss of the specimen. The over-all concentration of iodide formed in reaction (VI) will be unaffected by the hydrolysis of these products of reaction as suggested in reactions (VIII), (IX), and (X) since methyl iodide will give a quantitative test in aqueous solutions for iodide (17). However, reaction (IX), the interaction of hydrogen ions with aluminum, is a source of extra hydrogen gas; consequently it is believed that the difference between the actual and "calculated" weight loss may be due at least partly to this extra evolution of hydrogen resulting from reaction (IX).

The series of reactions believed to occur in solutions containing traces of water result in the over-all consumption of water, despite the fact that reaction (X) and a combination of reactions (VII) and (VIII) regenerate a portion of the water consumed. Thus, it would be expected that if the access of water to the solution were prevented, the water initially present might become exhausted, and insoluble aluminum methoxide might be precipitated. This actually occurred, as described earlier, in solutions of iodine in absolute methanol where the access of water vapor from the atmosphere was prevented by drying tubes. Consequently, this emphasizes the desirability of performing film isolation in contact with the atmosphere where the water that is consumed during reaction with the aluminum can be replenished by water vapor from the atmosphere.

Acknowledgments

The authors wish to express their appreciation to Mr. R. V. Paulson for his original contributions to the theory and to Dr. B. de B. Darwent, Professor H. H. Uhlig, Dr. J. F. Murphy, Dr. F. J. Bowen, Dr. T. R. Pritchett, and Mr. F. L. Howard for their helpful discussions and suggestions.

Any discussion of this paper will appear in a Discussion Section, to be published in the June 1956 JOURNAL.

REFERENCES

1. U. R. EVANS, *J. Chem. Soc.*, **1927**, 1020.
2. S. WERNICK, *J. Electrodepositors' Tech. Soc.*, **9**, 163 (1933–34).
3. H. FISCHER AND F. KURTZ, *Korrosion u. Metallschutz*, **18**, 42 (1952).
4. G. TAMMANN AND F. ARNTZ, *Z. anorg. allgem. Chem.*, **192**, 45 (1930).
5. W. H. WITHEY AND H. E. MILLAR, *J. Soc. Chem. Ind. (London)*, **45**, 173T (1926).

6. T. E. Rooney and A. G. Stapleton, *J. Iron Steel Inst.*, **131,** 249 (1935).
7. W. H. J. Vernon, F. Wormwell, and T. J. Nurse, *J. Chem. Soc.*, **1939,** 621.
8. J. E. O. Mayne and M. J. Pryor, *ibid.*, **1949,** 1831.
9. M. J. Pryor, *This Journal*, **101,** 141 (1954).
10. T. J. Nurse and F. Wormwell, *J. Appl. Chem.* (*London*), **2,** 550 (1952).
11. E. C. Pearson, H. J. Huff, and R. H. Hay, *Can. J. Technol.*, **30,** 311 (1952).
12. S. E. Turner and R. C. Anderson, *J. Am. Chem. Soc.*, **71,** 913 (1949).
13. C. V. King and E. Hillner, *This Journal*, **101,** 79 (1954).
14. W. J. Hickinbottom, "Reactions of Organic Compounds," p. 90, Longmans Green & Co., New York (1948).
15. M. T. Dangyan, *J. Gen. Chem.* (*U.S.S.R.*), **11,** 1215 (1941).
16. M. T. Dangyan, *Bull. Armenian Branch Acad. Sci. U.S.S.R.*, **63,** No. 3/4 (1942).
17. M. Kohn, *Anal. Chim. Acta*, **9,** 249 (1953).
18. F. C. Whitmore, "Organic Chemistry," p. 103, Van Nostrand & Co., New York (1946).
19. H. Gilman, "Organic Chemistry," Vol. I, p. 497, John Wiley & Sons, Inc., New York (1948).
20. H. Gilman, *op. cit.*, 499.
21. W. J. Hickinbottom, *op. cit.*, 409.
22. F. C. Whitmore, *op. cit.*, 112.
23. R. Seligman and P. Williams, *J. Soc. Chem. Ind.* (*London*), **35,** 88 (1916).
24. J. M. Bryan, "Aluminum and Aluminum Alloys in the Food Industry," Dept. of Scientific and Industrial Research Special Report #50, p. 22 (1948).
25. C. Brossett, *Acta Chem. Scand.*, **6,** 910 (1952).
26. N. Bjerrum, *Z. physik. Chem.*, **59,** 350 (1907).
27. W. M. Latimer, "The Oxidation States of the Elements and their Potentials in Aqueous Solutions," p. 264, Prentice Hall, New York (1938).
28. H. H. Uhlig, Private communication.
29. M. Stern and H. H. Uhlig, *This Journal*, **100,** 543 (1953).

The Rate and Mechanism of Dissolution of Purest Aluminum in Hydrofluoric Acid[1]

M. E. Straumanis and Y. N. Wang

University of Missouri School of Mines and Metallurgy, Department of Metallurgy, Rolla, Missouri

ABSTRACT

Pure aluminum (99.99%) dissolves in hydrofluoric acid with a rate comparable to that of titanium in the same acid. The rate of dissolution, V (mm³/cm² min of hydrogen), in 0.1–6N hydrofluoric acid is in agreement with the empirical equation $V = 28 + 275N$, and for 6-10N with $V = 20.44N^{2.35}$. Recrystallized aluminum showed the same rates within the error limits (±14%). Of the noble metal salts added to the acid, only nickel and gold increased the dissolution rate; deposits obtained from other salt solutions did not adhere to the surface of the dissolving aluminum. Ammonium fluoride and ammonium chloride additions to the acid decreased the dissolution rate (passivation) because a salt film was formed on the aluminum surface. The potential of aluminum in 2N hydrofluoric acid was −1.22 v, indicating that the extent or thickness of protective surface films was negligible. The dissolution rate of aluminum in sulfuric acid, phosphoric acid, and other acids can be increased considerably by addition of water-soluble fluorides. The behavior of aluminum in hydrofluoric acid, as well as in hydrochloric acid, could be explained qualitatively using the concept of local currents in a manner similar to that proposed earlier.

Introduction

Corrosion resistance of pure aluminum to atmospheric attack, as well as to the action of many acids, is explained by the presence of a thin but adherent and highly protective surface oxide film. If the oxide film is destroyed, e.g., by mercury or strong bases (1), the metal underneath quickly corrodes. Hydrofluoric acid attacks surface oxide layers also, e.g., on titanium, then dissolves the metal (2). So it was of importance to know whether the same is true in the case of aluminum (although aluminum fluoride formed during the reaction is difficultly soluble in the acid) and to elucidate the dissolution mechanism.

There is very little information in the literature about this dissolution process. Spacht has compiled all the available data (3), and Holmberg and Prange state that a film protects aluminum for a short time from attack by hydrofluoric acid (4).

Materials Used

Samples in the form of squares (1 cm²) were cut from a 1 mm thick, cold rolled, aluminum sheet supplied by the Aluminum Company of America. It was designated 99.99% pure, and contained as impurities: Si—0.0015, Fe—0.0007, Cu—0.0004, and Mg—0.0007%. To compare the corrosion properties of this metal with those of a 99.998% aluminum (5),[2] rate measurements in hydrochloric acid (6) were repeated using the 99.99% Alcoa aluminum. Plates made of this metal were relieved from internal stresses due to cold working by annealing them at 470°C for 1 hr. Specimens exactly 1 cm² were ground, polished, and mounted in Bakelite (2). From the rate of hydrogen evolution in 2N hydrochloric acid (reagent grade), the average dissolution rate of this aluminum during the 44 hr duration of the experiment was 18.6 mm³/cm²min in hydrogen units, while the French 99.998% aluminum developed a rate of only 0.56. Thus, the French metal was much purer, as was also indicated by its analysis of impurities: Si—0.0009, Fe—0.0002, and Cu—0.0003%.

All chemicals used were of reagent or of C.P. grade, and all experiments described below were performed with the 99.99% American aluminum.

Experimental Results

Rate of dissolution in pure hydrofluoric acid.—The rate was determined by collecting hydrogen developed according to the reaction

$$Al + 3HF \rightarrow AlF_3 + 1\tfrac{1}{2}H_2 \qquad (I)$$

as described previously (2). Glass parts of the apparatus were protected from attack by the acid by a brown wax.[3] The volume of acid in each experiment was 200 cc, the temperature was 25° ± 0.1°C, and the aluminum sample was mounted on the foot of stirrers rotating at 200 rpm. Glass joints were used wherever possible, in order to reduce the loss of hydrogen by diffusion through rubber connections.

Experiments were made in 0.1, 0.5, 1, 2, 4, 6, 8, and 10N hydrofluoric acid solutions, the normality of

[1] Manuscript received December 15, 1954.

[2] From Alais, Froges, et Camargue, France.

[3] Sunoco 1290, Sun Oil Company, Philadelphia, Pa.

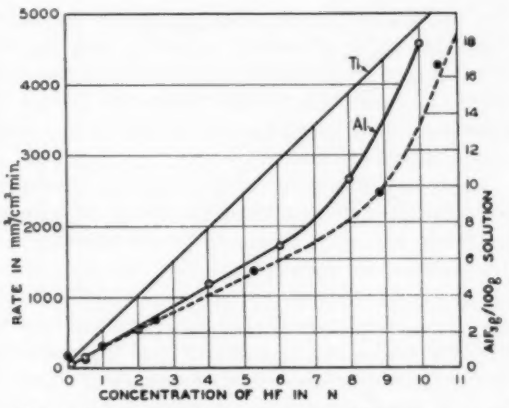

FIG. 1. Rate of dissolution of Al in different concentrations, N, of HF at 25°C. Each point represents an average of two runs. The volume of H_2 was reduced to normal conditions. 1 mm³ of H_2 corresponds to 0.000803 mg of Al metal. A similar curve for Ti is drawn for comparison (1 mm³ = 0.001424 mg Ti). Dashed line: solubility of AlF_3 in HF (in g/100 cm³ of solution) according to Seidell (7).

each being checked by titration. Reaction (I) started with an induction period of 30–50 min, then followed a flat maximum (about 120 min in diluted and 30 min in more concentrated acids), and finally declined gradually. In Fig. 1 the average maximum rate, a mean of two runs, is plotted against the acid concentration. For acids of lower concentrations (0.1 to 6N) the velocity of dissolution V conforms with the empirical equation

$$V = 28 + 275N \qquad \text{(II)}$$

and at higher concentrations (6–10N) with the equation

$$V = 20.44N^{2.35} \text{ mm}^3/\text{cm}^2\text{min} \qquad \text{(III)}$$

Deviation of observed from calculated rates [equations (II) and (III)] is within −7.2 and +5.8%. However, the difference between the average maximum rates of duplicated runs was within 0.3 and 16.6%. These deviations may be due to irregular distribution of small amounts of impurities in the aluminum. Other reasons, such as heterogenous stress distribution set up from cold work, are of minor importance, as is shown below.

The metal surfaces after dissolution were glossy, clearly showing the cold work fibers. The surfaces were partially covered with a loose white precipitate of aluminum fluoride, especially at the edges and corners of the sample, resulting from reaction (I). However, the sample was evenly attacked, indicating that the dissolution reaction was not retarded appreciably by the presence of aluminum fluoride on the surface of the dissolving metal. Solubility of the fluoride is limited to 0.55 g ($AlF_3 \cdot H_2O$) in 100 g water and decreases in low acid concentrations (7). Hence, if the solubility product is exceeded, the loose, white precipitate appears on the sample, and is also finally dispersed throughout the acid.

Experiments with aluminum samples recrystallized at temperatures of 400° and 575°C showed no appreciable difference in dissolution rates from those of cold worked metal (5). Differences of −7.5 to +14.3% were observed, but they are too small (and deviate to both sides) to state definite conclusions concerning the influence of cold work on the dissolution rate of aluminum.

Effect of additional reagents on the dissolution rate.—A series of qualitative tests were made to determine whether the dissolution rate of aluminum in sulfuric, nitric, phosphoric, acetic, and formic acids was increased by the presence of hydrofluoric acid. Pure aluminum reacts very slowly with 2N sulfuric acid. After addition of a small amount of ammonium fluoride to the acid, the sample was attacked immediately because of displacement of the free hydrofluoric acid, as was the case with titanium (8). Concentrated nitric, phosphoric, acetic, and formic acids did not react with the aluminum, even in the presence of ammonium fluoride, but there was a very slight reaction with phosphoric acid. However, when the fluoride was added to the diluted acids (1:1 and more), an immediate, rapid reaction went on for a considerable time. In the case of acetic acid the reaction was moderate.

To study the influence of salt additions on the dissolution rate of aluminum in hydrofluoric acid, ammonium fluoride and ammonium chloride were chosen. The results are shown in Fig. 2. This series of experiments began with aluminum dissolution in pure 1N hydrofluoric acid, and a rate of 344 mm³/cm²min was obtained instead of 303 (Fig. 1). The difference of 13.5% is still well within the error limits of the reproducibility of corrosion rate determinations, which is around 30%. While the reasons for

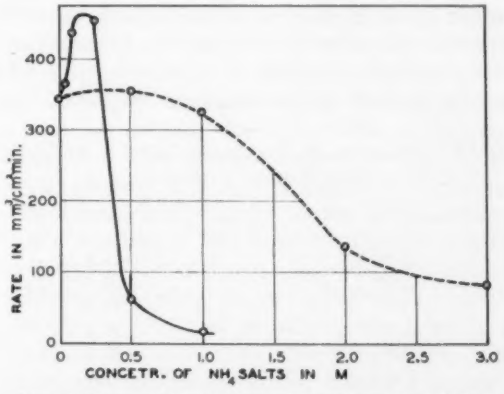

FIG. 2. Rate of dissolution of aluminum in 1N HF vs. concentration of ammonium salts added: NH_4F—solid curve, NH_4Cl—dashed curve.

increased rate of dissolution at small concentrations of the ammonium salts are not quite clear, the rate decrease at still higher salt concentrations can be explained satisfactorily. White salt films, porous, but adherent, were on the aluminum surface after such experiments, reducing the exposed metal surface. Evidently, at augmented concentrations of ammonium salts in the acid, the aluminum fluoride solubility was reduced, and a salt film, spreading in all directions with increasing ammonium salt concentrations, was formed on the surface and passivated the metal as was the case with titanium (8). The films were never thick enough to be collected for a complete chemical identification, but the presence of an ammonium radical could be proved in both kinds of films.

If a dissolution process is electrochemical in nature, metallic impurities present in the dissolving metal, or in the acid, in the form of noble metal salts should increase the reaction rate. Six salt solutions, $CuSO_4$, $HAuCl_4$, $NiCl_2$, $Pb(NO_3)_2$, $AgNO_3$, and $PtCl_4$ were added separately to the hydrofluoric acid in quantities of 2 cc of 0.1M aqueous solutions, in a manner, as previously described (2), so as not to dilute the acid. The runs with $PtCl_4$ were made in pure nitrogen to avoid any possible catalytic reaction in the formation of water from the liberated hydrogen and oxygen from the air. Results are shown in Table I.

The salt solutions of Table I were added to the acid when the dissolution rate of aluminum had reached its maximum. Only the nickel and gold solutions increased the rate, while the other solutions decreased it. Examination of aluminum samples after the runs showed that those in the nickel solution had a bright surface coating. Under the microscope the coating appeared tightly adherent to the aluminum surface, but had a porous appearance. This nickel film evidently acted as a local cathode accelerating the dissolution rate of aluminum. In the other instances no metal was observed on the sample surface, except in traces mixed up with the white salt deposit in the cases of gold, lead, and silver. Complete reduction occurred as evidenced by a dark metallic sediment on the bottom of the flask. Thus,

TABLE I. *The effect of salt solutions, added to the 1N* HF, *on the dissolution rate of* Al

Ions of the salts added	Change in rate in %
Cu^{2+}	−14.8
Au^{3+}	+25.1
Ni^{2+}	+118.0
Ag^{+}	−28.7
Pt^{4+}	−37.7
Pb^{2+}*	−72.0

* PbF_2 partly precipitated from the solution; but there was sufficient Pb^{++} to plate out on the Al.

the inefficiency of the salts mentioned is understandable, although not the severe drop in the dissolution rate after addition of the salts to the acid. Attempts were made to find the answer to this by measuring the potential of the dissolving aluminum under various conditions.

Potential measurements of the dissolving aluminum.—Potentials were measured against a 1*N* calomel electrode, and were converted to the standard hydrogen electrode scale (9, 10). Very few such measurements of the aluminum potential in hydrofluoric acid have been made (11). Just after immersion of the electrode in the hydrofluoric acid the potential dropped suddenly, then slowly became less negative. In most cases, there was a steady potential at the end of the experimental period. The potential is very negative and decreases with the acid concentration, approaching a limiting value (11).

Using an electrode freshly etched with hydrofluoric acid, slowly rising curves were obtained starting with the first minute (Fig. 3). If salt solutions were added to the acid of the etched electrode, changes in the electrode potential occurred immediately. Measurements were made in 100 cc 0.5*N* hydrofluoric acid; 1 cc of the 0.1M addition agent ($NiCl_2$, $PtCl_4$, $HAuCl_4$, $CuSO_4$) together with 1 cc of the 1*N* acid, in order not to dilute the electrolyte, were added to it. Results are summarized in Fig. 3. In all four cases the potential of the dissolving aluminum increased considerably after addition of the noble metal salts, especially when gold and copper salts were added, raising the potential by 0.52–0.54 v. However, a good deposit on the surface of the dissolving aluminum was observed only in the case of

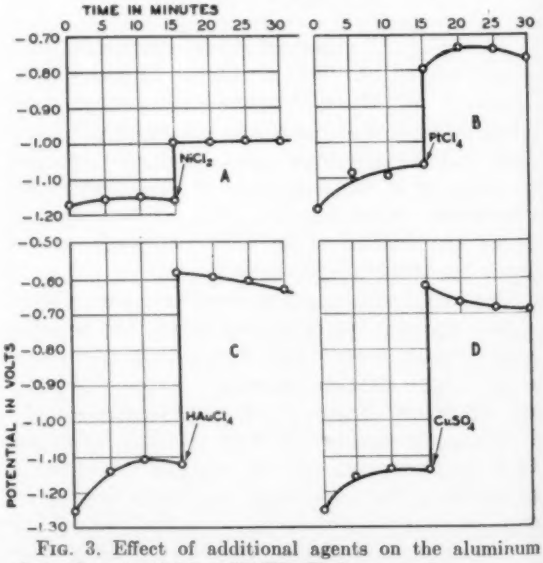

FIG. 3. Effect of additional agents on the aluminum electrode potential in 0.5*N* HF. Hydrogen scale.

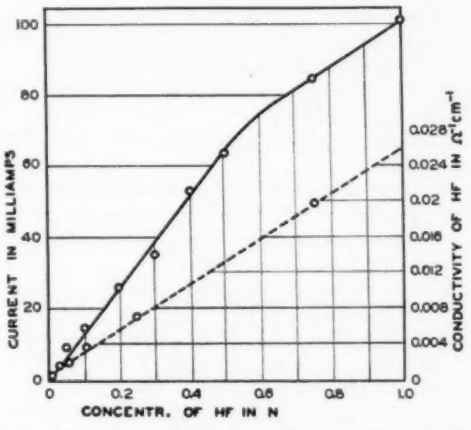

FIG. 4. Current produced by a cell Al-HF-Pt (platinized) vs. concentration of HF. Exposed electrode surfaces: 2 x 2 cm. Distance between the electrodes: 1 cm. Dashed curve: conductivity of the acid vs. concentration.

nickel chloride, and the presence of this metal was proved by qualitative tests. Other metals (Fig. 3 B, C, D) were reduced, but did not adhere to the electrode. A decrease in the rate of hydrogen evolution was observed after addition of the three salt solutions.

That aluminum, if in contact with particles of a noble metal, is capable of quickly going into solution in a bath of hydrofluoric acid, was proved by the behavior of the cell Al-HF-Pt (platinized). As soon as such a cell was closed through a milliammeter (9), current flowed. In dilute acids, the current was larger at first, dropped, then rose to a fairly steady value. At 0.75*N* and up no drop was observable, only an increase of current with time. The average current produced by the cell after 20 min of operation (usually between 20 and 50 min) is shown in Fig. 4, as a function of acid concentration.

Thus, local cathodes of low hydrogen overvoltage, being in contact with aluminum metal immersed in hydrofluoric acid, should accelerate the dissolution rate of the base metal.

DISCUSSION

Dissolution rates of pure aluminum in 2*N* hydrochloric acid and in hydrofluoric acid were 18.6 and 546 mm^3/cm^2min. This behavior is easily explained by the potential and difference effect measurements of the dissolving metal. The potential in 1*N* hydrochloric acid is around −0.6 v (12), and that in 2*N* hydrofluoric acid is −1.22 v (11). The consequence is that metallic impurities still present in the metal develop an emf about twice as large in the hydrofluoric acid. As aluminum dissolving in hydrochloric acid shows a negative difference effect, it is evident that the reacting surface of the metal is covered by a protective film (11). Consequently, dissolution occurs only through the pores, with part of them acting as anodes and those filled with metallic residues as cathodes (13, 14). The high anodic polarization of aluminum in the pores shows up in the less active potential of −0.6 v of the metal. On the other hand, aluminum dissolving in hydrofluoric acid exhibits a positive difference effect (11), so no appreciable protective films are on the metal. Therefore, anodic polarization is low, the aluminum shows a very negative potential of −1.22 v, and action of local currents on the metal surface is not limited by the film. Thus, a comparatively high dissolution rate is developed in hydrofluoric acid, in spite of the low solubility of aluminum fluoride formed in the acid. Furthermore, the concept of dissolution because of local element action is confirmed by the augmentation of the current produced by the cell Al-HF-Pt along a straight line (Fig. 4), a fact which can be explained by the increase in conductivity of the hydrofluoric acid with concentration (15). Deviations occur at higher current densities because of increased polarization of the cell.

It was expected that the aluminum dissolution rate should increase linearly with hydrofluoric acid concentration, as does that of titanium (Fig. 1). However, deviation from the straight line relationship above 6*N* can be explained by increased solubility of aluminum fluoride with hydrofluoric acid concentration (7), as shown by the dashed curve (Fig. 1). Then aluminum fluoride formed at low acid concentrations to a certain degree hampered the dissolution rate; indeed the addition of salts (NH_4F, NH_4Cl) decreased the rate (Fig. 2) because of formation of the salt film which covered part of the local cathodes. The appearance of the difference effect, which is explained on the basis of the local element theory (11), also testifies to such an electrochemical mechanism of dissolution.

The hydrogen overpotential on aluminum, as with titanium (16), should be very negative, at least more negative than the potential of aluminum in hydrofluoric acid (11). This negative potential, required for hydrogen development on aluminum, is the reason for the low dissolution rate of the purest aluminum. The appearance of local cathodes of a nobler metal with a less negative overpotential should, therefore, greatly increase the dissolution rate of the base metal. However, this was true only in the case of nickel and gold (Table I), while the other metals proved to be inefficient and even decreased the rate. One reason for this behavior has been mentioned already: the precipitates, except nickel, did not adhere to the dissolving surface, so no efficient local currents could be formed. The other reason is the shifting of the potential of aluminum

toward noble values after addition of the salt solution (Fig. 3). Of course, this shift decreased the emf of the local currents, with the effect of decreasing hydrogen evolution also. There is still a question as to why these shifts occurred, as particles of the displaced noble metal quickly dropped from the dissolving aluminum surface. There is still no answer to this question, but it is believed that the phenomenon is the same as noticed by Schlain and Smatko (17) upon immersion of a titanium electrode in a solution of hydrochloric acid containing small amounts of noble metal salts. The electrode became passive without showing the presence of the displaced metals on its surface (17).

It can be concluded that the dissolution of aluminum in hydrofluoric acid is an electrochemical process and that it can be satisfactorily described qualitatively, if not quantitatively.

Acknowledgment

The authors are grateful to Dr. C. B. Gill for correcting the English of this manuscript.

Any discussion of this paper will appear in a Discussion Section to be published in the June 1956 Journal.

REFERENCES

1. M. E. Straumanis and N. Brakšs, *This Journal*, **95**, 98 (1949); **96**, 21, 310 (1949); *Metall*, **3**, 41 (1949).
2. M. E. Straumanis and P. C. Chen, *This Journal*, **98**, 234 (1951).
3. R. B. Spacht, *J. Chem. Educ.*, **23**, 253 (1946).
4. M. E. Holmberg and F. A. Prange, *Ind. Eng. Chem.*, **37**, 1030 (1945).
5. B. Roald and M. A. Streicher, *This Journal*, **97**, 283 (1950).
6. M. Straumanis, *Korrosion u. Metallschutz*, **14**, 1 (1938).
7. A. Seidell, "Solubilities of Inorganic and Metal Organic Compounds," 3rd ed., D. Van Nostrand and Co., Inc., New York (1940).
8. M. E. Straumanis and C. B. Gill, *This Journal*, **101**, 11 (1954).
9. M. E. Straumanis and P. C. Chen, *Corrosion*, **7**, 229, 234 (1951).
10. A. J. deBéthune, *Corrosion*, **9**, 336 (1953).
11. M. E. Straumanis and Y. N. Wang, *This Journal*, **102**, 304 (1955).
12. C. J. de Gruyter, *Rec. trav. chim.*, **44**, 960 (1925).
13. M. E. Straumanis, *Korrosion u. Metallschutz*, **14**, 81, 82 (1938).
14. U. R. Evans, "Metallic Corrosion, Passivity and Protection," p. 204, Longmans, Green and Co., New York (1948).
15. Landolt-Börnstein (Roth-Scheel), "Physikalisch-chemische Tabellen," 5, Anflage II, pp. 1076–1077, Verl. J. Springer, Berlin (1923).
16. M. E. Straumanis, S. T. Shih, and A. W. Schlechten, *J. Phys. Chem.*, **59**, 317 (1955).
17. D. Schlain and J. S. Smatko, *This Journal*, **99**, 417 (1952).

Brightening Agents for the Tin-II Sulfate-Sulfuric Acid Electrolyte[1]

C. A. Discher[2] and F. C. Mathers

Indiana University, Bloomington, Indiana

ABSTRACT

Addition agents capable of producing specular deposits directly from the acid tin plating bath are described. Concentration ranges of electrolyte and operating conditions are discussed. Properties of the electrodeposit are described. The role played by each of the addition agents is discussed.

Introduction

In an intensive study of the literature of addition agents for the tin-II sulfate-sulfuric acid electrolyte, it was found that the reported addition agents tend to fall into certain well-defined classes of substances. In the claims for good deposits, two of these classes of addition agents were of special interest: the phenols, and the surface active agents.

The simple phenols, i.e., phenol and β-naphthol, are named too frequently to be listed, especially since the crude phenols, i.e., cresol and various mixtures containing phenols as constituents, are of greater interest. Cooper and Light (1) have patented the use of tar acids such as cresylic acid, and/or pyroligneous acids. Schlötter (2, 3) has patented the system using two or more substances from the groups glue, gelatine, and agar-agar on one hand and sulfonated oils, resins, bitumen, wood tar on the other. Felger and Mathers (4) have reported the crude products of the fractional distillation of coal tar as exceptional addition agents.

Surface active agents appear frequently, especially in the newer literature. Sulfonates are often mentioned (2–4). Nachtman (5) has patented a mixture containing a colloid, sulfonated cresols or naphthols, and a wetting agent consisting of the sodium salt of the sulfate ester of organic alcohols having 8–12 carbon atoms.

After preliminary study of the older work it was decided to investigate thoroughly these two classes of substances as brightening agents for acid tin electrolyte.

[1] Manuscript received November 22, 1954. This paper was prepared for delivery before the Boston Meeting, October 3 to 7, 1954, and is taken from a thesis submitted by C. A. Discher to the Graduate College of Indiana University in partial fulfillment of the requirements for the Ph.D. degree.

[2] Present address: Rutgers University College of Pharmacy, 1 Lincoln Ave., Newark 4, New Jersey.

Experimental

Test solutions contained 100 g/l tin-II sulfate (commercial quality) and 100 g/l concentrated sulfuric acid. One hundred milliliter portions of this solution were used for each addition agent or combination of addition agents tested. Cathodes were 2.5 cm x 2.5 cm steel sheet. Pure tin anodes giving a cathode:anode ratio of approximately 2:5 were used. Each anode was sheathed in an envelope of filter paper to prevent anode sludges from contaminating the bath. The electrodes were placed opposite each other and pressed tightly against the sides of a 150 ml beaker.

Current density was maintained at 1.55 amp/dm^2, except for tests made to determine maximum current density without gassing. Agitation, unless otherwise noted, was provided by a 7 mm glass rod, flattened at its end and rotated at about 100 rpm.

Results

It was found after many trials that the best brightening activity was obtained from the tars produced by the destructive distillation of saccharides: glucose, sucrose, starch, cellulose (cotton and filter paper), wood (pine and red wood), and the dried waste sulfite liquor of the paper industry. While the aqueous portions of the distillates possessed slight activity, it was shown that this was because they were saturated with respect to the tars. In order to eliminate much time-consuming work a commercial source of these tars was obtained.[3] All subsequent work reported in this paper was done with this wood tar. PT will be used as its symbol.

The work now centered about solubilizing the PT. Sulfonated *p*-cymene, *p*-ethyl benzene sulfonic

[3] Settled tar from destructive distillation of hardwood. Crossett Chemical Company, Crossett, Arkansas. Pyroligneous acid, methanol column slops, stripping oil, acetic acid still residue, and other by-products were also furnished, but were ineffective.

acid, sulfocarbolic acid, *p*-toluene sulfonic acid, sulfolane and dimethylsulfolane,[4] alkane sulfonic acid,[5] various sodium salts of aliphatic alcohol sulfates (i.e., Duponols, Tergitols), carbowaxes, cellusolves, and carbitals were tested. In most cases there was some improvement in the solubility of the PT and its effectiveness as an addition agent, but in no case could a bright deposit be obtained. Sodium aliphatic alcohol sulfate esters were more effective than the others. To see if further improvement of the deposit could be obtained it was decided to prepare and test the unneutralized sulfate esters.

The required quantity of concentrated sulfuric acid (to give 100 g/l in the finished electrolyte) was measured and the proper quantity of *n*-aliphatic alcohol added to it in 3–5 portions or rapidly dropwise good mixing. After standing 2–3 min the reaction mixture, which became warm, was added to water containing the tin-II sulfate. PT was added and the resulting electrolyte was filtered to remove any undissolved tin compounds and a small quantity of insoluble black sludge remaining from the tar.

Normal aliphatic alcohols having 2–12 carbon atoms were tested. Maximum solubilizing action was found in the *n*-octyl preparation, this solution giving mirror-bright deposits. Attempts to further increase the solubility of the PT by also including other surface active agents previously named were unsuccessful.

Composition of the bright bath.—The following composition appears to be the most effective: 100 g/l $SnSO_4$, 100 g/l H_2SO_4, 10 g/l *n*-octyl alcohol (reacted with the sulfuric acid), and 8 g/l PT. However, bright deposits are obtained with tin-II sulfate concentrations from 50 g/l to saturated. Concentrations as low as 30 g/l were tested, but matte deposits were obtained. Free sulfuric acid is essential. Bright deposits are obtained using 50–120 g/l. Lower concentrations cause excessive sludge; higher concentrations produce hard, rough deposits; very high concentrations (250 g/l) result in gassing.

The quantity of *n*-octyl alcohol used to prepare the acid sulfate ester may be varied from 5 to 15 g/l. Concentrations below the lower limit did not dissolve sufficient PT to give bright deposits; concentrations above 20 g/l give hard, gray, striated deposits. Nothing is gained by increasing the quantity of *n*-octyl alcohol above 10 g/l since the solubility of the PT does not improve beyond this level.

Concentration of the PT cannot be increased beyond 8 g/l. Baths prepared with higher concentrations of this substance separate into two phases, an oily upper layer and an aqueous layer. Neither layer is effective in producing bright deposits. As the PT level is allowed to drop below 8 g/l the deposit becomes progressively less bright, passing into white matte and, finally, at very low concentrations, giving a visibly grainy crystalline appearance.

Control of concentrations.—The usual analytical methods may be used for the tin-II and acid (6). PT acts as its own indicator. Solutions capable of giving mirror-bright deposits are dark brown, while matte deposits are obtained from solutions of a straw color. The bath may be regenerated as frequently as necessary by addition of PT to give the solution the depth of color necessary for the desired deposit. The *n*-octyl sulfate concentration may be controlled by making use of its foaming quality. As the electrolyte becomes depleted in this substance its foaming power decreases and its ability to dissolve PT decreases.

Operating conditions.—The bath has been operated successfully at temperatures as low as 5°C (some tin-II sulfate separates from the standard bath at this temperature) and as high as 65°C. The bath has been operated at current densities as high as 12 amp/dm^2. At this current density, with the stirring conditions used, gassing took place. With a higher stirring rate, higher current densities should be possible. Best brightening activity is obtained when the current density is maintained at a level just below that at which gassing begins.

Bath characteristics.—The cathode efficiency, for a series of 25 determinations, was found to be 98%. The anode efficiency is of the same order. Anode corrosion is very smooth and even. There is no intercrystalline corrosion.

The throwing power of *n*-octyl sulfate-PT bath is very good. A thick cathode was prepared by keeping it tightly against the side of the beaker. When cut in cross section the back side had $\frac{2}{3}$ the thickness of the front side. Irregular objects plate easily, even in deep crevices.

The life of the electrolyte is very good. One hundred milliliter baths were operated continuously for 4–5 month periods. Additions of various constituents were made as needed. The plate obtained at the end of this time was in every way comparable to that obtained initially.

Character of deposits.—Bright deposits have been produced on steel, copper, bronze, brass, and cast iron. Brightness on cast iron requires thicker deposits. On copper, at a current density of 5 amp/dm^2 bright plates are obtained at 0.00013 cm thickness, mirror bright at 0.00025 cm. Similar results were obtained on steel.

White matte deposits (obtained by using lower concentrations of PT) were flowed successfully in cottonseed oil (1% stearic acid) and by direct gas

[4] Shell Development Corporation, Emeryville, California.

[5] Standard Oil Company (Indiana), Chicago, Illinois.

heat (0.00007–0.0002 cm thickness at 1.5 amp/dm² and 0.0002–0.001 cm at 9.0 amp/dm²).

Deposits are soft and easily scratched. There is some increased hardness with brightness. Adhesion is excellent. Good adherent solder joints could be obtained with all plates.

The ferroxyl test gave results for this plate which were equal to or better than corresponding thicknesses of commercial plate.

Depletion of addition agents.—Study of baths in continuous operation for 3–5-month periods indicated that the octyl sulfate ester depletion can be accounted for entirely by dragout. This lends support to the theory that this substance serves solely as a solubilizing agent for the PT. On the other hand, the disappearance of PT is much greater than can be accounted for in the same way. Since no precipitates form during operation, it must be concluded that this substance is in some manner codeposited in the tin plate. Over a three-month period of continuous operation the following information was obtained. One hundred milliliters of electrolyte produced 630 g tin metal, consuming at the same time 0.5 g of *n*-octyl alcohol and 3.8 g of PT.

Nature of brightening agent.—A series of experiments were run in order to elucidate the chemical nature of the brightening agent. Fractional distillation of the PT established that the brightening activity is strongest in the highest boiling fractions and the still pot residue. This indicates a high boiling, high molecular weight substance.

Treatment of the solution of the PT in diethyl ether (a small amount of insoluble black solid forms which has no brightening action) with sodium hydroxide, potassium hydroxide, sodium carbonate, sodium bicarbonate (aqueous solution or solid) until basic gives two fractions, an ether-soluble portion and a water-soluble portion. The brightening activity is found to reside in the ether layer. This shows that the brightening agent is not an acid or phenol. (The phenols may be recovered from the water solubles. While they are of no value for the bath under discussion, with glue these phenols give white matte deposits.)

Use with other metals.—PT is an effective addition agent for lead electrodeposition. Obviously sulfuric acid with the sulfate esters is not applicable. However, using the fluorosilicate bath with carbowax-1500 to increase the solubility of the PT, excellent matte deposits of lead may be obtained over long periods of time. PT was added to the bath as needed.

A copper bath analogous to the tin electrolyte is capable of giving bright flash deposits. However, thick deposits were not obtainable.

Attempts to adapt the brightener to iron (iron-II sulfate), zinc (zinc sulfate), and zirconium (zirconium sulfate) were unsuccessful.

Conclusions

A tin-II sulfate-sulfuric acid bath using *n*-octyl sulfate in the form of the free acid as a solubilizing agent and pyroligneous tars from the destructive distillation of saccharides as brightening agents is capable of producing tin deposits possessing specular reflection. The brightening agent is a high boiling, nonacidic, probably neutral substance.

The composition of the solution is readily controlled to maintain it in a condition to give matte to mirror-bright deposits of tin. These deposits are adherent, soft, and malleable.

Any discussion of this paper will appear in a Discussion Section to be published in the June 1956 Journal.

REFERENCES

1. J. P. Cooper and D. W. Light, U.S. Pat. 2,156,427, May 2, 1939.
2. M. Schlötter, French Pat. 790,884, Nov. 28, 1935.
3. M. Schlötter, British Pat. 443,429, Feb. 27, 1936.
4. M. M. Felger and F. C. Mathers, *Trans. Electrochem. Soc.*, **90**, 81 (1946).
5. J. S. Nachtman, British Pat. 528,240, Oct. 25, 1940.
6. P. R. Pine, *Trans. Electrochem. Soc.*, **80**, 640 (1941).

Antimony Oxide Phosphor with Red Emission[1]

YOSHIHIDE KOTERA AND TADAO SEKINE

Fifth Division, Government Chemical Industrial Research Institute, Tokyo, Japan

ABSTRACT

A phosphor consisting of antimony oxide, boric oxide, and manganese activator is fairly efficiently excited by ultraviolet radiation. It emits a band spectrum with a peak at 6400 Å. The function of the boric oxide is to enhance fluorescent intensity, optimum composition being about 1 mole antimony oxide, 0.1 mole boric acid, and 0.002 mole manganese. Firing times, temperatures, and atmospheres (except hydrogen) are not critical. The structure of the phosphors is discussed on the basis of x-ray diffraction patterns.

INTRODUCTION

This is an account of a new phosphor which is capable of emitting red fluorescent light fairly efficiently when excited with ultraviolet radiation. It may, therefore, be used in fluorescent lamp applications. Heretofore, antimony oxide has been used rarely as a base material for phosphors. However, the present work shows that such phosphors do exist. While the manganese activator is responsible for the fluorescent emission, boric oxide serves mainly to enhance its intensity. Titanium may also be used as an activator, but its effect has not been investigated thoroughly as yet.

PREPARATION

In the preparation of phosphors, commercially available chemically pure grades of antimony trichloride, boric acid, and manganese sulfate were used as starting materials. Antimony chloride was dissolved in dilute HCl. After filtration, the solution was poured into about 10 times its volume of water. The precipitate formed was washed several times by decantation with water, then with dilute HCl and with ammonia, filtered, and dried at 110°C. Its purity was established spectrographically. After heating for 2 hr at 750°C the product became insoluble in solutions of acids and alkalies. It was found to be a mixture of Sb_2O_4 and Sb_2O_3 as determined by the method described below. Boric acid was purified by means of double recrystallization. Manganese sulfate was not further purified.

From preliminary work the optimum composition for the phosphor was found to be: antimony oxide—25.0 g; boric acid—0.50 g; manganese sulfate (anhyd.)—0.024 g.

These ingredients were thoroughly mixed in the dry state and then fired at 1100°C in air for 6 hr.

Experiments were also carried out with different experimental conditions. First, deviations from the above composition were tried, keeping the amount of antimony oxide constant and varying singly each of the other two components. These were increased in steps, from zero up to 10 or 25 times their quantities in the base formula above. Next, the firing temperatures were varied from 1000° to 1200°C, and the time of firing from 2 to 12 hr.

Possible losses of boric acid in firing were determined by chemical analysis of the phosphors. In most cases the losses were negligible, but in some samples they amounted to about one-half of the amounts added without, however, producing characteristic differences.

Phosphor samples were excited with a low pressure quartz mercury lamp and their relative brightness was measured with a Pulfrich photometer equipped with a red filter transmitting between 5500 and 7000 Å. Experimental data were taken several times by two observers for each sample. Average brightness values obtained are given in Table I.

The table shows that changes in boric acid concentration are not highly critical, that changes of manganese concentration are somewhat more characteristic, that manganese, in fact, is essential for the fluorescence of the phosphors to develop, and that a second brightness maximum is found at higher manganese concentrations. It is also evident that the base formula given above is close to the optimum composition. Firing times and temperatures are likewise not very critical, except that the material becomes too volatile at higher temperatures. Thus, most of the batch was volatilized after 1 hr firing at 1200°C, hence the firing temperature should be kept below 1200°C. At 1100°C, a 10-hr firing schedule of the base formula mix was nearly equal to 6-hr firing, such that 6 hr of firing is adequate for practical purposes. Under these conditions the loss of weight amounted to some 10–20%.

Samples of base formula composition were also fired in atmospheres of hydrogen, oxygen, nitrogen, water vapor, and some mixtures of these gases. Hydrogen is not suitable, as the material is completely volatilized following reduction to the ele-

[1] Manuscript received February 11, 1952.

TABLE I. *Factors affecting relative brightness*

Changes of boric acid concentration in % of amount in base formula		Rel. brightness
0		53
50		52
80		73
100		100
200		97
500		75
1000		74
Changes in $MnSO_4$ concentration in % of amount in base formula		
0		15
40		54
100		100
200		56
250		56
300		52
460		64
750		75
2500		64
Changes in firing schedule		
°C	*hr*	
1000	2	46
1000	4	39
1000	6	34
1000	8	87
1100	2	25
1100	4	71
1100	6	100
1100	8	96
1100	10	76
1100	12	65

mental state. The other gases showed some difference compared with air, as discussed later for oxygen and nitrogen.

The phosphor as prepared above was not attacked by acids. For example, the intensity of its fluorescence was fully retained after treating it with 2*N* HCl for ½ hr and then drying it. However, when treated with 2*N* NH_3, phosphor brightness decreased to 85%, although no change of color or of the state of aggregation was observed.

A number of phosphor preparations were made in which other compounds were substituted for boric acid and other elements for manganese and for part of the antimony. Also, double activation with manganese and other secondary activators was tried. All these phosphors were fired at 1100°C in air. Following is a survey of the substitutions (on molar basis) and of the other activators which were introduced in amounts of 0.001 mole for 1 mole of antimony oxide:

1. As_2O_3, SnO_2, P_2O_5 for ⅓ of the antimony oxide;
2. LiCl, $MgCl_2$, $CaCl_2$, MgF_2, CaF_2, KBr, $NaNO_3$, Na_2HPO_4, KH_2PO_4, $Na_2B_4O_7 \cdot 10H_2O$, Al_2O_3, SiO_2, TiO_2, V_2O_5, As_2O_5, for H_3BO_3;
3. Cu, Ag, Sn, Pb, Co, Ni, Cr, Th, Bi, Fe, Mo, Ti, W, V, Ce for Mn;
4. Ce, Sn, Pb as second activators with Mn.

None of the substituents and second activators listed above produced a good phosphor, with the exception of titanium which gave a yellow fluorescence when excited with 2537 Å radiation. Details will be reported in the future.

Properties and Structure

The phosphors are friable, free flowing powders which do not contain hard sintered particles when prepared as described. Fluorescence is weak to medium bright when excited by cathode rays and long ultraviolet of 3650 Å, respectively. It is fairly strong when excited with 2537 Å radiation. Under 3650 Å excitation with a high pressure mercury lamp and a Corning 5840 filter, the brightness as measured with a selenium photocell compares with that of manganese-activated strontium or magnesium aluminate phosphors. Under 2537 Å excitation the brightness is about one-half that of commercial magnesium arsenate phosphor.

The emission spectrum of a phosphor of base formula composition is shown in Fig. 1. The energy peak is at about 6400 Å and the wave lengths at which the energy is one-half of the peak value are 5830 and 6920 Å. No evidence of a spectral line structure was found. The emission curve is symmetrical with respect to frequency and has the general shape of the probability curve. The phosphor has a rather fast, probably exponential, decay. Other forms of excitation produce the same emission curve.

Considerable work was done in an effort to determine the exact composition and structure of the phosphors, by means of both chemical and x-ray diffraction analysis. The patterns were obtained by the Debye-Scherrer method using copper radiation and exposures of 3–5 hr. The x-ray tube was operated

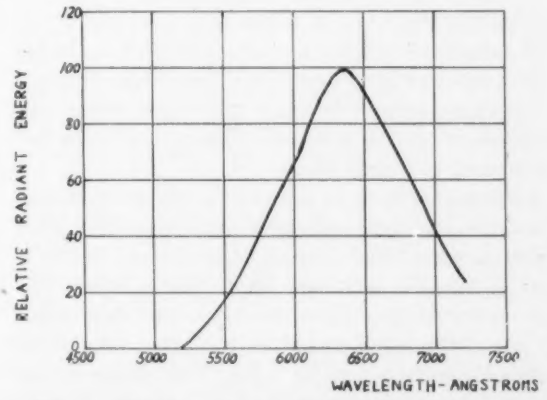

FIG. 1. Emission of manganese-activated antimony oxide phosphor with 2537 Å excitation.

TABLE II. *X-ray diffraction pattern of* Sb_2O_4Mn *phosphor*

d	Intensity	*d*	Intensity	*d*	Intensity	*d*	Intensity
3.19	m	1.498	m	1.110	s	0.937	w
3.03	w	1.479	v.w.	1.092	w	0.924	s
2.91	w	1.464	m	1.077	w	0.911	v.w.
2.86	m	1.430	w	1.066	m	0.907	v.w.
2.62	v.w.	1.394	m	1.062	m	0.899	s
2.41	w	1.316	v.w.	1.055	m	0.895	m
2.18	v.w.	1.293	v.w.	1.028	v.w.	0.885	s
1.98	v.w.	1.239	s	1.010	v.w.	0.881	m
1.82	m	1.214	v.w.	1.007	v.w.	0.875	v.w.
1.81	m	1.201	m	0.997	w	0.870	m
1.78	m	1.189	v.w.	0.988	m	0.858	m
1.71	v.w.	1.172	w	0.977	w	0.851	s
1.67	w	1.152	m	0.971	w	0.843	m
1.61	s	1.142	v.w.	0.968	w		
1.58	v.w.	1.127	v.w.	0.948	m		

TABLE III. *Antimony content of antimony oxides*

Sample	% Sb
b-0	83.13
b-2	79.65
b-4	80.88
Sb_2O_3 (theor.)	83.34
Sb_2O_4 (theor.)	79.19

at 35 kv and 10 ma. In addition to the phosphor samples, the following materials were prepared:

(*a*) The product of hydrolysis of antimony chloride was treated with dilute hydrochloric acid and ammonia, and dried at 110°C;

(*b*-0) Sample (*a*) was boiled with sodium carbonate solution and dried at 110°C;

(*b*-1) Sample (*b*-0) was heated at 300°C for 5 hr;

(*b*-2) Sample (*b*-0) was heated at 500°C for 5 hr;

(*b*-3) Sample (*b*-0) was heated at 600°C for 12 hr in an atmosphere of nitrogen;

(*b*-4) Sample (*b*-0) was treated with nitric acid and then heated at 750°C for 2 hr;

(*b*-5) Sample (*b*-4) was heated at 1100°C for 2 hr.

Results are shown in Tables II and III and Fig. 2. Data for cubic antimony trioxide and cubic antimony tetroxide in Fig. 2 were taken from Hanawalt and coworkers, from Dehlinger, and from Natta and coworkers (1). Conclusions drawn for these unactivated materials follow.

Sample (*b*-0) is a mixture of cubic antimony trioxide and hydrated antimony oxide. The latter also becomes cubic trioxide when heated to 300°C (*b*-1). Between 300° and 500°C the material (*b*-0) is converted into cubic antimony tetroxide, while some of the cubic trioxide is converted into orthorhombic trioxide [sample (*b*-2)]. This finding is supported by the results of chemical analysis. Gain in weight was not as high as would be expected on the

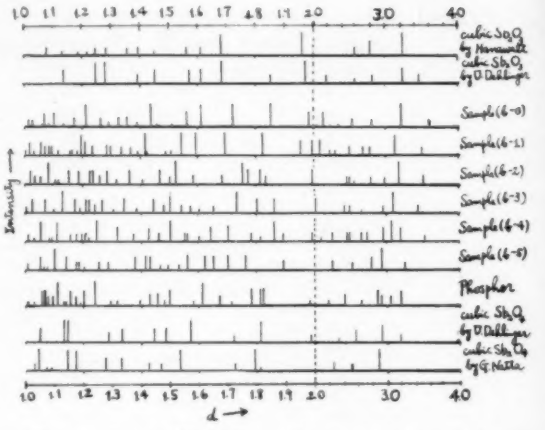

FIG. 2. X-ray diffraction patterns of various antimony oxide compositions.

basis of complete oxidation of trioxide to tetroxide. The sample gained only 4.48% compared with the theoretical value of 5.50% for complete oxidation. Fig. 3 shows that a final steady state was actually reached.

Diffraction lines of sample (*b*-2) were compared with the pattern for orthorhombic antimony trioxide as reported by Buerger (2) (not shown in Fig. 2). The latter material had been prepared by sublimation in a nitrogen atmosphere. Sample (*b*-3) is a comparable material. Sample (*b*-4), which was used for the preparation of phosphors, contains both antimony tetroxide and trioxide. The situation is similar in sample (*b*-5) and in the actual phosphor sample. Unfortunately, the structure of the phosphors themselves could not be determined satisfactorily. This is because of the lattice distortions brought about by additions of boric oxide and manganese. X-ray patterns of phosphors with low and with high manganese concentrations were taken of materials fired in air, oxygen, and nitrogen atmospheres, but they did not permit a clarification of the structure picture. Neither did the x-ray

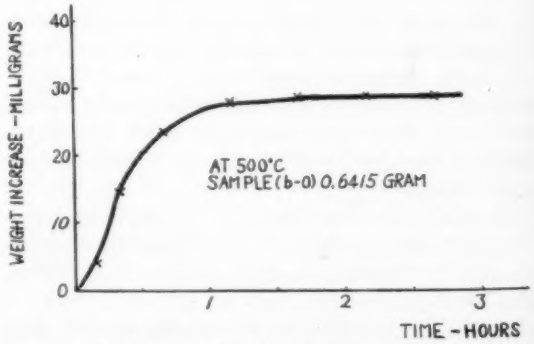

FIG. 3. Gain in weight of antimony oxide heated in air at 500°C.

TABLE IV. *Effect of firing atmosphere on brightness*

$MnSO_4$ in % of amount in base formula	Rel. brightness after firing in		
	Oxygen	Nitrogen	Air (from Table I)
40	36	54	54
100	40	65	100
200	38	49	56
300	33	26	52
500	43	39	75*
750	39	37	75
1000	30	20	72*
2500	33	29	64

* Data obtained by repeat tests.

patterns of materials prepared with boric acid or with manganese alone, in the absence of antimony oxide. Examination under a petrographic microscope showed the phosphors to contain noncubic portions. At present, the phosphors are believed to be a mixture of cubic antimony tetroxide and some orthorhombic trioxide in close association with the former.[2]

This view is supported by the dependency of phosphor brightness upon manganese concentration. As shown in Table I, there are two brightness maxima. Although this seems to be an unusual result, it has been confirmed by repeat experiments which were carried out in oxygen and nitrogen, as well as in air. Data are shown in Table IV. Compared with normal firing in air, brightness is decreased in oxygen as well as in nitrogen. In oxygen, both peak values are decreased, but the first maximum is decreased more strongly. In nitrogen, the decrease of the first maximum is not as strong.

[2] *Footnote added in print.*

Patterns made of materials prepared without boric acid and manganese (a), with manganese alone (no H_3BO_3, b) and with boric acid alone (no Mn, c) were compared with that of phosphor (d) by means of a Norelco x-ray spectrograph. Patterns of antimony oxide fired alone or mixed with manganese sulfate and/or boric acid at 1100°C for 4 hr were also compared. The x-ray tube was operated at 35 kv and 15 ma and copper radiation was used.

The results confirmed the fact that addition of boric acid simplified the patterns, perhaps because boric acid acts as a flux and regularizes the crystal structure of antimony oxide. They also showed that by the addition of manganese the lattice of antimony oxide was expanded (a and b), while that of antimony oxide prepared with boric acid (c) was contracted. The presence of free boric acid or of a possible borate was not evident.

A tentative explanation for this follows. The incorporation of manganese in the lattice may take place in two forms, namely, in the tetroxide and in the trioxide phase, each giving rise to an emission at nearly the same wave length. However, these two phases are not necessarily mechanically separated, nor are they a solid solution of one in the other. Rather, they are assumed to be substantially a tetroxide material in which some of the oxygen positions are left vacant, giving rise to "trioxidic" and to "tetroxidic" surroundings for the manganese activator. It is the relative proportion of these surroundings in the crystal which determines the brightness at low and high concentrations of manganese, the latter apparently having an effect upon these proportions.

Assuming that manganese enters preferentially in "trioxidic" surroundings, increasing amounts of manganese first serve to intensify the first maximum, while larger amounts intensify the second maximum in "tetroxidic" surroundings. The change of the relative height of the brightness peaks with the nature of the firing atmosphere favors this assumption. In an oxygen atmosphere the trioxide content is reduced which should lead to a relative increase of the second maximum, and vice versa.

The reason manganese preferentially enters "trioxidic" surroundings is not clear. It might be explained with the stability and distribution of manganese ions in different lattice structures. Further work on this phosphor system is under way.

Acknowledgments

The authors wish to express their thanks to M. Yamada and K. Mitsuhashi for the measurements of the spectral distribution, to E. Asada for the x-ray diffraction patterns, and to K. Nishida, N. Adachi, and S. Makishima for general discussions on the subject and some of their experimental work.

Any discussion of this paper will appear in a Discussion Section to be published in the June 1956 issue of the Journal.

References

1. J. D. Hanawalt, H. W. Rinn, and L. K. Frevel, *Ind. Eng. Chem. Anal. Ed.*, **10**, 457 (1938); U. Dehlinger, *Z. Krist.*, **66**, 108 (1927); G. Natta and M. Baccaredda, *Z. Krist.*, **85**, 271 (1933).
2. M. J. Buerger, *Am. Mineral.*, **21**, 206 (1936).

Bomb Reduction of Molybdenum Trioxide by Calcium Metal[1]

H. L. Gilbert[2] and F. E. Block

Northwest Electrodevelopment Experiment Station, U. S. Bureau of Mines, Albany, Oregon

ABSTRACT

Molybdenum trioxide has been reduced by calcium in a sealed bomb to produce massive reguli of molybdenum metal. A full description of the production of 25 lb reguli is given. Reguli are joined and employed as a consumable electrode in arc melting to produce ingot. Metal may be hot forged and rolled to desired form.

Introduction

Although the reduction of metallic compounds by carbonaceous materials may be dated in terms of the first use of bronze and iron by man, the use of more active metals as reducing agents perhaps was described first by Berzelius in 1825 in his salt bath reduction of zirconium fluoride by sodium metal (1). In 1898 Goldschmidt described his aluminothermic process for reducing oxides of metals, including molybdenum trioxide (2). These methods were re-examined by several workers, including Lely and Hamburger, who in 1914 developed the closed reactor or "bomb" for use in reducing various metal chlorides by sodium (3). Marden and Rich in 1926 applied this process to metal oxides in their work on the reduction of vanadium oxide by calcium metal in a bomb (4).

Many materials have been reduced on various scales under the supervision of Spedding (5). Gray (6) has described the production of certain rare earth metals, and the recent work of McKechnie and Seybolt (7) in the production of ductile vanadium answered questions remaining from the work of Marden (4) and Kroll (8).

The metal prepared by the early experimenters with bomb reductions was generally powder rather than massive metal. A powder product was frequently the result of a lack of thermal efficiency, but on occasion powder was desired in order to use powder metallurgy consolidation techniques. Also, most of the metal reduced in earlier work had a melting point considerably below that of molybdenum, hence experimental conditions did not require production of very high temperatures with the concurrent dangers involved as in the case of the reduction of molybdenum into a massive regulus. In the experiments about to be described, the objective was the production of massive metal rather than powder.

[1] Manuscript received September 29, 1954. This paper was prepared for delivery before the Cincinnati Meeting, May 1 to 5, 1955.

[2] Present address: Harvey Aluminum, Torrance, Calif.

Experimental Procedure

As a part of a larger research effort on new techniques for production of molybdenum metal, the bomb reduction of molybdenum oxide was first examined in a general manner. Successful bomb reduction requires the formation of massive metal if a high recovery is expected and, because the melting point of molybdenum is about 2600°C, one would perhaps not expect a massive regulus of molybdenum to be formed. Initial tests with molybdenum dioxide and calcium bore out expectations that only powder would be formed, while a rather rudimentary test with molybdenum trioxide, surprisingly enough, produced small metallic particles.

The reaction involved 525 g of molybdenum trioxide and 444 g of $\frac{1}{4}$-in. mesh calcium metal. The mixture was placed in a freshly burned calcium oxide-lined steel bomb and the bomb closed and heated to 725°C to fire the charge. The metallic particles shown in Fig. 1 were obtained.

Repeated tests on a 1-lb (MoO_3)-size bomb showed that the method of ignition of the bomb left much to be desired since the external heating weakened the wall of the bomb and caused some burnouts. It was also felt that the random efficiencies encountered indicated that the reaction could be initiated at different points within the charge with different end results. To check this, and at the same time permit reaction within a cold wall bomb, a resistance igniter, consisting of a standard automotive sparkplug with an 18-gauge molybdenum wire connected across the points, was developed. This igniter was the key that permitted expansion of the process to the scale herein described.

An increase in the scale of the operation, using a 5-lb charge, showed that the calcium oxide refractory employed to line and protect the steel bomb was fused down into the slag during the reaction, leaving the wall unprotected. Replacement of the calcium oxide refractory by electrofused magnesia solved this problem. It was shown on the larger scale that the erratic results obtained previously could be attributed to accidental location of the initiation of

FIG. 1. Pellets of molybdenum formed in reduction of MoO_3 by calcium in exploratory test.

reaction. Metal recovery effected when the charge was ignited at the bottom, middle, and top of the bomb was 47, 68, and 84%, respectively. This would indicate that the fall of molten metal progressively downward either accelerates the reaction or tends to collect the metal, or perhaps both. A concurrent study of bomb shape showed that, for optimum results, a bomb should have a height-diameter ratio of about 5:1.

Variations in the ratio of calcium to MoO_3 showed that the use of 50% excess calcium over the stoichiometric requirement substantially reduced the molybdenum yield but improved the quality of that metal produced. Use of 10% excess calcium gave the best yield of metal, but troublesome amounts of oxygen remained in the metal. A 20% excess of calcium appeared to be a good compromise and this was used in the majority of the tests.

As indicated by McKechnie and Seybolt (7), use of iodine to boost the thermal energy of the charge is of definite assistance, but since iodine is a rather expensive reagent, an effort was made to minimize the amount employed. Small-scale (1 lb MoO_3) reactions required 80 g of iodine per pound of MoO_3, while in larger (50 lb MoO_3) reactions this was reduced to 50 g of iodine per pound of MoO_3. Theoretical calculations show that somewhere in the charge range of 75–100 lb of MoO_3 iodine would no longer be required, except for a few grams in the immediate vicinity of the igniter.

Although a variety of techniques was developed during the course of this work, much of the exploratory effort may be summarized by describing in some detail the technique finally employed. The bomb was made from 11-in. ID $11\frac{1}{16}$-in. wall seamless-steel pipe with welded flanges at the ends. End plates were held in place by twelve $1\frac{1}{4}$-in. diameter alloy steel bolts. A high-pressure closure employing a round copper gasket sealed the bomb against leakage. The bomb was assembled with a paper-wrapped wooden mandrel located where the charge was desired. Electrofused magnesia, ground and mixed in an aggregate, 70% of which would pass 200-mesh size, was tamped into the space between the mandrel and the bomb wall to form a liner. An alternate method was the use of sodium silicate (waterglass) to bond the magnesia. The amount used contributed 0.37% silicon to the liner. After placement of the liner by either the wet or the dry method, firing was necessary to give the liner enough strength to withstand the loading operation. Firing was accomplished by means of a split graphite resistor placed inside the bomb and electrical strip-heaters clamped to the outside of the bomb. The graphite resistor was operated at 1500°–2000°C for 6 hr with an input of 1000 amp at 24 v a.c., at the conclusion of which time the liner had a moderately hard inner surface.

Molybdenum trioxide purchased on the open market was found to be pure and dry enough to use in making up bomb charges without further treatment. Commercial calcium metal is invariably contaminated with calcium oxide and nitride. The oxide, if not excessive, is of little consequence since the reaction involves an oxide, but nitrogen is very detrimental. Crude calcium metal was vacuum-sublimed to reduce the nitrogen level from the initial figure, 1700 ppm, to about 60 ppm. Sublimation had the further effect of creating a coarsely crystalline metal which was readily cut to pass $\frac{1}{4}$-in. mesh in a

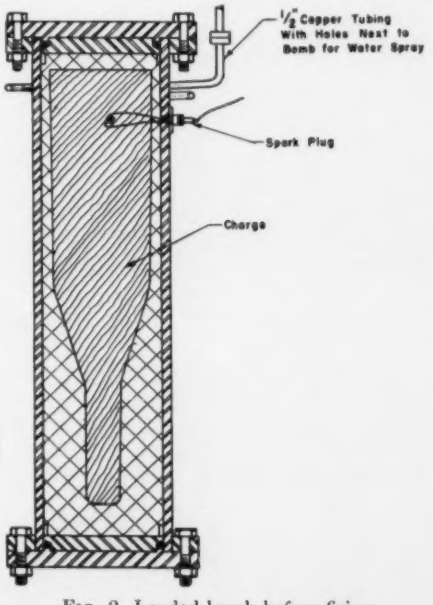

FIG. 2. Loaded bomb before firing

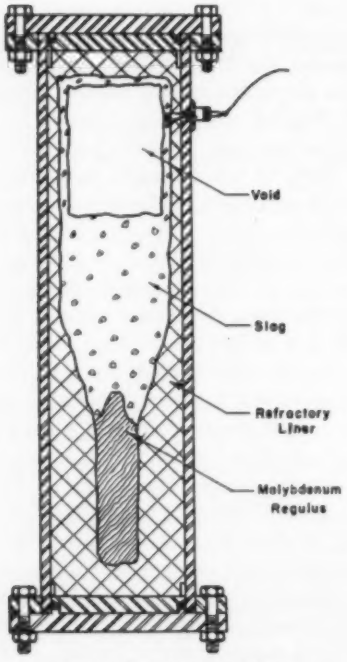

FIG. 3. Bomb after firing

FIG. 4. Sectioned regulus showing typical porosity

Mitts & Merrill hog machine. No commercial source of such metal was found at the time of the tests.

As a safety feature the charge was prepared in about 50 increments, each consisting of 1 lb of MoO_3, 1 lb of calcium, and 50 g of iodine.

The incremental charges were placed in the bomb, the igniter was inserted at the proper level, and a layer of magnesia was put in place to protect the lid of the bomb as shown in Fig. 2. The top seal was carefully placed in position since, if any leakage at all occurred due to a dirty closure or gasket, the bomb was destroyed in the ensuing explosion.

The bomb was moved to a remote location for firing, and personnel and equipment were protected by concrete revetments. Before firing a heavy spray of cooling water was fixed to play on the bomb.

The reaction was initiated by applying a source of a-c power to the igniter. No sound accompanied a successful firing. Twelve hours later the bomb was opened to show the result pictured in Fig. 3. The regulus of metal and the slag were separated from the liner material, which was saved for reuse. The regulus was easily recovered, but averaged only 80% of the theoretical density owing to inner porosity, as shown in Fig. 4. An average molybdenum recovery of 97% of the charge was obtained as a single mass of metal.

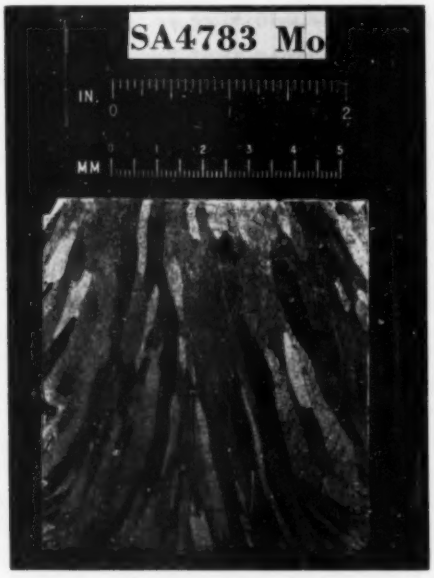

FIG. 5. Macro-etched test ingot showing typical large columnar grain structure.

FIG. 6. Microstructure of arc-melted calcium-reduced molybdenum. Etchant, NH_4OH-H_2O_2. 500× before reduction for publication.

Character of the Metal Produced

The quality of the reguli was studied by consumable-electrode arc melting them in a water-cooled copper mold and examining this ingot both metallographically and in forging tests. In the case illustrated, the 3½-in. diameter reguli were welded together and remelted into an 8-in. diameter ingot by a power input of 4500 amp at 32 v. A furnace atmosphere of 10% argon and 90% helium at atmospheric pressure was employed.

Ingot metal was sound and relatively clean. Macro- and microstructure of the metal is shown in Fig. 5 and 6. This material was not readily forgeable due to traces of residual oxygen, which, while present in only minute quantity, appeared to exert great influence through its location as thin planar crystals of molybdenum dioxide between the massive crystals of metal. Chemical analyses of typical reguli were as follows:

Chemical analyses of arc-melted molybdenum reguli

Sample No.	Assay, ppm		
	C	O_2	N_2
MoR62	380	55	190
MoR63	300	30	180
MoR65	190	70	110
MoR66	140	110	150
MoR68	300	150	70

To overcome the effect of the residual oxygen several materials capable of agglomerating the intergranular material were added to the bomb charge in small amounts.

Although this study is incomplete and no definite correlation can be made, additions of aluminum, thorium, or carbon in amounts ranging up to 2% of the weight of the molybdenum in the charge appear definitely to improve the ductility of the metal produced. It is believed that these materials influence the form of the oxygen in the final metal rather than actually removing it. The most ductile metal to date was produced by collecting the reduced molybdenum regulus in a graphite crucible embedded in the magnesia refractory inside the bomb.

FIG. 7. Microstructure of arc-melted molybdenum, calcium-reduced in the presence of 3% aluminum. Etchant, NH_4OH-H_2O_2. 75× before reduction for publication.

The microstructure of aluminum-treated material is shown in Fig. 7. Such treated material could be hot forged and rolled to sheet.

In an effort to lower the cost for producing molybdenum by this method attempts were made to substitute magnesium for the more expensive calcium as a reductant. By this means, a smaller quantity of less costly reductant was necessary, with the result that a greater portion of the bomb charge could be utilized for molybdenum trioxide. Although the yield of molybdenum metal did not suffer in a magnesium reduction, the fused reguli showed increased porosity and more oxide appeared to be occluded in the grains and grain boundaries. Major complications arose when magnesium reductions were performed in the larger bombs. Because magnesium has a substantially higher vapor pressure than calcium, greatly increased pressures were developed inside the bombs with the result that the bomb wall failed in several tests. For this reason, magnesium reductions were discontinued.

Bomb conditions were studied by physical and theoretical means. The thermodynamics of the reaction of molybdenum oxide with various metals has been studied by Ward and coworkers (9). From this information and various collected values, a temperature of 3000°C has been calculated as possible in the reaction of molybdenum trioxide and calcium under adiabatic conditions. Although conditions within the bomb are not adiabatic, the reaction apparently does reach its peak in a matter of some 35 sec. Molybdenum trioxide may be considered to be a peroxide type material which sublimes below its melting point of 795°C at atmospheric pressure. As calcium has a boiling point of 1690°C and the two reaction products, calcium oxide and molybdenum, have essentially no vapor pressure even at elevated temperature, it is likely that the reaction is essentially one between calcium vapor and molybdenum trioxide vapor, which form and then condense instantly on contact or between liquid MoO_3 and calcium vapor. The average pressure peak of 1200 psi, as determined by a variety of strain-gauge tests, occurs about 35 sec after ignition.

Conclusions

The method described here has permitted the production in a bomb of massive reguli of molybdenum with 97% efficiency through reduction of molybdenum trioxide by calcium metal in the presence of iodine. Addition of thorium, aluminum,

or carbon to the bomb charge improved the forgeability of the metal produced. The 20-lb reguli produced were not satisfactory for use until consumable-electrode arc melted. The principal problem at present is in placing the refractory lining in the bomb shell. The safety of personnel during the mixing of the reactants and bomb loading is subject to question. Further improvement in metal quality would be of interest.

Acknowledgments

Gratitude is expressed to John S. Nachtman of the Navy Bureau of Ordnance, under which this project was carried out, for permission to publish this article.

Bomb work was carried out by J. K. Hoy, M. M. Barr, and Gene Asai, supervised by H. A. Johansen, T. T. Campbell, and C. Q. Morrison. Arc melting was under the supervision of R. A. Beall, while metallographic work was performed through the courtesy of E. T. Hayes.

Any discussion of this paper will appear in a Discussion Section to be published in the June 1956 JOURNAL.

REFERENCES

1. J. Berzelius, *Pogg. Ann.*, **4**, 121 (1825).
2. H. Goldschmidt, *Lieb. Ann.*, **301**, 19 (1898).
3. D. Lely and L. Hamburger, *Z. anorg. u. allgem. Chem.*, **87**, 209 (1914).
4. J. W. Marden and M. N. Rich, *Ind. Eng. Chem.*, **19**, 786 (1927).
5. F. H. Spedding, H. A. Wilhelm, W. H. Keller, D. H. Ahmann, A. H. Doane, C. C. Hach, and R. P. Ericson, *ibid.*, **44**, 553 (1952).
6. P. M. J. Gray, *Metal Ind., London*, **80**, 43 (1952).
7. R. K. McKechnie and A. U. Seybolt, *This Journal*, **97**, 311 (1950).
8. W. J. Kroll, *Z. Metallkunde*, **28**, 30 (1936).
9. J. J. Ward, J. P. Ray, and S. A. Herres, Project Rand Report R-108, Battelle Memorial Institute, Columbus, Ohio, July 19, 1948.

The Thermodynamic Stability of Refractory Borides[1]

LEO BREWER

Department of Chemistry and Chemical Engineering, University of California, Berkeley, California

AND

HAAKSON HARALDSEN

Universitetes Kjemiske Institutt, Blindern, Oslo, Norway

ABSTRACT

Reactions between nitrogen gas and metal borides and between graphite and metal borides have been studied to obtain qualitative information on the relative stabilities of the metal boride phases. At high temperatures many borides are inert toward carbon or nitrogen. The most stable borides are found to be those of Ti, Zr, Nb, and Ta of the fourth and fifth groups of the periodic table. Data are summarized in terms of limits to the heats of formation.

INTRODUCTION

The determination of the thermodynamic properties of refractory borides such as the borides of the transition metals of the fourth to sixth groups of the periodic system is an especially difficult problem. These borides are very inert and are not easily dissolved in any solvents. Thus, conventional calorimetric methods cannot be used to determine their heats of formation. Combustion calorimeters are not readily applicable to these compounds because of the difficulty of obtaining complete combustion and definite final products. A method that appears to be generally applicable is the determination of high temperature equilibria conditions in systems containing these compounds. One promising type of experiment would be the determination of the boron decomposition pressure in equilibrium with the boride phase as a function of temperature. This method can be expected to give accurate results, but high temperatures are required. Equilibration of two metals with boron and determinations of the boride phases formed can also give information about the thermodynamic stability of the borides. Other experiments that could give useful thermodynamic data would be the determination of the equilibrium between nitrogen gas and the boride and nitride phases or the determination of the equilibrium between graphite and the boride and carbide phases. This paper will describe the results of experiments of the last three types that were carried out in an endeavor to obtain even qualitative information about the relative stability of boride phases.

Nitrogen systems.—The equilibria involving nitrogen gas can be expressed by the general equation:

$$MB_x(s) + \left(\frac{x+y}{2}\right) N_2(g) = MN_y(s) + xBN(s).$$

Knowing the free energies of formation of the nitride phases, the determination of the equilibrium constant for this reaction gives one the free energy of formation of the boride phase. For this result to apply to the pure boride phase, there must be little solubility of the solid phases in one another and no ternary phases must be formed. Evidence of such behavior can often be found by x-ray analysis. After these studies were under way, a paper by Kiessling and Liu (1) appeared in which they had carried out similar studies at much lower temperatures. Their experiments indicated that ammonia at atmospheric pressure always destroyed the metal boride phase yielding the metal nitride and boron nitride. The authors' experiments at higher temperatures had shown that the boride phases were stable in the presence of nitrogen. Thermodynamic calculations reconcile the two sets of results since the calculations show that increasing the temperature favors the borides over the nitrides. The authors' results obtained with the nitrogen system are tabulated in Table I. In the following discussion, these results will be combined with Kiessling's results and used in an attempt to evaluate thermodynamic data for the boride phases.

Carbon systems.—The equilibria in the carbon systems can be expressed by the general equation:

$$MB_x(s) + \left(\frac{x}{4} + y\right) C(s) = MC_y(s) + \frac{x}{4} B_4C(s).$$

This system was studied by heating various borides with graphite and determining by x-ray analysis the phases at equilibrium with one another. After this

[1] Manuscript received November 1, 1954. This paper was prepared for delivery before the Wrightsville Beach Meeting, September 13 to 16, 1953.

TABLE I. *Heatings in 0.5 atm N_2 using molybdenum crucibles*

Starting phases	Temp, °K	Final phases
Ti + B + BN + N_2(g)	2270	$\underline{TiB_2}_{s.}$ + $\underline{TiN}_{s.}$ + $\underline{BN}_{w.}$
Ti + 3B + N_2(g)	1820	$\underline{TiN}_{v.s.}$ + $\underline{TiB_2}_{w.}$ + BN?
Zr + 3B + N_2(g) Zr + 3B + ¼ BN + N_2(g)	1820	$\underline{ZrB_2}_{v.s.}$ + $\underline{ZrN}_{w.}$ + $\underline{BN}_{v.w.}$
Zr + B + BN + N_2(g)	2270	$\underline{ZrN}_{v.s.}$ + $\underline{ZrB_2}_{s.}$
W + 3B + ¼ BN + N_2(g)	1820	$\underline{W_2B_5}_{s.}$ + $\underline{WB}_{m.}$ + $\underline{\ ?\ }_{w.}$
W + 3B + N_2(g)	1820	$\underline{WB}_{s.}$ + $\underline{W_2B}_{m.s.}$ + $\underline{W_2B_5?}_{v.w.}$
Cr + 3B + N_2(g)	1820	$\underline{Cr_2N}_{m.s.}$ + ?
Cr + 3B + ¼ BN + N_2(g)	1820	$\underline{Cr_2N}_{m.s.}$ + $\underline{CrB_2}_{m.}$ + BN?

s. = strong, m. = medium, w. = weak, v. = very.

TABLE II. *Heating in 0.5 atm argon at 2050°K*

Starting phases	Final phases
Ce + 4B + C	$\underline{CeB_4}_{m.}$ + $\underline{CeB_6}_{m.w.}$
Ce + 6B + ½C	$\underline{CeB_6}_{s.}$ + $\underline{CeB_4}_{m.s.}$
Zr + 2B + C	$\underline{ZrB_2}_{s.}$ + $\underline{ZrC}_{s.}$ + ?
Nb + B + ½C	$\underline{NbB_2}_{s.}$ + $\underline{NbC}_{m.}$
Nb + 2B + C	$\underline{NbB_2}_{s.}$ + $\underline{NbC}_{s.}$
2Mo + B + ½C	$\underline{Mo_2B}_{m.}$ + $\underline{\alpha\text{-MoB}}_{m.}$
Mo + B + C	$\underline{\alpha\text{-MoB}}_{s.}$ + $\underline{\beta\text{-MoB?}}_{w.}$
2Mo + 5B + C	$\underline{MoB_2}_{s.}$ + $\underline{\alpha\text{-MoB}}_{m.}$

work had been completed, a paper by Glaser (2) appeared which presented similar experiments largely at higher temperatures. The authors' results are presented in Table II. In the following discussion all available data are used to attempt to fix the relative stabilities of the boride phases.

Metal exchange experiments.—The equation,

$$MB_x(s) + \left(\frac{x}{y}\right) R(s) = \left(\frac{x}{y}\right) RB_y(s) + M(s)$$

represents the equilibria obtained by heating two different metals together with boron such that there is insufficient boron for both metals. These experiments are more straightforward in principle than the experiments described above but are more complicated in practice due to more extensive solid solubilities among the boride phases than among the boride and nitride or boride and carbide phases. The results of these experiments are given in the following text.

Experimental Procedure

All experiments were done in the same equipment and in the same manner as the experiments described by Brewer, Sawyer, Templeton, and Dauben (3). Molybdenum crucibles were used as containers. The heatings were done in 0.5 atm nitrogen gases when equilibria involving nitrides were studied and in 0.5 atm argon for the other experiments. Each experiment was held for about 50 min within 100° of the temperature given in the tables. The boron used was obtained from the Fairmount Chemical Company, Newark, New Jersey, and was 99.5% pure. The main impurities were several tenths of a per cent of Ni, and less than 0.1% of Al and Mg. The metal powders were 99.9% pure except for Ti and Zr which contained oxide and nitride impurities.

Discussion of Experiments

Nitride equilibria.—The experiments described in Table I were carried out by mixing metal powder, boron powder, and boron nitride powder and heating in nitrogen gas or by just heating the mixture of metal and boron powders in nitrogen gas. The resulting phases are listed in order of importance with the main phases underlined. The intensities of the x-ray powder patterns are indicated, although it is understood that these do not indicate the actual abundances, as phases with simple patterns will give strong patterns even when not abundant. The question mark after BN indicates that only the strongest line of the pattern was observed. A question mark alone indicates the pattern of an unidentified phase. In addition to the experiments described in Table I, mixtures with sufficient metal to result in both boride and nitride phases were heated to determine if ternary compounds or solid solution formation could be expected. No ternary phases were observed and within the experimental uncertainty of ±0.003 Å, no evidence could be obtained for sufficient solid solution formation in the quenched products to cause variation of lattice constants.

Table I shows that strong x-ray patterns of TiN and ZrN, or solid solutions of these compounds with TiB and ZrB, are observed when the boron-to-metal ratio does not exceed two. This is due to the

nitride impurity in the metals as well as to some boron loss to the crucible. With higher boron-to-metal ratios the nitride diffraction patterns appear only weakly. As patterns of cubic phases appear very sensitively, the amount of the nitride phases must be very small and their occurrence is undoubtedly due to formation during cooling. Thus, the results of Table I indicate that ZrB_2, WB, W_2B, and W_2B_5 are stable in the presence of N_2 at 1820°K. TiB_2 is largely converted to TiN at 1820° K but it is quite stable at 2270°K. At 1820°K borides of Cr are also largely converted to Cr metal which is converted to Cr_2N on cooling. Since the reaction of nitrogen with these borides can be shown to be exothermic with a large entropy decrease, the borides will be stable at high temperatures but become less stable with respect to nitrides as the temperature is lowered, and virtually all borides can be expected to react with nitrogen at lower temperatures. This explains why Kiessling and Liu (1) found tungsten borides to be converted to the metal or nitride at temperatures below 1370°K while the authors find the tungsten borides stable at 1820°K. Also Kiessling and Liu's use of ammonia tends to give the nitriding reaction a greater driving force as is indicated by the formation of metastable nitrides such as the iron nitrides in the ammonia stream, but at 1370°K the effect should not be large.

The experimental data can be expressed in thermodynamic quantities as indicated by the following equations.

$$TiB_2(s) + \tfrac{3}{2}\,N_2(g) = TiN(s) + 2BN(s), \quad \Delta F^\circ_{2280} > 0 \text{ and } \Delta F^\circ_{1820} \sim 0 \qquad (I)$$

$$ZrB_2(s) + \tfrac{3}{2}\,N_2(g) = ZrN(s) + 2BN(s), \quad \Delta F^\circ_{1820} > 0 \qquad (II)$$

$$W_2B(s) + \tfrac{1}{2}\,N_2(g) = 2W(s) + BN(s), \quad \Delta F^\circ_{1820} > 0 \text{ and } \Delta F^\circ_{1373} < 0 \qquad (III)$$

$$CrB_2(s) + N_2(g) = Cr(s) + 2BN(s), \quad \Delta F^\circ_{1820} \leq 0 \qquad (IV)$$

To obtain limits to the heats of formation of the borides, the following thermodynamic data were used. Data for the elements were obtained from Brewer (4). For BN at 1820°K, $\Delta F^\circ = -15.7$ kcal was calculated from data given by Dworkin, Sasmor, and van Artsdalen (5) and Kelley (6). For TiN at 1820°K, $\Delta F^\circ = -40.0$ kcal was obtained from data given by Humphrey (7) and Kelley (6).

Thus for TiB_2, $\Delta F^\circ_{1820} \sim -71.4$ kcal and $\Delta H^\circ_{298} \sim -71$ kcal since ΔS° and ΔC°_p will be close to zero.

For ZrN, $\Delta H^\circ_{298} = -87.3$ kcal (8), $\Delta S^\circ_{298} = -22.9$ e.u. (6), and $\Delta C^\circ_p = 0$ were used to obtain for $ZrB_2(s)$, $\Delta H^\circ_{298} < -77$ kcal.

In a similar manner one obtains for CrB_2, $\Delta H^\circ_{298} \geq -31$ kcal and for W_2B, $\Delta H^\circ_{298} < -16$ kcal. From Kiessling and Liu's ammonia results, one can also give for W_2B, $\Delta H^\circ_{298} > -28$ kcal and for WB, $\Delta H^\circ_{298} > -22$ kcal.

In addition to the metals listed in Table I, cerium metal was also heated with boron and boron nitride in nitrogen gas at 2280°K. CeO_2, Ce, and CeN x-ray diffraction patterns were obtained, but the main phases present after heating could not be identified from the diffraction patterns. Also the molybdenum crucible reacted with the sample to a considerable extent. CeB_4 and CeB_6 definitely were not present. It would seem that cerium borides are less stable than nitride or ternary phases at this temperature. This would fix ΔH°_{298} for CeB_4 as > -84 kcal using $\Delta H = -78.0$ kcal for CeN from Brewer (9).

Carbide equilibria.—The experiments presented in Table II were carried out by heating a mixture of metal powder with boron and graphite powders. From the results of Table II, one would conclude that CeB_6, ZrB_2, NbB_2, Mo_2B, MoB, and MoB_2 are stable in the presence of graphite. Due to the low atomic weight of carbon, the graphite phase is difficult to demonstrate. ZrC and NbC patterns can be detected due to some boron loss to the crucible which leaves metal free to react with the graphite. No evidence was found for changes in lattice constant at room temperature due to solid solution formation. The combination of molybdenum with boron and graphite did not always give clear-cut results. Unidentified lines found in some of the samples are apparently due to high temperature modifications. Hexagonal MoB_2 was definitely identified and by comparison with the NbB x-ray pattern, some of the lines can be taken as a probable indication of the presence of MoB with the CrB structure. Two samples of the composition 2Mo + B + C did not give any identifiable phases after heating between 2170° and 2240°K. Although Glaser (2) reports Mo_2B stable in the presence of C and the authors find Mo_2B in a 2Mo + B + ½ C mixture, a reaction $2Mo_2B + C \rightarrow Mo_2B + MoB + MoCB_x$ could account for the authors' results if x is small. In a similar way the high CeB_6 content found for the Ce + 4B + C composition indicates a reaction. This has been recently confirmed by Engelke (19) who finds evidence for a ternary Ce-B-C compound.

The above results together with those reported by Brewer, Sawyer, Templeton, and Dauben (3), Glaser (2), Steinitz (10), and Nelson, Willmore, and Womeldorph (11) allow the borides to be divided into the two groups shown in Table III.

Where different investigators have carried out similar experiments, all of them agree except for W_2B. Glaser (2) and Schwarzkopf and Glaser (12)

TABLE III

Borides stable in presence of graphite	Borides unstable in presence of graphite
CeB_6	CeB_4
TiB_2	Ti_2B, TiB, Ti_2B_5
ZrB_2	ZrB, ZrB_{12}
ThB_6	ThB_4
NbB_2	Nb_2B, NbB, Nb_3B_4, NbB_m
TaB_2	Ta_2B, TaB, Ta_3B_4, TaB_m
Cr_2B, Cr_5B_3, CrB, Cr_3B_4, CrB_2	Cr_4B?, Cr_2B_5?
Mo_2B?, Mo_3B_2, α-MoB, β-MoB, MoB_2, Mo_2B_5	Mo_2B?
WB, W_2B_5	W_2B
Fe_2B, FeB	
Co_2B, CoB	
Ni_2B	

report preparation of W_2B in a graphite crucible and conclude that W_2B is stable in graphite. However Brewer, Sawyer, Templeton, and Dauben found a definite reaction between W_2B and C, when intimately mixed, to form WB and WC. Thus Glaser's result would seem to be due to poor contact. Krikorian (13) has recently rechecked this and has confirmed the reaction of W_2B and C to yield WC and WB. He has also shown that W_2C, WC, and W_2B exist together without reaction. Nelson, Willmore, and Womeldorph (11) report Cr borides stable in the presence of graphite without indicating which ones. Glaser reports that five chromium boride phases are stable, but gives no information for Cr_4B or Cr_2B_5 which probably react with carbon.

From the results given in Table III, one can write equations for the reactions of the borides with graphite for which one can indicate $\Delta F°$ as greater than or less than zero. The temperature is not of great importance for the carbide equilibria in contrast to the nitrogen systems, as $\Delta S°$ and $\Delta C°_p$ for the reactions of borides with graphite will be close to zero and $\Delta F°$ will change little with temperature. Also $\Delta H°_{298}$ can be used in place of $\Delta F°_T$ at any temperature for these approximate considerations. The following heats of formation limits can be derived on this basis.

TiB_2	$\Delta H°$	<-51	TaB_2	$\Delta H°$	<-45
ZrB_2		<-51	NbB_2		<-37
ThB_4		<-54	W_2B		<-22
ThB_6		<-66	WB		<-13 kcal

In deriving these values, $\Delta H°_{298} = -43.85$ kcal was used for TiC (7), $\Delta H°_{298} = -44.4$ kcal was used for ZrC (8), $\Delta H°_{298} = -8.41$ kcal was used for WC (14), $\Delta H°_{298} = -38.5$ kcal was used for TaC (8), and $\Delta H°_{298} = -46$ kcal for ThC_2 (9), and $\Delta H°_{298} = -13.8 \pm 2.7$ kcal was used for B_4C (15). The entropies of formation were obtained from Brewer, Bromley, Gilles, and Lofgren (9). $\Delta H°_{298} = -30$ kcal was estimated for NbC. Where values are given for different boride phases of the same metal, disproportionation reactions were also considered. The types of equations used will be illustrated for the tungsten system.

$$W_2B + C = WB + WC,\ \Delta F < 0$$
$$\Delta H_{WB} < \Delta H_{W_2B} + 8.4 \text{ kcal}$$

$$2WB + \tfrac{1}{4}C = W_2B + \tfrac{1}{4}B_4C,\ \Delta F > 0$$
$$\Delta H_{WB} < \tfrac{1}{2}\Delta H_{W_2B} - 1.8 \text{ kcal}$$

$$W_2B = WB + W,\ \Delta F > 0 \qquad \Delta H_{WB} > \Delta H_{W_2B}$$

$$W_2B + B = 2WB,\ \Delta F < 0 \qquad 2\Delta H_{WB} < \Delta H_{W_2B}$$

$$WB + 1\tfrac{1}{4}C = WC + \tfrac{1}{4}B_4C,\ \Delta F > 0$$
$$\Delta H_{WB} < -11.9$$

All of these equations can be satisfied by $\Delta H < -12$ kcal for WB and $\Delta H < -20$ kcal for W_2B, and the two ΔH values should not differ by more than 8 kcal.

Metal Exchange

Ce and B were heated at 1775°K with Mo, W, Nb, and Ta, respectively. The resultant samples were powdered and x-ray powder diffraction patterns of CeO_2 or Ce but no other Ce phases were obtained. Borides of the other metal were found in every instance. These experiments demonstrate that the cerium borides are less stable than Mo_2B, MoB, W_2B, NbB, and TaB. By similar experiments, Brewer, Sawyer, Templeton, and Dauben (3) have shown that Ta, Ti, and Zr can reduce the Mo and W borides. This fixes the ΔH limit given in Table IV for the Ta borides. Thus, the Mo and W borides are less stable than those of Ta, Ti, and Zr. They have also shown that the Mo and W borides are of similar stability. At most they could differ only by 10 kcal

TABLE IV. *Summary of ΔH of formation in kcal per gram atom boron*

	ΔH		ΔH
$\frac{1}{4}$ CeB_4	>-21	$1/x$ CrB_x	<-15
		$\frac{1}{2}$ CrB_2	<-15
$1/x$ TiB_x	~-36		
$\frac{1}{2}$ TiB_2	~-36	Mo_2B	-25.5
$\frac{1}{5}$ Ti_2B_5	<-21	$\frac{1}{2}$ Mo_2B_2	-21
		MoB	
ZrB	<-39		-16.3
$\frac{1}{2}$ ZrB_2	<-39	$\frac{1}{2}$ MoB_2	-11.5
$\frac{1}{12}$ ZrB_{12}	<-10	$\frac{1}{5}$ Mo_2B_5	-10
$\frac{1}{4}$ ThB_4	<-13	W_2B	-28 to -20
$\frac{1}{6}$ ThB_6	<-11	WB	-22 to -12
$1/x$ NbB_x	<-18	$\frac{1}{5}$ W_2B_5	-9 to -5
$\frac{1}{2}$ NbB_2	<-18	$1/x$ MB_x refers to all phases lower in boron composition than MB_2	
$1/x$ TaB_x	<-26		
$\frac{1}{2}$ TaB_2	<-26		

per gram atom of boron. In Table IV, the authors' results for the W borides are compared with those determined for the Mo borides by Gilles and Pollock (16). Within our uncertainty, one cannot distinguish any difference in stability between tungsten and molybdenum borides.

Summary

By consideration of all available chemical data including information concerning disproportionation reactions, one can finally summarize all the data in terms of the composition triangles of the ternary phase diagrams as given in Fig. 1–11 or in terms of the thermodynamic values given in Table IV.

The phase diagrams show at a glance the reactions that can take place, as only phases with a common composition triangle can be at equilibrium with each other. Where some phases have only a limited temperature range of stability, the tempera-

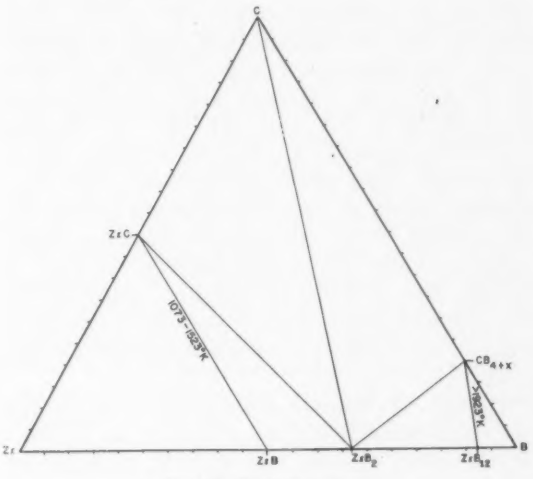

Fig. 3. Zr-B-C system

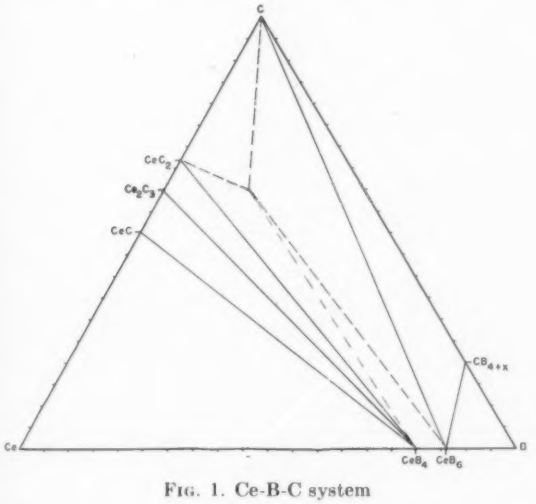

Fig. 1. Ce-B-C system

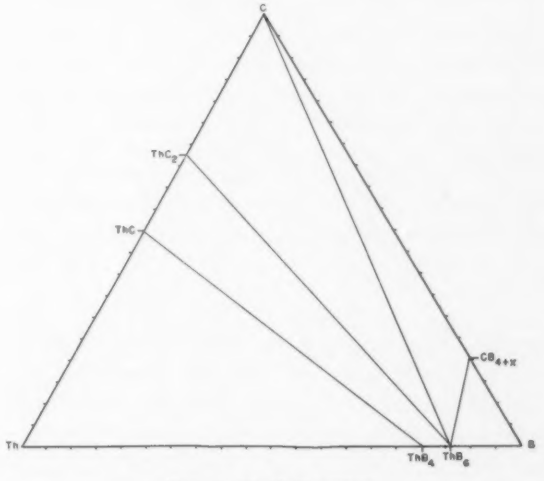

Fig. 4. Th-B-C system

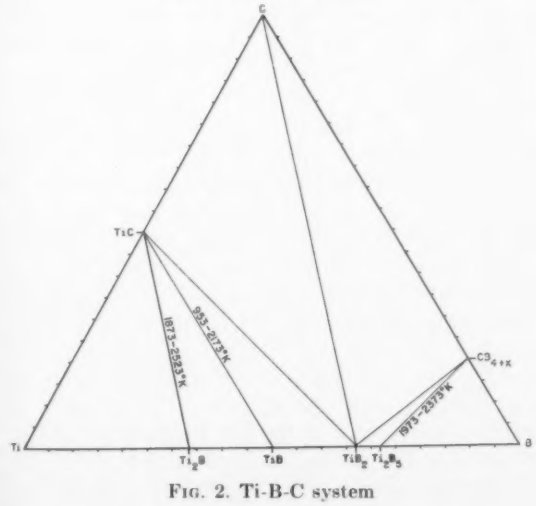

Fig. 2. Ti-B-C system

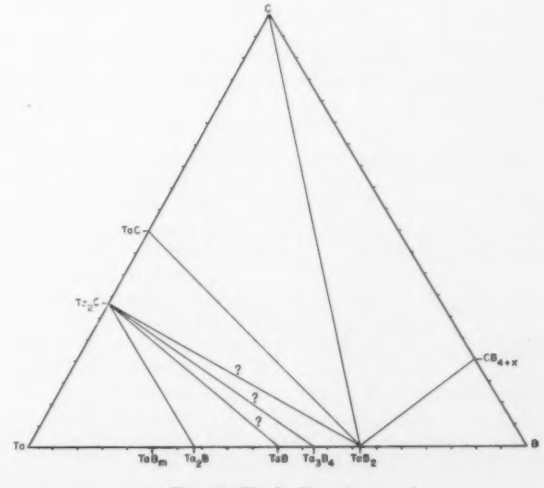

Fig. 5. Ta-B-C system

ture range is indicated on the joins when known. Thus in Fig. 3, the ZrC-ZrB join is to be considered only in the temperature range 1073°–1523°K which is the approximate stability range of ZrB as given by Schwarzkopf and Glaser. The last four diagrams that contain gaseous nitrogen as a component change considerably with temperature because of the large entropy change of reactions involving gaseous N_2. Thus in Fig. 8, the TiN-BN join exists only below 1900°K. Above 1900°K TiN and BN will react to produce TiB_2 and N_2 which can coexist above 1900°K. The joins that are important only at low temperatures are dotted and the temperature limits are indicated.

The Nb-B-C diagram is not given, as the ternary diagram features are the same as shown for Ta-B-C. The Nb-B-N_2, Ta-B-N_2, and Mo-B-N_2 diagrams can be expected to be very similar to the W-B-N_2 diagram. No attempt is made to indicate the homogeneity

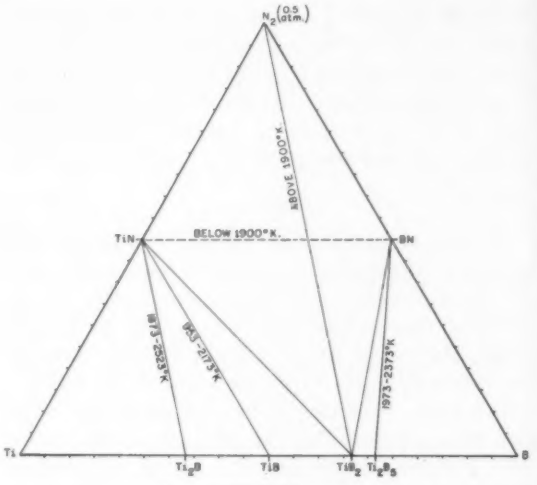

FIG. 8. Ti-B-N_2 system

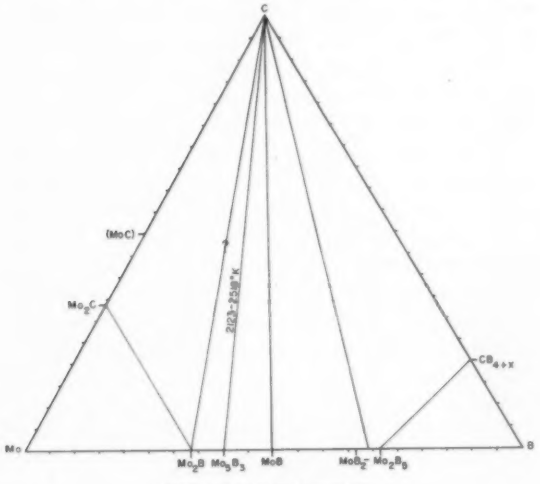

FIG. 6. Mo-B-C system

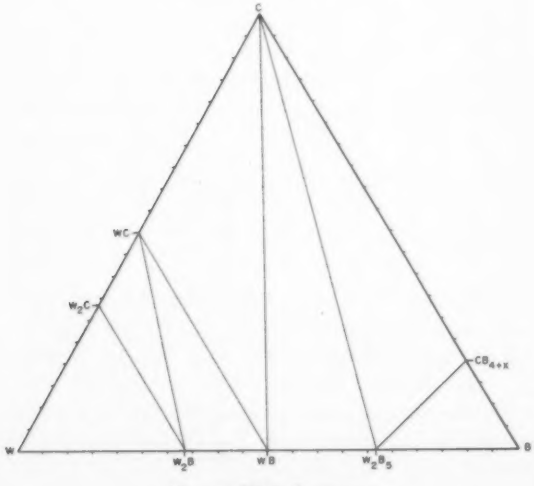

FIG. 7. W-B-C system

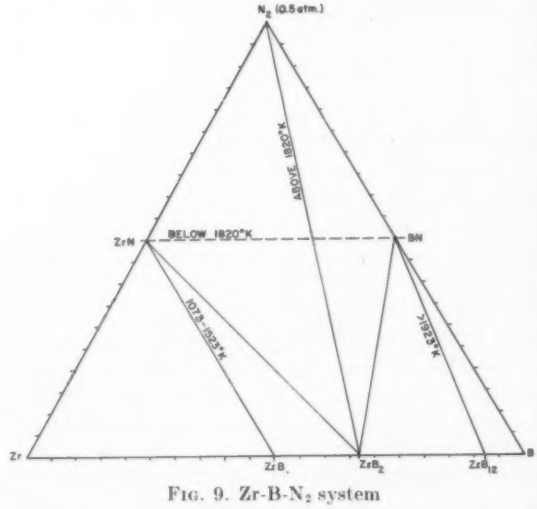

FIG. 9. Zr-B-N_2 system

ranges of the phases other than to recognize the B_4C-B range by use of the term CB_{4+x}. The designation MoB_2-Mo_2B_5 represents the two allotropic phases with homogeneity ranges in this composition region.

Kiessling (17) has noted that the stability of borides decreases in the order Mn, Fe, Co, Ni, Cu, and has pointed out that this behavior is similar to that for the nitrides and carbides in that the stability decreases as one moves to the right in the periodic table through the transition metals. In this work it is found that the most stable borides of the sixth group elements Mo and W are less stable than those of the fourth and fifth group elements Ti, Zr, and Ta. However, there is a maximum stability in the fourth groups and a decrease in stability is found if one moves to the left to the third group. Thus, as one compares compounds of F, O, N, C, and B, one finds that the region of maximum sta-

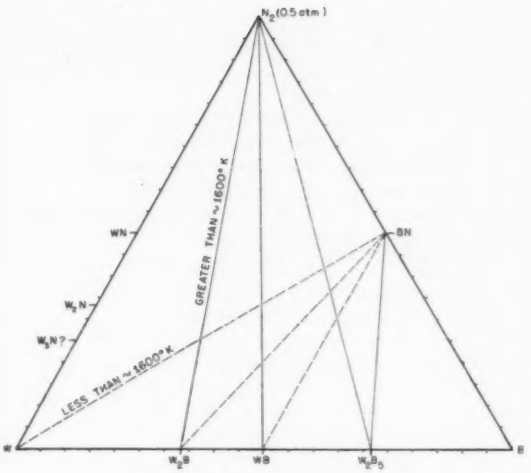

FIG. 10. W-B-N_2 system

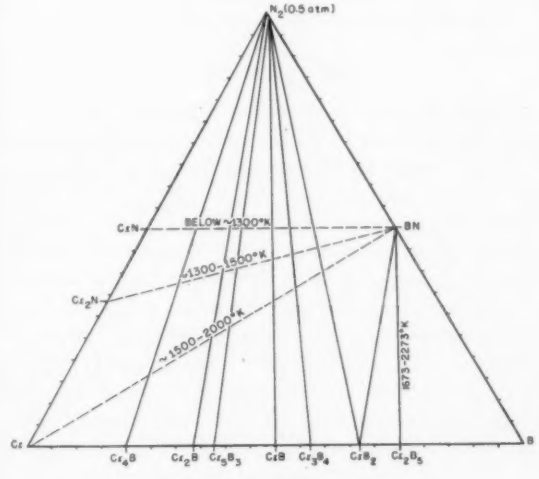

FIG. 11. Cr-B-N_2 system

bility in the periodic table is decidedly shifted to the right as one goes from F to B. Except for the indication by the nitride studies that ZrB_2 is more stable than TiB_2, it is not known how stability varies with atomic weight within a group. It might be noted that ZrC is more stable than TiC and the tungsten carbides are more stable than those of molybdenum.

It is of interest to speculate as to the reason for the shift of the region of maximum stability toward the fourth and fifth groups of the periodic tables for the nitrides, carbides, and borides. One may note that the most stable metal lattices are found near this same region of the periodic table where a large number of *d*-electrons and orbitals are available for bonding. It would appear that the *d*-electrons of the metals play an important part in the bonding in the nitride, carbide, and boride lattices. The metal-like properties of these phases also indicate a common type of bonding. Magnetic susceptibility measurements will be of special interest for possible insight into the type of bonding.

The data in Table IV may now be combined with the heat of sublimation of boron at 298°K of 141 kcal, recently determined by Searcy and Myers (18), to obtain qualitative information about the vaporization behavior of the borides. For borides decomposing to the solid metal and boron vapor at 2500°K, those with heats of formation as negative as −50 kcal per gram atom boron will have boron vapor pressures around 10^{-9} atm. Those with heats of formation as negative as −30 kcal per gram atom boron will have boron vapor pressures around 10^{-7} atm. Those with heats of formation near −10 kcal per gram atom boron will have boron vapor pressures around $10^{-5.5}$ atm. Thus it should be quite practical to obtain accurate thermodynamic data for the refractory boride phases by study of the boron vapor pressure in the range of 2000–2500°K.

Since the borides of the fourth and fifth groups appear to have the most negative heats of formation of any borides, these borides should be resistant against reduction by other metals. They should especially be resistant against attack by the alkali and alkaline earth metals on one hand and the low melting metals like Bi, Sn, Zn, Pb, etc., on the other hand if phases not too high in either boron or metal are used.

Acknowledgments

The x-ray diffraction photographs were taken by Mrs. Helena Ruben and the x-ray diffraction patterns were interpreted by Mrs. Carol Dauben. The authors wish to express their thanks for their help, which was essential to this research. This work was made possible by Smith-Mundt and Fulbright grants for travel to Berkeley, California, in 1952, which are gratefully acknowledged.

Any discussion of this paper will appear in a Discussion Section to be published in the June 1956 JOURNAL.

REFERENCES

1. R. KIESSLING AND Y. H. LIU, *J. Metals*, **3**, 639 (1951).
2. F. W. GLASER, *ibid.*, **4**, 391 (1952).
3. L. BREWER, D. SAWYER, D. H. TEMPLETON, AND C. DAUBEN, *J. Am. Ceramic Soc.*, **34**, 173 (1951).
4. L. BREWER, National Nuclear Energy Series, Vol. 19B, Paper 3 (1950).
5. A. S. DWORKIN, D. J. SASMOR, AND E. R. VAN ARTSDALEN, *J. Chem. Phys.*, **22**, 837 (1954).
6. K. K. KELLEY, U. S. Bur. of Mines Bulls. 476 (1949) and 477 (1950).
7. G. L. HUMPHREY, *J. Am. Chem. Soc.*, **73**, 2261 (1951).
8. K. K. KELLEY, Private communication.
9. L. BREWER, L. A. BROMLEY, N. L. LOFGREN, AND P. W. GILLES, National Nuclear Energy Series, Vol. 19B, Paper 4 (1950).

10. R. Steinitz, *Powder Met. Bull.*, **6,** 54 (1951).
11. J. A. Nelson, T. A. Millmore, and R. C. Womeldorph, *This Journal*, **98,** 465 (1951).
12. P. Schwarzkopf and F. W. Glaser, "Structural and Chemical Characteristics of the Borides of the Transition Metals of the Fourth, Fifth and Sixth Group," presented at the III^e Congrès International D'Électrothermie, and at Wrightsville Beach Meeting, ECS, September 1953.
13. O. Krikorian, Unpublished work, University of California, Berkeley.
14. G. Huff, E. Squitieri, and P. Snyder, *J. Am. Chem. Soc.*, **70,** 3380 (1948).
15. E. R. van Artsdalen, Private communication.
16. P. Gilles and D. Pollock, *Trans. Am. Inst. Mining Met. Engrs.*, **197,** 1537 (1953); and unpublished work.
17. R. Kiessling, *This Journal*, **98,** 417 (1951).
18. A. W. Searcy and C. E. Myers, Unpublished work.
19. J. Engelke, Unpublished work.

High Temperature Oxidation of Two Zirconium-Tin Alloys[1]

M. W. Mallett and W. M. Albrecht

Battelle Memorial Institute, Columbus, Ohio

ABSTRACT

The rate of oxidation of a zirconium-1.5 wt % tin alloy followed a cubic law in the temperature range 600°–900°C at 1 atm pressure. However, two different energies of activation were obtained. In the range 600°–800°C the activation energy was calculated to be 38,400 ± 1100 cal/mole and the cubic rate constant in $(ml/cm^2)^3/sec$ can be expressed as $k = 5.34 \times 10^4 \exp(-38{,}400/RT)$. An activation energy of 22,600 ± 1400 cal/mole was obtained in the range 825°–900°C and the cubic rate constant is $k = 87.2 \exp(-22{,}600/RT)$.

For a zirconium-2.5 wt % tin alloy, the rate of oxidation followed a parabolic law in the range 550°–900°C. The parabolic rate constant in $(ml/cm^2)^2/sec$ was calculated to be $k = 2.63 \times 10^3 \exp(-32{,}400/RT)$, where 32,400 ± 1000 cal/mole is the activation energy.

Adherent gray-black oxidation films were found to be *N*-type semiconductors and from this a mechanism for the oxidation of zirconium is proposed. The effect of tin in the zirconium is to increase the porosity of films and decrease the time before breakdown of the protective properties of the films.

Introduction

A previous study was made on the high temperature oxidation of zirconium (1). This study has been expanded to include the high temperature oxidation of two zirconium-tin alloys containing 1.5 and 2.5 wt % tin. In the zirconium study (1) the initial oxidation followed the cubic rate law for long times in the range 575°–950°C. This was one of the very few times that the cubic rate law was observed over a wide temperature range. Other investigators to report cubic oxidation were Tylecote (2), who studied the oxidation of copper, and Waber (3), who cited data on the oxidation of titanium and tantalum. Cabrera and Mott (4) have developed a theory for cubic oxidation for the growth of thin films containing excess anions and space charges. Besides studying the kinetics of the oxidation of the zirconium-tin alloys it was planned to carry out additional experimental work to determine some of the processes that occur during the cubic oxidation of zirconium and to determine what effect tin may have on these processes.

Experimental

Method.—Rates of reaction of oxygen with the zirconium-tin alloys were determined by measuring rates of consumption of the gas by the alloys in a modified Sieverts apparatus (1, 5).

The zirconium-tin alloy specimens were machined cylinders, 4 cm long by 0.7 cm in diameter. All specimens were abraded with kerosene-soaked 240-, 400-, and 600-grit silicon carbide papers and washed in successive baths of naphtha, ether, and acetone.

Rate data were obtained as follows. A specimen was placed in the reaction tube of the apparatus and degassed in a vacuum for one hour at a temperature 50°C above the temperature of the run in the range 550°C–750°C and at temperature in the range 800°–950°C. All temperatures were maintained to ±5°C. Measured amounts of oxygen were added to the reaction tube to atmospheric pressure. Pressure measurements were made every two minutes at the start of the reaction and at longer time intervals as the reaction rate decreased. Amounts of oxygen remaining in the apparatus as a gas phase were determined from pressure measurements on an open-end mercury manometer and the calibrated dead space of the reaction tube. The difference (to ±0.04 ml STP) between the quantity of oxygen added and that remaining in the gas phase was the quantity reacted with the specimen. Original geometrical dimensions of the specimens were used to compute the quantity of gas reacted per unit surface area.

Materials.—Two zirconium-tin alloys, containing 1.5 and 2.5 wt % tin, were fabricated into ⅜-in. diameter rods. Test specimens were machined from these rods. Analyses of the alloys were obtained by spectrographic, chemical, and vacuum-fusion techniques. Results are given in Table I.

Oxygen was prepared from degassed potassium permanganate by the method described by Hoge (6). It was dried by passing through a dry ice-acetone cold trap.

[1] Manuscript received October 9, 1954. This paper was prepared for delivery before the Cincinnati Meeting, May 1 to 5, 1955. Work performed under AEC Contract W-7405-eng-92.

TABLE I. *Analyses of zirconium-tin alloys*

Element	Amount present, wt %	
	Zr-1.5 wt % Sn	Zr-2.5 wt % Sn
Fe	0.20	0.03
Cr	0.05	NF*
Ni	0.03	0.001
Si	0.007	0.002
Al	0.006	0.001
Mn	0.002	NF
Mg	0.002	NF
Pb	0.002	NF
O_2	0.09	0.06
N_2	0.003	0.002
H_2	0.002†	0.004†

* NF—not found.
† Analysis before degassing.

Results

Zirconium-1.5 wt % tin.—Rates of consumption of oxygen at 1 atm pressure by zirconium-1.5 wt % tin alloy were measured from 600° to 900°C. Below 600°C the reaction was too slow and above 900°C the rapidity of the reaction made it difficult to control. It was found that the data could be fitted to the cubic law, $w^3 = kt$, where w is the ml STP of oxygen consumed per square centimeter of surface, t is time, and k is the cubic rate constant. Fig. 1 and 2 are plots of w^3 vs. t for a number of runs and it is seen that the data fall on straight lines. For cubic oxidation, a plot of log w vs. log t should be a straight line with a slope equal to 0.33. Values of rate constants, calculated from the various plots, and slopes of log-log plots are given in Table II. Rate constants range from 1.5×10^{-5} $(ml/cm^2)^3/sec$ at 600°C to 5.5×10^{-3} $(ml/cm^2)^3/sec$ at 900°C.

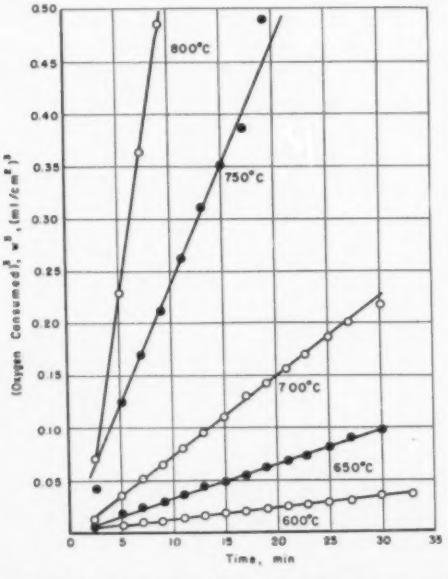

FIG. 1. Cubic plot of oxidation of zirconium-1.5 wt % tin alloy at 600°–800°C.

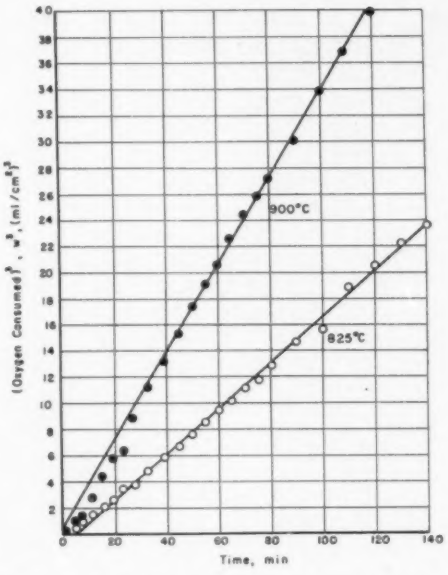

FIG. 2. Cubic plot of oxidation of zirconium-1.5 wt % tin alloy at 825° and 900°C.

Temperature dependence of the cubic rates of oxidation can be seen in Fig. 3. Two different straight lines were obtained, one in the range 600°–800°C, the other for 825°–900°C. Equations for the best straight lines through the two sets of points were determined by the method of least squares. Using the Arrhenius-type equation, $k = A \exp(-Q/RT)$, energies of activation and frequency factors were calculated. At 600°–800°C, the rate constant in $(ml/cm^2)^3/sec$ is $k = 5.34 \times 10^4 \exp(-38{,}400/RT)$ where 38,400 ± 1100 cal/mole is the activation

TABLE II. *Rate constants for the reaction of zirconium-1.5 wt % tin alloy with oxygen*

Temp, °C	Rate constant (k), $(ml/cm^2)^3$ sec	Slope of log-log plot
600	1.5×10^{-5}	0.30
650	5.4×10^{-5}	0.33
650	3.0×10^{-5}	0.39
700	1.3×10^{-4}	0.34
750	3.9×10^{-4}	0.32
750	2.7×10^{-4}	0.34
800	7.3×10^{-4}	0.37
800	1.0×10^{-3}	0.35
825	3.0×10^{-3}	0.35
825	2.7×10^{-3}	0.34
850	3.5×10^{-3}	0.35
850	3.2×10^{-3}	0.32
900	5.4×10^{-3}	0.33
900	5.5×10^{-3}	0.32

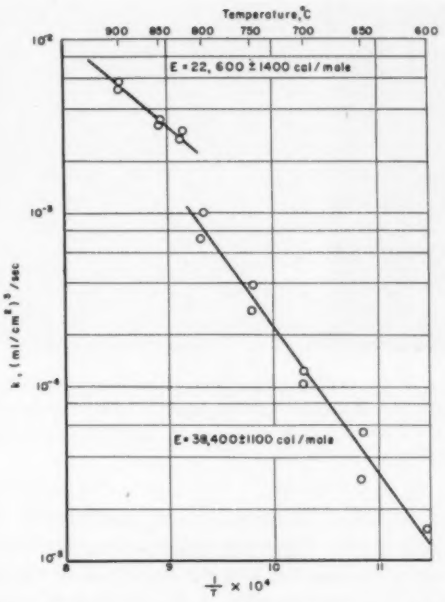

FIG. 3. Temperature dependence of cubic rate constant for zirconium-1.5 wt % tin alloy.

energy and the probable error[2] in a calculated k is approximately 16%. For 825°–900°C $k = 87.2 \exp(-22{,}600/RT)$ where 22,600 ± 1400 cal/mole is the activation energy and 4.3% is the probable error in a calculated k.

Zirconium-2.5 wt % tin.—Rates of oxidation at 1 atm pressure for the zirconium-2.5 wt % tin alloy were measured from 550° to 900°C. The data were found to follow a parabolic law, $w^2 = kt$, where k is the parabolic rate constant. In Fig. 4, the square of w is plotted as a function of t for a number of runs, and it is seen that the data fall on straight lines. For the parabolic law, a plot of log w vs. log t is a straight line with a slope of 0.50. Values of rate constant and slopes of log-log plots are given in Table III. Rate constants range from 3.8×10^{-6} $(\text{ml/cm}^2)^2/\text{sec}$ at 550°C to 2.5×10^{-3} $(\text{ml/cm}^2)^2/\text{sec}$ at 900°C.

Temperature dependence for the parabolic oxidation is given in Fig. 5. Between 550° and 900°C, the rate constant is $k = 2.63 \times 10^3 \exp(-32{,}400/RT)$ $(\text{ml/cm}^2)^2/\text{sec}$, where 32,400 ± 1000 cal/mole is the activation energy and the probable error in a calculated k is 18%.

[2] From the least square calculation, the probable error in k can be calculated by the equation $k = A \exp(-Q/RT) \exp \pm PE_k$. The probable error in log k is $PE_k = 0.6745 \sqrt{\Sigma d^2/n - 2}$, where Σd^2 is the summation of the squares of the differences between the least square calculated values of log k and the experimental values of log k, and n is the number of experimental values of log k used. For this work the approximation is used that $\exp \pm PE_k \approx 1 \pm PE_k$.

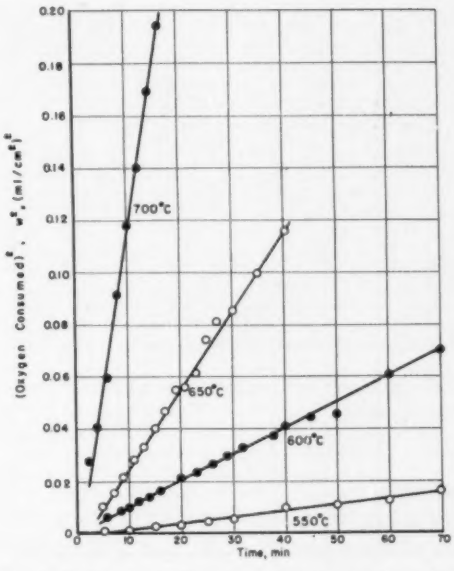

FIG. 4. Parabolic plot of oxidation of zirconium-2.5 wt % tin alloy at 550°–700°C.

FILMS

At the end of reaction-rate runs, specimens were cooled to room temperature in a vacuum and examined. In all cases throughout the temperature ranges investigated, reacted specimens were covered with a gray-black film which adhered very strongly to the metal. Growth of this film is associated with the forementioned rate laws for the tin alloys. Where breakdown of these laws occurred and the rate increased toward linear behavior, a tan to white film started forming on the specimens. After a time, these light-colored films tended to flake off the specimens.

TABLE III. *Rate constants for the reaction of zirconium-2.5 wt % tin alloy with oxygen*

Temp, °C	Rate constant (k), $(\text{ml/cm}^2)^2/\text{sec}$	Slope of log-log plot
550	3.8×10^{-6}	0.56
600	1.7×10^{-5}	0.51
600	3.1×10^{-5}	0.44
650	5.1×10^{-5}	0.54
650	6.4×10^{-5}	0.46
700	1.2×10^{-4}	0.56
700	2.1×10^{-4}	0.53
750	3.1×10^{-4}	0.59
750	3.2×10^{-4}	0.48
800	5.5×10^{-4}	0.48
800	5.6×10^{-4}	0.40
850	9.8×10^{-4}	0.44
900	2.5×10^{-3}	0.45

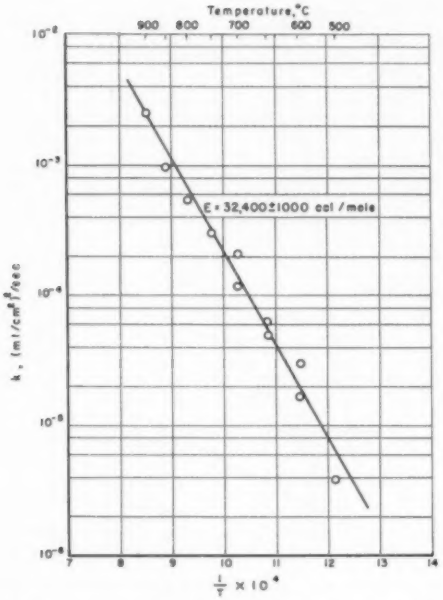

FIG. 5. Temperature dependence of parabolic rate constant for zirconium-2.5 wt % tin alloy.

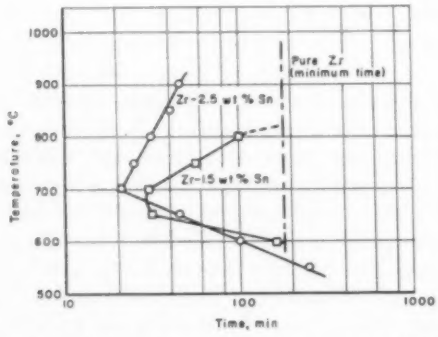

FIG. 6. Variation of breakdown time of gray-black film with temperature.

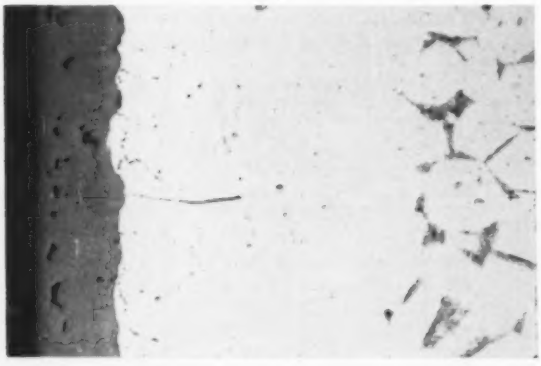

FIG. 7. Zirconium-1.5 wt % tin alloy reacted with oxygen at 825°C for 180 min. Surface layer is a gray-black film about 0.0025 cm thick. Aqua regia-HF etch. 500× before reduction for publication.

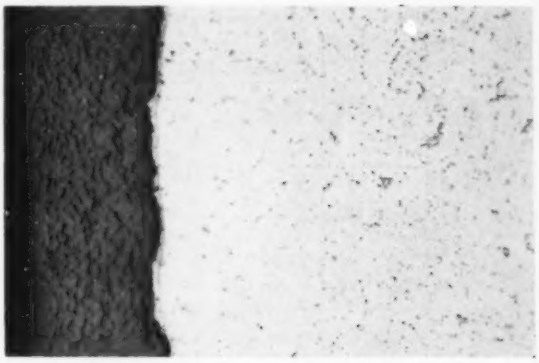

FIG. 8. Zirconium-1.5 wt % tin alloy reacted with oxygen at 700°C for 240 min. Surface layer is a light-colored film about 0.0050 cm thick. Aqua regia-HF etch. 500× before reduction for publication.

The time before occurrence of the breakdown of the gray-black film depended on temperature and tin content (see Fig. 6). During oxidation of the pure zirconium (1) the gray-black film persisted for times greater than 180 min in the entire range 575°–950°C. However, for the tin alloys in general the breakdown time of the dark film decreases with increasing tin content, and the minimum breakdown time comes at about 700°C (Fig. 6). No breakdown occurred for 180 min during the oxidation of the 1.5 wt % tin alloy in the range 825°–900°C.

Metallographic examination of the gray-black films of both tin alloys showed them to be a dense phase containing pores and a darker second phase (Fig. 7 and 9). Generally, it was found that films of the zirconium-2.5 wt % tin alloy contained more of the pores and second phase than the zirconium-1.5 wt % tin alloy. Maximum thicknesses of the gray-black films were of the order of 2 to 4 × 10^{-3} cm for the 1.5 wt % tin alloy and 0.6 to 2 × 10^{-3} cm

FIG. 9. Zirconium-2.5 wt % tin alloy reacted with oxygen at 800°C for 60 min. Surface layer is a gray-black film about 0.0012-0.0020 cm thick. Aqua regia-HF etch. 500× before reduction for publication.

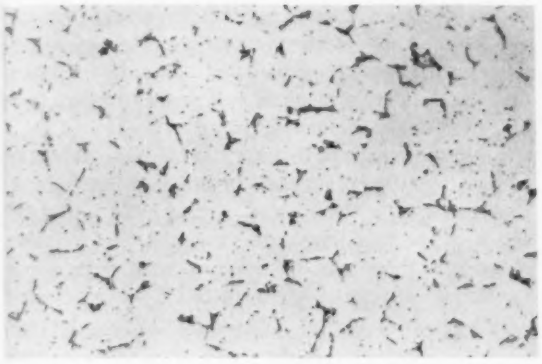

FIG. 10. Zirconium-1.5 wt % tin alloy vacuum annealed at 825°C for 1 hr. Aqua regia-HF etch. 500× before reduction for publication.

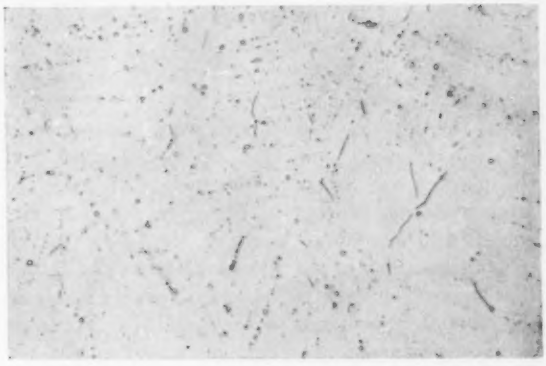

FIG. 12. Zirconium-2.5 wt % tin alloy vacuum annealed at 800°C for 1 hr. Aqua regia-HF etch. 500× before reduction for publication.

for the 2.5 wt % tin alloy. X-ray patterns taken at room temperature indicated that these films were preferentially oriented monoclinic ZrO_2. The tan to white films that formed after longer times were found to be randomly oriented monoclinic ZrO_2 (Fig. 8). No identification could be made readily of the second phase (particles marked A in Fig. 9) in the dark films. However, this phase was also present in the bulky light-colored films and could be mechanically separated in the cases of the zirconium-2.5 wt % tin alloy. X-ray analysis gave patterns of metallic zirconium and of ZrO_2. Apparently these particles are portions of the base metal which oxidize more slowly than the bulk of the metal. This phase was not noted in the oxidation films of pure zirconium (1).

Microstructures of the base alloys at the end of oxidation-rate experiments can be seen in Fig. 7, 8, and 9. Microstructures of the unoxidized alloys after a vacuum anneal of one hour appearing in Fig. 10, 11, and 12 show the condition of the specimens at the start of oxidation. A fine, random precipitate is noted in alpha zirconium-1.5 wt % Sn alloy at 700°C (see Fig. 8 and 11). This precipitate is caused by the chromium, iron, and nickel contents of the alloy. At 825°C for the zirconium-1.5 wt % tin alloy, the transformed-beta structure is evident at the alpha grain boundaries (Fig. 7 and 10). Adjacent to the oxidation film (Fig. 7) is an area devoid of the transformed-beta structure. This was caused by diffused oxygen which stabilized the alpha phase. From these considerations it appears that there is a eutectoid temperature around 800°C that may be related to the change in the activation energy occurring between 800° and 825°C. In the case of the zirconium-2.5 wt % tin alloy where alloying constituents other than tin were very low, the alpha structure was stable over the entire temperature range investigated. However, the 800°C specimen in Fig. 9 and 12 shows some precipitation of intermetallic (not tin) compounds at the grain boundaries.

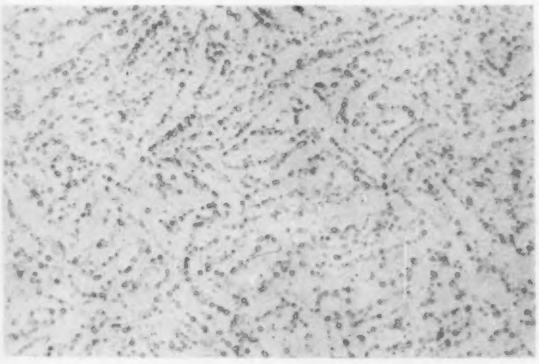

FIG. 11. Zirconium-1.5 wt % tin alloy vacuum annealed at 700°C for 1 hr. Aqua regia-HF etch. 500× before reduction for publication.

Semiquantitative spectrographic analyses for the presence of tin were obtained on the oxidation films of both alloys. About 2 wt % tin was found in each film. Calculations based on these crude analyses indicate that there was very little diffusion of the tin at the metal-film interface.

MECHANISMS

Formation of thick protective oxidation films is predominantly a diffusion-controlled process. The films are semiconductors and, according to Wagner (7), they are not of exactly stoichiometric composition, but are stable with an excess of either cation or anion. Various means have been devised to distinguish the diffusion mechanisms in semiconductors. A number of such tests were applied to the experimental oxidation films.

Marker experiments were made on the zirconium-tin alloys, pure zirconium, and a copper control. The marker was a thin layer of Cr_2O_3 powder (in

water) painted on the specimens. Specimens were then reacted with one atmosphere of oxygen at 800°C for 6 hr. In the case of copper, it was determined by various investigations that the cuprous ion is the diffusion specie. This work was reviewed by Kubaschewski and Hopkins (8). Accordingly, the marker was found at the metal-film interface after oxidation of copper. However, for pure zirconium and zirconium-tin alloys, the Cr_2O_3 marker remained entirely at the film-gas interface indicating that the oxygen ion is diffusing through the film and the reaction is occurring at the metal-film interface. From experiments of Weininger and Zemany (9) with a Nernst glower (85 mole % ZrO_2 and 15 mole % Y_2O_3), one would expect the oxygen ions to be the diffusing specie.

Theoretically, diffusion of the oxygen ion (anion) can occur by two mechanisms, either by anion holes (defects) in the zirconia lattice, or by interstitial anion diffusion through the lattice. Consideration of the ionic radii of Zr^{+4} (0.90 Å) and $O^{=}$ (1.36 Å) gives a ratio for R_+/R_- of 0.66 for ZrO_2. Therefore, in the zirconia lattice, oxygen ions are in contact and zirconium ions fit in positions between the oxygen ions. Because of the size of oxygen ions, they could not occupy interstitial positions in the zirconia lattice. In view of these considerations, it is concluded that the mechanism of the anion diffusion is by lattice defects or holes.

Thermoelectric power measurements were made on the gray-black films to determine the type of electronic conduction. Negative thermoelectric power indicates that excess electrons are responsible for the conductivity, while a positive thermoelectric power indicates electron defects are responsible. Measurements made on films of pure zirconium and zirconium-tin alloys, using a hot (700°C) tungsten probe, gave negative thermoelectric powers. Therefore, electronic conduction in the films is through excess electrons. Since diffusion in the films is through anion holes and electronic conduction is by excess electrons, it was concluded that the dark oxidation films in the pure zirconium and zirconium-tin alloys are anion-deficit semiconductors (N-type).

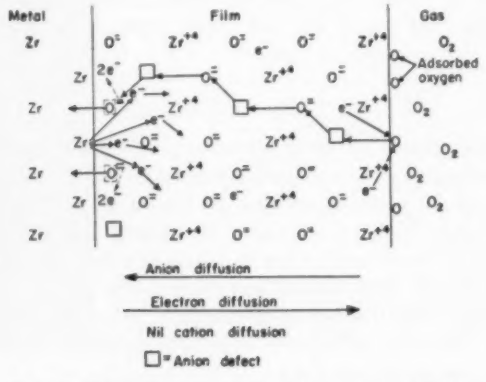

FIG. 13. Proposed mechanism for the oxidation of zirconium.

From the results of this work, a mechanism for the surface reaction of oxygen is proposed as follows. Starting with a clean metal surface, the initial reaction of the zirconium with oxygen is the formation of an adsorbed layer of oxygen with subsequent solution of oxygen into the metal. This is followed by the reaction

$$Zr + 2O_{(ads)} \rightarrow Zr^{+4} + 2O^{=} \qquad (I)$$

to form oxide. As soon as a finite layer has formed, anion holes are produced by solution of some of the anions into the metal, that is

$$Zr + xO^{=} \rightarrow Zr^{+4} + xO_{(\text{in } Zr)} + x\square + (4 + 2x)e^{-} \qquad (II)$$

which is the reaction occurring at the metal-film interface. Thus, anion holes are supplied to the oxide lattice and the gray-black film of substoichiometric ZrO_2 is produced. The reaction at the film-gas interface is

$$2O_{(ads)} + 4e^{-} \rightarrow 2O^{=} \qquad (III)$$

The summation of (II) and (III) is the equation for the over-all reaction.

$$Zr + 2O_{(ads)} \rightarrow Zr^{+4} + (2 - x)\ O^{=} + xO_{(\text{in } Zr)} + x\square + 2x\ e^{-} \qquad (IV)$$

The proposed mechanism for the formation of the gray-black film is shown in Fig. 13. At the metal-film boundary where the reaction to form oxide is occurring, zirconium atoms at the metal surface are ionized to tetravalent cations. The freed electrons

TABLE IV. *Oxygen consumed at various temperatures by zirconium and zirconium-tin alloys*

Temp, °C	Reaction time, min	Oxygen consumed, ml STP per cm² of surface		
		Zr	Zr-1.5 wt % Sn	Zr-2.5 wt % Sn
600	10	0.19	0.24	0.10
600	20	0.21	0.29	0.14
600	100	0.35	0.46	0.34
700	10	0.38	0.42	0.38
700	20	0.43	0.53	0.49
700	30	0.51	0.60	—
800	10	1.0	0.82	0.59
800	30	1.3	1.2	1.0
800	100	2.1	1.8	—
900	10	1.9	1.3	1.4
900	30	2.4	2.2	2.2
900	100	3.6	3.2	—

enter the conduction bands of the zirconia lattice and start diffusing toward the film-gas boundary. About the newly formed cation, anion holes are produced by solution of the anions into the metal, and anions moving toward the metal surface fill these holes leaving anion holes behind. The greatest concentration of the holes is near the metal-film boundary and the smallest concentration is near the film-gas boundary. The reaction proceeds by a countercurrent of anion diffusion inward and anion holes diffusing outward through the film. The metal-film boundary is continually moving into the metal. Meanwhile, anions are formed at the film-gas boundary as adsorbed oxygen atoms pick up two electrons from the conduction bands of the film. To keep the film electrically neutral, there are two electrons in the conduction bands of the lattice for each anion hole.

Consideration is now given to the role of tin in the proposed mechanism. In Table IV are listed the amounts of oxygen consumed per square centimeter surface of pure zirconium and zirconium-tin alloys for various temperatures and reaction times. It is seen that, for equal times at any one temperature, the amount of oxygen consumed varied little with the tin content of the zirconium. However, as would be expected in view of the differences in oxidation rates and rate types, the relative positions of the materials in respect to amount of oxygen consumed changed as time progressed. At 600°C the zirconium-1.5 wt % tin alloy consumed the greatest quantity of oxygen, while at 900°C the pure zirconium consumed the most oxygen after equal times.

Room temperature specific resistivity measurements were made on the oxidation films to determine whether the tin has an effect on their electrical properties. Gray-black films of equal thickness (0.001 cm) were prepared at 800°C on pure zirconium and on the zirconium-tin alloys. Resistivities were determined by measuring the current flow from a small area of deposited silver (silver paste) through the oxide film to the base zirconium using a field strength of 3.7×10^4 v/cm. The values obtained were of the order of 6×10^{13} ohm-cm for pure zirconium and about 1×10^{14} ohm-cm for the two zirconium-tin alloys. These are only approximate values and it is believed that there is very little if any effect of tin on the electrical properties of the films.

Discussion

The over-all oxidation mechanism of pure zirconium and zirconium-tin alloys is a complex process and changes with tin content. The kinetics of high temperature oxidation of zirconium, reported in an earlier paper (1), followed a cubic rate law. In the present study, the zirconium-1.5 wt % tin alloy also oxidized according to the cubic law; however, oxidation of the zirconium-2.5 wt % tin alloy followed the parabolic law. These rate laws are associated with the formation of an adherent gray-black film of preferentially oriented monoclinic ZrO_2 (oxygen deficit) on the metal.

The natural volume ratio of monoclinic ZrO_2 to Zr is about 1.5. Therefore, for the gray-black film to be adherent to the metal, it must grow under highly compressive stresses. When the continuity of this film is disrupted, part of the oxide is no longer a part of the restrained coherent film. Consequently, it oxidizes to stoichiometric composition forming the light-colored randomly-oriented monoclinic ZrO_2. Metallographic examination indicates that films on the 2.5 wt % tin alloy are more porous than films on zirconium and the 1.5 wt % tin alloy. This increased porosity could result in the parabolic behavior. Tylecote (2) found that the oxidation of annealed copper in moist air initially followed the cubic law at 210°C and in the range 520°–750°C. Between 210° and 520°C, the oxidation approached parabolic behavior. This was explained on the basis of porosity (blistering) of the films. However, in the range 520°–700°C, where the films were compact and nonporous, the cubic law was obeyed.

As in the present study, the film thicknesses (1 to 3×10^{-3} cm) obtained by Tylecote were greater than the limiting thickness (2×10^{-4} cm) permitted by the cubic growth mechanism proposed by Cabrera and Mott (4) for films containing excess anions (*P*-type semiconductor). Moreover, the present data show the formation of relatively thick films on zirconium and zirconium-1.5 wt % tin alloy during cubic-rate oxidation to form an anion-deficit semiconductor film (*N*-type semiconductor). Therefore, the theory of Cabrera and Mott cannot be applied to the cubic oxidation of zirconium and the zirconium-1.5 wt % tin alloy.

In comparing energies of activation for the cubic oxidation of zirconium and zirconium-tin alloy, the energy of activation decreases with increasing tin content of the zirconium. For zirconium, the energy of activation is 47,200 cal/mole (1), and for zirconium-1.5 wt % tin, 38,300 cal/mole. A still lower energy of activation of 22,500 cal/mole was found for the 1.5 wt % alloy (cubic reaction) in the high temperature range (825°–900°C). It was found that there is a eutectoid temperature at about 800°C for the zirconium-1.5 wt % tin alloy which could cause the change in the activation energy. The eutectoid temperature apparently results from the alloying constituents chromium, iron, and nickel.

For the parabolic oxidation of the zirconium-2.5 wt % tin alloy the energy of activation is 32,500 cal/mole. This value cannot be compared with those obtained for the cubic reactions.

Acknowledgments

The authors gratefully acknowledge the assistance of Mr. B. G. Koehl in making the experimental reaction rate runs and of Mr. R. K. Willardson who did the thermoelectric power and resistivity measurements on the oxide films.

Any discussion of this paper will appear in a Discussion Section to be published in the June 1956 JOURNAL.

REFERENCES

1. J. BELLE AND M. W. MALLETT, *This Journal*, **101**, 339 (1954).
2. R. F. TYLECOTE, *J. Inst. Metals*, **81**, 681 (1952-53).
3. J. T. WABER, *J. Chem. Phys.*, **20**, 734 (1952).
4. N. CABRERA AND N. F. MOTT, *Repts. Progr. Phys.*, **12**, 163 (1949).
5. M. W. MALLETT, J. BELLE, AND B. B. CLELAND, *This Journal*, **100**, 1 (1954).
6. H. J. HOGE, *J. Research Natl. Bur. Standards*, **44**, 321 (1950).
7. C. WAGNER, *Z. Phys. Chem.*, **B 22**, 181 (1933).
8. O. KUBASCHEWSKI AND B. E. HOPKINS, "Oxidation of Metals and Alloys," p. 30, Academic Press, Inc., New York (1953).
9. J. L. WEININGER AND P. D. ZEMANY, *J. Chem. Phys.*, **22**, 1469 (1954).

Application of Backside Luggin Capillaries in the Measurement of Nonuniform Polarization[1]

M. Eisenberg,[2] C. W. Tobias, and C. R. Wilke

Department of Chemistry and Chemical Engineering, University of California, Berkeley, California

ABSTRACT

The backside capillary is demonstrated to be a suitable tool in the measurement of local values of polarization, particularly when interference with hydrodynamic conditions at the solution electrolyte interface needs to be avoided. The design and performance of several capillaries are described. A simple capillary machined of Teflon plastic is shown to yield satisfactory accuracy in polarization measurements. When the current distribution is nonuniform due to geometry or convection, cathodic polarization is shown to depend on the position of the capillary opening in the cathode.

Introduction

In the measurement of polarization, electrical contact on the solution side between the working electrode and reference electrode is established by means of a column of a suitable electrolyte, enclosed in a plastic or glass tube, which has a small (capillary) opening in the working cell (Fig. 1). The capillary serves to prevent flow of electrolyte between the reference half-cell and the main body of electrolyte, and also permits the assignment of a more or less exact location of the junction within the electric field of the working cell.

The capillary tube, if placed close to the electrode surface, *shields the current* from it (1), and the measured polarization values are lower than the "true" polarization corresponding to the average current density over the electrode. If the measurement of polarization is effected while the current is flowing across the cell (direct method), the emf measured between the electrode and the reference half-cell includes besides the half-cell potentials the *ohmic potential drop* between the working electrode and the end of the capillary tube. Recognition of the proper significance of these factors is due to Piontelli and co-workers (2, 3), who estimated the errors incurred in polarization measurements by various capillary designs and locations on the basis of studies conducted with scaled up models. Barnartt (4) extended these observations by the electric trough method, using models of somewhat improved accuracy. The conclusions of these researches indicate that the shielding effect may be eliminated for all practical purposes by locating the capillary end at a distance larger than four times the external radius of the capillary from the surface [Fig. 1(a)]. The ohmic potential drop on the basis of Barnartt's model studies can be computed if the conductivity of the electrolyte, average current density, and exact dimensions and location of the capillary are known. Piontelli (3) recommended the use of a small diameter glass tube, closed at the end by a thin glass membrane, placing it tightly against the electrode surface, with its axis normal to the surface [Fig. 1(b)]. In this arrangement the area covered by the membrane is completely shielded. However, the electric field remains unaffected if the lines of flow in the field of the cell are parallel to the axis of the tube. The liquid junction between the solution in the cell and in the tube is established by a circular corona-shaped opening in the glass wall, 10–40μ from the electrode surface. The ohmic drop in this arrangement is negligibly small. This junction has the added advantage of eliminating the error incurred when the ohmic drop between the capillary tip and surface is computed by assuming that the conductivity of the electrolyte adjacent to the working electrode is identical to the bulk value.

Both the above arrangements can be assumed to function satisfactorily as long as the geometry of the working cell and the hydrodynamic conditions are such that the current distribution over the electrodes is uniform. Parallel plane electrodes, connected by insulating planes normal to the electrodes, or concentric circular cylindrical electrodes terminated by insulator planes normal to the axis provide uniform primary distribution (5). (The concentric spherical arrangement is not practical.)

Secondary distribution, however, is affected by convection in the vicinity of the electrodes. In the absence of stirring this can cause a significant departure from the uniform primary current distribution.[3] It has been shown that current density may

[1] Manuscript received July 19, 1954. This paper was prepared for delivery before the Philadelphia Meeting, May 4 to 8, 1952.

[2] Present address: Stanford Research Institute, Stanford, California.

[3] Convection is suppressed in the vicinity of an electrode if the concentration changes established by the current

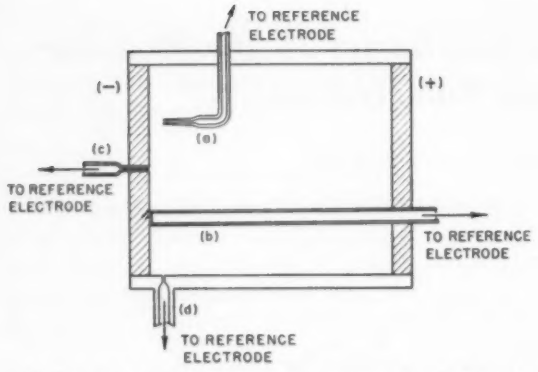

FIG. 1. Methods for coupling reference electrodes with working electrode surfaces.

vary as much as 100% over relatively short vertical distances (in the order of 10 cm) due to differences in ionic mass transfer rates (6, 7). Therefore, in polarization studies, effective stirring is of great importance. Establishment of a condition of uniform turbulence along the electrode surface cannot be achieved in the presence of an obstruction (such as the frontal capillary tube) in the hydrodynamic boundary layer. As a result, current density distribution may vary in the vicinity of the capillary tip, whether or not the latter is in contact with the surface.

When the effect of convection on current distribution is studied, introduction of a frontal capillary tube causes a more or less significant departure from the hydrodynamic conditions prevailing in the absence of such a disturbance. Since the quantitative prediction of these effects is extremely cumbersome, if not impossible, the *backside capillary* arrangement [Fig. 1(c)] possesses definite advantages over a frontal tube.

This junction was first suggested and used by Piontelli (8, 9) and Poli (8) and since subjected to thorough investigation with regard to errors resulting from the introduction of a discontinuity in the electrode surface. A small ohmic potential drop is included between the inside of the capillary hole and the electrode surface. In Barnartt's model experiments (4) this drop was found to be equal to the potential drop across an electrolyte layer of thickness 0.559 r (r = external radius of capillary) in a direction normal to the electrode. (Wall thickness was $\frac{1}{3}$ r.) It is evident from these data that, if one uses small capillary openings and electrolytes of high conductivity, the error incurred up to moderately high current densities (0.01–0.1 amp/cm^2) will not exceed a few millivolts.

are such that only vertical density gradients result, with the density decreasing with increasing elevation. The deposition of a metal on a horizontal top end plate of a vertical cell is a model where convection is negligible (10).

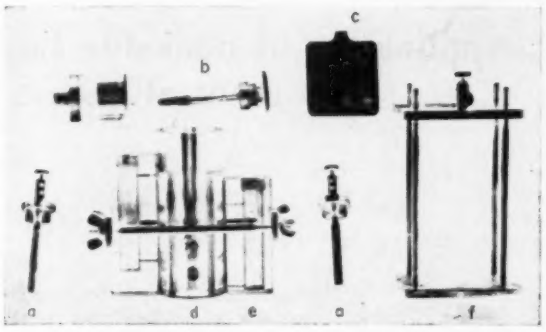

FIG. 2. Parts of cell for measurement of total polarization by the sidewall and backside capillaries. (a) Cu reference electrode; (b) Cu cathode disk with backside capillary; (c) Cu anode plate; (d) Lucite tube (for electrolysis); (e) side compartments, for reference electrodes; (f) clamp for holding anode and cathode in place.

WORKING TEST OF BACKSIDE CAPILLARY MODELS

In the following the development and testing of a backside capillary (designated by BSC) suitable for the measurement of local polarization is described.

A 1-in. ID, 5-in. long circular cylindrical Lucite tube was closed off at both ends by $\frac{1}{4}$-in. thick copper plates, held in place by a clamping structure (Fig. 2). The BSC to be tested was mounted in the center of one of the electrodes and was connected by a glass or plastic tube to the reference half-cell, containing copper reference electrodes. In addition, two $\frac{1}{64}$-in. holes were drilled through the Lucite wall, normal to the axis of the tube, at 0.1- and 1.0-in. distances, respectively, from the electrode containing the BSC. Each hole served to connect the cell to separate side compartments containing a copper reference electrode and filled with electrolyte of the same composition as in the working cell. When external potential is applied across the two end-plate electrodes, the ohmic potential drop in the column between them is proportional to the distance along the axis of the tube (10), provided the composition of the electrolyte remains uniform during the passage of the current. Knowing the conductivity of the electrolyte and the distance of a sidewall capillary (SWC) [Fig. 1(d)] from the electrode under investigation, the ohmic potential drop between the working electrode and either of the holes can be evaluated[4] for any given current.

EXPERIMENTAL PROCEDURE

The cylinder equipped with sidewall capillaries (SWC) provided a convenient means for the investigation of the performance of several BSC de-

[4] Uniform conductivity can be maintained approximately by effective stirring (electrolyte circulation) and the use of excess "supporting electrolyte" (10).

signs. The electrolyte was either 0.5M or 0.6M $CuSO_4$ in 1.45M H_2SO_4. Both the cathode and the reference electrodes (¼-in. diameter, 2-in. long copper rods) were carefully preplated from a similar solution prior to each experimental series. After the cell, capillary connections, and reference half-cell compartments have been filled with the electrolyte, the desired current was applied across the cell, and after 5–15 min the potential between each reference electrode and the cathode was simultaneously measured.[5] The potential difference between the two side compartment reference electrodes was also recorded [Fig. 2(a)] in order to establish the ohmic drop between the planes of the sidewall capillary openings.

Polarization values were obtained in the unsteady state. They included both chemical and concentration polarization. These measurements were intended only to clarify how closely a particular BSC yields the same polarization value as those obtained simultaneously by the sidewall capillaries.

The ohmic component was subtracted from the values measured by the sidewall capillaries, and then the polarization values obtained by the SWC and the BSC were plotted. (In all calculations the potential difference between the reference electrodes was taken into account.)

In the design of the BS capillaries the authors considered the following:

1. The diameter of the capillary should be as small as possible since both the ohmic potential drop and the current density at the edge of the hole in the metal increase with hole size (4).

2. The inside of the capillary hole must be effectively insulated from the metal surface inside the hole, and from the back side of the electrode, otherwise the polarization values measured will be smaller than the value corresponding to the uniform current density on the surface.

3. The outer end of the capillary must be smooth and flush with the working electrode surface (10).

Fig. 3 shows some of the capillaries tested by the above described method. Glass capillaries were found to be too fragile. Sealing the gap between the metal and the glass capillary and fitting the outer end of the capillary exactly in the plane of the electrode is a tedious operation. In type (a) (Fig. 3) a thin wire was inserted in the hole drilled through the electrode, and a resin lacquer[6] was applied. After hardening, the wire was pulled out, leaving a well-defined capillary hole behind. In model (b), the ruby was a standard watchmaker's stone, inserted in the predrilled hole by a special tool. Model (b) gave very well-defined

[5] Instruments: (*a*) Leeds and Northrup potentiometer Type K2; (*b*) Potentiometer-Recorder, G.E. Model 8 CE-SCM19A.

[6] G.E. Glyptal.

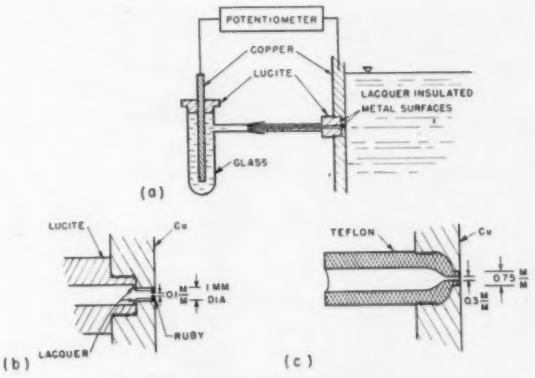

FIG. 3. Backside capillaries

hole geometry on the solution side, but still required lacquer insulation inside the hole. Capillaries (a) and (b) showed similar behavior in the authors' tests in the cylindrical cell (Fig. 2). Polarization values were consistently lower than the ones measured by the SWC, differences increased with increasing current density and hole diameter. This indicates that the lacquer layers were imperfect and the solution came into contact with the electrode inside the hole. Fig. 4 and 5 give typical sets of results for types (a) and (b).

The Teflon capillary (model c) was the easiest to manufacture, and yielded by far the most satisfactory results (Fig. 6). Fig. 7 shows the increase of total polarization of the cathode with time, at constant current in a horizontal position on the top of the cell. Again satisfactory agreement can be observed between values obtained by the two capillaries.

The Teflon need not be machined accurately to the dimensions of the hole in the electrode, because under pressure (provided by the thread) it can be forced

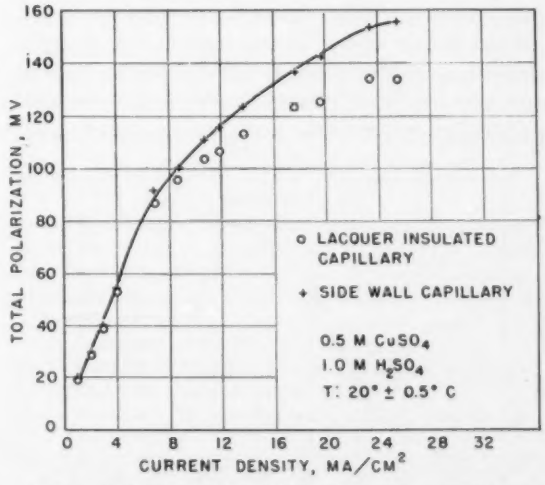

FIG. 4. Total cathode polarization as a function of current density.

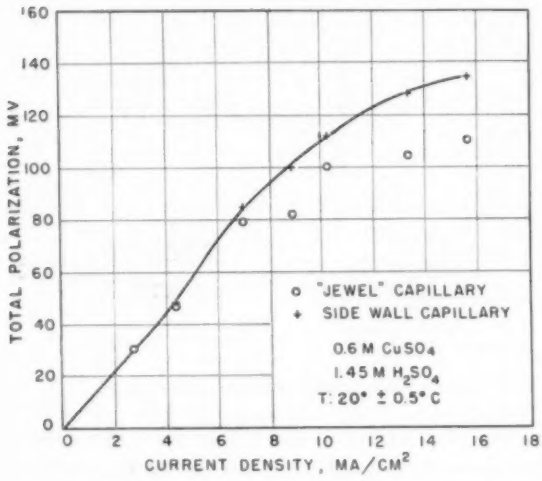

FIG. 5. Total cathode polarization as a function of current density.

through the capillary opening. The hole in the Teflon can be drilled after it has been fitted into the electrode. The solution side of the capillary was machined to eliminate any protrusions. This Teflon piece was attached to the reference half-cell by a piece of plastic tubing or by fitting it directly into a glass joint.

The Teflon capillary yielded consistently close agreement with values measured by the sidewall capillaries. (None of the values in Fig. 4, 5, 6, and 7 were corrected for the small *IR* drop that existed between the surface and the inside of the BSC.)

Measurement of Polarization Variation along Electrode Surfaces

The copper end plate of a rectangular Lucite cell of square cross section (Fig. 8) was equipped with three identical Teflon capillaries located on a line parallel to the bottom of the cell. The three capillaries connected to separate half-cell compartments, each provided with identical copper reference electrodes. Each reference electrode was connected to the

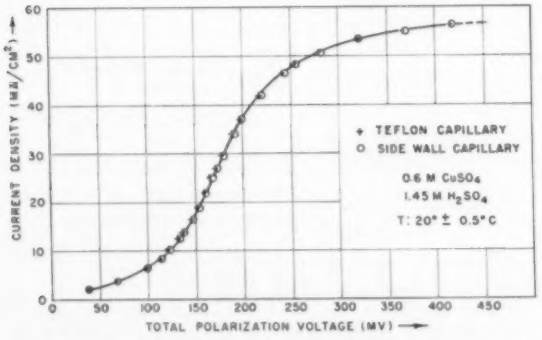

FIG. 6. Total cathode polarization as a function of current density.

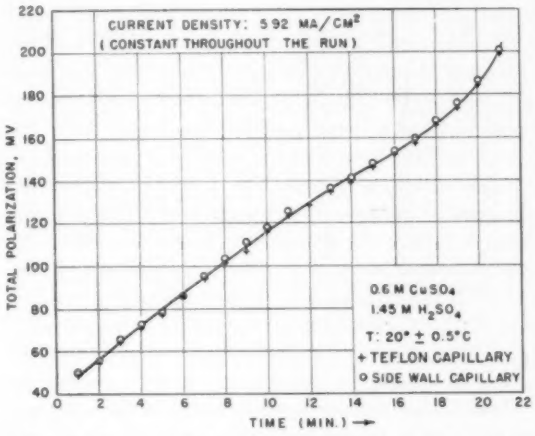

FIG. 7. Growth of the polarization of a "top" cathode with time, followed up simultaneously with the sidewall (0) and Teflon (+) capillary methods.

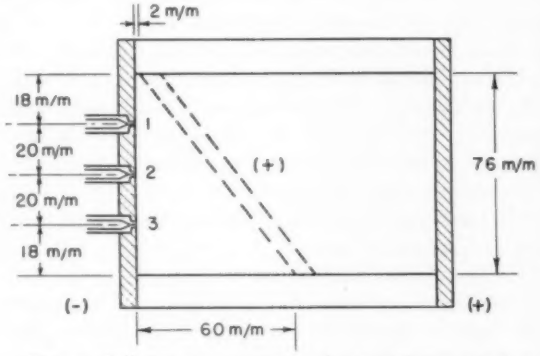

FIG. 8. Cell for measurement of nonuniform polarization; dashed lines indicate position of inclined anode.

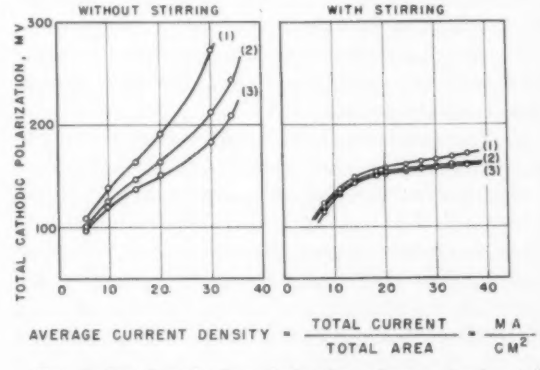

FIG. 9. Total cathode polarization along a horizontal line; inclined anode.

end plate through a potentiometer, and polarization was measured simultaneously for all three locations.

(*a*) *Line of capillaries in horizontal position.* Since the mass transfer boundary layer thickness along a horizontal line is the same (7) it is expected that all three locations yield the same polarization value. As shown in Fig. 9, indeed the values measured were identical within experimental accuracy (±2 mv).

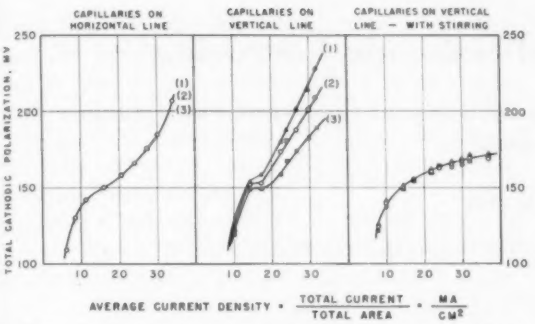

FIG. 10. Total cathode polarization vs. current density on a vertical Cu-cathode; uniform primary current distribution.

(*b*) *Line of capillaries in vertical position.* The end plate was turned by 90°, so that the lowest opening, 3, was 18 mm from the bottom. Due to natural convection the lower part of the electrode received a better supply of copper ions than the upper region. As a result, concentration polarization is higher at the top of the electrode than at the bottom (7). This fact is well illustrated by the appreciable difference between polarization values measured by the three capillaries, as illustrated in Fig. 10.

Stirring in the center of the cell by a small propeller at 1500 rpm almost completely eliminated the difference between locations.

(*c*) *Line of capillaries in horizontal position, anode in an inclined position.* The primary distribution of current is nonuniform, decreases with location 1 to 3. Without stirring, differences in polarization are quite pronounced, due to concentration polarization. With stirring, chemical polarization dominates, and polarization values fall close together (Fig. 9).

REMARKS

The backside capillary does not yield completely correct polarization values because of the ohmic drop included between the inside of the capillary and the electrode surface, and also because the current density, hence the polarization, is higher around the capillary wall than it would be on the electrode at the location where the hole was drilled in the metal in the absence of the hole. The ohmic correction is small unless the conductivity of the electrolyte is low and can be calculated approximately on the basis of Barnartt's recommendations (4). The error incurred due to higher polarization around the edge of the hole is negligible, provided the hole diameter is small and the conductivity is high.

Series of BS capillaries can be conveniently built into large electrode surfaces. In this laboratory one of the cells built for the study of the effect of forced convection (laminar and turbulent flow past flat plates) on ionic mass transfer and current distribution (10) was equipped with BS capillaries (Fig. 11). Any frontal tube or capillary would seriously affect the nature of the hydrodynamic boundary layer in such a model.

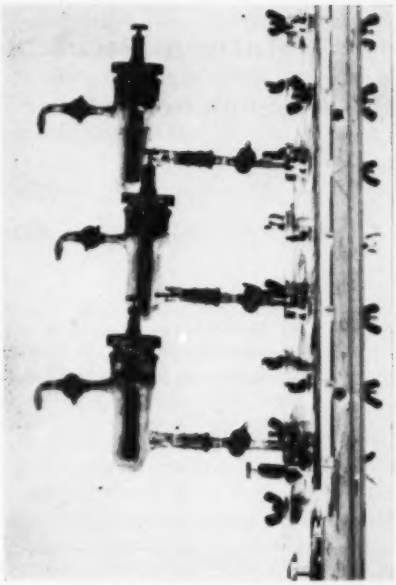

FIG. 11. Detail of cell for study of effect of laminar and turbulent flow past flat plate electrodes with reference half-cells connected to the cathode by backside capillaries.

CONCLUSION

1. Due to relatively low interference with the flow of electricity and hydrodynamic conditions, the backside capillary was found to be a suitable means for establishing junction between working electrode surfaces and reference electrodes.

2. Properly designed capillary junctions lead to potential values which are in excellent agreement with those obtained simultaneously by independent methods of established accuracy.

3. Such backside Luggin capillaries permit the measurement of local (point) values of polarization and can serve as a valuable tool in obtaining data for mass transfer and overvoltage studies.

Any discussion of this paper will appear in a Discussion Section to be published in the June 1956 JOURNAL.

REFERENCES

1. A. E. MATTSON, *Svensk Kem. Tidskr.*, **62,** 83 (1950).
2. R. PIONTELLI, G. BIANCHI, AND R. ALETTI, *Z. Elektrochem.*, **56,** 86 (1952).
3. R. PIONTELLI AND G. BIANCHI, *This Journal*, **100,** 295 (1953).
4. S. BARNARTT, *ibid.*, **99,** 549 (1952).
5. C. KASPER, *Trans. Electrochem. Soc.*, **77,** 353 (1940).
6. C. WAGNER, *This Journal*, **95,** 161 (1949).
7. C. R. WILKE, M. EISENBERG, AND C. W. TOBIAS, *ibid.*, **100,** 513 (1953).
8. R. PIONTELLI AND G. POLI, *Gazz. Chim. Ital.*, **78,** 717 (1948).
9. R. PIONTELLI, *Z. Elektrochem.*, **55,** 128 (1951).
10. M. EISENBERG, M.S. thesis, University of California, Berkeley (1951).

Mathematical Studies of Galvanic Corrosion

III. Semi-infinite Coplanar Electrodes with Equal Constant Polarization Parameters[1]

JAMES T. WABER

Los Alamos Scientific Laboratory of the University of California, Los Alamos, New Mexico

ABSTRACT

Mathematical analysis of a coplanar alternating array of long narrow electrodes was conducted subject to the limitation that polarization parameters for the anodes and cathodes are constant and equal. Interfacial potential and corrosion current parameters were computed for 18 values of $a/\mathfrak{P}$ and for a/c equal to $\frac{1}{2}$ and $\frac{1}{4}$. Four perspective drawings of the distribution of potential throughout the corrodent were made to scale to illustrate the influence of polarization. Two experimental studies were found to be in reasonably good agreement with the present theoretical analysis.

INTRODUCTION

Two important limiting cases, namely that polarization was negligible and that one electrode was infinitely larger than the other have been discussed elsewhere (1, 2). It is difficult to find experimental studies of potential distribution or of variation of corrosion attack which correspond to these limiting cases. However, several studies (3–6) have been undertaken to demonstrate such distribution of corrosion and potential in the corrodent, and, in these, finite anode-cathode ratios were employed. Thus the distribution of corrosion attack using models similar in detail to these experimental conditions has been computed.

The most serious limitation imposed on this investigation, largely by convenience, is the assumption that the anode and cathode polarization parameters are equal. This parameter, $\mathfrak{P}$ as defined by Wagner (7), has the dimensions of length and, as discussed previously (1, 2, 7), is extremely important in characterizing the behavior of a given galvanic cell. The use of equal parameters renders the case amenable to straightforward mathematical treatment, whereas, if the assumption were made that they are not equal, one would have to use cumbersome methods for solution of integral equations. Solutions require, in general, iterative or trial-and-error methods.

Previously (2) the magnitude of this parameter was calculated from various experimental data; it was found to lie in the range $\frac{1}{4}$–25 mm. This indicates that in many cases, and particularly those cases in which extensive experimental work was done, the assumption of equal polarization parameters would be a reasonable approximation.[2] This special case of equality illustrates the effect of polarization and is useful for a qualitative discussion of the more accurate and general case of unequal parameters.

This investigation was undertaken to provide numerical data which could be compared with the experimental data of Copson (3) and Daniel-Bek (4). In a separate study (8) values of the potential were tabulated for nine widely different values of the ratio of the anode width to the polarization parameter and for each of these at over a hundred locations within the electrolyte. Detailed comparison of these potential values with the experimental results have not been made here.

A comparison of the variation of the current density can be made. These data indicate that there is good agreement between the mathematical and experimental results.

Important Limiting Cases

There are four pertinent lengths needed to characterize an alternating array of long, narrow, coplanar, galvanic cells, namely, the anode width, cathode width, and anodic and cathodic polarization parameters. In agreement with the notation of the previous papers these are identified as $2a$, $2(c - a)$, $\mathfrak{P}_a$ and $\mathfrak{P}_c$, respectively. The behavior of a given galvanic system can be characterized by three dimensionless groups, $(a/\mathfrak{P}_a)$, $(c - a/\mathfrak{P}_c)$, and a/c. If even five values of each of these groups are used to illustrate the behavior of galvanic systems, 125 curves would have to be presented. The alternative is to

[1] Manuscript received October 25, 1954. This paper was prepared for delivery before the Cincinnati Meeting, May 1 to 5, 1955.

[2] That is, the electrodes employed by others range from 10 to 160 cm in width and are, therefore, macroscopically large in comparison with $\mathfrak{P}_c$. Even several fold variations between $\mathfrak{P}_a$ or $\mathfrak{P}_c$ will have a small influence on the corrosion current over much of these "large" electrodes.

discuss only limiting values of each ratio, and this procedure has been adopted in the present series of reports. One may distinguish four limiting conditions:

[1] *Negligible polarization* $a \gg \varrho_a (c - a) \gg \varrho_c$. This was considered earlier (1) with the further condition that $\varrho_a = \varrho_c$.

[2] *Strong polarization and high conductivity* $a \ll \varrho_a (c - a) \ll \varrho_c$. In this case as Wagner pointed out, IR drops within the solution represent a minor correction which can be disregarded. One may therefore use the usual diagram of electrode potential vs. current density in order to derive the corrosion potential and the operating current density.

[3] *Cathodic control and protection* $a \gg \varrho_a (c - a) \ll \varrho_c$. The case of cathodic control on dissolution of an almost pure metal has been discussed by Wagner (9). He also adopted this assumption in his contribution to cathodic protection (10). The special condition that $\varrho_a = \varrho_c$ has already been discussed briefly (2).

[4] *Anodic control* $a \ll \varrho_a (c - a) \gg \varrho_c$. This case has not been treated in general; however an analysis of the special condition that $\varrho_a = \varrho_c$ has been made (2).

In a preceding paper ϱ was assumed to be zero, and several values of the anode-cathode ratio a/c were investigated (1). Later, ϱ was permitted to vary over a wide range, but it was assumed that one electrode was infinitely larger than the other (2). In the present paper both these restrictions are removed, but ϱ_a still equals ϱ_c.

Important Experimental Studies

Electrostatic potentials have been known to exist in solution for many years, and many electrochemical problems and phenomena have been explained in terms of them. However, it was apparently not until 1938 that they were shown to exist in the vicinity of corroding specimens (10). About this time a number of independent investigations were started in Europe. The most significant contributions were made by Jaenicke and Bonhoeffer (6) and by Daniel-Bek (4). World War II interrupted similar work at Cambridge, and Copson (3) undertook to complete the work of Agar (12) here in the United States.

Jaenicke and Bonhoeffer (6) showed that, in a given medium, the absolute cathode size has a definite effect on potentials measured in the vicinity of the electrode surface. The ratio $(c - a/\varrho_c)$ has important physical significance and thus should be applied in the discussion of galvanic systems in general.

Daniel-Bek (4) measured variation in corrosion attack near the anode-cathode junction by measuring potentiometrically the approximate variation in normal potential gradient. Copson (3) obtained the variation in corrosion attack, as indicated by changes in thickness, by measuring with a micrometer the penetration into the metal.

Mathematical Analysis and Evaluation

The techniques used have been well illustrated earlier (1, 2).

Boundary Conditions

Inasmuch as corrosion currents enter and leave a solution only at the electrodes, it is necessary to have the flow lines begin and end on the electrode surfaces. In order to eliminate edge effects at the boundary line of the electrode, an infinite repetition of the electrode arrangement with even symmetry has been assumed. This assumption restricts attention to what is happening at the anode-cathode boundary. Such an arrangement can be studied mathematically by using an even periodic function such as a Fourier cosine series which alternately takes on the potential of the anode and the cathode as a boundary condition, and which will give the potential within the corrodent. Consideration can thus be restricted to one period.

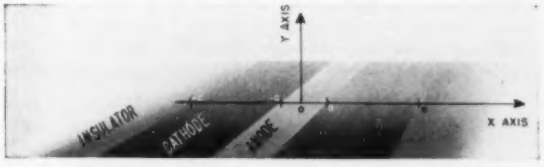

Fig. 1. Geometric relation and orientation of the electrodes.

The model galvanic cell consists of two bimetallic coplanar, juxtaposed infinite strips as indicated in Fig. 1. Since current is assumed not to flow between the electrodes in different cells or periods, one can place insulators at the remote electrode boundaries as shown in Fig. 1.

The unpolarized potential difference between the anode and cathode when immersed in the corrosive medium is designated as E_a. Conditions appropriate to the use of the slope of the polarization curve as though it were a linear polarization law have been discussed by Wagner (7). This reduces the problem to the solution of a simple Sturm-Liouville problem. As in the other papers of this series, both E_a and the potential $P(x, y)$ within the solution have been measured with respect to the cathode. Clearly P is bounded in the region under consideration.

Interfacial conditions for the solution of this

problem are:

$$P^*(x, 0) - \mathfrak{P} \left.\frac{\partial P^*}{\partial y}\right|_{y=0} = E_a S_a(x) \qquad \text{(I)}$$

$$\left.\frac{\partial P^*}{\partial x}\right|_{x=c} = \left.\frac{\partial P^*}{\partial x}\right|_{x=c} = 0 \qquad \text{(II)}$$

where the step function S_a is defined as

$$S_a(x) = \begin{cases} 1 \\ 0 \end{cases} \text{for} \begin{cases} 0 \le x \le a - 0 \\ a + 0 \le x \le c \end{cases} \qquad \text{(III)}$$

and in which $2c$ is the period of repetition. The quantity a is half of the width of the anode. The potential at the solution interface is illustrated in Fig. 2.

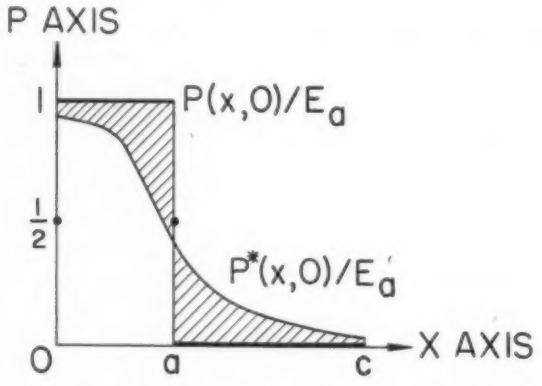

FIG. 2. Polarized interfacial potential. Variation is due to the changing current density in the two electrode regions.

Solution of the Problem

A Fourier Series which will satisfy the two boundary conditions, satisfy Laplace's equation, and converge for infinite nonnegative y is

$$P^*(x, y) = A_o^* + \sum_{n=1}^{\infty} A_n^* \exp\left(-\frac{n\pi y}{c}\right) \cdot \cos\left(\frac{n\pi x}{c}\right) \qquad \text{(IV)}$$

The starred coefficients may be determined by the boundary conditions (I) and (III). The asterisks indicate that polarization is being considered, in agreement with the convention adopted in earlier papers (2, 8). Substitution of this series into equation (I) leads to

$$A_o^* + \sum_{n=1}^{\infty} A_n^* \left(1 + \frac{n\pi\mathfrak{P}}{c}\right)^{-1} \cdot \cos\left(\frac{n\pi x}{c}\right) = E_a S_a(x) \qquad \text{(V)}$$

The orthogonal properties of a cosine series can then be used to determine the coefficients. If this equation is multiplied by $\cos(m\pi x/c)$ and then integrated with respect to x, it is clear on using definition (III) that

$$\sum_{n=1}^{\infty} A_n^* \left(1 + \frac{n\pi\mathfrak{P}}{c}\right)^{-1} \left(\frac{c}{2}\right) \delta_{mn} = \frac{cE_a}{\pi m} \sin\left(\frac{m\pi a}{c}\right) \qquad \text{(VI)}$$

where δ_{mn} is the Kronecker delta function. The left hand side of (VI) reduces to a single term of the series. The quantity A_o^* is determined in the usual way. The resulting coefficients A_m^* and A_o^* are presented in Table I, together with A_m and A_o which were derived earlier (1). The resulting equation for the potential is

$$P^*(x, y) = \frac{E_a a}{c} + \frac{2E_a}{\pi} \sum_{n=1}^{\infty} \cdot \frac{\exp\left(-\frac{n\pi y}{c}\right) \cos\left(\frac{n\pi x}{c}\right) \sin\left(\frac{n\pi a}{c}\right)}{n\left(1 + \frac{n\pi\mathfrak{P}}{c}\right)} \qquad \text{(VII)}$$

It is clear that A_m^* reduces to A_m when $\mathfrak{P}$ is zero as would be expected.

As long as the electrodes polarize similarly, the remote reference potential of this composite electrode is equal to A_o or $E_a(a/c)$. This important result can be seen by setting y equal to infinity in equation (VII).

TABLE I. *Comparison of the coefficients obtained in the two reports*

	$\mathfrak{P} = 0$ Part I	$\mathfrak{P} \neq 0$ Part III
A_o	$E_a(a/c)$	$E_a(a/c)$
A_m	$\dfrac{2E_a \sin\left(\frac{m\pi a}{c}\right)}{m\pi}$	$\dfrac{2E_a \sin\left(\frac{m\pi a}{c}\right)}{\pi m(1 + m\pi\mathfrak{P}/c)}$

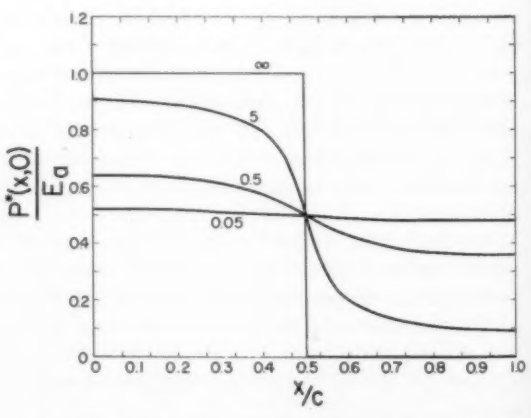

FIG. 3. Plot of the reduced interfacial potential, $P^*(x, 0)/E_a$, for four values of $a/\mathfrak{P}$ and with $2a = c$.

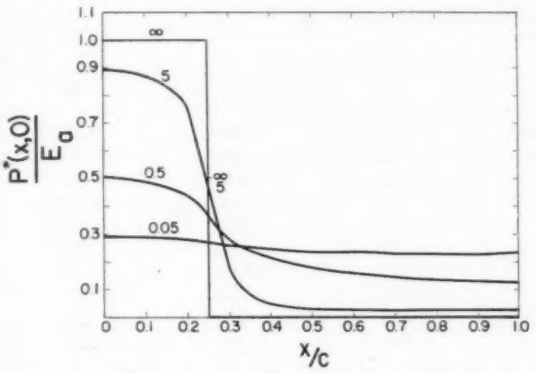

FIG. 4. Plot of the reduced interfacial potential, $P^*(x, 0)/E_a$, for four values of a/ℓ and with $4a = c$.

To give the mathematical results more general significance and applicability, the potential function can be reduced to the dimensionless group $P^*(x, 0)/E_a$. The reduced dimensionless groups x/c and a/c may also be used for the linear dimensions of the cell.

Distribution of the Interfacial Potential

The reduced interfacial potential $P^*(x, 0)/E_a$ was evaluated from (VII) using the Dual Coding Program on the Type 701 IBM computer of this laboratory. This quantity is presented in Tables II and III as a function of various x/c, a/ℓ, and a/c values. The influence of these parameters is illustrated in Fig. 3 for $a/c = \frac{1}{2}$ and in Fig. 4 for $a/c = \frac{1}{4}$.

TABLE II. *The reduced interfacial potential function $P^*(x, 0)/E_a$ evaluated for $a/c = \frac{1}{2}$ and equal polarization parameters (Part 1)*

	x/c				
a/ℓ	0	0.1	0.2	0.3	0.4
0	0.50000	0.50000	0.50000	0.50000	0.50000
0.01	0.50369	0.50359	0.50328	0.50272	0.50180
0.05	0.51796	0.51748	0.51598	0.51328	0.50885
0.1	0.53477	0.53386	0.53101	0.52582	0.51728
0.5	0.63848	0.63525	0.62505	0.60603	0.57320
1.0	0.72010	0.71564	0.70132	0.67385	0.62397
5	0.90724	0.90351	0.89077	0.86270	0.79719
10	0.95110	0.94880	0.94071	0.92164	0.87036
50	0.98997	0.98946	0.98762	0.98300	0.96809
100	0.99493	0.99467	0.99373	0.99138	0.98366
∞	1.00000	1.00000	1.00000	1.00000	1.00000

TABLE II. (*Part 2*)

	x/c					
a/ℓ	0.5	0.6	0.7	0.8	0.9	1.0
0	0.50000	0.50000	0.50000	0.50000	0.50000	0.50000
0.01	0.50000	0.49820	0.49728	0.49672	0.49641	0.49631
0.05	0.50000	0.49115	0.48672	0.48402	0.48252	0.48204
0.1	0.50000	0.48272	0.47418	0.46899	0.46614	0.46523
0.5	0.50000	0.42680	0.39397	0.37495	0.36475	0.36152
1.0	0.50000	0.37603	0.32615	0.29868	0.28437	0.27990
5	0.50000	0.20281	0.13730	0.10923	0.096492	0.092755
10	0.50000	0.12964	0.078357	0.05929	0.051205	0.048895
50	0.50000	0.031908	0.017000	0.012383	0.010542	0.010028
100	0.50000	0.016335	0.008619	0.006266	0.005331	0.005071
∞	0.50000	0.00000	0.00000	0.00000	0.000000	0.000000

TABLE III. *Reduced interfacial potential function $P^*(x, 0)/E_a$ evaluated for $a/c = \frac{1}{4}$ (Part 1)*

	x/c					
a/ℓ	0	0.1	0.2	0.249	0.251	0.3
0	0.25000	0.25000	0.25000	0.25000	0.25000	0.25000
0.005	0.25396	0.25371	0.25285	0.25188	0.25181	0.25082
0.05	0.28773	0.28538	0.27711	0.26777	0.26700	0.25743
0.5	0.50883	0.49384	0.43711	0.36394	0.35616	0.28189
5	0.88684	0.86980	0.77438	0.50215	0.44896	0.17618
50	0.98811	0.98574	0.96638	0.62632	0.36869	0.02862
∞	1.00000	1.00000	1.00000	1.00000	0.00000	0.00000

TABLE III. (*Part 2*)

	x/c						
a/ℓ	0.4	0.5	0.6	0.7	0.8	0.9	1.0
0	0.25000	0.25000	0.25000	0.25000	0.25000	0.25000	0.25000
0.005	0.24975	0.24908	0.24861	0.24828	0.24806	0.24793	0.24789
0.05	0.24731	0.24102	0.23671	0.23372	0.23173	0.23060	0.23023
0.5	0.21600	0.18076	0.15894	0.14491	0.13609	0.13121	0.12965
5	0.07588	0.04638	0.03333	0.02656	0.02288	0.02100	0.02042
50	0.008731	0.004923	0.003427	0.002690	0.002298	0.002101	0.002041
∞	0.00000	0.00000	0.00000	0.00000	0.00000	0.00000	0.00000

TABLE IV. *Corrosion current parameter evaluated for $a/c = \frac{1}{2}$ (Part 1)*

	x/c					
$a/\mathfrak{P}$	0	0.1	0.2	0.3	0.4	0.499
0.01	0.009926	0.009928	0.009934	0.009946	0.009964	0.009999
0.05	0.04820	0.04825	0.04840	0.04867	0.04912	0.04998
0.1	0.09304	0.09323	0.09380	0.09484	0.09654	0.09992
0.5	0.3615	0.3647	0.3749	0.3940	0.4268	0.4979
1.0	0.5598	0.5687	0.5974	0.6523	0.7521	0.9920
5	0.9276	0.9649	1.0923	1.3730	2.0281	4.8454
10	0.9779	1.0241	1.1859	1.5671	2.5928	9.4673
50	1.0028	1.0542	1.2383	1.6999	3.1908	41.588
100	1.0141	1.0663	1.2532	1.7238	3.2671	74.236
∞	1.0000	1.0515	1.2361	1.7013	3.2360	318.47

TABLE IV. (*Part* 2)

	x/c					
$a/\mathfrak{P}$	0.501	0.6	0.7	0.8	0.9	1.0
0.01	−0.009999	−0.009964	−0.009946	−0.009934	−0.009928	−0.009926
0.05	−0.04998	−0.04912	−0.04867	−0.04840	−0.04825	−0.04820
0.1	−0.09992	−0.09654	−0.09484	−0.09380	−0.09323	−0.09304
0.5	−0.4979	−0.4268	−0.3940	−0.3749	−0.3647	−0.3615
1.0	−0.9920	−0.7521	−0.6523	−0.5974	−0.5687	−0.5598
5	−4.8454	−2.0281	−1.3730	−1.0923	−0.9649	−0.9276
10	−9.4673	−2.5928	−1.5671	−1.1859	−1.0241	−0.9779
50	−41.588	−3.1908	−1.6999	−1.2383	−1.0542	−1.0028
100	−74.236	−3.2671	−1.7238	−1.2532	−1.0663	−1.0141
∞	−318.47	−3.2360	−1.7013	−1.2361	−1.0515	−1.0000

Corrosion Current Density

More important than the interfacial potential is the distribution of corrosion attack over the anode and the cathodic current density over the other electrode. In agreement with the definition used elsewhere (1, 2), the corrosion current parameter

$$C^*(x) = \frac{-2a}{E_a} \frac{\partial P^*}{\partial y}\bigg|_{y=0} \qquad \text{(VIII)}$$

It is clear that the normal gradient in (VIII) may be calculated by means of boundary condition (I) from the interfacial potential. Thus

$$C^*(x) = \frac{2a}{\mathfrak{P}}\left[S_a(x) - \frac{P^*(x,0)}{E_a}\right] \qquad \text{(IX)}$$

An additional and important merit of calculating the interfacial potential is the facility with which current density can subsequently be calculated. It is apparent that this equation cannot be used if the polarization parameter is negligibly small, i.e., when $\mathfrak{P}$ is zero. The current density distribution has been discussed for zero $\mathfrak{P}$ elsewhere (1).

Values of this dimensionless parameter $C^*(x)$ which represents the corrosion current have been computed from (IX) and are presented in Tables IV and V. The dimensionless quantity employed to represent the current parameter (1) was $r(x)/E_aR_oh$ which is equal to $(c/4a)C(x)$.

Distribution of Potential in the Solution

Distribution of the potential can be obtained in the corrodent from equation (VII). Because the exponential factor is present in each term of the series, computation of the potential at a point in the solution is more rapid than equivalent computation of a value of the interfacial potential. That is, the series converges more rapidly in the former case.

As indicated above, the reduced and dimensionless polarization parameter $P^*(x, y)/E_a$ has been used to render the mathematical results applicable to the general problem. When this parameter is tabulated in terms of the reduced groups x/c, a/c, and $a/\mathfrak{P}$, which represent the physical dimensions of the galvanic cell, the results are independent of the actual quantities of any given galvanic cell, namely, E_a, a, c, σ, etc. By calculating the several pertinent ratios, a given problem can be solved.

Values of the reduced potential have been computed and presented elsewhere (8) for a variety of $a/\mathfrak{P}$ and a/c values. The effect of $\mathfrak{P}$ on the distribution of potential is best illustrated by the four perspective drawings of $P^*(x/c, y/c)$ which have been made to scale. In these drawings, the anodic material is assumed to be 50% of the total. Fig. 5 was constructed for the condition that $\mathfrak{P} = 0$. The cross hatching represents the portion of the interfacial potential which is hidden from view by the po-

TABLE V. *Corrosion current parameter $C^*(x)$ evaluated for $a/c = \frac{1}{4}$ (Part 1)*

	x/c					
$a/\mathfrak{L}$	0	0.1	0.2	0.249	0.251	0.3
0.005	0.007460	0.007463	0.007472	0.007481	−0.002518	−0.002508
0.05	0.07123	0.07146	0.07229	0.07322	−0.02670	−0.02574
0.5	0.4192	0.5062	0.5629	0.6361	−0.3561	−0.2819
5	1.1316	1.3020	2.2561	4.9784	−4.4896	−1.7618
50	1.1887	1.4259	3.3617	37.368	−36.869	−2.8629
∞	1.207	1.4493	3.4693	159.26	−158.54	−2.9631

TABLE V. (*Part 2*)

	x/c						
$a/\mathfrak{L}$	0.4	0.5	0.6	0.7	0.8	0.9	1.0
0.005	−0.002497	−0.002491	−0.002486	−0.002483	−0.002481	−0.002479	−0.002479
0.05	−0.02473	−0.02410	−0.02367	−0.02337	−0.02317	−0.02306	−0.02302
0.5	−0.2160	−0.1808	−0.1589	−0.1449	−0.1361	−0.1312	−0.1296
5	−0.7588	−0.4637	−0.3333	−0.2657	−0.2288	−0.2100	−0.2042
50	−0.8731	−0.4923	−0.3428	−0.2690	−0.2298	−0.2101	−0.2042
∞	−0.8881	−0.5000	−0.3479	−0.2735	−0.2332	−0.2132	−0.2071

tential surface. Fig. 6, 7, and 8 were constructed for the conditions that $a/\mathfrak{L}$ was 10, 1, and 0.1, respectively. In these figures the cross hatching represents the changes in the interfacial potential from the unpolarized values 1 and 0 caused by polarization.

Comparison between Theory and Experiments

Adequate comparison can be made only when values of $\mathfrak{L}_a$ and $\mathfrak{L}_c$ have been obtained under conditions comparable to the experimental conditions that were employed. In the studies made to date, the author is not aware of any experimental study of current or potential distribution in which both $\mathfrak{L}_a$ and $\mathfrak{L}_c$ are available or can be computed. Any observed discrepancy revealed by comparing experiments with the present analysis will reveal mainly the degree to which $\mathfrak{L}_a$ and $\mathfrak{L}_c$ are dissimilar and will not reveal any fundamental error in the analysis.

There is a fairly large mass of experimental data available on the distribution of potential throughout the corroding medium (3–6, 11, 12). However, comparison is complicated by the difficulty of estimating the unpolarized potential difference E_a and the subject

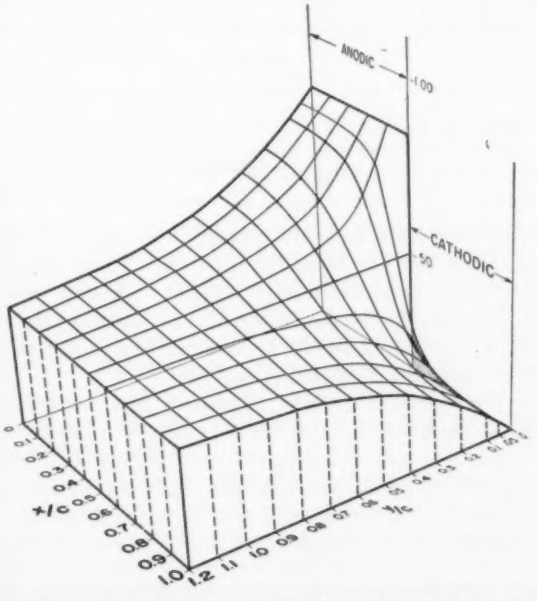

FIG. 5. Perspective scale drawing of the reduced potential function evaluated for $\mathfrak{L} = 0$.

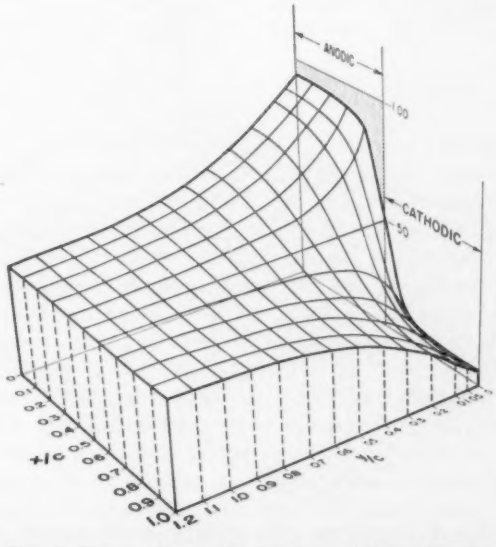

FIG. 6. Perspective scale drawing of the reduced potential function evaluated for $a/\mathfrak{L} = 10$.

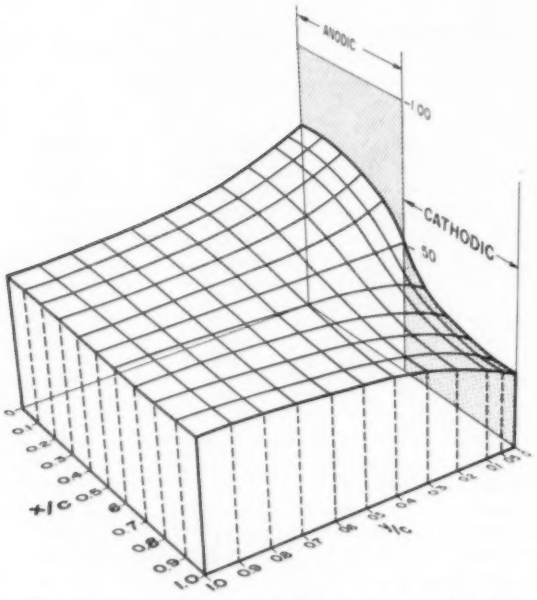

FIG. 7. Perspective scale drawing of the reduced potential function evaluated for $a/\mathfrak{P} = 1$.

is not as interesting, in the main, as the question of the distribution of the corrosion attack. Copson's (3) and Daniel-Bek's third paper (4) will be used for the comparison. Although only an experimental study designed for making this comparison can be adequate, these two investigations approximate the ideal conditions closely enough to merit consideration below.

Comparison with Daniel-Bek's Results

Daniel-Bek(4) employed an approximate form of equation (VIII) to calculate the distribution of corrosion attack over the anode in the vicinity of the anode-cathode junction. He estimated $\partial P^*/\partial y|_y = 0$ by drilling tiny holes at several positions in the anode and fitting the capillary tip of a reference electrode into them. By measuring the potential difference between these electrodes and another held constant 0.55 mm in front of the metal surface, the normal potential gradient could be made roughly proportional to this potential difference. The assembly, consisting of one anode and one cathode, was 320 cm long, so that the ratio y/c appearing in the exponential term of the present series would be equal to 1.72×10^{-4} for his work. The difference form of the gradient $\Delta P/\Delta y$ was evaluated at approximately $y = 0$.

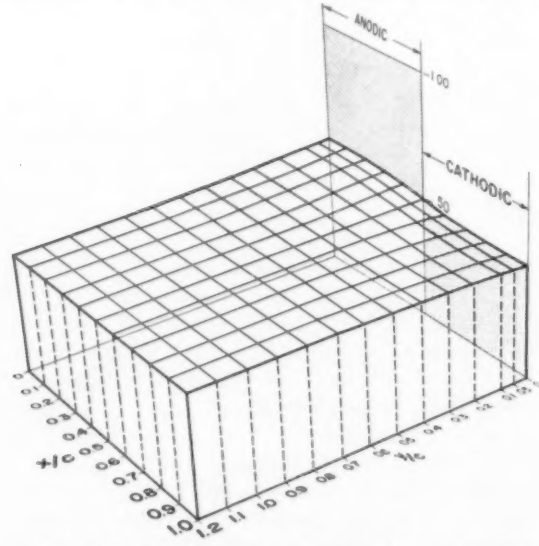

FIG. 8. Perspective scale drawing of the reduced potential function evaluated for $a/\mathfrak{P} = 0.1$.

With this clever, approximate method he was able to show that there was a considerable variation in the amount of corrosion attack over the anode and in different strong electrolytes. Although conductivities of the solutions were high the anode width was equal to 160 cm, and thus $\mathfrak{P}/a$ would be very small.

$\mathfrak{P}$ can be estimated from the data which he gives since $a/c = \frac{1}{2}$. In such a case it can be shown that[3]

$$J_a(a - s) = -J_c(a + s) \qquad (X)$$

Employing $s = \frac{1}{2}$ cm, the largest J_c is 4.6 ma/cm² for $0.2N$ $KClO_3$, and the smallest J_c for $s = 8$ cm is 0.36 ma/cm² for $0.05N$ KCl. One may estimate the derivative of the overvoltage curve, $\partial \Delta E_c/\partial J_c$ from Tafel's equation

$$\Delta E_c = a + 0.050 \ln J_c \qquad (XI)$$

if hydrogen evolution is the principal cathodic process. On substitution into the definition of $\mathfrak{P}$,

$$\mathfrak{P}_i = \left| \frac{\partial \Delta E_i}{\partial J_i} \right| \sigma \qquad (XII)$$

it is evident that

$$\mathfrak{P}_c = \frac{0.050\sigma}{J_c} \qquad (XIII)$$

The smallest value of the polarization parameter is 0.207 cm and the largest is 0.775 cm. These values are quite compatible with values estimated elsewhere (2). The largest value of $\mathfrak{P}_a/c$ then would be 24×10^{-4} since in the theoretical analysis it has been assumed that $\mathfrak{P}_a = \mathfrak{P}_c$.

The corrosion current parameter was computed from equation (IX) for $\mathfrak{P}/c$, namely, 5×10^{-4}. When $\mathfrak{P}$ is zero, equation [24] of reference (1) can be used to obtain the corrosion current parameter. Theoretical curves as well as experimental data for three electrolytes are presented in Fig. 9. Specifically,

[3] Note that $J_a(x)$, the actual current density, is equal to $(\sigma E_a/2a)\zeta^*_a(x)$.

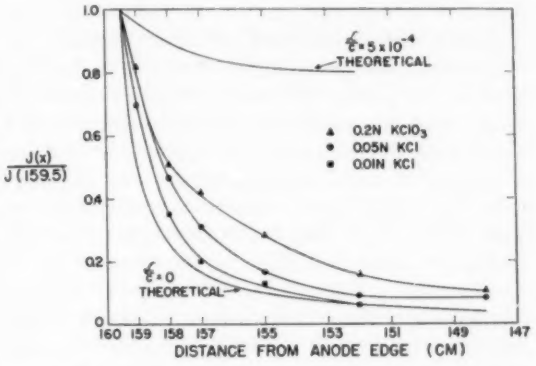

FIG. 9. Comparison of the theoretical current densities evaluated for $\ell/c = 5 \times 10^{-4}$ and 0 with Daniel-Bek's experimental results.

the ordinate is $J(160\text{-}s)/J(159.5)$ and the abscissa is $a - s$. The experimental data are well bracketed by $\ell = 0$ and $\ell = 1.6$ mm. Therefore, the agreement would appear to be quite satisfactory considering the idealizations which have been employed.

Comparison with Copson's Results

It is not practical to compare the potentials which Copson (3) measured in the corrodent, Bayonne tap water; however, the galvanic corrosion attack on the steel part of his steel-nickel couple can be compared with corrosion current parameter obtained in the theoretical analysis of this paper. He estimated the distribution of corrosion attack by graphically estimating the potential gradient from a map of the measured potentials. Fig. 7 of reference (3) shows the comparison between the actual change in thickness and the calculated attack. The graphical method is clearly inadequate near the steel-nickel junction as would be expected from the tables of the corrosion current parameter presented above. Near the junction the current increases very rapidly, and a linear average between two gradients is not very representative. In general, one would expect the average to be low because of the strong influence of the value taken more remotely from the junction. The estimated anodic current densities range from 0.138 ma/dm² or 1.38 μa/cm² at a point ½ in. from the center of the anode ($x = ½$) to 8.62 μa/cm² at 3.95 in. The cathodic current was estimated to vary from 4.32 μa/cm² at $x = 4.00$ to 1.45 μa/cm² at 7.80 in. In terms of the definitions employed herein, a is 4 in. and c is 16 in.

An estimate of the polarization parameter can be obtained from these data, using equation (XIII) for ℓ_c. It would range from 0.81 cm to 2.42 cm. If an expression such as Tafel's equation could be used properly to represent the anodic polarization, the estimated values of ℓ_a would lie in the range 0.41 to 2.54 cm. The justification for making this crude estimate of ℓ_a is to indicate that ℓ_a and ℓ_c are approximately equal, and that the present idealized analysis is pertinent.

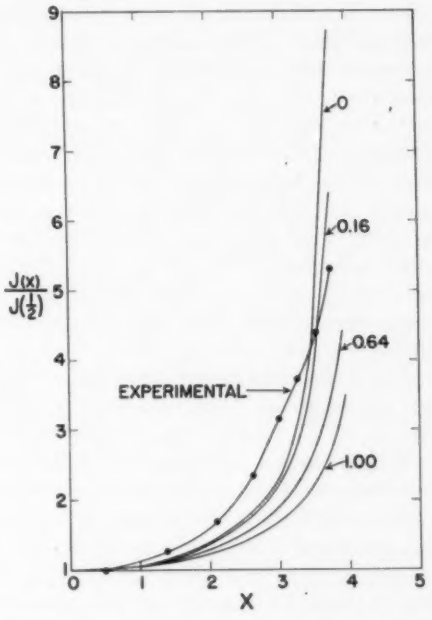

FIG. 10. Comparison between the distribution of Copson's experimental current densities and the theoretical variation evaluated for four ℓ values.

Values of the corrosion current parameter were computed using four values of ℓ: 0.0, 0.16, 0.64, and 1.0 in. These data were plotted in Fig. 10 in the form of $C_a^*(x)/C_a^*(½)$ which is equal to $J_a(x)/J_a(x = ½)$. Copson's experimental data are also plotted in Fig. 10 for comparison. Agreement is fairly good considering the idealizations involved in the theoretical analysis.

DISCUSSION

These numerical values of the polarized potential bear out the conclusions which have been deduced by others from experimental studies. The interfacial potential becomes more nearly the same for the anode and cathode as the parameter ℓ increases.

This polarization parameter is very important in characterizing actual galvanic cells. In a given environment, irrespective of physical size, a galvanic cell may behave as though it were "macroscopic" or "microscopic" depending on whether the ratio of the critical dimension to ℓ is large or small. This critical dimension cannot easily be defined in a precise manner, but it is that physical dimension which affects most strongly the distribution of current over the electrodes. Thus, it depends on the geometry of the cell.

If the critical dimension is small in comparison to $\mathfrak{L}$, that galvanic cell will behave as though it were microscopic. Since $\mathfrak{L}$ is directly proportional to the conductivity of the solution, a particular system may appear to be either microscopic, or not, depending on whether the electrical resistance of the corrodent is small or large, respectively. That is, more uniform potentials over the electrodes are observed in solutions which have good conductivity as shown by Jaenicke and Bonhoeffer (6), among others. The "microscopic" cells are characterized by nearly uniform current distributions, hence nearly uniform interfacial potentials.

It should be emphasized here again that the present investigation is an idealization since the restriction $\mathfrak{L}_a = \mathfrak{L}_c$ has been imposed. However, as indicated above, experimental values of $\mathfrak{L}_c$ taken from a variety of studies range from a fraction of a millimeter to 3 cm. The assumption that $\mathfrak{L}_a$ and $\mathfrak{L}_c$ are equal is not seriously in error if either $\lambda/\mathfrak{L}$ is very small or very large, since in either range fivefold changes, for instance, of this ratio do not significantly affect the interfacial potential or the current density.

Further, it is clear from the discussion that $\mathfrak{L}$ is difficult to estimate from the current density and must be obtained properly from the polarization curve. For example, one choses a value of $\mathfrak{L}$ and then computes the current density. When these are taken to compute $\mathfrak{L}_c$ one obtains a large range of values. This discrepancy becomes most serious when the ratio $a/\mathfrak{L}$ is large, i.e., when there is small or negligible polarization.

Without going into it here, it is apparent from Wagner's analysis (7) of $\mathfrak{L}$ that it is not a fixed quantity but depends upon the curvature of the polarization curve and, therefore, will in general vary over the electrodes in a macroscopic assemblage in the same way that the current density does. A further feature which may not be recognized at first is that $E_{a(a)}$ is not a fixed quantity and is not necessarily the difference between the two equilibrium single electrode potentials but is somewhat dependent upon the shape of the polarization curve [See Fig. 2, Ref. (7)]. Nevertheless, these simplifications in the treatment and accompanying increase in the tractability in mathematic analysis which is required, lead one to a more understandable picture of the influence of the various factors. The present analysis becomes increasingly accurate and pertinent if "microscopic" galvanic cells are considered.

The estimation of $\mathfrak{L}_a$ depends upon a questionable technique if the anodic polarization curve is not obtained in any practical study. This is so because there is no recognized expression such as Tafel's equation for relating anodic polarization to current density. A thorough analysis of the limited and scattered experimental data would be desirable.

It is clear from inspecting the perspective drawings that the variation in potential in a direction parallel to the electrode surface is greatest at the interface between the electrodes and the liquid. This variation in potential diminishes as one recedes from the interface and approaches a constant potential value at great distances. It has been shown (13) that this constant is equal to $E_a(a/c)$ for the condition $\mathfrak{L}_a = \mathfrak{L}_c$. This value has been called the potential of a composite electrode (1). Therefore, it is evident that this potential, which is obtained with a remote reference electrode, is dependent not only on the potential difference E_a but also on the relative proportions of anodic to cathodic material.

This qualitative effect of $\mathfrak{L}$ is brought out in a previous paper (2). In the two experimental cases under consideration, the critical dimension was a, the half-width of the anode. Dependence of the maximum potential difference on $a/\mathfrak{L}$ is clearly illustrated by the tables.

It is interesting to point out that

$$\lim_{\mathfrak{L}\to\infty} P^*(x, y) = E_a(a/c) \qquad \text{(XIV)}$$

since the coefficients A_m^* become zero. Thus, since the interfacial potential must converge to this value, it is clear that

$$\lim_{\mathfrak{L}\to\infty} P^*(x, 0) = P^*(x, \infty) = E_a(a/c) \qquad \text{(XV)}$$

As discussed above in connection with equation (VII), the right-hand side of this equation applies for all $\mathfrak{L}$. Thus the potential distribution within the solution must become more uniform as $\mathfrak{L}$ increases, since these potentials are being squeezed between the limiting interfacial potential and the remote potential value of the galvanic cell. That is, any potential variation in the solution is smaller than that present on the interface. This feature has not been brought out clearly in any of the previous experimental studies.

Using the definition employed in a previous paper (2), that the anodic region in the electrolyte is that in which the potential exceeds $\frac{1}{2}E_a$, it is evident from the tables that shrinkage of the anodic region occurs as $\mathfrak{L}$ increases and vanishes for sufficiently large $\mathfrak{L}$, if a/c is less than $\frac{1}{2}$. The use of $(a/c)E_a$ is not really more satisfactory since a study of Fig. 4 shows that for certain values of $\mathfrak{L}/a$, the liquid adjacent to the cathode is at potentials which lie between $\frac{1}{2}E_a$ and a/cE_a. No satisfactory definition has been suggested.

The current density and total anodic current remain finite for a given width of the anode. Consideration of tiny cathodes leads to equivalent re-

sults. This finite current density is different from calculations in which the effect of polarization is ignored. This fact justifies the present calculations in spite of the rather artificial condition of equal polarization parameters.

Summary

A theoretical analysis of the influence of the percentage of anodic material and of the polarization parameter on corrosion attack has been made subject to the condition that anodic and cathodic polarization parameters are constant and equal. Two experimental studies of the distribution of corrosion attack were compared with the theoretical results and were found to be in reasonable agreement. Analysis shows that the potentials in the solution lie between the interfacial potential, as polarized, which is variable over the electrodes, and a constant value which is dependent upon the relative amounts of anodic and cathodic material. The variation in solution decreases with a/ℓ, that is, as the galvanic system approaches "microscopic" behavior.

Acknowledgments

The author is deeply indebted to Professor Carl Wagner for his continuing interest, deep insight, and fruitful suggestions during this study. Many members of this laboratory have assisted in the preparation of this manuscript, and the author would like to thank particularly Max Goldstein, Mark Wells, and Bertha Fagan for having obtained the numerical evaluations, and Elizabeth Scott for preparing the perspective drawings.

Any discussion of this paper will appear in a Discussion Section to be published in the June 1956 JOURNAL.

REFERENCES

1. J. T. WABER, *This Journal*, **101**, 271 (1954).
2. J. T. WABER AND MARSHALL ROSENBLUTH, *This Journal*, **102**, 344 (1955).
3. H. R. COPSON, *This Journal*, **84**, 71 (1943).
4. V. S. DANIEL-BEK, *Zhur. Fiz. Khim.*, **15**, 382 (1941); **18**, 247 (1944); **20**, 567 (1946).
5. G. V. AKIMOV AND A. I. GOLUBEV, *Zhur. Fiz. Khim.*, **20**, 303, 309 (1946).
6. W. JAENICKE AND K. F. BONHOEFFER, *Z. physik. Chem.*, **A191**, 193 (1942); **193**, 301 (1944).
7. C. WAGNER, *This Journal*, **98**, 116 (1951).
8. J. T. WABER, A. I. BENSON, AND M. GOLDSTEIN, Report No. LA-1651, Los Alamos Scientific Laboratory, April 1954.
9. C. WAGNER, "Handbuch der Metallphysik," (G. Masing, ed.) Vol. I, Part 2, pp. 195-200, Akademische Verlagsgesellshaft Becker and Erler K. G., Leipzig (1940).
10. C. WAGNER, *This Journal* **99**, 1 (1952).
11. R. S. THORNHILL AND U. R. EVANS, *J. Chem. Soc. (London)*, **1938**, 614.
12. J. N. AGAR, reported by U. R. EVANS, *J. Iron Steel Inst.*, **141**, 221 (1940).
13. J. T. WABER, Report No. LA-1386, Los Alamos Scientific Laboratory, March 1952.

Conductances of Some Moderately Concentrated Solutions of Metallic Perchlorates in the Mixed Solvent Methanol-Acetone at Low Temperatures[1]

PAUL G. SEARS, WALTER W. WHARTON, AND LYLE R. DAWSON

Department of Chemistry, University of Kentucky, Lexington, Kentucky

ABSTRACT

Conductances and viscosities of solutions of lithium perchlorate in 50-50 wt % methanol-acetone at concentrations up to 4.75*M* have been measured over the temperature range −50° to 20°C. Similar measurements have been made on solutions of magnesium, zinc, and strontium perchlorates to concentrations slightly above 1.0*M*.

The maximum, which appears in the plot of conductivity as a function of concentration, shifts toward lower concentrations as the temperature is decreased. It has been shown that the four solutes studied exhibit very similar behavior and that the properties of solutions of the mixed solutes in this system depend primarily upon the total electrolyte concentration rather than the particular salts used.

Addition of water causes an increase in conductivity at room temperature; however, at low temperatures the presence of water markedly decreases the conductivity.

INTRODUCTION

This study was designed to investigate the conductance of some moderately concentrated solutions of metallic perchlorates in methanol-acetone mixtures at temperatures in the range −50° to 20°C. Magnesium, zinc, strontium, and lithium perchlorates were known to be rather remarkably soluble in both methanol and acetone (1, 2). An earlier investigation of conducting solutions of magnesium perchlorate in methanol and in acetone at 25°C had been reported by van Rysselberghe and Fristom (3). Their work was directed primarily toward the comparison of experimental and theoretically-predicted conductance behavior at low concentrations, whereas that reported in this paper has been concerned with a study of some factors affecting conductance at low temperatures.

EXPERIMENTAL

Materials.—Commercially available materials of good quality were used without further purification. Essentially anhydrous metallic perchlorates were obtained from the G. Frederick Smith Chemical Company. 'Baker Analyzed' reagent methanol and acetone had conductivities which amounted to less than 0.1% of that of the least conducting solution studied.

[1] Manuscript received December 2, 1954. This paper was prepared for delivery before the Cincinnati Meeting, May 1 to 5, 1955.

Based on research performed under a contract with the U. S. Army Signal Corps.

Procedure.—Solutions were prepared on a weight basis with all material transfers made in a dry box. A Jones bridge, manufactured by the Leeds and Northrup Company, was used to measure the resistance of the solutions by employing three conductance cells having constants of 31.99, 31.58, and 30.68 cm^{-1}. These constants were determined at 25°C through the intercomparison of resistances with cells having constants evaluated by the method of Jones and Bradshaw (4). Other aspects of the experimental procedure have been described adequately in a previous paper (5).

Measurements on each solution were completed within 48 hr after its preparation so that the results would not be altered appreciably because of instability effects which might appear.

DISCUSSION OF RESULTS

The conductance of lithium perchlorate in a 50-50 weight mixture of methanol and acetone was investigated rather extensively. The conductivity of this system, and of some solutions of magnesium perchlorate, at the various temperatures is shown in Fig. 1 as a function of the concentration expressed as gram-equivalent weights per 1000 g of solvent. It may be observed that the conductivity passes through a maximum at each temperature and that the concentration at which the maximum occurs decreases as the temperature is lowered. The corresponding viscosity data for these solutions have been incorporated into Fig. 2, where it may be seen that the viscosity of solutions of lithium perchlorate in

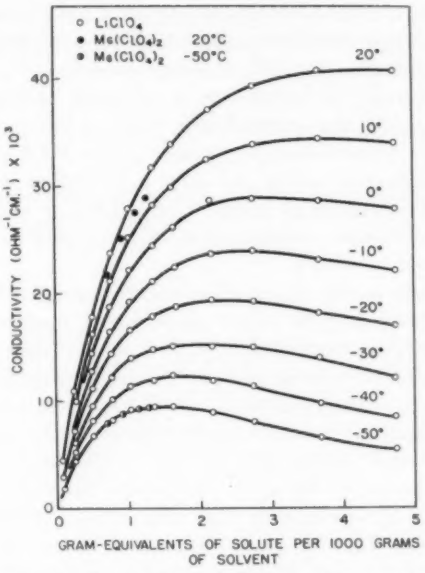

FIG. 1. Conductivities of lithium and magnesium perchlorates in 50-50 methanol-acetone as a function of the concentration.

50-50 methanol-acetone increases markedly with concentration at low temperatures. If the change of viscosity with concentration were relatively the same at each temperature, the concentration at which the maximum conductivity occurs should increase with decreasing temperature owing to increased dissociation of the solute resulting from the greater dielectric constant of the solvent. However, it appears that the more rapid increase of viscosity with concentration at lower temperatures has a counter-

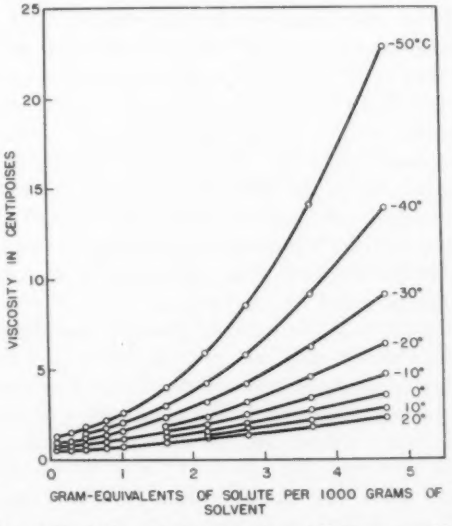

FIG. 2 Variation of the viscosity of lithium perchlorate solutions with concentration.

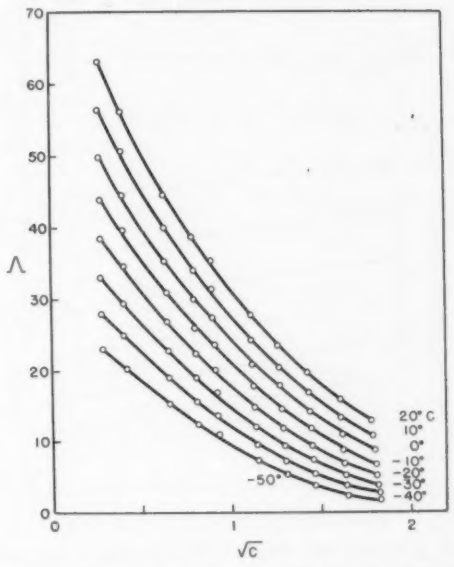

FIG. 3. Kohlrausch plots for some moderately concentrated solutions of lithium perchlorate in 50-50 methanol-acetone.

balancing effect great enough to shift the conductivity maximum toward a lesser rather than a greater concentration.

Kohlrausch plots for concentrated solutions of lithium perchlorate in 50-50 methanol-acetone are shown in Fig. 3. Graphs for the various temperatures are quite similar and are displaced at different magnitudes along the ordinate. No attempt has been

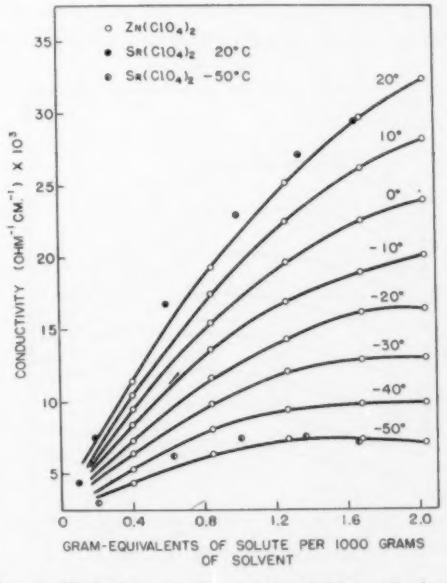

FIG. 4. Variation of the conductivities of zinc and strontium perchlorates with concentration.

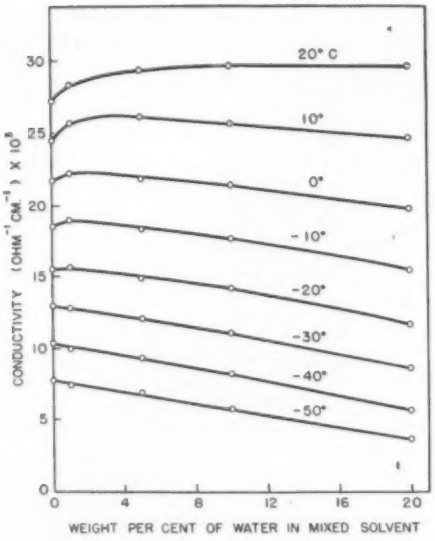

FIG. 5. Conductivities of 0.6*M* solutions of magnesium perchlorate in solvent mixtures of water and 50-50 methanol-acetone.

made to evaluate the limiting equivalent conductance from these data.

It may be observed from Fig. 1 that the conductivity of a magnesium perchlorate solution is approximately equal to that of a lithium perchlorate solution containing the same number of gram-equivalents of solute per 1000 g of solvent. Points representing conductance data for magnesium perchlorate solutions at intermediate temperatures have been omitted from this figure for purposes of clarity.

Fig. 4 shows conductivities of solutions of zinc perchlorate and strontium perchlorate in 50-50 methanol-acetone as a function of the concentration. Conductances of these salts, which are almost equal, are approximately 15% less than that for the same concentration of magnesium perchlorate. It may be noted that the conductivity maxima for −50°C in Fig. 4 occur at a concentration of 1.2–1.4 gram-equivalents of solute per 1000 g of solvent which may be compared to about 1.4 on the same concentration basis for magnesium and lithium perchlorates as shown in Fig. 1.

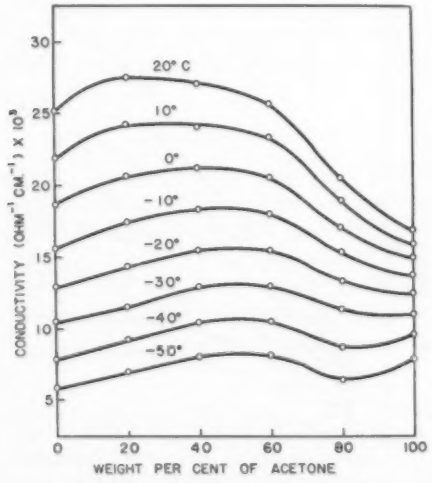

FIG. 6. Conductivities of 0.6*M* solutions of magnesium perchlorate in mixtures of methanol and acetone.

Conductances of several solutions containing both magnesium and strontium perchlorates, magnesium and lithium perchlorates, or zinc and lithium perchlorates were measured at various temperatures; however, conductances of all of these perchlorate solutions of the same total electrolyte concentration were found to differ no more than a few per cent.

The effect of water in perchlorate solutions was studied by measuring the conductance of 0.6*M* solutions (i.e., 1.2 gram-equivalents of solute per 1000 g of solvent) of the magnesium salt in solvent mixtures of water and 50-50 methanol-acetone at temperatures within the range −50° to 20°C. Results are presented in Fig. 5. As may be observed from this figure, the presence of approximately 20% water at 20°C causes a 10% increase in the conductance; however, at −50°C 20% water in the solvent reduces the conductivity to approximately half that when water is absent.

Another study of the effect of solvent composition upon conductance was made by determining the conductance of 0.6*M* magnesium perchlorate solutions in solvent mixtures of methanol and acetone ranging from pure methanol to pure acetone. Results are shown in Fig. 6. For the particular concentration of magnesium perchlorate used, the most conducting solution at −50°C was in the 50-50 solvent and that at 20°C was in the 80-20 methanol-acetone mixture. Whether this is true for all concentrations of solute is unknown. In connection with this study, it is rather interesting that the conductivity of the 0.6*M* solution of the magnesium salt at 20°C divided by that at −50°C gives values of 4.26 and 2.13, respectively, for methanol and acetone. It seems to be merely fortuitous that the value for acetone is exactly half that for methanol.

In order to obtain some information regarding the stability of the solutions, the resistance of a 0.6*M* solution of magnesium perchlorate in 50-50 methanol-acetone was measured periodically over a period of nearly seven weeks. The resistance was found to increase steadily until after 47 days it was 8.5% greater than the initial value. Another solution 0.617 and 0.099*M* with respect to magnesium and strontium perchlorates was found to increase in

resistance 12% at 20°C and 23% at −50°C over a period of 82 days. The cause of the increase in resistance (or decrease in conductance) upon standing is unknown; however, it was observed that a very small amount of white flocculent precipitate usually appeared in most of the solutions after a few days.

Any discussion of this paper will appear in a Discussion Section to be published in the June 1956 JOURNAL.

REFERENCES

1. H. H. WILLARD AND G. F. SMITH, *J. Am. Chem. Soc.*, **45,** 286 (1923).
2. R. SALVADORI, *Gaz.*, **42,** i, 482 (1912).
3. P. VAN RYSSELBERGHE AND R. M. FRISTOM, *J. Am. Chem. Soc.*, **67,** 680 (1945).
4. G. JONES AND B. C. BRADSHAW, *ibid.*, **55,** 1780 (1933).
5. P. G. SEARS, R. R. HOLMES, AND L. R. DAWSON, *This Journal*, **102,** 145 (1955).

FUTURE MEETINGS OF
The Electrochemical Society

Pittsburgh, October 9, 10, 11, 12, and 13, 1955

Headquarters at the William Penn Hotel

Sessions will be scheduled on

Batteries, Corrosion, Electrodeposition,
Electro-Organics, and Electrothermics and Metallurgy

* * *

San Francisco, April 29 and 30, and May 1, 2, and 3, 1956

Headquarters at the Mark-Hopkins Hotel

Sessions will be scheduled on

Electric Insulation, Electronics, Industrial Electrolytics,
and probably Electrothermics and
Metallurgy and Theoretical Electrochemistry

* * *

Cleveland, October 28, 29, 30, and 31, and November 1, 1956

Headquarters at the Statler Hotel

* * *

Washington, D. C., May 12, 13, 14, 15, and 16, 1957

Headquarters at the Statler Hotel

* * *

Buffalo, October 6, 7, 8, 9, and 10, 1957

* * *

Papers are now being solicited for the meeting to be held in San Francisco. Triplicate copies of each abstract (not exceeding 75 words in length) are due at the Secretary's office, 216 West 102nd Street, New York 25, N. Y., *not later than January 2, 1956*. Complete manuscripts should be sent in triplicate to the Managing Editor of the JOURNAL at the same address.